ISTANBUL TECHNICAL UNIVERSITY ★ INSTITUTE OF SCIENCE AND TECHNOLOGY

EXPERIMENTAL ASSESSMENT OF HETEROTROPHIC ENDOGENOUS DECAY AND DENITRIFICATION KINETICS USING HYDROLYZED CARBON SOURCES

Ph.D. Thesis by

Ebru AVCIOĞLU, M.Sc.

501930023012

Date of submission: 30 June 2000
Date of defence examination: 20 November 2000

Supervisor (Chairman) : Prof. Dr. Derin ORHON
Members of Examining Committe : Prof. Dr. Nazik ARTAN (İ.T.Ü.)
Prof. Dr. İzzet ÖZTÜRK (İ.T.Ü.)
Prof. Dr. Ülkü YETİŞ (O.D.T.Ü.)
Prof. Dr. Orhan YENİGÜN (B.Ü.)

NOVEMBER 2000

İSTANBUL TEKNİK ÜNİVERSİTESİ ★ FEN BİLİMLERİ ENSTİTÜSÜ

İÇSEL SOLUNUM MEKANİZMASI VE DENİTRİFİKASYON KİNETİĞİNİN HİDROLİZ KAYNAKLI KARBON TÜRLERİ İÇİN BELİRLENMESİ

DOKTORA TEZİ

Y. Müh. Ebru AVCIOĞLU

501930023012

Tezin Enstitüye Verildiği Tarih: 30 Haziran 2000
Tezin Savunulduğu Tarih: 20 Kasım 2000

Tez Danışmanı : Prof. Dr. Derin ORHON
Diğer Jüri Üyeleri : Prof. Dr. Nazik ARTAN (İ.T.Ü.)
Prof. Dr. İzzet ÖZTÜRK (İ.T.Ü.)
Prof. Dr. Ülkü YETİŞ (O.D.T.Ü.)
Prof. Dr. Orhan YENİGÜN (B.Ü.)

KASIM 2000

ACKNOWLEDGEMENTS

The completion of a scientific study requires moral support as well as scientific and technical assistance. In this aspect, I would like to thank to all of my family for their encouragement and endless support throughout this study. I would like to express my sincerest gratitude to my supervisor, Prof. Derin Orhon for his creative and brilliant suggestions and positive support. For all times, I was able to receive valuable contributions and encouragement from Assoc. Prof. Seval Sözen. Assoc. Prof. Erdem Görgün has always been outstandingly supportive. Mr. Cengiz Baske and all the laboratory staff was incredibly gentle in providing me the excellent laboratory conditions. I should also thank to my friends who have provided the best kind of support I needed during this time.

June 2000 Ebru Avcıoğlu

TABLE OF CONTENTS

LIST OF TABLES

LIST OF FIGURES

Page No

Page No

NOTATION LIST

A_1, A_0 : Steady state and influent concentrations of volatile acids in Ghosh model
b_H : Endogenous decay rate coefficient in endogenous decay model [1/T]
b_H' : Endogenous decay rate coefficient in death-regeneration model [1/T]
b_{HD} : Anoxic endogenous decay rate coefficient [1/T]
b_{STOD} : Anoxic respiration rate coefficient for storage products [1/T]
f_E : Inert fraction of the biomass in endogenous decay model
f_E' : Inert fraction of the biomass in death-regeneration model
f_a : Activity coefficient
F/M : Food to microorganism ratio
G'_1 : Steady-state gas production rate from acid fermentation, [M/T]
i_{XB} : Nitrogen content of the active sludge fraction [M N/M COD]
k_d : Decay coefficient [1/T]
k_h : Rate constant for the hydrolysis of slowly biodegradable biomass [M COD/M COD.T]
k_{HD} : Anoxic maximum specific hydrolysis rate [M COD/M COD.T]
k_1 : Rate of denitrification during growth phase [M N/M VSS.T or M N/M COD]
k_2 : Rate of denitrification during hydrolysis phase [M N/M VSS.T or M N/M COD]
k_3 : Rate of denitrification during endogenous respiration phase [M N/M VSS.T or M N/M COD]
k_h :Hydrolysis rate constant [M COD/M COD.T or M COD/M VSS.T]
k_{hs} : Hydrolysis rate constant for S_H [M COD/M COD.T or M COD/M VSS.T]
K_{OH} : Half velocity coefficient for dissolved oxygen [M/L^3]
K_{NO} : Half-saturation constant for nitrate-nitrogen, [M NO_3^--N/L^3]
K_S : Half-saturation constant for the carbon source, [M COD/L^3]
K_{STO} : Half-saturation constant for X_{STO}, [M COD/L^3]
k_{STO} : Storage rate constant, [M COD/M COD.T]
K_X : Half velocity coefficient for hydrolysis [M COD/M VSS or M COD/M COD]
K_{XS} : Half velocity coefficient for hydrolysis of S_H [M COD/M VSS or M COD/M COD]
L : Substrate loading [M/L^3.T] or [L^3/T]
m : Maintenance coefficient for acid formers in Ghosh model [1/T]
$m_s(s)$: Consumption rate of substrate to supply catabolic energy for maintenance requirements
$M_0(s)$: A substrate function
NUR : Nitrate utilization rate [M N/L^3.T]
NUR_1 : Nitrate utilization rate exerted during growth on readily biodegradable substrate according to the model proposed by Marais and Ekama [M N/L^3.T]
OC_T : Total oxygen consumed [M O_2/L^3]
OUR : Oxygen utilization rate [M O_2/L^3.T]

OUR_1 : Oxygen utilization rate exerted during growth on readily biodegradable substrate according to the model proposed by Marais and Ekama [M $O_2/L^3.T$]

P' : Steady-state formation rate of acidogenesis product at given detention time [$M/L^3.T$]

q_D : Specific nitrate utilization rate [M N/M VSS.T]

$q_{obs}(s)$: Observed consumption rate of substrate

$q_{gr}(s)$: Growth related consumption rate of substrate

r^2 : Coefficient of determination

S_1 : Steady-state substrate concentration for acid formers [M/L^3]

S_H : Soluble slowly hydrolyzable organic matter concentration [M COD/L^3]

S_0 : Dissolved oxygen concentration [M O_2/L^3]

S_{OI} : Initial dissolved oxygen concentration [M N/L^3]

S_{NO} : Concentration of nitrate plus nitrite-nitrogen [mg N/L^3]

S_{NO3} : Initial nitrate-nitrogen concentration [M N/L^3]

S_{NO2} : Initial nitrite-nitrogen concentration [M N/L^3]

S_S : Readily biodegradable substrate concentration [M COD/L^3]

S_R : Bulk substrate removed [M COD/L^3]

X_E : Particulate inert endogenous mass concentration [M VSS/L^3 or M COD/L^3]

X_P : Inert particulate organics [M VSS/L^3 or M COD/L^3]

X_H : Active heterotrophic biomass concentration [M VSS/L^3 or M COD/L^3]

X_{HD} : Concentration of denitrifiers [M VSS/L^3 or M COD/L^3]

X_s : Slowly biodegradable particulate organic matter concentration [M VSS/L^3 or M COD/L^3]

X_{STO} : Organics stored by heterotrophs [M COD/L^3]

X_T : Total biomass concentation [M VSS/L^3 or M COD/L^3]

V : Digester volume [L^3]

V_{ml} : Biomass volume [L^3]

V_{ww} : Wastewater volume [L^3]

U_p, U_e : Substrate utilization coefficients for growth and energy respectively in Ghosh model

Y_D : Denitrification yield [M COD/M N]

Y_H : Heterotrophic yield coefficient [M COD/M COD]

Y_{HD} : Heterotrophic yield coefficient for denitrifiers [M COD/M COD]

Y_{STOD} : Anoxic storage yield [M COD/M COD]

$\hat{\mu}$: Maximum specific growth rate [1/T]

$\hat{\mu}_H$: Maximum growth rate for heterotrophic biomass [1/T]

μ_{HD} : Specific growth rate for denitrifiers [1/T]

$\hat{\mu}_{HD}$: Maximum growth rate for denitrifiers [1/T]

$\mu_{obs}(s)$: Observed growth at a specific rate

$\mu_{true}(s)$: True growth at a specific rate

$\mu_e(s)$: Negative endogenous growth at a specific rate

η_g : Correction factor for growth under anoxic conditions

η_h : Correction factor for hydrolysis under anoxic conditions

η_E : Correction factor for endogenous respiration under anoxic conditions

η_D : Correction factor for anoxic conditions

α : True product yield constant

α_i : True yield of acidogenesis

θ : Theoretical detention time [T]

θ_c : Critical detention time [T]

θ_x : Sludge age [T]

$\Delta_1 NO_3$: Mass of nitrogen utilized per unit volume during readily biodegradable substrate consumption, [M N/L^3]

ΔO : Mass of oxygen utilized per unit volume during readily biodegradable substrate consumption [M O_2/L^3]

EXPERIMENTAL ASSESSMENT OF HETEROTROPHIC ENDOGENOUS DECAY AND DENITRIFICATION KINETICS USING HYDROLYZED CARBON SOURCES

SUMMARY

Endogenous metabolism can be defined as the sum of all the chemical activities performed by organisms in the absence of utilizable extracellular materials serving as sources of energy and building stones for assimilation and growth. Water, molecular oxygen, and non-carbonaceous and non-nitrogenous mineral salts present in the external environment may participate in endogenous metabolism. Thus, endogenous metabolism can be viewed as all those chemical activities in the starving cell

Endogenous respiration acts as the controlling mechanism for sludge production and oxygen utilization in activated sludge systems. In aerobic sludge digestion, the only need for oxygen is to supply the endogenous respiration requirement. Extended aeration, which is an activated sludge process modification and is widely used in summer resort areas, operates in endogenous phase. In the post-denitrification compartment of the Bardenpho process commonly used for nutrient removal, the anoxic endogenous respiration is regarded as the sole carbon source. Despite the engineering significance of endogenous respiration, very limited information exists in the literature in terms of experimental assessment and modelling purposes.

The first part of the experimental studies covers the experimental assessment of endogenous respiration rate For this purpose, the method proposed by Marais and Ekama in 1976 was carried out by using activated sludge cultures acclimated to meat processing effluents, leather tanning effluents, and domestic wastewaters. The method is based on the monitoring of oxygen utilization rates (OUR) for 10 to 20 days. The most obvious deficiency associated with the current procedure was detected as imprecise OUR measurements due to the low initial electron acceptor utilization rates (in a range of 8 to 2 mg/l.hr) associated with endogenous respiration The observed data was scattered, exhibiting cyclic variations with remarkably low coefficients of determination (r^2). Hence, it was deduced that hydrolysis of adsorbed particulate organic matter was interfering with the OUR values associated with endogenous respiration. Since the application of the current practice led to results with insufficient accuracy and reliability, an alternative method was proposed to overcome the major drawbacks experienced with the current practice.

The proposed method aims to shift OUR measurements to the growth phase i.e., to replace $b_H X_H$ term with $\mu_H X_H$ term. Thus, the variation of X_H is reflected by providing a constant unlimited growth medium which would ensure a constant $\hat{\mu}_H$ level. The experimental process involves running of an aerobic "main reactor" and an aerobic "feed reactor" in parallel. The main reactor contains heterotrophic biomass which undergoes endogenous respiration during the whole experimental period. The feed reactor, on other hand, is put into operation whenever (preferably at

daily intervals) seeded with the biomass transferred from the main reactor. To ensure maximum growth conditions, the feed reactor is fed with a synthetic solution representing readily biodegradable substrate, of fixed quantity and composition together with the mixed liquor of a pre-selected volume, transferred from the main reactor. OUR in the feed reactor is monitored long enough to detect the corresponding initial plateau. The procedure outlined above is repeated after a time period t by transferring the pre-selected volume of mixed liquor to a second batch feed reactor and adding the same amount of substrate. Obviously, a lower initial OUR value is observed at time t due to the gradually decreasing activity of the biomass in the main reactor. After this procedure is repeated for 10 to 20 days, the slope of the plot of the initial plateau OUR values versus time yields the aerobic endogenous respiration rate, b_H. In the same manner, a main anoxic reactor may be run in parallel to an anoxic feed reactor and the same procedure can be carried out for the determination of anoxic endogenous rate coefficient, b_{HD}.

The proposed method was applied to domestic wastewaters. Five experimental sets were conducted at 20 ± 1°C and one experiment was performed at 10 ± 1°C. Based on these results the following conclusions can be drawn:

1. The arithmetic mean of the b_H value obtained at the end of five experimental runs was 0.08 1/day whereas an arithmetic average of 0.05 1/day was obtained for b_{HD} at 20 ± 1°C

2. At 10 ± 1°C, a value of 0.04 1/ day was obtained for both b_H and b_{HD} at the end of one experimental run

3. The statistical analysis of the experimental data indicates a high percentage of consistency between results obtained within each experimental set and among individual sets

4. At 20 ± 1°C an η_E value of 0.6 was assessed which yields to the practical conclusion that the anoxic digester tank volume has to be almost as twice as the aerobic tank volume to achieve the same treatment efficiency

When a comparison is established between the observed values of b_H and η_E with the values reported in the literature, it is evident that the values obtained in this study are appreciably lower than the values in the literature. This may either be attributed to the variations in wastewater characteristics or to the above mentioned limitations of the current method. Since, no procedures are present in the literature for the determination of b_{HD}, a comparison with the literature values would not be possible.

During the course of this study, the method was practiced only for domestic wastewaters. It should be emphasized that further experimental work is required both on domestic and industrial wastewaters at various temperatures to support the results of this study.

The second part of the experimental work is based on the investigation of primary sludge as a carbon source for denitrification. Domestic sewage is mainly composed of volatile fatty acids (VFA's), carbohydrates, alcohols, peptones and amino acids, which are biodegradable at different rates. VFA's are mainly associated with the hydrolysis of primary sludge, which itself is an internal source of organic carbon, and

are usually produced within wastewater treatment facilities. They are most beneficial in cases where suitable industrial wastes are not available containing adequate concentrations of short chain organic substrates. VFA's include formic, acetic, propionic, n-butyric, iso-butyric, n-valeric, isovaleric, and caproic acids. They are recognized as ideal substrates for *Acinebacter* species and denitrifiers, therefore, employed in biological nutrient removal processes (BNR) to achieve high rates of phosphorus removal and denitrification.

Biological sludge hydrolysis is gaining popularity in the recent years. The process makes it possible to increase biological nutrient removal by at least 10-15 %. It increases the potential of process stability and flexibility through production and storage of easily degradable organics and subsequently dosing when needed in the process. Making the most of the fermentation process at the wastewater treatment plant may allow reactor volumes to be reduced and increase the treatment capacity without requiring much more space. It is also cost effective as compared with the addition of chemical materials, such as methanol, as supplemental carbon sources.

In order to assess the performance of primary sludge as a carbon source, denitrification rates obtained with primary sludge were compared with the rates obtained with acetate, which is accepted as a well-defined external carbon source. For this purpose, batch experiments were conducted for equivalent initial S_S concentrations of both substrates in parallel tests.

Filtered primary sludge and acetate yielded similar denitrification rates (k_1) indicating that primary sludge proved to be an efficient carbon source as acetate. This observation agrees well with most of the literature findings. It should also be noted that observed denitrification rates for both filtered primary sludge and acetate are relatively higher than literature values. This might be due to the expression of denitrification rates on the active biomass (X_H) basis rather than volatile suspended solids (VSS) as reported in the literature.

Experimental data obtained from denitrification tests for acetate and filtered primary sludge were simulated by using two models, namely Endogenous Decay Model (EDM) and, a more recent one, Activated Sludge Model No 3 (ASM3). ASM3 involves mechanisms such as storage and respiration of storage products both of which are defined as energy consuming processes. These two processes have not been included in the prior model structures such as EDM and ASM1. Storage process involves the conversion of S_S into the form of cell internal storage products referred as X_{STO}, which includes poly-hydroxy-alkanoates (PHA), glycogen, etc. Respiration of storage products involves the decay of storage products, analogous to endogenous respiration. This model assumes that X_S is converted to S_S at a comparably higher rate as compared to growth on X_{STO}, thus, in contrast to EDM, hydrolysis is not a rate-limiting mechanism.

The experimental electron acceptor utilization profiles, for both acetate and filtered primary sludge are found to be compliant with the model simulation of EDM. The maximum growth rate ($\hat{\mu}_H$) and anoxic yield (Y_{HD}) values for acetate are obtained as 6 1/d and 0.58 g COD/g COD respectively. A range of $\hat{\mu}_H$ (6-6.5 1/d) and Y_{HD} (0.62-0.66 g COD/g COD) values used for filtered primary sludge can be explained by the variable content and/or fractions of filtered primary sludge components

produced in a settling tank rather than a steady-state fermentor. $\hat{\mu}_H$ values considered for acetate and filtered primary sludge, both of which contain acetate, are consistent with each other. These values can also be regarded as compatible with the default value reported in EDM (6 1/d) for domestic wastewaters in which acetate, again, forms a substantial fraction of S_S. Y_{HD} values adopted in the model are reasonably lower than the default value of Y_H (0.67 g COD/g COD), stated in EDM for domestic wastewaters. Literature findings also support the lower magnitudes of the Y_{HD} values as compared to Y_H. On the other hand, the second phase of the electron acceptor utilization profile (k_2) for filtered primary sludge was found to be too high to be associated with endogenous respiration in EDM. This finding was justified by the presence of hydrolyzable soluble COD fraction, S_H, within the structure of the primary sludge besides the readily biodegradable portion, S_S. This situation has been validated by the good correlation of experimental data with the model simulation.

The experimental results' compliance with the model simulation run with a range of meaningful parameter values show that the processes and parameters within the structure of EDM are proficient in explaining the behaviour of acetate and filtered primary sludge as carbon sources for denitrification.

While an increased number of processes are considered in ASM3, the model simplifies the definition of the readily biodegradable content, S_S, by assessing this fraction simply by filtration instead of employing the respirometric analysis method as adopted in EDM. This definition brings the inclusion of the slowly hydrolyzable fraction, S_H, defined in EDM, within the content of S_S. Thus, the S_S content of systems composed of more than one fraction of COD, such as primary sludge, becomes greater in magnitude than the S_S fraction considered in EDM.

The experimentally obtained electron acceptor utilization profiles for acetate and filtered primary sludge exhibit quite similar trends. However, during the simulation of ASM3, it became apparent that the model and experimental fit could be provided by the use of different values of parameters associated with storage. For acetate, the anoxic storage yield (Y_{STOD}) was assessed as 0.63 g COD/g COD while for filtered primary sludge Y_{STOD} assumed values between 0.78 g COD/g COD and 0.8 g COD/g COD. Although, Y_{STOD} value determined for filtered primary sludge is in good agreement with the default value of Y_{STOD} (0.8 g COD/g COD) as stated in ASM3, it was found to be much lower for acetate. On the other hand, for acetate the storage rate was assessed as 12 g COD/g CODd and for filtered primary sludge, the rates of storage (k_{STO}) varied between 16 and 20 g COD/g CODd respectively. Hence, the storage rates compliant with the experimental data were quite high for both cases, as compared with the default value for k_{STO} as 5 g COD/g COD. Based on these observations, it can be stated that, although acetate and primary sludge are similar in content, which is also reflected in similar experimental behaviour, the model parameters associated with storage do not exhibit the expected consistency as already observed in EDM, mainly due to the COD fractionation approach adopted in ASM3.

The model simulation studies for ASM3 has provided evidence that monitoring of the storage products should be an essential part of the experimental studies. Based on this consideration, an experimental database should be formed towards the assessment of kinetic and stochiometric parameters associated with storage.

İÇSEL SOLUNUM MEKANİZMASI VE DENİTRİFİKASYON KİNETİĞİNİN HİDROLİZ KAYNAKLI KARBON TÜRLERİ İÇİN BELİRLENMESİ

ÖZET

İçsel solunum metabolizması, asimilasyon ve büyüme için gerekli enerji kaynağı ve yapı taşı olarak görev yapan dış kaynakların yokluğunda organizma tarafından sürdürülen tüm kimyasal aktiviteler şeklinde tanımlanabilir. Dış çevrede bulunan su, oksijen, ve karbon ve azot kaynaklı olmayan mineral tuzlar içsel solunum mekanizmasına katkıda bulunabilirler. Böylelikle içsel solunum metabolizması, aç hücredeki kimyasal aktiviteler şeklinde özetlenebilir.

İçsel solunum, aktif çamur sistemlerinde oluşan çamur miktarı ve elektron alıcısı ihtiyacını belirlemesi açısından önemli bir kontrol mekanizmasıdır. Çamur arıtımında yaygın olarak kullanılan aerobik çamur çürütmesi işleminde gerekli oksijen miktarı, tamamıyla içsel solunum ihtiyacından kaynaklanmaktadır. Özellikle yazlık yerleşim bölgelerinde yaygın olarak kullanılan ve bir aktif çamur modifikasyonu olan uzatmalı havalandırma prosesi de içsel solunum fazında çalıştırılmaktadır. Biyolojik azot arıtımında sıkça kullanılan Bardenpho prosesinin post denitrifikasyon ünitesinde karbon ihtiyacı, içsel solunum mekanizması sonucu salınan karbon ile karşılanmaktadır. Görüldüğü gibi içsel solunum mekanizması mühendislik uygulamaları açısından büyük önem taşımasına rağmen literatürde bu konuda hem deneysel belirleme hem de modelleme uygulamaları açısından yeterli bilgiye rastlanmamaktadır.

Bu tez çalışmasının ilk araştırma konusunu içsel solunum katsayısının deneysel olarak belirlenmesi oluşturmaktadır. Bu amaçla, öncelikle literatürde mevcut ve 1976 yılında Marais ve Ekama tarafından önerilen deneysel yöntem uygulanmıştır. Bu yöntem, içsel solunum fazında çalıştırılan kesikli bir aktif çamur sisteminde 10 ila 20 gün boyunca oksijen tüketim hızı (OTH) ölçümlerinin izlenmesine dayanmaktadır. Yöntem, et işleme endüstrisi ve deri endüstrisi atıksularına, ve evsel kökenli atıksulara uygulanmış ve bu uygulama sonucunda gözlenen en büyük aksaklık içsel solunum fazında elde edilen oldukça düşük (2-8 mg O_2/l.saat) OTH değerlerinin mevcut oksijen metre teknolojisi ile bu yöntemin gerektirdiği titizlikte ölçülememesi olmuştur. Elde edilen deneysel veriler gözlenmesi beklenen lineer trende uygun olmayarak, önemli ölçüde salınımlar göstermiştir. Buna bağlı istatistiksel analiz sonuçlarının korelasyon yüzdesi ise oldukça düşüktür. Deney başlangıcında yavaş ayrışan partiküler organik maddenin hidrolizine bağlı olarak daha yüksek nümerik değerler elde edilmiştir. Bu değerler, içsel solunum fazında elde edilen daha düşük değerler ile uyum sağlamadığı için, gözönüne alınan süreye bağlı olarak birbirinden farklı içsel solunum hızı (b_H) değerleri elde edilmiştir.

Bu gözlemlere dayanarak, mevcut yöntemin kullanımı ile elde edilen deney sonuçlarının bilimsel bir araştırmanın gerektirdiği güvenilirlikte olmadığı sonucuna varılmıştır. Bu noktadan hareketle, alternatif bir yöntem arayışına gidilmiş ve bu tez kapsamında yeni bir yöntem önerilmesi uygun görülmüştür.

Önerilen yöntemin temeli mevcut yöntemin getirdiği aksaklıkları gidermeye yöneliktir. Yöntemin amacı, kısıtlayıcı olmayan bir çoğalma ortamı sağlanması ve bu şekilde biyokütlenin aktivitesindeki azalımın içsel solunuma oranla oldukça yüksek bir ölçekte izlenmesidir. Deneysel yöntem, deney süresi boyunca aerobik fazda bir 'ana' bir de 'besleme' reaktörü işletilmesini içerir. Ana reaktör deney süresi boyunca içsel solunum fazında çalıştırılmaktadır. Besleme reaktörü ise istenilen aralıklarda (tercihen günlük) işleme konur ve ana reaktörden transfer edilen biyokütle ile beslenir. Maksimum büyüme koşullarını sağlamak amacıyla, besleme reaktörüne miktarı önceden belirlenmiş kolay ayrışabilir nitelikte substrat ile ana reaktörden aktarılan sabit hacimde askıda katı madde eklenir. Besleme reaktöründe OTH değerleri yaklaşık sabit bir değerin gözlendiği ilk plato boyunca izlenir. Aynı prosedür 't' süresi sonunda kurulacak bir besleme reaktörüne yine ana reaktörden transfer edilen sabit hacimde askıda katı madde, ve sabit miktarda kolay ayrışabilir nitelikli substrat eklenmesiyle tekrarlanır. 't' süresi sonunda gözlenecek ilk OTH plato değeri biyokütlenin azalan aktivitesine bağlı olarak deney başlangıcında elde edilen plato değerinden daha düşük olacaktır. Deney prosedürünün 10 ila 20 gün boyunca tekrarı ile elde edilecek ilk platoya ait OTH değerleri zamana karşı çizildiğinde, grafiğin eğimi aerobik içsel solunum hızı olan b_H değerini verecektir. Aynı yöntem çerçevesinde, anoksik ortamda çalıştırılacak ana ve besleme reaktörlerinden elde edilecek nitrat tüketim hızı (NTH) profillerinin benzer şekilde değerlendirilmesiyle anoksik içsel solunum katsayısı (b_{HD}) elde edilebilecektir.

Önerilen yöntem evsel atıksulara aklime edilmiş aktif çamur kültürleri üzerinde uygulanmıştır. 20 ± 1° C'de beş set ve 10 ± 1° C'de bir set deney yapılmıştır. Elde edilen sonuçlar aşağıdaki şekilde özetlenebilir:

1. b_H için beş set deney sonucu elde edilen aritmetik ortalama 0.08 1/gün, aynı setlerden elde edilen b_{HD} değerlerinin aritmetik ortalaması ise 0.05 1/gün'dür.

2. 10 ± 1° C'de yapılan tek deneme sonucunda b_H ve b_{HD} değerleri için 0.04 1/gün değeri elde edilmiştir

3. Deneysel verilerin istatistiki değerlendirmesi deney setleri içindeki ve aynı sıcaklıkta yapılan farklı deney setleri arasındaki tutarlılığın oldukça yüksek olduğunu göstermektedir

4. 20 ± 1° C'de anoksik ve aerobik elektron alıcısı tüketim hızlarının karşılaştırması sonucu elde edilen η_E faktörü 0.6 olarak bulunmuştur. Bu değerin pratikteki anlamı, aynı verimi elde etmek için gereken anoksik çürütme tank hacminin gerekli aerobik tank hacminin yaklaşık iki katı olması gerektiğidir

Elde edilen b_H ve η_E değerlerinin literatürdeki değerlerden oldukça düşük olduğu gözlenmiştir. Bu farkın atıksu özelliklerindeki değişikliklerden ya da literatürde mevcut yöntemin uygulanması sonucu ortaya çıkan ve yukarıda sözü geçen aksaklıklardan kaynaklandığı düşünülmektedir. Anoksik içsel solunum katsayısı (b_{HD}) için ise, literatürde bu katsayı için bir belirleme yöntemi bulunmaması nedeniyle, bir karşılaştırma yapmak mümkün olamamaktadır.

Bu tez çerçevesinde önerilen aerobik ve anoksik heterotrofik içsel solunum katsayısının bulunmasına yönelik yöntem yalnızca evsel nitelikli atıksulara aklime olmuş biyokütle için uygulanmıştır. Elde edilen sonuçları desteklemesi açısından,

yöntemin değişik sıcaklıklarda hem evsel hem de endüstriyel nitelikli atıksulara aklime olmuş biyokütle üzerinde uygulanmasında yarar görülmektedir.

Deneysel çalışmanın ikinci aşamasını evsel kaynaklı ön çöktürme çamurunun karbon kaynağı olarak kullanıldığı ortamlarda denitrifikasyon kinetiğinin incelenmesi oluşturmaktadır. Evsel kaynaklı ön çöktürme çamuru genel olarak uçucu yağ asitleri, karbonhidratlar, alkoller, peptonlar ve aminoasitleri içerir. Uçucu yağ asitlerinin oluşumu için ön çöktürme çamurunun hidrolizi yaygın olarak kullanılan bir yöntemdir. Bu asitlerin tesis içinde üretilmesi yeterli miktarda kısa zincirli organik substrat içeren endüstriyel atıksuların bulunmadığı durumlarda daha büyük avantaj sağlamaktadır. Uçucu yağ asitleri başlıca asetik, propionik, n-bütirik, izo-bütirik, n-valerik, izo-valerik ve kaproik asitleri içerir. Fosfor ve azot gideren bakteriler için ideal substrat olarak kabul edilmeleri nedeniyle uçucu yağ asitleri biyolojik nütrient giderimi proseslerinde yaygın olarak kullanılmaktadırlar.

Biyolojik çamur hidrolizi son yıllarda pratikte sıkça uygulanmaktadır. Bu prosesin biyolojik nütrient giderimini % 10 ila 15 oranında artırdığı düşünülmektedir. Kolay ayrışabilir organik maddenin depolanabilmesi ve gerektiği durumlarda kullanılabilmesi proses stabilitesini önemli ölçüde artırmaktadır. Bu ürünlerin tesis içinde üretilmesi metanol gibi dışarıdan eklenen karbon kaynaklarının maliyeti ile karşılaştırıldığında avantaj sağlamaktadır. Ayrıca bu yol ile, tesiste gerekli reaktör hacimleri azalacak ve arıtma kapasitesi hacim artışı olmaksızın artacaktır.

Ön çöktürme çamurunun denitrifikasyon verimini araştırmak amacıyla bir ön çöktürme tankının geri devir hattından elde edilen çamur ile literatürde kolay ayrışabilir karbon kaynakları arasında en iyi örneklerden biri olarak kabul edilen asetat, denitrifikasyon hızları bazında karşılaştırılmıştır. Karşılaştırma amacıyla yapılan paralel kesikli deneylerde ortama önceden seçilen ve eşit miktarda kolay ayrışabilir KOİ eşdeğeri substrat eklenmiştir. Denitrifikasyon hızlarının yanısıra kolay ayrışabilir substrat konsantrasyonu (S_s) da denitrifikasyon deneylerinin verim açısından değerlendirilmesinde incelenmiştir.

Deneysel çalışmalar sonucu süzülmüş ön çöktürme çamuru ve asetat ile elde edilen denitrifikasyon hızlarının (k_1) birbirine oldukça yakın olduğu görülmüştür. Bu yöndeki bulgulara literatürde de sıkça rastlanmaktadır. Ancak elde edilen denitrifikasyon hızları literatürde rastlanan değerler ile karşılaştırıldığında daha yüksektir. Bunun nedeni olarak denitrifikasyon hızlarının literatürde olduğu gibi uçucu askıda katı madde bazında değil biyokütlenin aktif fraksiyonu bazında ifade edilmesi gösterilebilir.

Asetat ve ön çöktürme çamurunun karşılaştırılması ile elde edilen deneysel veri sonuçları için, literatürde sıkça kullanılan İçsel Solunum Modeli (İSM) ve daha yakın bir tarihte sunulmuş olan Aktif Çamur Modeli No 3 (ASM3) ile simülasyon çalışmaları yapılmıştır. ASM3, yapısında İSM'den farklı olarak, depolama ve depolanan ürünlerin solunumu olarak adlandırılan ve enerji tüketen iki farklı proses içermektedir. Depolama prosesi, kolay ayrışabilir organik maddenin X_{STO} olarak tanımlanan hücre içi ürünlere dönüştürülmesini kapsar. Bu ürünlerin genel içeriği polihidroksialkanlar (PHA) ve glikojendir. Depolanan ürünlerin solunumu ise içsel solunum mekanizmasına benzer şekilde depolanmış ürünlerin ayrışmasını içerir. ASM3 modelinde yavaş ayrışan partiküler maddenin hidrolizi X_{STO} üzerindeki

çoğalma hızına oranla daha hızlı gerçekleşmekte, bu nedenle İSM'nin aksine, hidroliz kademesi hız kısıtlayıcı adım olarak kabul edilmemektedir.

Deneysel olarak elde edilen verilerin, içsel solunum modeli simülasyon sonuçları ile uyum içinde olduğu görülmüştür. Model çalışmaları sonucunda asetat için maksimum çoğalma hızı ($\hat{\mu}_H$) değeri 6 1/gün ve anoksik dönüşüm oranı (Y_{HD}) 0.58 g KOİ/g KOİ olarak elde edilmiştir. Süzülmüş ön çöktürme çamuru için ise $\hat{\mu}_H$ için 6 ile 6.5 1/gün, Y_{HD} için ise 0.62 g KOİ/g KOİ ile 0.66 g KOİ/g KOİ aralığında değerler kullanılmıştır. Bu değerlerin ön çöktürme çamuru için değişkenlik göstermesinin, ön çöktürme tankının işletiminde görülebilecek istikrarsızlığa ve/veya ön çöktürme çamurunun içeriğinde oluşabilecek değişikliklere bağlı olduğu düşünülmektedir. Elde edilen $\hat{\mu}_H$ değerleri, içsel solunum modelinde evsel atıksu için öngörülen $\hat{\mu}_H$ değerine (6 1/gün) oldukça yakındır. Y_{HD} değerleri ise aynı modelde yine evsel atıksu için öngörülen Y_H değerinden (0.67 g KOİ/g KOİ) daha düşüktür. Literatürdeki bulgular da anoksik dönüşüm oranının aerobik dönüşüm oranına göre daha düşük olduğu yönündedir. Asetatın evsel atıksu içindeki kolay ayrışabilir organik madde fraksiyonunun önemli bir kısmını oluşturduğu düşünülürse, simülasyon sonuçlarının içsel solunum modelinde öngörülen değerler ile tutarlı olduğu söylenebilir. Öte yandan, süzülmüş ön çöktürme çamuru için elektron alıcısı tüketim profilinin ikinci fazında elde edilen hızın içsel solunum hızına oranla daha yüksek olduğu, bu bulgunun ise çamur yapısında mevcut olabilecek yavaş hidroliz olabilen fraksiyonun (S_H) varlığıyla açıklanabileceği düşünülmüştür. İçsel solunum modeli bu bağlamda değerlendirildiğinde, deney sonuçlarının model ile son derece uyumlu olduğu görülmüştür.

Elde edilen sonuçlar gözönüne alındığında, içsel solunum modeli yapısındaki prosesler ile, birbirine benzer nitelikte iki karbon kaynağı için birbiri ile uyumlu değerlere sahip parametreler kullanılarak, elektron alıcısı tüketim profilleri açıklanabilmektedir.

ASM3, model yapısındaki proses sayısını artırıken KOİ fraksiyonları tanımına basitlik getirmektedir. İçsel solunum modelinde S_S fraksiyonu respirometrik yöntemlerle belirlenirken, ASM3, 0.45 μm'den süzülmüş miktarın inert fraksiyon dışındaki kısmını kolay ayrışabilir organik madde olarak yorumlamaktadır. Bu kapsamda, içsel solunum modelinde yavaş hidroliz olabilen fraksiyon, S_H, olarak yorumlanan kısım ASM3'te kolay ayrışabilir KOİ olarak kabul edilmekte ve S_S içeriği ön çöktürme çamuru gibi birden fazla KOİ fraksiyonu içeren sistemler için, içsel solunum modeline göre daha yüksek olmaktadır. Bu çerçevede, asetat ve süzülmüş ön çöktürme çamuru için deneysel elektron alıcısı tüketim profilleri benzerlik gösterirken, ASM3 simülasyonunda kullanılan, depolama prosesi için anoksik dönüşüm oranı, Y_{STOD}, ve depolama hızı, k_{STO} gibi profile en fazla etkisi olan parametrelerin değerleri, S_S tanımındaki farklılıktan dolayı değişiklik göstermektedir. Buna göre, asetat için Y_{STOD} değeri 0.63 g KOİ/g KOİ iken süzülmüş ön çöktürme çamuru için bu değer 0.78 g KOİ/g KOİ ile 0.8 g KOİ/g KOİ arasındadır. Ön çöktürme çamuru için bulunan değerler ASM3'te öngörülen Y_{STOD} değerlerine uyum sağlamaktadır. Öte yandan, asetat için uygun depolama hızı değeri 12 g KOİ/g KOİgün iken süzülmüş ön çöktürme çamuru için elde edilen hızlar 16 ile 20 g KOİ/g KOİgün arasında değişiklik göstermektedir. Her iki durumda da depolama hızları modelde öngörülen depolama hızına göre (5 g KOİ/g KOİgün) oldukça yüksektir. Deney sonuçlarından da görüldüğü gibi içeriğinde asetatın da

yeraldığı ön çöktürme çamuru denitrifikasyon için karbon kaynağı olarak değerlendirildiğinde asetat ile benzer performans göstermiştir. Ancak, her iki karbon kaynağına ait deney sonuçları ASM3 için simüle edildiğinde önemli model parametrelerinin içsel solunum modelinde gözlenenin aksine, asetat ve çamur için birbirleriyle tutarlı olmadığı görülmüştür.

ASM3 için yapılan simülasyon çalışmalarından da görüldüğü gibi depolama ürünlerinin izlenmesi model yorumu açısından büyük önem taşımaktadır. Bu çerçevede oluşturulacak bir veri tabanıyla, depolama prosesiyle ilgili stokiometrik ve kinetik büyüklüklerin belirlenmesi de mümkün olacaktır.

CHAPTER 1 INTRODUCTION

1.1 Significance of the Study

The growing demand for water sources throughout the world has generated an equivalent need for effective water and wastewater management strategies. These strategies require a thorough understanding of the principles of treatment processes and operations. Improved knowledge of mechanisms involved in flow-schemes is a prerequisite for successful design.

Among other pollutants, control of nitrogen has been identified as an important environmental activity because of its adverse effects on aquatic systems. Among other methods of treatment (chemical, physical), biological removal of nitrogen has become increasingly popular due to its operational and economical feasibility. Denitrification is the second step in the removal of nitrogen after nitrification process in which nitrogen in raw wastewater is converted to ammonia-nitrogen. In this study, it is intended to provide the conceptual basis for the design of nitrogen removal systems employing carbon sources including products of endogenous respiration and fermentation.

Endogenous respiration acts as the controlling mechanism for sludge production and oxygen utilization in activated sludge systems. In aerobic sludge digestion, the only need for oxygen is to supply the endogenous respiration requirement. Extended aeration, which is an activated sludge process modification and is widely used in summer resort areas, operates in endogenous phase. In the post-denitrification compartment of the Bardenpho process commonly used for nutrient removal, the anoxic endogenous respiration is regarded as the sole carbon source. Despite the engineering significance of endogenous respiration, very limited information exists in the literature in terms of experimental assessment and modelling purposes.

Recent research has demonstrated that substantial improvement may be realized by the use of primary sludge as a carbon source for denitrification. Since hydrolysis of

primary sludge is achieved within treatment plant facilities, investment costs are remarkably reduced. This process can also be regarded as cost effective compared to external supplies of carbon. In the mean time, further research has to be conducted in terms of process efficiency and reliability.

Experimental research is an essential part of the design strategy for water and wastewater treatment facilities. This study aims to generate accurate data towards successful design of activated sludge processes.

1.2 Objective and Scope of the Study

The first part of the experimental studies covers the assessment of the endogenous respiration rate by the current method available in the literature. The current experimental method is criticized for its deficiencies by the presentation of experimental results for domestic, meat processing and leather tanning effluents. A new respirometric method is introduced for the assessment of aerobic and anoxic endogenous respiration rates. The proposed method is evaluated in terms of experimental results for domestic wastewaters. An evaluation is also performed with the values reported in the literature. Additionally, a comparison of aerobic and anoxic rates of electron acceptor utilization is established to investigate the possibility of applying anoxic sludge stabilization as an alternative to aerobic stabilization, the former having apparent economic advantages as commonly cited in the literature.

The second period of the experimental studies involves evaluating the performance of primary sludge as a carbon source for denitrification. Experimental assessment is obtained by performing parallel batch tests where the rates of denitrification obtained with primary sludge are compared with acetate, which is accepted in the literature as a well-defined external carbon source. The experimental and model compliance is investigated by employing two mathematical models, namely Endogenous Decay Model and Activated Sludge Model No 3. Since Activated Sludge Model No 3 introduces processes and parameters, which have not been included in the prior model structures, special emphasis will be paid for the evaluation of these concepts.

CHAPTER 2 FUNDAMENTAL BASIS OF MICROBIAL DECAY AND BIOLOGICAL DENITRIFICATION

2.1 Microbial Decay

Microbial decay is the term used to represent loss of cell mass. It incorporates a large number of mechanisms including endogenous metabolism, death, predation, and lysis. Among these mechanisms, predation is the feeding of predators on bacteria. The efficiency of growth of predators upon bacteria is similar to that of bacteria upon the original substrate. A reduction in microbial mass results even though new predators are being formed. Cell lysis is the leakage of internal contents of microorganisms into the medium as they die. After lysis only the remaining cell wall is large enough to be measured as insoluble cell mass. Due to its significance, endogenous metabolism will be studied in detail in the following section. In the microbiological literature, the maintenance concept is also used as another description of microbial behaviour. There is a growing consensus that from a modelling and measuring point of view, both maintenance and endogenous concepts are able to represent this specific process behaviour. Therefore in this chapter, it has been decided to investigate microbial decay under two headlines as endogenous respiration and energy of maintenance.

Microbial decay is defined by a first order rate expression with respect to the biomass concentration:

$$\frac{dX_T}{dt} = -k_d X \tag{2.1}$$

where the units for k_d and X_T are generally expressed as:

k_d = Decay coefficient [1/day],

X_T= Total biomass concentation [mg VSS/l].

Most work dealing with the microbial decay has not considered the viability of the culture but has instead measured the overall decay coefficient by the decrease in the mixed liquor volatile suspended solids concentration (VSS).

Table 2.1 contains k_d values for pure and mixed cultures. For pure cultures it can be seen that the species of organisms influence the value of k_d. The carbon source also affects k_d probably because of the effect it has upon the type of endogenous reserves in the cells. It should also be emphasized that there is a noticeable difference between values for pure and mixed cultures such that the values obtained with mixed cultures are often an order of magnitude lower than those obtained with pure cultures (Grady and Lim, 1980).

Table 2.2 presents k_d values for mixed cultures growing on various wastewaters. Most of the values in the table are similar to those of the slowly growing mixed cultures in Table 2.1. Although Barnard (1975) has concluded that for most wastewater treatment systems k_d values lie around 0.05 1/day, it can be seen from Table 2.2 that this is true for domestic sewage but k_d values vary significantly for other wastewaters. The table also reveals that, k_d value for the biological nutrient removal process (BNR) as 0.063 1/day, was lower than in the fully aerobic process, 0.110 1/day, indicating that decay occurs at a much lower rate in the anoxic and anaerobic zones of the BNR process.

Table 2.1 Typical values of k_d for cultures grown on simple substrates (Grady and Lim, 1980)

Organism	Substrate	k_d (1/day)	Reference
A. aerogenes	Glucose	1.920	Topiwala and Sinclair, 1971
A. aerogenes	Glycerol	1.008	Pirt, 1965
A. cloacae	Glucose	0.984	Pirt, 1965
E. coli	Glucose	0.672	Marr et al., 1963
P. fluorescens	Glucose	2.880	Mennett and Nakayama, 1971
P. fluorescens	Glucose	2.640	Palumbo and Witter, 1969
Mixed culture	Glucose	0.456	Chiu et al., 1972
Mixed culture	Glucose	0.552 (30°C)	Muck and Grady, 1974
Mixed culture	Glucose	0.0864	Stack and Conway, 1959
Mixed culture	Sucrose and Peptone	0.0432	Sherrard, 1971
Mixed culture	Peptone	0.0792	Sherrard, 1971
Mixed culture	Skim milk	0.0456	Gram, 1956

k_d values determined by Koers as shown in Table 2.3 at 20 and 25°C are close to those reported in Table 2.2 for domestic wastewaters. At lower temperatures, there is a corresponding decrease in k_d values. Values determined by Jenkins are somewhat higher at the low temperature range studied and somewhat lower at 20°C.

Table 2.2 Typical values of k_d for cultures grown on wastewaters (Grady and Lim, 1980)

Wastewater Type	k_d (1/day)	Reference
Domestic sewage	0.048 – 0.0696	Lawrence and McCarty, 1970
Domestic sewage	0.063 (BNR process) 0.110 (Aerobic process)	McClintock et al, 1992
Poultry processing	0.720	Jorden et al., 1971
Pulp and paper	0.1992	Kormanik, 1972
Pulp and paper	0.036	Gray et al., 1973
Refinery	0.240	Kormanik, 1972
Shrimp processing	1.608	Horn and Pohland, 1973
Soybean	0.144	Jorden et al., 1971
Textile	0.720 – 1.200	Domey, 1973
Textile	0.0336	Mahloch et al., 1974
Thiosulfate	0.01008 – 0.01992	Kreye et al., 1974
Vegetable and fruit processing	0.0288 – 0.1896	Gray et al., 1973
Whey, cottage cheese manufacturing	0.0552	Quirk and Hellman, 1972

Table 2.3 k_d values with reported temperature and sludge age (Anderson and Mavinic, 1992)

Temperature (°C)	Sludge Age (d)	k_d (1/day)	Reference
25	10	0.055 – 0.076	Koers, 1979*
20	12.5	0.038 – 0.070	
15	16.7	0.027 – 0.044	
10	25	0.014 – 0.020	
5	50	0.007 – 0.010	
20	20	0.0229	Jenkins, 1988**
	15	0.0132	
	10	0.0277	
10	20	0.0130	
	15	0.0156	
	10	0.0135	

* High rate sludge

** Extended aeration biological nutrient removal sludge

2.1.1 Concept of endogenous respiration

Endogenous metabolism can be defined as the sum of all the chemical activities performed by organisms in the absence of utilizable extracellular materials serving as sources of energy and building stones for assimilation and growth. Water, molecular oxygen, and non-carbonaceous and non-nitrogenous mineral salts present in the external environment may participate in endogenous metabolism. Thus, endogenous metabolism can be viewed as all those chemical activities in the starving cell (Lamanna , 1963).

Organisms deprived of nutrients become dependant exclusively upon internal resources for maintaining their lives. At the moment of deprivation, the cell finds itself with a complement of enzymes for access to endogenous substrates.

Ribbons and Dawes studied some of the factors that affected the endogenous metabolism of two strains of bacteria, namely, *Sarcina Lutea* and *Escherichia coli.* They observed that the respirable endogenous reserves of *S. lutea* vary with the composition of the growth medium. Peptone grown cells oxidize their amino acid and peptide pools during starvation: lipid and carbohydrate content of the cells remain constant. Glucose-peptone grown cells additionally oxidize polyglucose with amino acid pool depletion and ammonia release. They also investigated the patterns of endogenous respiration of *E. coli* harvested from glucose-ammonium salts, glucose, tryptone, and tryptone media with respect to glycogen utilization and ammonia release. Glucose-ammonium salts and glucose media yield stationary phase cells containing glycogen, which is initially utilized as an endogenous substrate with ammonia release after glycogen depletion. Tryptone grown cells release ammonia immediately on starvation, but they contain no glycogen. Only anaerobically grown cells release carbon dioxide and hydrogen in the process.

Studies about the chemical changes occuring in the cells or in the supernatant fluid of Pseudomonas by Campbell et al. revealed the revolution of ammonia during endogenous respiration. According to the experiments of Kjeldgaar and of others, the ratio between the amount of cellular RNA and the rate of protein synthesis is relatively constant in *Pseudomonas aeruginosa* which is an obligate aerobic bacteria. Therefore, in starving cells where there is no net synthesis of protein, the level of cellular RNA and, in particular, ribosomal RNA is in excess of the requirements of

the cell during this period. RNA was strongly implicated as a major endogenous substrate but it was found under some circumstances that protein was also used (Lamanna , 1963).

The endogenous respiration rate of activated sludge can be defined in operational terms as the oxygen consumption rate in the absence of substrate from external sources (Spanjers et al., 1998). By this definition, endogenous respiration not only includes the decay of bacteria but also oxygen consumption by protozoa. In most experiments with protozoans, motility was observed as the evidence of viability. Hutchens et al., (1948) observed in *Chilomonas* that 55 per cent of the acetate utilized during the growth of the organism is assimilated to form a polymer indistinguishable from β-amylose. Under conditions of starvation, that is after washing and suspending the organisms in buffered salts, the amount of carbohydrate reserve decreased approximately 70 per cent in a four hour period (Mast and Pace, 1933): the polymer is apparently hydrolyzed and then metabolized to an easily oxidizable material. Oxidation is apparently through the Kreb's cycle since malonate inhibits the endogenous metabolism of the organism (Holz, 1954). As the age of *Chilomonas* culture increases, the rate of endogenous metabolism of the cells decreases: the highest endogenous activity is observed during the early logarithmic phase of growth and decreases by almost 70 per cent as the cell reaches the stationary phase of growth (Hutchens, 1941). Hunter and Lee (1962) found that the endogenous metabolism of the euglenid organism, *Astasia*, remains the same when cells are cultured in media of wide pH variations. In contrast to the situation with *Chilomonas*, the endogenous respiration of *Tetrahymena* increases at a rate almost parallel to the increase in growth of the culture, at least until the initiation of the stationary phase of the growth (Ormsbee, 1942). Warren (1960) has shown that the endogenous metabolism of *Trypanosoma cruzi* also increases with the age of the culture. Brachet (1955) has suggested that in *Amoeba proteus* glycogen stores serve as reserve material, but in the soil amoeba, *Acanthamoeba*, lipid serves this function; glucose, although utilized by cell free extracts, does not alter the rate of endogenous metabolism (Neff et al., 1958) (Lamanna , 1963).

Studies on endogenous metabolism bring a number of queries such as the nature of the endogenous reserves, their variation with environmental conditions, their biosynthesis and turnover, and their subsequent dissimilation under conditions of

nutrient deficiency. The relation of endogenous metabolism to the survival of vegetative (metabolically active) forms has not been well documented. In an investigation of the survival characteristics of *Aerobacter aerogenes*, Strange, Dark and Ness showed that profound changes in chemical composition could occur without appreciable loss of viability, and demonstrated that the presence of glycogen in the cell favors survival. On the other hand with *Pseudomonas aeruginosa*, an organism which does not reserve carbohydrate, Campbell has shown that loss of protein and RNA occurs. Almost 40 per cent of the RNA of *Escherichia coli* may be released without the loss of viability (Lamanna , 1963).

In the literature, basically, two models are utilized to describe endogenous metabolism, namely, endogenous decay and death regeneration models. In the following sections, fundamentals of these models will be presented.

2.1.1.1 Endogenous decay model

In this model, a new parameter is introduced involving the concept of viability. This new parameter, named as the endogenous decay coefficient, (b_H), is more representative in terms of microbial kinetics as compared to the conventional decay coefficient, k_d. In this manner, it is intended to reflect the behaviour of active biomass (X_H) rather than monitoring the concentration of volatile suspended solids which includes particulate inert matter and inert residual products in addition to the active fraction.

Table 2.4. b_H values for domestic wastewaters as reported in the literature

Sludge age, θ_x (day)	Temperature (°C)	b_H (1/day)	Reference
-	20	0.24	Sollfrank & Gujer, 1991
-	10	0.12	Sollfrank & Gujer, 1991
2	20	0.25	Kappeler & Gujer, 1992
10	22	0.1	Kappeler & Gujer, 1992
2	22	0.4	Kappeler & Gujer, 1992
11	13	0.05	Kappeler & Gujer, 1992
4	13	0.1	Kappeler & Gujer, 1992
-	15	0.08	Kappeler & Gujer, 1992
-	15	0.11	Sarıkaya et al., 1997
-	20	0.24	Ekama & Marais, 1976
-	14	0.20	Warner et al., 1983
-	20	0.24	Henze et al., 1987
-	10	0.077	Henze et al., 1987
-	20	0.153	Henze et al., 1995
-	10	0.077	Henze et al., 1995

Table 2.4 presents b_H values reported in the literature which are either determined experimentally or assumed for mathematical modelling. As the table shows, at 20°C, a b_H value of 0.24 1/day is generally adopted.

According to the endogenous decay model, a fraction, f_E, of the active biomass does not undergo any further reaction and accumulates in the activated sludge leading to the generation of inert endogenous mass or particulate inert organic products, X_E. The rate of decrease of the total biomass (X_T) is defined by McKinney as the sum of the endogenous decay rate of the active biomass (X_H) and the rate of generation of the particulate inert products (X_E) (Orhon and Artan, 1994):

$$\frac{dX_T}{dt} = \frac{dX_H}{dt} + \frac{dX_E}{dt} \tag{2.2}$$

Since f_E units of the active biomass generates X_E:

$$\frac{dX_E}{dt} = -f_E \frac{dX_H}{dt} \tag{2.3}$$

For f_E, a value of 0.2 is adopted universally. The decrease of active biomass can be expressed as a first order reaction as in equation 2.1, so:

$$\frac{dX_H}{dt} = -b_H X_H \tag{2.4}$$

By combining equations (2.3) and (2.4), the rate of generation of particulate inert organic products can be defined as a first order expression with respect to active biomass:

$$\frac{dX_E}{dt} = f_E b_H X_H \tag{2.5}$$

Combining equations (2.2), (2.3), and (2.4), the rate for the total biomass can be obtained as:

$$\frac{dX_T}{dt} = -(1-f_E) b_H X_H \tag{2.6}$$

Equalizing equations (2.1) and (2.6) yields the relationship between the two decay coefficients k_d and b_H:

$$k_d = (1 - f_E)\frac{X_H}{X_T} b_H \tag{2.7}$$

Equation (2.7) reveals that k_d is not a constant, and varies as a function of the active fraction of the biomass which leads to smaller k_d values for longer sludge ages (Orhon and Artan, 1994).

The rate of electron acceptor utilization through endogenous decay, which is the rate of dissolved oxygen consumption under aerobic conditions can be defined as:

$$\frac{dS_0}{dt} = -(1 - f_E) b_H X_H \tag{2.8}$$

2.1.1.2 Death-regeneration model

This is the second approach adopted for modelling the decay of the heterotrophic biomass which was proposed by Dold et al. (1980). In this case, biomass is assumed to be converted to a combination of particulate products and slowly biodegradable substrate. No loss of COD is involved and no electron acceptor is utilized. Furthermore, decay continues at a constant rate independent of the environmental conditions i.e., the decay coefficient b_H` is not a function of the type of electron acceptor or its concentration (ASM1, 1986). Equation (2.9) is used to express the rate of microbial decay:

$$\frac{dX_H}{dt} = -b'_H X_H \tag{2.9}$$

The rate of formation of inert endogenous mass (X_E) and slowly biodegradable substrate (X_S) are shown by equations (2.10) and (2.11):

$$\frac{dX_E}{dt} = f'_E b'_H X_H \tag{2.10}$$

$$\frac{dX_S}{dt} = (1 - f'_E) b'_H X_H \tag{2.11}$$

where f'_E = inert fraction of the endogenous particulate matter.

The slowly biodegradable substrate formed is hydrolyzed, releasing an equivalent amount of readily biodegradable COD. Under aerobic conditions, new cells are produced by the utilization of this substrate together with oxygen uptake. Under anoxic conditions, nitrate nitrogen will be used for cell growth. If neither oxygen, nor nitrate nitrogen is available, no conversion occurs with the accumulation of slowly biodegradable substrate.

Dold et al. have claimed that the two approaches would lead to the same quantitative results in aerobic systems operated at steady state by selecting appropriate values for the kinetic and stoichiometric coefficients. For this purpose, the respective rates of inert particulate organics generation and oxygen consumption can be compared. By the aid of equation (2.11), which gives the rate of biodegradable COD release into the mixed liquor in the death regeneration model, the rate of active biomass synthesized from the recycled substrate can be expressed as follows (Orhon and Artan, 1994):

$$\frac{dX_H}{dt} = Y_H(1-f'_E)b'_H X_H \qquad (2.12)$$

where Y_H = Heterotrophic yield coefficient

The resulting rate of oxygen consumption is:

$$\frac{dS_0}{dt} = -(1-Y_H)(1-f'_E)b'_H X_H \qquad (2.13)$$

For the generation of inert particulate organics, equations (2.5) and (2.10), and, for the rate of dissolved oxygen utilization, equations (2.8) and (2.13) can be compared. Thus:

$$f_E b_H X_H = f'_E b'_H X_H \qquad (2.14)$$

$$(1-f_E)b_H X_H = (1-Y_H)(1-f'_E)b'_H X_H \qquad (2.15)$$

If these equations are solved simultaneously the following relationships can be obtained:

$$b'_H = \frac{b_H}{1 - Y_H(1 - f'_E)} \tag{2.16}$$

$$f'_E = \frac{(1 - Y_H)}{1 - Y_H f_E} f_E \tag{2.17}$$

Using values proposed by Marais and Ekama as f_E = 0.2, b_H = 0.24 1/day and Y_H = 0.67 cell COD/COD, the above expressions give f'_E = 0.08 and $b`_H$ = 0.62 1/day. These values are adopted for typical domestic sewage at 20°C, in the Task group model (Orhon and Artan, 1994).

The magnitude of the decay coefficient used in the death-regeneration model ($b`_H$) is different from the rate coefficient used in the endogenous decay model (b_H). In the endogenous decay model, the loss of one unit of cell mass COD leads to the utilization of one unit of oxygen minus the COD of the inert particulate products formed. In the death-regeneration model, the loss of one unit of cell mass COD results in the formation of one unit of COD due to the readily biodegradable substrate minus the COD of the inert particulate products formed (ASM1, 1986).

Figure 2.1 provides a schematic representation of death-regeneration and endogenous decay models. Although, the death-regeneration approach involves a better interpretation of biomass decay under anoxic and anaerobic conditions, the direct or indirect (by the recirculation of readily biodegradable substrate) consumption of the endogenous material does not seem to have any practical importance for aerobic systems. Besides, it should also be noted that, this model does not provide the differentiation between particulate slowly biodegradable substrate of influent origin , and its counterpart, generated as part of the endogenous biomass. The rate of hydrolysis of the former fraction depends apparently on the nature of the wastewater and could significantly be different than that of endogenous biomass. In relation with this, an experimental study with synthetic soluble waste yielded the rate constant for the hydrolysis of slowly biodegradable endogenous biomass, k_h, as 0.65 1/day which is lower than the value proposed in the Task Group Model where the death-regeneration approach was adopted (Orhon and Artan, 1994).

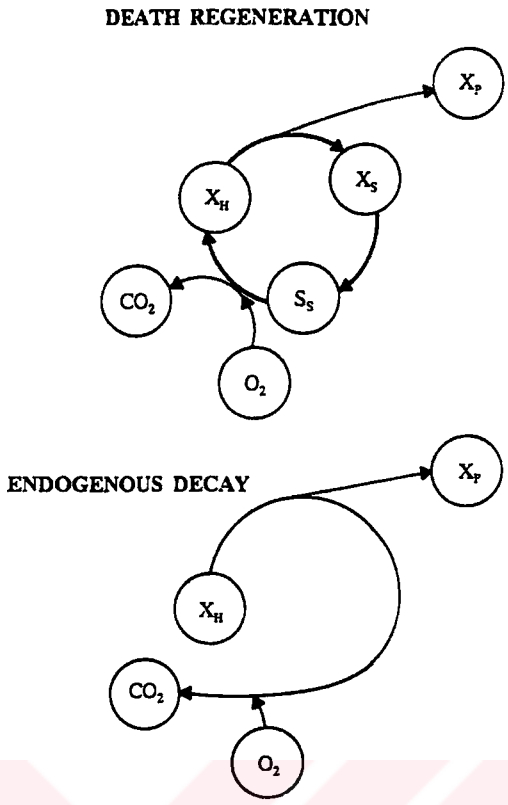

Figure 2.1 Schematic representation of death-regeneration and endogenous decay models (Orhon and Artan, 1994)

2.1.2 Concept of energy of maintenance

The thermodynamic and kinetic instabilities of many biochemical molecules suggest a need for sources of free energy in preserving or replacing such unstable structures in cells. Since the environment may be devoid temporarily of useful free energy, evolution should have favored development of species capable both of storing reserve energy and utilizing it for the preservation or replacement of essential cellular components. Thus, the direct source of the free energy for this purpose probably is endogenous without permitting the direct utilization of suitable exogenous compounds when available.

Some steps in endogenous metabolism may be essential to the vitality of the organism. Others may occur simply because the substrates and enzymes are present and in contact with each other. In either case, metabolism of exogenous energy sources replaces the energy reserves consumed by endogenous reactions. As suggested by Rahn (1932) that level of exogenous energy just sufficient to replace the energy used endogenously, but without inducing growth, is termed "energy of

maintenance". Rahn assigned to the energy of maintenance the role of overcoming the effects of "chemical wear and tear" resulting from hydrolysis and decomposition. In studies conducted by many bacteriologists, the existence of an energy of maintenance has been shown for *E. coli* and verified by the kinetic approach by Marr (1962). Presumably, other bacteria should behave similarly, although probably with quantitative differences (Lamanna, 1963).

In the following section, the models presented for the description of energy of maintenance will be mentioned.

2.1.2.1 Models for the energy of maintenance

Maintenance requirements are mathematically expressed in two alternative ways. Herbert (1958) modified a common balance equation on biomass reactions so as to contain a maintenance term in addition to a growth associated term. As an alternative, a common balance on substrate reactions was modified by Pirt (1965).

According to the concept of Herbert, two fundamental reactions involving biomass and one reaction involving substrate were assumed. Thus, observed growth at a specific rate, $\mu_{obs}(s)$, results from true growth at a specific rate, $\mu_{true}(s)$, and from negative endogenous growth or biomass degradation at a specific rate $\mu_e(s)$. The latter decay process is thought to supply the energy (ATP) required for maintenance purposes. As opposed to the Pirt approach, which will be mentioned below, observed consumption of substrate at a rate $q_{obs}(s)$ results only from growth related consumption at a rate $q_{gr}(s)$, reflecting anabolism and growth associated catabolism (Beeftink et al., 1990).

Pirt presents a modification of the balance equation for the carbon source and substrate. In agreement with earlier concepts, he proposed one fundamental reaction for biomass and two for substrate. Here, substrate is consumed at a rate $q_{gr}(s)$ for growth requirements, but in addition at a rate $m_s(s)$ to supply catabolic energy for maintenance requirements. Contrary to the Herbert approach, there is no biomass degradation and the observed growth rate $\mu_{obs}(s)$ equals the true growth rate $\mu_{true}(s)$ (Beeftink et al., 1990).

Both models consist of two independent equations for the dependent variables $\mu_{obs}(s)$ and $q_{obs}(s)$, involving three unknowns, namely $q_{gr}(s)$, $\mu_{true}(s)$, $m_s(s)$ in the Pirt model, and $q_{gr}(s)$, $\mu_{true}(s)$ and $\mu_e(s)$ in the Herbert model. In both models one of these unknowns is eliminated by postulating a fixed ratio between true growth and growth associated substrate consumption called the true yield of biomass on substrate:

$$Y = \frac{\mu_{true}(s)}{q_{gr}(s)} \tag{2.18}$$

The final Herbert model is represented by the following equations:

$$\mu_{obs}(s) = \hat{\mu}_{true} \frac{S}{K_S + S} - \mu_e \tag{2.19}$$

$$q_{obs}(s) = \hat{\mu}_{true} \frac{S}{Y(K_S + S)} \tag{2.20}$$

Alternatively, for the Pirt model:

$$\mu_{obs}(s) = \hat{\mu}_{true} \frac{S}{K_S + S} \tag{2.21}$$

$$q_{obs}(s) = \hat{\mu}_{true} \frac{S}{Y(K_S + S)} + m_s \tag{2.22}$$

Beeftink et al. (1990) attempted to combine "attractive features" of the previous models and view maintenance energy as being supplied from either substrate or biomass, depending on environmental conditions. They assumed:

- Negative growth at S = 0
- No substrate consumption at S = 0
- No endogenous decay at S = ∞
- $\mu_{obs}(\infty) = \hat{\mu}$

The basis of the equations suggested by Beeftink et al. includes four fundamental rates (instead of three for the models discussed above). Thus, the biomass balance (see equation 2.23) contains, besides an observed rate, a true growth rate and a

maintenance rate following the approach of Herbert. In addition, however, the substrate balance (see equation 2.24) contains terms for observed consumption, growth related consumption, and maintenance consumption; as such it follows the approach of Pirt.

$$\mu_{obs}(s) = \hat{\mu}\, M_0(s) - M\,(1 - M_0(s)) \tag{2.23}$$

$$q_{obs}(s) = \frac{\hat{\mu}}{Y} M_0(s) + \frac{M}{Y} M_0(s) \tag{2.24}$$

Here $M_0(s)$ represents a substrate function such that $M_0(0) = 0$ and $M_0(\infty) = 1$. By the second terms on the right hand side of the equations (2.23) and (2.24), two separate maintenance processes are postulated; both are substrate dependent and are represented by a constant M and a substrate dependent factor involving $M_0(s)$.

During feast conditions (i.e. at S = ∞ and hence $M_0(\infty) = 1$), the observed growth rate approaches $\hat{\mu}$, while the microorganism covers its maintenance ATP requirements entirely from non-growth related substrate consumption (Pirt situation).

During famine conditions on the other hand, endogenous respiration dominates: at S = 0 and $M_0(0) = 0$ there is no observed substrate consumption and maintenance ATP is obtained from biomass degradation ($\mu_{obs}(s) < 0$; the Herbert situation).

At intermediate substrate concentrations, the mechanism of maintenance energy generation shifts between these extremes. This shift is brought about by the factors $(1 - M_0)$ and (M_0) in the biomass and substrate balances in equations (2.23) and (2.24).

This model by Beeftink et al. regards maintenance ATP requirements by microorganisms as being constant; they are supplied by both substrate catabolism and biomass degradation in substrate dependent ratios. It seems that, equations (2.23) and (2.24) presented in this model may be derived directly from Herbert's equations (2.19) and (2.20) by simple rearrangement and a redefinition of kinetic parameters. While the result obtained from equations (2.23) and (2.24) seems identical, there is an essential difference in terms of interpretation. Herbert's model assumes three fundamental rates as previously explained, therefore, it can not be interpreted in

terms of the latter model's assumptions (four fundamental rates). Beeftink et al. further stress that their model features a total demand for maintenance energy in ATP terms that is a constant (δ). The relative contributions to this demand from both ATP supplying routes, however are substrate dependent. Maintenance from biomass degradation in itself is growth rate dependent, as is the supply from substrate catabolism. This flexibility has been obtained without the addition of extra parameters as compared to the Herbert and Pirt models.

It should be noted that, although the models described above have substantial importance from microbiological point of view, models used to describe the endogenous metabolism, i.e., endogenous decay and death regeneration models, are more conveniently used for environmental engineering applications.

2.2 Biological Nitrogen Control

Nitrogen in raw wastewater is usually in the form of reduced organic nitrogen and ammonia. After conventional biological treatment it exists mainly in the form of ammonia nitrogen. There are only three biological approaches available to prevent nitrogen contamination of waters (Christensen and Harremoes, 1985):

1. Oxidation of the reduced forms to nitrate to prevent oxygen depletion and some of the toxic effects which is known as nitrification
2. Removal of nitrogen from wastewater by assimilation into sludge
3. Reduction of oxidized nitrogen to elementary nitrogen by denitrification preceded by nitrification of the ammonia in the wastewater

Denitrification is a key process in biological nitrogen control of wastewaters as well as an important step in the natural nitrogen cycle, which occurs concurrently with nitrification.

2.2.1 Microbiology of denitrification

Denitrification is the name given to the dissimilatory process by which nitrate and nitrite are reduced to gaseous oxides of nitrogen, i.e., nitric and nitrous oxides, which may then be further reduced to give gaseous nitrogen as below:

$$\overset{(+5)}{NO_3^-} \rightarrow \overset{(+3)}{NO_2^-} \rightarrow \overset{(+2)}{NO} \rightarrow \overset{(+1)}{N_2O} \rightarrow \overset{(0)}{N_2}$$

Denitrifying bacteria are biochemically and taxonomically diverse, but most are heterotrophic and utilize complex organic substances as oxidizable substrates, some utilize one carbon compound, some are autotrophic and utilize hydrogen and carbon dioxide or reduced sulphur compounds, and one group is photosynthetic. The most significant genera of denitrifying bacteria are *Pseudomonas*, *Alcaligenes*, *Bacillus*, *Aerobacter*, *Micrococcus*, *Flavobacterium*, and *Proteus,* many of which are abundant in sewage. This fact is extremely useful since a population of denitrifiers containing many different species are capable of growing in a wide variety of conditions being less sensitive to the environment in contrast to nitrifiers which involve one or two specialized organisms (Winkler, 1984).

Most denitrifiers are capable of reducing nitrate to nitrogen gas, some can reduce only nitrite to nitrogen, and are called nitrite dependent, some can not reduce nitrous oxide and so produce nitrous oxide as an end product, and others can reduce nitrous oxide, but can not produce nitrous oxide from nitrate or nitrite. The proportion of denitrifiers, like any microbial species present in a mixed culture will depend on the relative abundance of appropriate electron donor (usually but not necessarily organic molecules), the relative abundance of appropriate electron acceptor (nitrate for denitrifiers), and the energy by using a particular electron acceptor. In a wastewater which has undergone biological nitrification, the concentration of nitrate ions would be expected to be greater than the concentration of phosphate or sulphate ions. Therefore, under conditions of low oxygen concentration biological denitrification can be expected to occur (Barnes and Bliss, 1983).

The same series of enzymatic reactions occur in aerobic and anoxic biochemical processes except *nitrate reductase* , an enzyme generated in the absence of oxygen. Due to the similarity in the respiration processes, facultative bacteria in a single sludge process can switch easily from oxygen to nitrate as terminal electron acceptors.

2.2.2 Stochiometry of denitrification

In denitrification as opposed to organics removal, it is the nitrate that is the pollutant to be removed and the carbon source that is added. In organics removal, it is the carbon that is the pollutant to be removed and the oxygen that is added. Only sufficient carbon is added in denitrification to accomplish nitrate removal as excess dosing causes organics to reappear in the effluent unless control measures are taken.

The sources of electron donors for denitrification can be investigated in three major categories:

1. External sources added at the denitrification stage
2. Internal sources which include wastewater carbon
3. Endogenous carbon sources generated by the death and lysis of biomass

These carbon sources will be discussed in detail in Section 2.3.

During denitrification, an organic compound serves as an electron donor and carbon source while nitrate acts as the electron acceptor according to the following half reaction:

$$\frac{1}{5}NO_3^- + \frac{6}{5}H^+ + e^- \rightarrow \frac{1}{10}N_2 + \frac{3}{5}H_2O \qquad (2.25)$$

When oxygen acts as the electron acceptor, the half reaction can be written as follows:

$$\frac{1}{4}O_2 + H^+ + e^- \rightarrow \frac{1}{2}H_2O \qquad (2.26)$$

These two half reactions reveal that, in case of oxygen one electron transferred from the organic matter requires (1/4*32)=8 g of oxygen and in case of nitrate, one electron transferred from the organic matter requires (1/5*14)=2.8 g nitrate-nitrogen. Equalizing on the electron basis:

$$2.8\ g\ NO_3^- - N = 8\ g\ O_2 \qquad (2.27)$$

This means 1 g of $NO_3^- - N$ will be reduced for 2.86 g O_2 equivalent of substrate. Y_{HD} denoting the yield coefficient for denitrifier microorganisms and $(1-Y_{HD})$ expressed as [e^-.e electron acceptor/e^-.e substrate], for the removal of 1 gr COD, 2.86 gr of nitrate-nitrogen has to be reduced as follows:

$$(1-Y_{HD})\frac{2.8}{8} = \frac{(1-Y_{HD})}{2.86}\ g\ NO_3^- - N / gCOD \qquad (2.28)$$

If equation (2.28) is multiplied by $1/Y_{HD}$, the same expression can also be expressed in terms of cell COD:

$$\frac{(1-Y_{HD})}{2.86Y_{HD}}\ g\ NO_3^- - N / g\ cellCOD \qquad (2.29)$$

Equation (2.29) relates the concentration of oxidized nitrogen to the growth of denitrifiers.

The overall stochiometric coefficient (Y_{NHD}) involves the assumption of nitrate being utilized in endogenous respiration as well. This can be written as:

$$\frac{(1-Y_{NHD})}{2.86}\ g\ NO_3^- - N / g\ COD \qquad (2.30)$$

The above expression shows that, (1/2.86)=0.35 g of NO_3^--N would be required for each g of COD removed, if all the organic matter in the denitrification reactor were only converted to CO_2 and H_2O. However, this is a theoretical value and only reflects the requirements of the energy reactions of the denitrifiers. A portion of the organic matter is converted into cell material so the amount of NO_3^--N required is reduced by a factor ($1-Y_{NHD}$). Additionally, in the absence of ammonia nitrogen, $i_{XB}Y_{NHD}$ g of nitrate has to be incorporated into biomass for each g of COD removed. The value of i_{XB} was recommended by Henze et al. (1987) as 0.086 g N/g cell COD. Thus, the total NO_3^--N consumption can be expressed as:

$$N / COD = [0.35(1-Y_{NHD}) + 0.086Y_{NHD}]\ g\ NO_3^- - N / g\ COD \qquad (2.31)$$

Other factors to be considered for the calculation of COD/N ratio are NO_2^--N and dissolved oxygen. NO_2^--N is reduced according to the below reaction:

$$\frac{1}{3}NO_2^- + \frac{4}{3}H^+ + e^- \rightarrow \frac{1}{6}N_2 + \frac{2}{3}H_2O \qquad (2.32)$$

The above relationship shows that, one electron transferred from the organic matter requires (1/3*14)=4.67 g nitrite-nitrogen so:

$$(1-Y_{NHD})\frac{4.67}{8} = \frac{(1-Y_{NHD})}{1.71}\ g\ NO_2^- - N / g\ COD \qquad (2.33)$$

will be required.

Dissolved oxygen might be carried to the reactor by the return sludge stream. In this case, it will be consumed by the microorganisms and the total organic matter requirement for the reduction of nitrate, nitrite and deoxygenation will be expressed as:

$$C_T = \frac{2.86}{1-Y_{NHD}} S_{NO3} + \frac{1.71}{1-Y_{NHD}} S_{NO2} + \frac{1}{1-Y_{HD}} S_{O1} \quad (2.34)$$

where

C_T = required biodegradable COD concentration

S_{NO3} = initial nitrate-nitrogen concentration

S_{NO2} = initial nitrite-nitrogen concentration

S_{O1} = initial dissolved oxygen concentration

Methanol has been widely used in biological denitrification as an external carbon and energy source. Nitrate dissimilation with methanol can be depicted as a two step reaction (Monteith et al., 1980):

$$NO_3^- + 0.33CH_3OH \rightarrow NO_2^- + 0.67H_2O + 0.33CO_2 \quad (2.35)$$

$$NO_2^- + 0.5CH_3OH \rightarrow 0.5N_2 + 0.5CO_2 + 0.5H_2O + OH^- \quad (2.36)$$

$$NO_3^- + 0.83CH_3OH \rightarrow 0.5N_2 + 0.83CO_2 + 1.17H_2O + OH^- \quad (2.37)$$

Equation (2.37) shows the overall reaction, revealing the stochiometric quantity of methanol required for nitrate dissimilation. Additional methanol is required for deoygenation and cell synthesis according to the following equations:

$$O_2 + 0.93CH_3OH + 0.056NO_3^- + 0.056H^+ \rightarrow 0.056C_5H_7NO_2 + 0.65CO_2 + 1.69H_2O \quad (2.38)$$

$$14CH_3OH + 3NO_3^- + 4H_2CO_3 \rightarrow 3C_5H_7NO_2 + 2H_2O + 3HCO_3^- \quad (2.39)$$

The methanol requirement, C_m, for nitrate dissimilation and deoxygenation can be written as (US EPA, 1975):

$$C_m = 2.47S_{NO3} + 1.53S_{NO2} + 0.87S_{O1} \quad (2.40)$$

In practice, a common value of 3 kg methanol per kg nitrate-nitrogen is adopted rather than the stochiometric amount of 2.47 kg.

The methanol requirement can be combined and related to that required for nitrogen removal and deoxygenation. McCarty, Beck and St. Amant (1969) referred to this as the consumptive ratio, C_r, represented by the relationship:

$$C_r = \frac{Total\ FOC\ utilized}{FOC\ required\ for\ denitrification\ and\ deoxygenation}$$

FOC denotes filterable organic carbon. In a reactor in which nitrate, nitrite, and oxygen are reduced stochiometrically by organic carbon sources, the C_r is equal to one. Since a supplemental quantity is required for cell synthesis, experimentally the consumptive ratio is observed to be greater than one. As the C_r of an organic compound increases, cell synthesis also increases. Thus, an organic waste that has a high consumptive ratio would tend to generate larger volumes of sludge (cells) than a waste with a lower C_r. The mean C_r for methanol was found by Monteith et al. as 1.65 while McCarty, Beck, and St. Amant obtained an average C_r of 1.30 in semi-continuos field experiments.

Stochiometric equations for nitrate reduction by organic compounds were developed by Monteith et al. (1980) in order to calculate the consumptive ratios. Equations similar to equation (2.37) for methanol were derived. The equations are as follows:

For glycol:

$$0.5(CH_2OH)_2 + NO_3^- \rightarrow 0.5N_2 + CO_2 + H_2O + OH^- \qquad (2.41)$$

For formaldehyde:

$$1.25HCHO + NO_3^- \rightarrow 0.5N_2 + 1.25CO_2 + 0.75H_2O + OH^- \qquad (2.42)$$

For acetic acid:

$$0.625CH_3COOH + NO_3^- \rightarrow 0.5N_2 + 1.25CO_2 + 0.75H_2O + OH^- \qquad (2.43)$$

For isopropanol:

$$0.278C_3H_7OH + NO_3^- \rightarrow 0.5N_2 + 0.833CO_2 + 0.611H_2O + OH^- \qquad (2.44)$$

For fusel oil (as amyl alcohol):

$$0.167C_5H_{11}OH + NO_3^- \rightarrow 0.5N_2 + 0.833CO_2 + 0.5H_2O + OH^- \quad (2.45)$$

For dextrose:

$$0.208C_6H_{12}O_6 + NO_3^- \rightarrow 0.5N_2 + 1.25CO_2 + 0.75H_2O + OH^- \quad (2.46)$$

For these equations, Monteith et al. calculated the stochiometric quantities of organic carbon required for nitrate reduction. They used the observed depletions of organic carbon in the batch tests. The calculated C_r values for wastes as above are summarized in Table (2.5).

Biological denitrification is accomponied by an increase in alkalinity. From stochiometry, for 1 mg of nitrate-N denitrified, (50/14=3.57) mg alkalinity as CaCO3 is produced. On the other hand, (50/14 i_{XB}) mg $CaCO_3$ is utilized for each mg of cell COD due to the utilization of ammonia-nitrogen for cell synthesis. Here, i_{XB} denotes the nitrogen content of the active sludge fraction. Thus, the resulting expression can be written as follows:

$$\frac{1-Y_{HD}}{2.86Y_{HD}}\frac{50}{14} - i_{XB}\frac{50}{14} \quad (2.47)$$

or

$$\frac{1-Y_{HD}}{2.86Y_{HD}}\frac{1}{14} - i_{XB}\frac{1}{14} \quad (2.48)$$

Table 2.5 Calculated values of consumptive ratios (C_r) for some industrial wastes (Monteith et al., 1980)

Type of Industry	C_r
Methanol (Commercial)	1.65
Methanol heads	1.15
Methanol still bottoms	1.00
Methyl fuel	2.58
Glycol waste	1.07
Formaldehyde waste	1.29
Acetic acid waste	1.60
Fusel oil as $C_5H_{11}OH$	2.04
Waste dextrose solution	2.40
Isopropanol waste	2.53

2.2.3 Process kinetics in denitrification

The process kinetics of denitrification will be discussed mainly under three circumstances, namely, growth of denitrifiers, hydrolysis of particulate organic matter, and decay of denitrifiers.

A double Monod type function is used to express the growth of denitrifiers which includes both the organic matter and nitrate concentrations:

$$\mu_{HD} = \hat{\mu}_{HD} \frac{S_S}{K_S + S_S} \frac{S_{NO}}{K_{NO} + S_{NO}} \tag{2.49}$$

Each parameter is commonly expressed with the units indicated below:

μ_{HD} = Specific growth rate for denitrifiers, [1/day],

$\hat{\mu}_{HD}$ = Maximum growth rate for denitrifiers, [1/day],

K_S= Half-saturation constant for the carbon source, [mg COD/l],

K_{NO}= Half-saturation constant for nitrate-nitrogen, [mg NO_3-N/l],

S_S= Carbon source concentration, [mg COD/l],

S_{NO}= Concentration of NO_3-N, [mg NO_3-N/l].

Experimental values cited for K_{NO} in the literature are in a range of 0.1-0.5 mg NO_3-N/l (Orhon and Artan, 1994). Due to these low values, K_{NO} may often be neglected as compared to S_{NO} values of greater than 1 mg/l, consequently leading to zero-order expressions with respect to NO_3-N concentration.

The rate of change in the denitrifier concentration can be expressed in terms of growth and decay as follows:

$$\frac{dX_{HD}}{dt} = \mu_{HD} X_{HD} - b_{HD} X_{HD} \tag{2.50}$$

where

X_{HD}= Concentration of denitrifiers, [mg VSS/l],

b_{HD}= anoxic endogenous decay rate coefficient, [1/day].

Anoxic yield coefficient Y_{HD}, relates the rate of removal of the carbon source to the rate of anoxic growth:

$$\frac{dS_S}{dt} = -\frac{\mu_{HD}}{Y_{HD}} X_{HD} = \frac{\hat{\mu}_{HD}}{Y_{HD}} \frac{S_S}{K_S + S_S} X_{HD} \quad (2.51)$$

The rate of nitrate utilization, dS_{NO}/dt, can be expressed as follows:

$$\frac{dS_{NO}}{dt} = -\frac{1 - Y_{HD}}{2.86 Y_{HD}} \mu_{HD} X_{HD} \quad (2.52)$$

Equation (2.52) involves an expression defined as denitrification yield, Y_D, which is the amount of cell COD produced per unit amount of NO_3^--N consumed:

$$Y_D = \frac{2.86 Y_{HD}}{1 - Y_{HD}} \quad (2.53)$$

When equations (2.52) and (2.53) are combined, a parameter which is used as a measure of denitrification performance is evolved, named as specific nitrate utilization rate, q_D:

$$\frac{dS_{NO}}{dt} = -\frac{\mu_{HD}}{Y_D} X_{HD} = -q_D X_{HD} \quad (2.54)$$

q_D is usually expressed in a unit of g NO_3^--N/g VSS.time.

Single sludge systems are commonly employed for simultaneous carbon and nitrogen removal in activated sludge systems. In such systems, activated sludge comprises heterotrophic bacteria which are expected to take part during aerobic and anoxic respiration. Recent knowledge suggests, however, that the rate of nitrate removal is lower than the rate observed under aerobic conditions. Two explanations brought by the researchers for this fact are given as below:

1. Not all the heterotrophic bacteria take active part in denitrification
2. The rate of heterotrophic growth under anoxic conditions is lower than the aerobic heterotrophic growth rate

Since no experimental procedure has been suggested so far for the discrete impacts of $\hat{\mu}_{HD}$, X_{HD}, and Y_{HD} which are the apparent parameters to affect the rate of substrate removal (see equation (2.51)), a simplifying assumption was adopted in the current modelling approach. This assumption brings the definition of an overall correction factor, denoted as η_g, for anoxic conditions. Thus, η_g is the respective

ratio of the rates of readily biodegradable substrate consumption under anoxic and aerobic conditions. Therefore, equation (2.51) can be rewritten as:

$$\frac{dS_S}{dt} = -\eta_g \frac{\mu_H}{Y_H} X_H \tag{2.55}$$

η_g values cited in the literature are between 0.7 and 1, i.e. less than one (Orhon and Artan, 1994).

After the depletion of readily biodegradable substrate in a medium, heterotrophic microorganisms start to grow on slowly biodegradable particulate substrate (X_S), first, by converting it into the readily biodegradable form by a hydrolysis mechanism as suggested by Dold and Marais (1986). This rate is shown to be slower than the rate of growth on S_s, hydrolysis being the rate-limiting step. The rate of growth on particulate slowly biodegradable substrate under anoxic conditions can be expressed as:

$$\frac{dX_S}{dt} = -k_{HD} \frac{X_S / X_{HD}}{K_X + X_S / X_{HD}} X_{HD} \tag{2.56}$$

where

k_{HD}= Anoxic maximum specific hydrolysis rate [mg COD/mg COD.day]
K_X= Half velocity coefficient for hydrolysis [mg COD/mg VSS]

The same expression can be written in the following form by involving a correction factor for hydrolysis under anoxic conditions (η_h):

$$\frac{dX_S}{dt} = -\eta_h k_h \frac{X_S / X_H}{K_X + X_S / X_H} X_H \tag{2.57}$$

In the literature the suggested value of η_h is 0.4 (Orhon and Artan, 1994).

As previously mentioned in section 2.1, microbial decay can be expressed as a first order reaction with respect to active biomass concentration. During growth conditions, decay occurs as well, but is usually neglected if the rate of growth is considerably high. Two models, namely endogenous decay and death and regeneration, exist in the literature to describe endogenous metabolism (see sections 2.1.1.1 and 2.1.1.2). Due to similar reasons as described above, for endogenous

respiration just as for growth and hydrolysis phases, a correction factor under anoxic conditions, η_E is again adopted:

$$\frac{dX_{HD}}{dt} = -b_{HD}X_{HD} = -\eta_E b_H X_H \tag{2.58}$$

The only information in the literature about η_E was reported by Kristensen et al. (1992) as a range from 0.79 to 1.07. This implies that the behaviour of heterotrophs is quite similar during endogenous decay in both aerobic and anoxic media.

As also stated above, denitrification rate is affected by growth and decay processes:

$$\frac{dS_{NO}}{dt} = -\frac{1-Y_{HD}}{2.86Y_{HD}}\hat{\mu}_{HD}\frac{S_S}{K_S+S_S}\frac{S_{NO}}{K_{NO}+S_S}X_{HD} - \frac{1-f_E}{2.86}b_{HD}X_{HD} \tag{2.59}$$

In predenitrification systems, the concentration of the readily biodegradable substrate, S_s, is high enough so that maximum growth conditions prevail ($\hat{\mu}_{HD}$), and denitrification occurs at a constant rate k_1:

$$\frac{dS_{NO}}{dt} = -\frac{1-Y_{HD}}{2.86Y_{HD}}\hat{\mu}_{HD}X_{HD} - \frac{1-f_E}{2.86}b_{HD}X_{HD} \tag{2.60}$$

or in terms of η_g:

$$\frac{dS_{NO}}{dt} = -\frac{1-Y_H}{2.86Y_H}\hat{\mu}_H\eta_g X_H - \frac{1-f_E}{2.86}\eta_E b_H X_H \tag{2.61}$$

where

$$k_1 = \frac{1-Y_H}{2.86Y_H}\hat{\mu}_H\eta_g \tag{2.62}$$

After the depletion of the readily biodegradable substrate, biomass starts to consume slowly biodegradable particulate substrate after hydrolysis as previously described above. During that phase, the rate of denitrification proceeds at a constant rate k_2 as indicated below:

$$\left(\frac{dS_{NO}}{dt}\right)_2 = -\frac{1-Y_H}{2.86}\eta_h K_h X_H - \frac{1-f_E}{2.86}b_{HD}X_{HD} \tag{2.63}$$

Here, K_h is the aerobic maximum hydrolysis rate [mg COD/mg COD/day]. When the decay term is expressed in terms of η_E:

$$\left(\frac{dS_{NO}}{dt}\right)_2 = -k_2 X_H - \frac{1-f_E}{2.86}\eta_E b_H X_H \tag{2.64}$$

where,

$$k_2 = \frac{1-Y_H}{2.86}\eta_h K_h \tag{2.65}$$

Endogenous phase occurs in the absence of external carbon sources as in the post denitrification reactors of biological nutrient removal systems. For this third phase, the rate of nitrate depletion can be written as:

$$\left(\frac{dS_{NO}}{dt}\right)_3 = -\frac{1-f_E}{2.86}\eta_E b_H X_H \tag{2.66}$$

Since,

$$k_3 = \frac{1-f_E}{2.86}\eta_E b_H \tag{2.67}$$

Equation (2.66) can be rewritten as:

$$\left(\frac{dS_{NO}}{dt}\right)_3 = -k_3 X_H \tag{2.68}$$

Table 2.6 shows the denitrification rate constants observed for the three phases of growth for domestic sewage. These constants are calculated from zero order rate expressions with respect to substrate. It is apparent from the table that the rate constant varies with the type of the carbon source available. Since the rate expression is zero order, nitrate removal efficiency is independent of the hydraulic characteristics of the reactors and remains unchanged for plug flow and completely mixed systems.

A rate constant, k_4, was defined for anoxic/aerobic digesters by Warner et al. (1986), as 0.0019 g N/g VSS.hr, which is smaller than k_3.

Table 2.6 Denitrification rates for different carbon sources in sewage (Orhon and Artan, 1994)

Rate Constant	Value (g N/g VSS.hr)	Carbon Source
k_1	0.0342	Readily biodegradable substrate
k_2	0.0043	Particulate substrate
k_3	0.0032	Endogenous biomass

A crucial point in the assessment of denitrification rates is the consideration of nitrite accumulation in the media (Henze 1986; Sözen, 1995). For the reduction of nitrate to nitrogen gas the following reaction holds:

$$NO_3^- + 6H^+ + 5e^- \rightarrow \frac{1}{2}N_2 + \frac{3}{5}H_2O \qquad (2.69)$$

Equation (2.69) shows that nitrate accepts 5 electrons from the organic substrate for the whole process of reduction. 2 of these 5 electrons participate in the reduction of nitrate to nitrite while 3 electrons are used for reducing nitrite to nitrogen gas as also depicted by the following equations:

$$NO_3^- + 2H^+ + 2e^- \rightarrow NO_2^- + H_2O \qquad (2.70)$$

$$NO_2^- + 4H^+ + 3e^- \rightarrow \frac{1}{2}N_2 + 2H_2O \qquad (2.71)$$

In terms of electron equivalents, the reduction of nitrate to nitrite results in the following relationship between oxygen and nitrogen:

$$\frac{8\ g\ O_2 / e^-\ eq}{(14/2)\ gN / e^-\ eq} = 1.14\ g\ O_2 / N \qquad (2.72)$$

For the reduction of nitrite to nitrogen gas:

$$\frac{8\ g\ O_2 / e^-\ eq}{(14/3)\ g\ N / e^-\ eq} = 1.72\ g\ O_2 / g\ N \qquad (2.73)$$

equation (2.73) applies.

Transfer of 5 electrons result in the following relationship:

$$1.14 + 1.72 = 2.86\ g\ O_2 / g\ N$$

When nitrite is not further reduced to nitrogen gas, mainly due to environmental conditions (type of carbon source, absence/presence of certain species of bacteria, etc.), 3 electrons equivalent of substrate is not oxidized. In this case, to get a nitrate rate based on nitrate reduction to nitrogen gas, 60 % of the nitrite rate should be subtracted from the nitrate rate. Then, oxygen equivalent of electron acceptor consumption rate will be as follows:

$$2.86\Delta N = 2.86\Delta NO_3^- - N - 1.72\Delta NO_2^- - N \quad (2.74)$$

$$2.86\Delta N = 2.86(\Delta NO_3^- - N - 0.6\Delta NO_2^- - N) \quad (2.75)$$

Without nitrite correction, the rate of denitrification will appear to be higher, since, 60 % of nitrite will then, be assumed to be reduced, instead of being accumulating in the system.

Effect of environmental factors

Many environmental factors including, temperature, ambient oxygen concentration, pH and toxic substances influence the activity of denitrifiying organisms.

A mixed bacterial culture responds to a temperature change with a change in the reaction rate. It is important to distinguish between short-term (shock temperature response) and long term temperature dependence. The short-term dependence reflects the immediate ability of the organisms to change reaction rates. The long-term temperature dependence is a combination of adaptation by organisms originally present and selection of organisms favored by the new temperature conditions. Figure 2.2 shows that the temperature to which the bacterial population adapted has considerable influence on the result of a short term temperature dependence test. Cooling, in this case, will give a higher dependence and heating will give a lower dependence compared to long term temperature dependence.

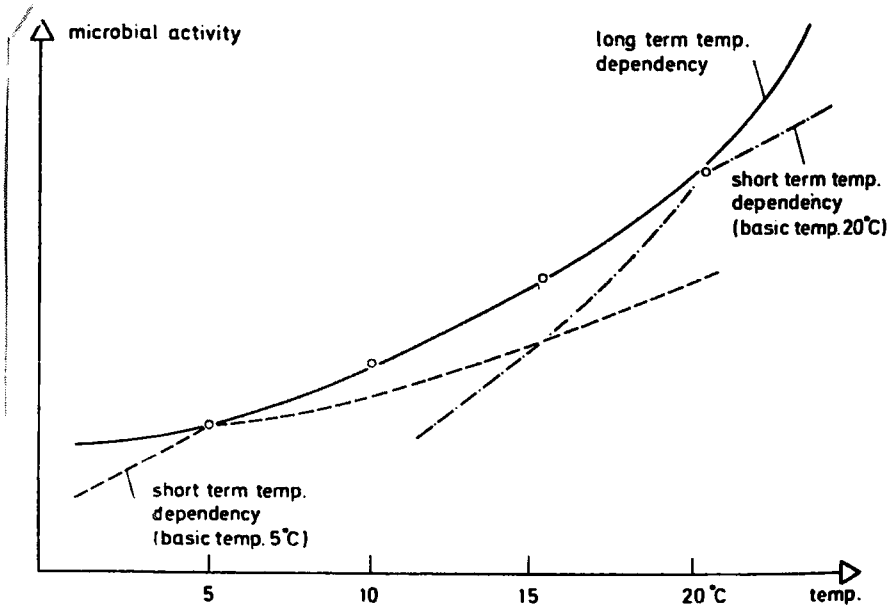

Figure 2.2 Temperature dependence of denitrification (Christensen and Harremoes, 1985)

Mathematically, temperature dependence can be described by an exponential expression:

$$\hat{\mu}_{(t)} = \hat{\mu}_{(20)}.10^{k_t(t-20)} \tag{2.76}$$

which can also be written as:

$$\hat{\mu}_{(t)} = \hat{\mu}_{(20)}.\theta^{t-20} \tag{2.77}$$

Table 2.7 Long term temperature constants for denitrifiying microorganisms (Christensen and Harremoes, 1985)

Denitrification Process	Carbon Source	k_t (1/°C)	θ	Temperature Range (°C)
Suspended separate culture	Methanol	0.05	1.12	10-25
Suspended combined culture	Raw sewage	0.06	1.15	5-20
	Endogenous	0.08	1.20	15-25
Attached separate culture	Methanol	0.02	1.05	5-20

These expressions are only valid in the range from the minimum temperature of the organisms to some temperature (30-35°C) where destruction of the bacterial enzymes begins to be important. As temperature in most cases changes slowly (such as an annual variation), long term temperature dependence is the most important for practical purposes.

Table 2.7 lists the long-term temperature constants k_t and θ for various denitrification processes.

The role of dissolved oxygen concentration on denitrification depends on a distinction between a micro and macro environment. It has been suggested that a dissolved oxygen concentration above 0.2 mg/l ceases denitrification. Accordingly, the growth rate of denitrifiers is expressed as functions of carbon, dissolved oxygen, and nitrate-nitrogen concentrations:

$$\frac{dX_H}{dt} = \hat{\mu}_H \eta_g \frac{S_S}{K_S + S_S} \frac{K_{OH}}{K_{OH} + S_O} \frac{S_{NO}}{K_{NO} + S_{NO}} X_H \qquad (2.78)$$

$K_{OH}/K_{OH}+S_{NO}$ represents a switching function whose value decreases with increasing concentration of dissolved oxygen (S_{NO}), thus, decreasing overall growth rate of denitrifiers. Here, K_{OH} denotes the half velocity coefficient for dissolved oxygen with a suggested value of 0.2 mg/l.

On the other hand, for a macro environment, conditions suitable for denitrification may prevail in the interior of flocs and biofilms despite high concentrations of oxygen in the bulk liquid. In such a case, oxygen is consumed in the outer regions of flocs and biofilms, thus, denitrification may occur in spite of the presence of oxygen.

It is also appropriate to use the distinction between long term and short term pH effects. Both types of effects are important because pH may vary over short (hours, days) or long (months, years) periods. All investigations of pH dependence have been short term. The optimum pH range for denitrification is suggested to be between 7 and 7.5.

2.3 Carbon Sources for Denitrification

In all biological systems, almost all of the organic carbon is depleted in the nitrification process. Thus, the addition of preferably a nitrogen-free electron donor, is necessary for the denitrification of the nitrates formed during nitrification.

The main requirements for a suitable carbon source are a very high concentration of soluble organic carbon, uniformity in composition from day to day, availability in sufficient quantities to provide regular supply, proximity to treatment plants to be transported economically, a non-toxic, non-dangerous nature, a low sludge yield, and the ability to stimulate a complete denitrification without the need for adaptation of the microflora, so that environmentally detrimental intermediary products such as nitrite and nitrogenous oxides can be avoided.

In this context, four categories of carbon sources can be listed:

1. Internal carbon sources
2. Endogenous carbon sources
3. External carbon sources
4. Hydrolyzed carbon sources

Each category of carbon source will be discussed below in terms of advantages, disadvantages, and denitrification kinetics.

2.3.1 Internal carbon sources

In recent years, there is an increasing trend of using internal carbon for the reasons of better economy, less sludge production, and more optimal usage of organics within the wastewater.

Mainly two points have to be considered when employing internal carbon in a process. First, it should be made sure that enough carbon must be available for the complete denitrification of nitrate formed during nitrification. Thus, the necessary carbon to nitrogen ratio (C/N) should be supplied. Since a part of the COD in the combined nitrification-denitrification process is oxidized by oxygen, C/N requirement in practice is higher. Henze (1991) suggests typical values in a range of 5-10 g COD/g N. Second, complete denitrification may not occur due to a low denitrification rate . The denitrification rate is affected by the nature of the carbon

source besides temperature. It is well known that the highest rates are obtained with the easily degradable forms.

When the organic carbon necessary to drive denitrification reactions is supplied from internal sources, the overall nitrogen removal efficiency can be limited since raw wastewater introduces ammonium and organic nitrogen as well as carbon.

All of the systems using wastewater as the main organic carbon source use an alternating aerobic-anoxic sequence of stages without intermediate clarification to avoid ammonia-nitrogen release. The rates of denitrification obtained with internal sources exhibit wide variations. Henze (1986) reported rates in a range of 1.5-16.7 mg NO_3-N/(g VSS.hr) for various wastewater treatment plants. Thus, rates vary considerably from one type of wastewater to another type, and for a certain type of wastewater, variation tends to be smaller. Therefore, pilot investigations should be conducted to verify design parameters for denitrification when wastewater is the carbon source. Henze (1989) also found that the rate of denitrification with wastewater is about one third of the value obtained with acetic acid or methanol. This postulates the practical conclusion that a denitrification reactor using a wastewater carbon source would have to be about three times larger than a denitrification reactor using easily degradable external carbon sources.

2.3.2 Endogenous carbon sources

When endogenous carbon sources are employed for denitrification, the rate-limiting step becomes the organism's endogenous decay rate in an anoxic environment.

Various studies were conducted for the determination of the endogenous denitrification rates where a fairly high mixed liquor solids were employed (5200-5300 mg/l) and detention times of 2.2 to 2.8 hours were used in the denitrification section, in sequential carbon oxidation-nitrification-denitrification systems. Table 2.8 shows the results of these studies.

Although, endogenous respiration of activated sludge microorganisms contribute to volatile suspended solids destruction at no apparent cost, it results in very low denitrification rates, and consequently, larger reactor volume requirements. De Renzo (1978) noted that the rates obtained with endogenous carbon sources fall considerably below the rates for methanol as the carbon source. For instance, the

median values at 20°C for methanol and endogenous carbon are about 0.25 g NO_3^--N removed/(g VSS.d) and 0.04 g NO_3^--N removed/(g VSS.d). Therefore, a denitrification reactor using an endogenous carbon source would have to be about six times larger than a reactor with a methanol carbon source at 20°C.

2.3.3 External carbon sources

For wastewaters with a low C/N ratio, external carbon source often has to be added to achieve a satisfactory degree of denitrification. This situation usually arises with industrial wastewaters having a very high nitrate concentration, such as those from the explosives and fertilizer industries and also with waters with very low nitrate concentrations as well as very low organic carbon contents. Examples for the latter are, water in water treatment and the effluent from a nitrification process as in a separate sludge system. Furthermore, external carbon source generally has to be supplied to post-denitrification processes in which the rate of denitrification is quite low as mentioned above.

Table 2.8 Results of pilot tests conducted in Wuhrman's sequential carbon oxidation-nitrification-denitrification system for the determination of peak denitrification rates (De Renzo, 1978)

Location	Temperature (°C)	Peak Denitrification Rate (kg NO_3^--N/ kg VSS.d)	Effluent NO_3^--N (mg /l)	Range of Total Nitrogen Removal (%)
Switzerland[a]	13.6	0.0168	2	82-90
	17.1	0.041		
Germany[a]	16	0.022	-	40-60
	16	0.026		
Germany[a]	12-16	0.038	3	36-88
Germany[b]	20	0.048	7.8	46 (average)
Seattle[a]	20	0.026	-	31-65
New York[c]	-	-	1.5-3.1	84-89

[a] Pilot-scale
[b] Lab-scale
[c] Full-scale

The use of external carbon sources is considered as a back-up, which can increase denitrification rates, for example during periods of low temperature, peak nitrogen loads, or similar stress situations. This may also provide a reduction in the minimal plant size for a given wastewater load.

On the other hand, during the recent history of nitrogen removal processes, external carbon sources have not been regarded as very preferential for the benefit of process economics. The use of external carbon sources will increase the overall sludge production by 10-20 % in the treatment plant. The overall cost of the treatment process will increase due to sludge handling costs apart from the individual cost of the carbon source.

The range of organic materials that can be used as external carbon sources is very wide, including methanol as the most common source, ethanol, carbohydrates, organic acids, n-alkanes, benzoate and other benzene derivatives, molasses and sugars, and nitrogen deficient industrial wastes (Winkler,1984).

Table 2.9 presents values for optimum C/N ratios for various external carbon sources to achieve complete denitrification as they are reported in the literature. Table 2.10 submits maximum rates of denitrification obtained with external carbon sources. Apparently, these rates are much higher than the rates observed with endogenous and most of the internal carbon sources.

Table 2.9 C/N ratios for various external carbon sources as reported in the literature

Form of Carbon	Ratio (g C/ g NO_3^--N)	Reference
Ethanol (continuos)	3.85	Christensson et al., (1994)
Methanol (continuos)	4.45	
Ethanol (pure culture)	6.1	
Methanol (pure culture)	4.1	
Glucose	5.6 (as COD)	Akunna et al., (1993)
Glycerol	5.6 (as COD)	
Acetic acid	3.7 (as COD)	
Lactic acid	4.1 (as COD)	
Methanol	2.3 (as g BOD/g N_{OX}-N)	Narkis et al., (1979)
Sodium acetate	2.3 (as g BOD/g N_{OX}-N)	
Methanol	2.4	Winkler, (1984)
Methanol	2.5 (as COD)	Skrinde and Bhagat, (1982)
Methanol	2.6	Claus and Kutzner, (1985)
Methanol	4.9	Nyberg et al., (1992)

Various findings have been reported in the literature about the efficiency of external carbon sources in denitrification. McCarty et al., (1966) investigated the use of five commercially available organic compounds: methanol, acetic acid, ethanol, acetone and sugar. Methanol was selected as the most suitable and it is the least expensive on an equivalent basis besides being very effective. Paskins et al. (1978), found the

maximum rates of removal of nitrate with methanol, glucose and peptone as 2.3, 2.9 and 9.3 mg N/(g sludge.hr) respectively.

Table 2.10 Literature values for the rates of denitrification obtained with various external carbon sources

Carbon Substrate	Denitrification Rate ($g NO_3^-$-N/ kg VSS.hr)	Reference
Acetic acid		Henze, (1991)[a]
Brewery wastewater	7-20	
Hydrolyzed starch		
Ethanol		
Whey	1-5	
Molasses		
Methane	0.2-0.5	
Glucose	2.7	Akunna et al., (1993)[b]
Glycerol	7.4	
Acetic acid	27.8	
Lactic acid	27.8	
Fusel oil	14	Monteith et al., (1980)[d]
Methanol	4	
Methanol	8	Bonomo et al., (1981)[g]
	3-21[e]	
Methanol	13	Beccari et al., (1983)[c,g]
Fusel oil	16.7	Klapwijk et al.,(1981)[f,g]

[a] Full-scale plants, 20°C
[b] Laboratory batch tests
[c] Laboratory batch tests, 25°C, pH=7.5
[d] Laboratory batch tests, 20°C
[e] Fixed film systems
[f] Up-flow sludge blanket reactor

On the contrary, Gerber and his coworkers (1987) found that substances such as acetate, propionate, butyrate and lactate consistently produced higher denitrification rates than substrates such as glucose, methanol and citrate. Carley and Mavinic (1991) reported that acetate was the most efficient substrate for complete denitrification of a high-ammonium leachate, followed by methanol and glucose. As a reason, sodium acetate enters the pathways directly without any preliminary process while methanol must undergo a condensation process to form 3-C or 4-C intermediates before entering the TCA cycle. Tam et al. (1992) reported that sodium acetate was the most effective carbon source, followed by methanol and glucose in terms of total inorganic nitrogen reduction.

Lee and Welander (1996) observed that carbohydrate products had a higher sludge yield, a lower denitrification yield, and stimulated not only denitrifiying bacteria but also fermentative and nitrite producing bacteria. The hydrolysis of these carbon sources were rather slow, therefore, acetate and methanol appeared to be more advantageous carbon sources for denitrification processes. On the other hand, the methanol-denitrifiying microbial system yielded a specialized microflora with a substantially lower growth rate than the acetate-denitrifiying system. Thus, they concluded that, a higher denitrification rate and also a faster response can be expected with acetate than with methanol.

Recent research work has demonstrated that glucose is a less reliable carbon source with inconsistent denitrification performance. Manoharan et al. (1989) and Carley and Mavinic (1991) reported nitrate removal efficiencies fluctuating between 10 and 100 %. Glucose in the anoxic phase might promote the growth of facultative anaerobes rather than true denitrifiers, leading to poor denitrification (Tam et al., 1992).

Monteith et al. (1980), used a range of 30 different industrial wastes including brewing, distillery, and paper making wastes as carbon sources for denitrification and showed that 27 of them gave higher denitrification rates than methanol, the highest rate being obtained with distillery fusel oil (mixed higher alcohols). Fusel oil was also successfully employed in denitrification using an upflow sludge blanket reactor (Klapwick et al., 1981) and several industrial wastes, including whey, sulphite waste liquor, and a maize silage derivative, were as effective as methanol in fluidized column denitrification (Skrinde and Bhagat, 1992) (Winkler, 1984).

2.3.4 Hydrolyzed carbon sources

Volatile fatty acids (VFA), are mainly associated with the hydrolysis of primary sludge, which itself is an internal source of organic carbon, and are usually produced within wastewater treatment facilities. They are most beneficial in cases where suitable industrial wastes are not available containing adequate concentrations of short chain organic substrates. VFA's include formic, acetic, propionic, n-butyric, iso-butyric, n-valeric, isovaleric, and caproic acids. They are recognized as ideal substrates for *Acinebacter* species and denitrifiers, therefore, employed in biological

nutrient removal processes (BNR) (see section 2.3.2) to achieve high rates of phosphorus removal and denitrification.

The organic content of primary sludge is approximately 90 times that of raw wastewater. The organic carbon to nitrogenous matter ratio of primary sludge is very high (approximately 16) (Abufayed and Schroeder, 1986). In 1983, Pitman et al. proposed the addition of acid supernatant liquor from a high rate digester to the feed of the biological excess phosphorus removal process (BEPR). In 1985, Nicholls et al. confirmed that the supply of high rate anaerobic fermentation products to the BNR process was beneficial both for nitrogen and phosphorus removal. Osborn et al. (1986) concluded that the composition of the wastewater feed to the BEPR process was important for good nutrient removal. They reported that in many wastewaters such substrates would not be present in adequate concentrations and supplementation from other sources would be required (Pitman et al., 1992).

Generally, primary sedimentation tanks are not regarded as beneficial to BNR since total nitrogen to COD and total phosphorus to COD ratios are adversely affected by primary sedimentation although the load on the biological step is reduced. However, primary sedimentation tanks are used in most modern BNR plants where their role is to remove and thicken primary sludge for its acid fermentation to increase the VFA content of the wastewater fed to the BNR reactors, thus to improve process performance.

Biological sludge hydrolysis is gaining popularity in the recent years. The process makes it possible to increase biological nutrient removal by at least 10-15 %. It increases the potential of process stability and flexibility through production and storage of easily degradable organics and subsequently dosing when needed in the process. Making the most of the fermentation process at the wastewater treatment plant may allow reactor volumes to be reduced and increase the treatment capacity without requiring much more space. It is also cost effective as compared with the addition of chemical materials, such as methanol, as supplemental carbon sources.

The main disadvantage of addition of VFA's to BNR processes is the increased loads of nitrogen, phosphorus, and suspended solids. However, since most of the carbonaceous and nitrogenous matter is in the particulate form and because the organic carbon release rate from sludge particulate matter is significantly higher than

that of nitrogenous matter, less ammonia-nitrogen will be introduced into the BNR system.

In the following section, anaerobic digestion of primary sludge will be studied in detail.

2.3.4.1 Anaerobic digestion of primary sludge

The process of sludge digestion can be considered as three discrete stages; hydrolysis and acid formation (non-methanogenic phase), followed by methane formation (methanogenic phase) as depicted in Figure 2.3. As can be seen from the figure, insoluble organics are hydrolyzed to soluble organics by hydrolytic bacteria after which acid forming bacteria converts soluble organics to volatile acids. Finally, methanogenic bacteria produces gases by using volatile acids.

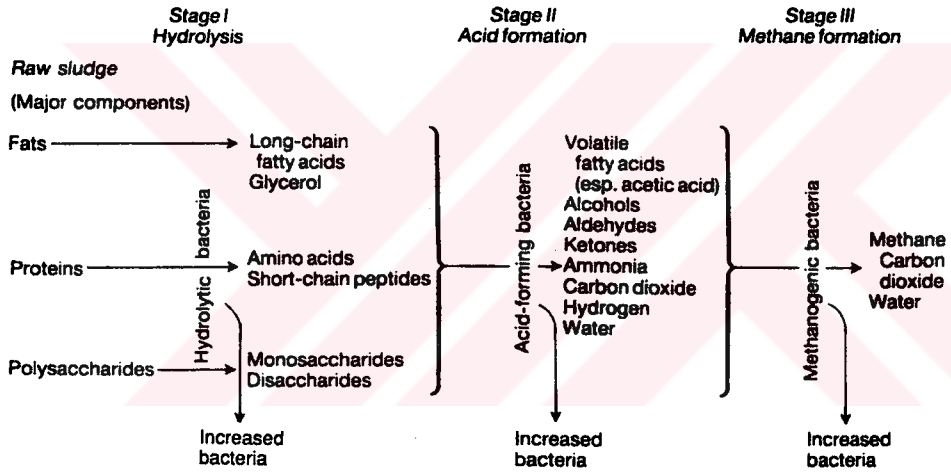

Figure 2.3 Three stages involved in sludge digestion (Gray, 1989)

Although, the microorganisms involved at each stage are metabolically dependent on each other, the growth and metabolism of acid forming and methanogenic bacteria are very different in terms of physiology, nutritional requirements, growth kinetic capabilities, and sensitivity to environmental stresses. An instability occurring between these groups may lead to the accumulation of intermediary products and inhibit the methane formers.

Besides bacteria as the major group of microorganisms involved in anaerobic digestion, fermentative ciliate and flagellate protozoa and some anaerobic fungi also occur. No electron acceptors such as oxygen, sulphate, or nitrate are utilized in the

process. Energy transformation is by the ATP system with energy being stored by the reaction of ADP and inorganic phosphate (P_i) to form ATP (Gray, 1989).

In general, bacteria are unable to take up particulate organic material and first it has to be broken down into soluble polymers or monomers. Thus, in the first stage of anaerobic digestion, the major substrates in the sludge are hydrolyzed to basic components: proteins to amino acids, fats to glycerol and long-chain fatty acids, and polysaccharides to mono- or disaccharides.

Proteins are hydrolyzed to smaller units such as polypeptides, oligopeptides, or amino acids by extracellular enzymes called proteases, which are produced by only a small proportion of the bacteria. The majority of the bacteria are able to utilize these smaller peptides or the amino acids, which pass through the cell wall and are broken down intracellularly. The production of protease is in far excess of that required, even though protease producing bacteria represent a small percentage of the total bacteria present. The most active proteolytic bacteria are the spore-forming *Clostridium* sp. In sewage sludge, the ability to hydrolyze starch is the most common activity of anaerobic cellulolytic bacteria which are predominantly gram-negative coccobacci, with *Bacteroides ruminicola* being a particularly common species and present in anaerobic sludge at concentrations of between 10^4-10^5/ml. Other species, including gram-positive species forming curved rods have been isolated by Hobson and Shaw (1971) (Gray, 1989).

The heterogenous group of facultative and anaerobic bacteria, which are responsible for hydrolysis, are also responsible for acid formation. In this second stage, the hydrolysed substrate is converted to organic acids and alcohols, with new cells also being produced. Various biochemical pathways are utilized including fermentation and β-oxidation. Fermentation is defined as a microbial process in which organic compounds serve both as electron donors and as electron acceptors, and is an anaerobic form of energy production. There is very little stabilization of the substrate in terms of BOD_5 or COD removal, with the products of acid fermentation being large organic molecules. The major acid-forming organisms are Bacillus sp., Micrococcus sp., and Pseudomonas sp. Mono- and disaccharides, long-chain fatty acids, glycerol, amino acids, and short-chain peptides provide the main carbon source for growth with saturated fatty acids, carbon dioxide and ammonia being the main end-products. Alcohols, aldehyde, and, ketones are also produced but only in

small quantities. When no external electron acceptor is present, as is the case in acid fermentation, pyruvate can undergo several alternative reactions, which regenerate NAD from NADH. Acetic, propionic, butyric, and lactic acids are the most frequently produced end-products during the second stage and Toerien (1970) found that these acids were produced by 87, 67, 10, and 70 % respectively of the 92 acid forming bacterial isolates he examined. Propionic and longer chain fatty acids are degraded by an intermediate microbial group called the obligate hydrogen-producing acetogenic bacteria, whereas other acid-producing bacteria, referred to as the homoacetogenic bacteria, produce acetic and sometimes other acids (McInerney et al., 1980) (Gray, 1989). Ethanol, propionic acid, and butyric acid are converted to acetic acid by acetogenic (acetate and hydrogen producing bacteria) according to the following reactions (Bitton, 1994):

$$\underset{\text{ethanol}}{CH_3CH_2OH} + CO_2 \rightarrow \underset{\text{acetic acid}}{CH_3COOH} + 2H_2 \qquad (2.79)$$

$$\underset{\text{propionic acid}}{CH_3CH_2COOH} + 2H_2O \rightarrow \underset{\text{acetic acid}}{CH_3COOH} + CO_2 + 3H_2 \qquad (2.80)$$

$$\underset{\text{butyric acid}}{CH_3CH_2CH_2COOH} + 2H_2O \rightarrow \underset{\text{acetic acid}}{2CH_3COOH} + 2H_2 \qquad (2.81)$$

Table 2.11 Enumeration and identification of anaerobic bacterial populations in sewage sludge digesters after Zeikus (1980) (Gray, 1989)

Group	Numbers (per ml)	Genetic Identity
Hydroltytic bacteria		Majority unidentified
Total	10^8-10^9	Gram-negative rods
Proteolytic	10^7	Eubacterium
Cellulolytic	10^5	Clostridium
Hydrogen producing acetogenic bacteria	10^6	Unidentified Gram-negative rods
Homoacetogenic bacteria	10^5-10^6	Clostridium Acetobacterium
Methanogens	10^6-10^7	Methanobacterium Methanospirillum Methanococcus Methanosarcina Methanothrix
Sulphate reducers	10^4	Desulfovibrio Desulfotomaculum

The third and final stage in anaerobic digestion is methane fermentation where the end-products of acid fermentation are converted to gases, mainly methane and carbon dioxide, by several different species of obligate anaerobic bacteria. Since the subject of methanogenesis is beyond the scope of this thesis, this stage will not be discussed.

Table 2.11 presents species of anaerobic bacteria in sewage sludge digesters.

2.3.4.2 Optimization of acidogenic digestion

Recognizing the substantial difference in the metabolic characteristics of the acid and methane formers, a two-stage process may be optimized by concentrating on either hydrolysis of the substrate or on the slowly growing methanogenic bacteria. To optimize acid phase digestion, the use of primary sedimentation tanks, separate high rate digesters, or activated sludge digesters for the fermentation of primary sludge can be considered (Osborn et al., 1986).

When suspended organic solids are removed from sewage in primary sedimentation tanks, they readily undergo anaerobic fermentation in the accumulated sludge layer in the bottom of these tanks. On some installations, it might not be possible to carry out fermentation in sedimentation tanks or thickeners, i.e., the sedimentation tanks could have inadequate facilities to handle larger volumes of sludge and the plant may not have thickeners. The use of a separate anaerobic digester can have further advantages such as manipulation of process conditions like retention time, mixing temperature. A further source of fermentation products could be activated sludge where the fermentable substrate would be the biomass itself or adsorbed colloidal and other suspended solids. Some researchers (Barnard, 1974; Nicholls, 1975; Venter et al., 1978) have reported that considerable success could be obtained by allowing activated sludge to undergo fermentation (Osborn et al., 1986).

Once fermentation products have been produced, they have to be made available to the microorganisms. In order to achieve this objective, basically three methods are employed in the literature, namely, addition of whole fermented primary sludge, addition of fermented primary sludge to the inlet of primary sedimentation tanks, and recycling of primary sludge.

In the first option, fermented primary sludge either from the bottom of sedimentation tanks or from an acid digester is added back into the feed of the stage where deficiency of carbon occurs. This might be the anaerobic zone of the five stage Bardenpho process for phosphorus removal or post-denitrification reactor where the amount of carbon available for denitrification usually becomes limited. Particularly, in large treatment plants, it is not economical to return all the acid sludge from a digester or a primary sedimentation tank to the activated sludge process due to additional power and tank volume requirements. In such cases, it is necessary to elutriate the volatile fatty acids and other substrates out of the acid sludge. Therefore, it might be considered to feed the acid sludge into the inlet to the primary sedimentation tanks where it comes into contact with a large volume of sewage for elutriation. Finally, for the option of recycling of primary sludge, accumulated sludge in the bottom of primary sedimentation tanks is allowed to go anaerobic and a portion of the acid sludge is recycled to the tank inlet. This recycle allows for the elutriation of the fermentation products into the main flow and increases the sludge retention period in the sedimentation tanks. The degree of recycling depends on the quantity of the fermentation products required by the process.

Studies with the acid phase (Eastman and Ferguson, 1981) have shown that the rate-limiting step in the conversion of primary sludge to fermentation products in the acid phase of anaerobic digestion is the hydrolysis of particulates to soluble substrates. Thus, the kinetics of the overall process are determined primarily by the rate of hydrolysis, not by the bacterial growth kinetics. However, favorable conditions for bacterial growth must be provided because hydrolysis is accomplished with enzymes elaborated by the organisms.

Ghosh et al. (1975), proposed a model in order to evaluate the biokinetic characteristics of the acidogenic organisms in an acid-phase digester. The equations were derived from mass balances around an acid digester and based on the growth kinetic model proposed by Monod. A general equation describing the rate of formation of any product, liquid or gas, in terms of mass of the product per unit time per unit volume of the acid digester is as follows:

$$P' = \frac{\alpha(U_e + m\theta)(L\theta - S_1)}{\theta(U_e + U_p + m\theta)} \qquad (2.82)$$

where:

P' = Steady-state formation rate of acidogenesis product at given detention time, [g/l.hr],

α = True product yield constant,

U_p, U_e = Substrate utilization coefficients for growth and energy respectively,

m = Maintenance coefficient for acid formers, [1/hr],

θ = Theoretical detention time, [hr],

L = Substrate loading, [g/l.hr] or [ft^3/day],

S_1 = Steady-state substrate concentration for acid formers, [g/l].

Ghosh et al. proposed the following linear equations for the determination of biokinetic constants, $\hat{\mu}$, K_S, U_p, U_e, m, α_i, α_g, and Y:

$$\theta = \frac{1}{\hat{\mu}} + \frac{1}{S_1}\left(\frac{K_S}{\hat{\mu}}\right) \tag{2.83}$$

$$\frac{L\theta - S_1}{\alpha} = U_p + U_e + m\theta \tag{2.84}$$

$$\frac{L\theta - S_1}{A_1 - A_0} = \frac{1}{\alpha_i} + \frac{X(U_p)}{A_1 - A_0} \tag{2.85}$$

$$\frac{\theta G'_1}{(L\theta - S_1)} = \alpha_g V - \frac{\alpha_g V U_p(X)}{L\theta - S_1} \tag{2.86}$$

where:

$\hat{\mu}$ = Maximum specific growth rate, [1/hr],

K_S = Saturation concentration, [g/l],

X = Biomass concentration, [g VSS/l],

A_1, A_0 = Concentrations of volatile acids at steady state and influent respectively,

α_i = True yield of acidogenesis,

G'_1 = Steady-state gas production rate from acid fermentation, [g/hr],

V = Digester volume, [l].

The critical detention time for any given organic loading is given by the formula:

$$\theta_c = \frac{L + \sqrt{L + 4K\hat{\mu}}}{2\hat{\mu}L} \qquad (2.87)$$

Useful information on the acid phase has been obtained from various studies. Eastman and Ferguson (1981) did an extensive investigation about the acidogenic phase at 35°C. They performed two series of studies, on completely mixed flow through reactor and batch reactor systems. The production of soluble organic carbon in the acid phase was significantly affected by pH but not by the influent solids concentration. Although pH was not controlled, it did not fall below 5.1 because of the buffering of ammonia released from amino acid fermentation. In flow through reactors, at a detention time of 36 hours, the soluble COD was 42 % greater at pH 6.67 than at pH 5.15. However, the maximum amount of soluble COD obtained in batch tests before active methanogenesis began was only 15 % higher at pH 6.6 than at pH 5.2. The soluble organic carbon produced during the acid phase consisted primarily of volatile acids about 85 % to 95 %. Acetic and propionic acids were about equally important on a COD basis. From batch tests in which the pH was controlled between 5.1 and 6.8, both the short chain fatty acids and soluble COD production was higher at the higher pH values. They also found that the lipids in the influent were not degraded to VFA's. Figure 2.4 shows the composition of acid phase influent and effluent for domestic primary sludge. Another important conclusion of their study is that a relatively low yield of VFA's was obtained. The maximum estimated yield was about 0.223 mg VFA (as COD)/mg influent total COD. The yields obtained from the flow through systems, at 3 days sludge age, were only 0.161 mg VFA (as COD)/mg influent total COD.

In bench and pilot-scale tests, Bundgaard et al. observed that, in hydrolysis stage 20-30 % of the carbohydrate fraction and about 15-25 % of the protein fraction was degraded. No degradation of the lipid fraction was recorded since hydrogen partial pressures exceeding 10^{-3} atm inhibited degradation of the long chain fatty acids in the acetogenic phase. They also claimed that, the dry solid content in the fermenter must not exceed 10 % to avoid the loss of easily degradable organic matter. The loss of easily degradable organic matter increased with a higher dry solid percentage in the fermenter.

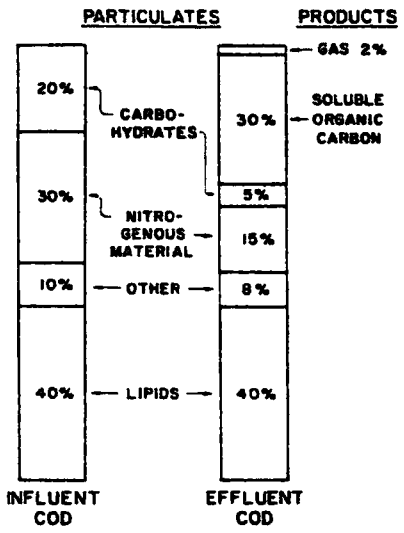

Figure 2.4 General composition of acid phase influent and effluent for domestic primary sludge (Eastman and Ferguson, 1981)

Ghosh et al. (1975) performed experiments in a continuous flow acid digester. A 15 to 120 % increase in total volatile acid (as acetic acid) and a 20 to 90 % increase in ammonia-nitrogen was observed as compared to the influent concentrations. These increases were accompanied by decreases in volatile solids, pH, and an increase in alkalinity from about 300 mg/l as $CaCO_3$ in the influents to 700 mg/l in the effluents. They observed that volatile solids was the fraction which served as the major substrate for the acid formers. Under mesophilic conditions, acidogenesis of activated sludge occurred at a pH of 5.7 and an oxidation-reduction potential of –240 mV. The following biokinetic properties were exhibited by acid formers: Maximium specific growth rate of 0.16 1/day; minimum generation time of 4.3 hr; saturation constant of 26 g volatile solids/l; maintenance coefficient of 0.033 1/hr; growth yield coefficient of 0.40; acetic acid yield constant of 0.28; propionic acid yield constant of 0.11; butyric acid yield constant of 0.25; valeric acid yield constant of 0.25; and gas yield constant of 0.071. The optimum range of loadings and detention times were between 2 to 5 lb volatile solids/day.ft^3 (1.33 to 3.34 g/hr.l) and 10 to 24 hr respectively.

Zoetemeyer et al. (1979) studied the influence of the pH value on acidogenesis. An acid reactor was operated and the main products of the acid fermentation were butyric, propionic, acetic, formic and lactic acid and ethanol. They observed that product distribution at 90 % of the maximum growth rate was fairly constant up to the pH value of 6, after which dramatic changes of the main products occurred from

butyric acid to lactic acid, and subsequently to acetic acid, formic acid and ethanol (Figure 2.5). They stated that the stable operation of acidogenesis of carbohydrates in a single as well as a two stage anaerobic process was barely possible in a pH range of 6 and 8.

Rabinowitz and Oldham (1985b) operated a fermenter in a pilot biological excess phosphorus removal (BEPR) plant. The fermenter sludge age was maintained at 2.5, 3.5, 5 and 10 days. The fermenter was operated at ambient temperatures, except during winter when the temperature was controlled around 20°C. VFA's produced in decreasing order were acetic, propionic and butyric acids. Acetic and propionic acids made up more than 95 % of the total VFA's. The ratio of acetic to propionic acids (as acetic acid) was approximately 55/45 which appeared to be independent of the fermenter sludge age. At 3.5 and 5 days of sludge ages, optimum VFA yields were obtained as 0.093 mg HAc/mg influent COD. Slightly lower yields were observed as 0.078 and 0.082 HAc/mg influent COD at the 2.5 and 10 day sludge ages respectively (Lilley et al., 1990).

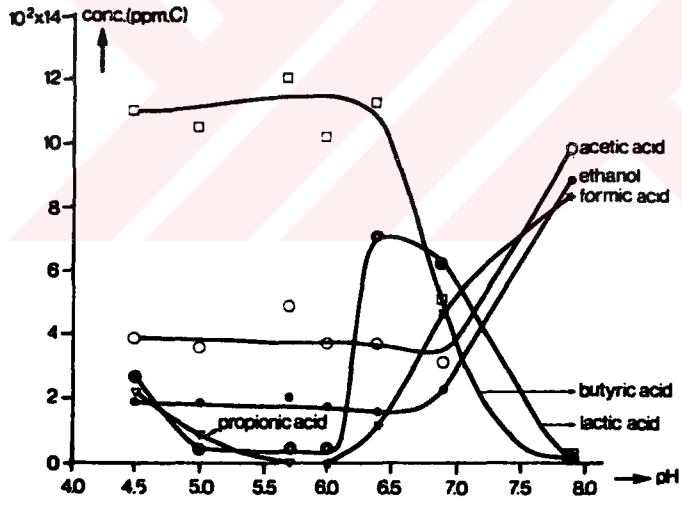

Figure 2.5 Product distribution (at μ=0.9 $\hat{\mu}$) as a function of pH (Zoetemeyer et al., 1979)

Gupta et al. (1985) investigated the effects of temperature, pH and retention time on VFA production. During the study, temperatures of 10, 20 and 30°C, retention times of 3, 6 and 9 days were tested. pH was either uncontrolled or controlled at 7. They observed that the control of pH at 7 did not affect the net total VFA production but affected the relative concentrations of acetic and propionic acids. Maximum net total VFA production was obtained at 6 days retention time at 30°C. The lower yield at 9

days at 30°C was attributed to methane fermentation. During uncontrolled pH tests, the lowest average pH was 5.63. Lower pH values were not observed probably due to the natural buffering capacity of the sludge. Very low yield values were obtained during this study. At 9 days sludge age, for example, the yield was 0.064 mg VFA (as COD)/mg fermenter influent COD (Lilley et al., 1990).

Lotter and Murphy (1986) suggested that acid fermentation could be improved by raising the temperature. Only the total amount of generated VFA's was affected by temperature and the ratio of generated acetic to propionic acids at 14°C and 20°C appeared to be similar.

Pitman and Lotter (1986) investigated the generation of VFA's in two anaerobic digesters and in a primary settling tank. Comparing the two systems they concluded that considerably higher levels of VFA's were achieved in primary sedimentation tanks than in acid digesters. However, elutriation of the sludge in the primary sedimentation tank added non-VFA COD to the primary sedimentation tank overflow.

Kristensen et al. (1992) performed a pilot study to investigate biological nitrogen removal supported by biological sludge hydrolysis, together with chemical pre-precipitation. They observed that COD solubilization (COD yield), during sludge hydrolysis, depended strongly on temperature. At a retention time of 1 day at 15°C, the COD yield was just above 2 %, but when the temperature was raised to 30°C, the yield raised to 10 %. At a retention time of 2 days, the COD yield seemed to be less dependent on temperature. Thus, at 15°C the COD yield was 8 %, and increased to 13 % at 30°C. In the hydrolysate, VFA-COD made up to 60 % of total COD. Acetate constituted 50 % of total VFA-COD, while the rest was made up by longer chained acids, mainly propionate and butyrate. They also noted that, the activated sludge settling characteristics could be negatively influenced by the addition of hydrolysate. The filamentous growth was probably favored by a combination of sulphide and easily degradable organics in the hydrolysate.

Elefsiniotis and Oldham (1994) investigated the effect of hydraulic retention time (HRT) on acidogenic digestion of primary sludge. For this purpose bench-scale continous-flow experiments were performed in completely mixed and up-flow anaerobic sludge blanket reactors. Their results showed that both VFA production

and COD solubilization increased significantly with increasing HRT up to 12 hours, but dropped moderately at a longer HRT. Acetic and propionic acids were the most prevalent VFA's produced averaging in either reactor, 46 % and 32 % of the total. Butyric acid followed with an average value of 8 %. However, the percent VFA distribution appeared to be independent of HRT. On the contrary to the findings of Eastman and Ferguson and Bundgaard et al., they found that, regardless of the experimental conditions, lipids and carbohydrates were converted at higher percentages than proteins. Furthermore, protein utilization appeared to be independent of reactor configuration, but carbohydrate and lipid degradation patterns were a function of the reactor regime.

Lilley et al. (1990) did a thorough investigation about the acid fermentation of primary sludge at 20°C. Their results indicated that raw sludge had an acid fermentation potential for the production of VFA, of about 17 % of the influent sludge COD, i.e., a specific potential yield of 0.17 mg VFA as COD/mg influent sludge COD and this potential did not appear to be influenced by the concentration of the influent primary sludge. The production of VFA seemed to follow a first order reaction with a reaction rate constant of about 0.16 1/day at 20°C. Besides generating VFA, acid fermentation also generated soluble complex molecules approximately equal in concentration of VFA. Thus, of the total COD concentration generated, approximately half was VFA (as COD) and the other half was non-VFA soluble COD. The rate of production of the total soluble COD appeared to follow a first order reaction not influenced by the sludge concentration. They observed that, at hydraulic retention times of longer than 6 days at 20°C, methane fermentation could occur reducing the net VFA yield. At 6 days of hydraulic retention time at 20°C, the COD yield of the VFA was approximately 38 % of the potential yield, i.e., 0.065 mg VFA as COD/mg influent sludge COD, revealing that only a minor fraction of the VFA potential could be generated at short retention times.

Ragazzi et al. operated psychrophilic (lab-scale) and mesophilic (pilot-scale) fermentors to evaluate the efficiency of biological nutrient removal processes. HRT for the lab-scale fermenters were selected as 3, 4, 5, 10 and 15 days while the mesophilic pilot-plant was tested at 0.5,1 and 2 days HRT. They concluded that, both psychrophilic and mesophilic hydrolysis followed first order kinetics. Mesophilic conditions favored methanogenesis even at short hydraulic retention times and pH

control was recommended at HRT higher than 1 day. Mesophilic conditions allowed for hydrolysis of a bigger portion of the particulate COD and the rate of hydrolysis was much higher under mesophilic conditions.

Rodriguez et al. (1998) analyzed the performance of an SBR reactor fed with anaerobically fermented wastewater. For this purpose, they used two SBR reactors, one as a fermenter and the other as an activated sludge SBR. Without pH neutralization, VFA concentrations up to 223±24 mg/l were achieved. 63 % of the VFA comprised acetic and 12 % propionic acids. Inorganic nitrogen removal was 88, 66, and 81 percent for the 0.13, 0.25, and 0.35 kg COD_{tot}/kg TSS.d organic loading rates respectively. The settleability of the sludge was improved with SVI values around 80 ml/g.

Engeler et al. (1998) investigated the suitability of fermented sludge (a mixture of primary and excess sludge) for phosphorus and nitrogen removal. At the end of first five days of fermentation at 20°C, 17 % of the total COD as soluble carbon was produced while this fraction was increased by another 5 % for another five days. Therefore, it was concluded that, longer fermentation periods were not efficient. For denitrification experiments, two strategies were considered. First, for a direct comparison of the different products of fermentation, six short chain fatty acids were mixed (the mixture was equimolar) and added to the activated sludge. Two groups were characterized: The preferentially used linear short chain fatty acids (acetate, propionate, n-butyrate, n-valeriate) and the branched forms (iso-butyrate, methyl-butyrate). It was found out that the degradation rates of substrates based on COD are lower for the branched fatty acids. Second, for testing the real mixture of fermentation products, filtrate from fermentation was used. Denitrification based on dissolved fermentation products resulted in a rate of 6 g NO_3-N/kg COD_{tot}.hr which was higher than for acetate (3.8 g NO_3-N/kg COD_{tot}.hr) and for propionate (1.7 g NO_3-N/kg COD_{tot}.hr). 8 % of the dissolved COD identified at the end of the experiment, which might consist of long chain fatty acids, were either degraded or adsorbed. The mean value for COD yield during the whole respiration time with fermentation products was found as 0.57. In a similar experiment with acetate as the sole substrate, yield was calculated as 0.63. During biological phosphorus removal tests, acetate and propionate were identified as the most important substrates among the six fatty acids examined.

2.3.4.3 Bacterial storage mechanism

Recent research has demonstrated that microorganisms are able to store fermentation products as organic internal storage polymers in the forms of polyhydroxyalkanoates (PHA), mainly polyhydroxybutyrate (PHB), lipids and glycogen or inorganic storage polymers such as polyphosphate, under transient (unbalanced) conditions. Accumulation of substrates could also occur in which substrate is taken up in an unchanged form. Transient conditions take place when the microorganisms have external substrate available only for relatively short periods of time. Under such conditions, two main types of physiological adaptation can occur, depending on the nature of the biomass, on the nature and the concentration of substrate, and on previous operating conditions: The biomass can adapt itself to the new conditions by increasing the growth rate from the previous level (growth response) and/or by rapidly storing the available substrate (storage response). If the microorganisms are able to store substrates during imposed transients and subsequently reuse them for growth, they will gain a competitive advantage (Majone et al., 1998).

Activated sludge processes where storage polymers play a significant role can be investigated in four categories (Loosdrecht et al., 1997): Biological phophorus elimination, bulking sludge control, contact stabilization and A/B processes and COD conversion.

Although, the storage phenomena have not been studied in detail and are usually excluded in modelling, in the process of biological phosphorus elimination, it is generally accepted that storage polymers are of prime importance in the metabolism of biological phosphorus bacteria. After it was recognized that, fatty acids serve as the major substrates for biological phosphorus bacteria, it was also clear that this substrate is accumulated in the cell during the anaerobic phase and storage forms a crucial part of the bacterial metabolism. The same fact also applies to the recently introduced "G-bacteria" which can also store substrates under conditions where an electron acceptor is absent. Here, storage is based on the energy released in the conversion of sugars to polyhydroxyalkanoates (Loosdrecht et al., 1997).

Competition of filamentous and non-filamentous bacteria is based on the difference of substrate affinity. Because filamentous bacteria have a lower maximum growth rate but higher substrate affinity than floc-formers, they can dominate at low

substrate concentrations. Selectors have been designed as a remediation for bulking sludge problems. In the selector, the soluble COD is taken up by the sludge and accumulated in the cells as storage polymer. The good performance of aerobic selectors or intermittent feeding seems to indicate that floc-formers have an advantage over filaments. According to the accumulation-regeneration theory (Grau et al., 1982), the selection of floc formers also requires a second aeration tank where the floc formers grow on accumulated/stored substrate regenerating the limited accumulation/storage capacity.

In both contact stabilization (Ulrich and Smith, 1951) and A/B (Bohnke, 1977) processes, sludge and influent are mixed and after a relatively short time separated again. The non-soluble compounds are incorporated physically in the sludge floc. The soluble components are accumulated inside the cells as storage polymers. In the contact stabilization process, the return sludge is aerated in the sludge regeneration tank where stored substrate is oxidized and cell growth occurs. Storage pools are also emptied for a new cycle. In the A/B process, the majority of the stored material will be removed with the excess sludge and fermented in the sludge digester.

Recent studies with respirometry and pure substrates point out to the occurrence of storage phenomena during COD removal processes. The relationship between oxygen and substrate consumed is much lower than found in pure culture studies. This deviation also observed by Chudoba et al. (1973), between observed and pure culture yields, strongly indicates the formation of storage polymers.

It should also be noted that, in addition to the above described processes, transient conditions are typical for sequential batch reactors where biomass experiences alternately high and low substrate conditions, nutrient removal processes where alternating anaerobic, anoxic, and aerobic environments are exposed and a metabolic stress is added to the kinetic one, or where a concentration gradient of the substrate is produced like in plug-flow configuration of the aeration tanks.

Very little literature information exists about storage under anoxic conditions. Similar situations arise in nitrogen removal processes (denitrification) where an external source of readily biodegradable substrate has to be added to increase the denitrification rate. Fatty acids or other COD sources added can be partially stored inside the cells resulting in a relatively high COD/N ratio needed for the

denitrification process. On the other hand, a significant situation arises where denitrification on the stored products increases "endogenous" denitrification rate. As an example, an aerobic contact/anoxic stabilization process has been proposed (Jones et al., 1990a and 1990b) where a higher "endogenous" denitrification rate is achieved in the anoxic tank due to biosorption and storage of COD in the aerobic one (Majone et al., 1998).

Cech and Chudoba (1983) investigated the kinetics of COD removal in non-proliferating glucose-acclimated activated sludge systems. The general differential equation describing the process involved a rate constant for storing processes (zero order), a rate constant for accumulation processes (first order), and volumetric accumulation capacity. The rate constant of accumulation capacity was found to be independent of the initial concentration of biomass but dependent on the type of cultivation or on the composition of a mixed culture. For activated sludge cultivated semi-continuously (non-filamentous), it was assigned a range of 1.8 to 2.6 1/hr and another range of 0.8 to 1.0 hr for activated sludge cultivated continuously in a completely mixed unit (highly filamentous). Activated sludge microorganisms cultivated semi-continuously had a specific accumulation capacity around 600-750 mg/g, whereas those cultivated continuously in a completely mixed unit had their accumulation capacity totally saturated.

Alleman and Irvine (1980) studied bacterial storage as the electron source for denitrification process. They found that sequencing batch reactor operation could provide repetitive cycling of environmental phases which would lead to the activation of the storage mechanism. Using a synthetic, high-strength waste stream they achieved over 92 % total nitrogen removal without addition of a supplemental carbon source. During the denitrification reaction, depletion of the cellular glycogen reserve was observed.

Majone et al. (1996) investigated the transient response, and the effect of the S_0/X_0 ratio and of the starvation time on two different mixed cultures (bulking and non-bulking) by continuous or intermittent feeding of a CSTR. In most experimental conditions, PHB storage was shown to be the prevailing mechanism of substrate removal. In particular, the culture dominated by floc- formers showed a very fast response to the substrate spike with a high observed yield. According to their findings, on the contrary to Chudoba et al. (1992), the ratio of substrate/biomass

initial concentration did not play a major role in determining the type and extent of the response. Starvation did not affect the response of the floc-formers to transient conditions whereas it significantly decreased filamentous bacteria response. For the filamentous bacteria, both growth, and even more significantly, storage were negatively affected.

Goel et al. (1998), did an experimental study to quantify the effects of intracellular storage polymers on the oxygen uptake rate (OUR) profile and biomass yield coefficients, for acetate, glucose and starch, using a sludge from anaerobic-aerobic sequencing batch reactor. In case of acetate as substrate, two different OUR areas were observed as, OUR due to external substrate and OUR due to storage. PHA concentration in the biomass increased significantly, indicating that the major storage polymer was PHA. After depletion of bulk substrate in acetate reactors, PHA did not start depleting immediately. It was deduced that there might have been be a pool of some intermediate intracellular metabolite which were utilized by biomass before switching to the stored PHA. The maximum storage was about 45 %, 68 % and 36 % of total acetate, glucose and starch COD removed from bulk respectively. Equation (2.88) was proposed to calculate biomass yield coefficients considering the storage compounds.

$$Y_{G,P} = 1 - \frac{OC_T}{(S_R - S_S)} \qquad (2.88)$$

In this equation the following abbreviations apply:

S_R = Bulk substrate removed, [mg COD/l],
S_S = Storage as glycogen or PHA [mg COD/l],
OC_T = Total oxygen consumed, [mg O_2/l].

The calculated yield coefficients based on equation (2.88) were 0.24-0.28, 0.58-0.50, and 0.64 for acetate, glucose, and starch respectively, indicating the dependence of yield factors on the types of the substrates. Besides, they were significantly lower than the yield coefficients calculated based on the conventional approach where storage was not accounted for.

Van Aalst-van Leeuwen et al. (1997) investigated the behaviour of *Paracoccus panthatrophus* under feast-famine conditions. They stated that after the depletion of

the external substrate, the stored PHB was used as growth substrate. PHB accumulation was found to be strongly dependent of the growth rate of the organism before the pulse addition of acetate. PHB accumulation was correlated to the difference in maximum acetate uptake and the acetate required for growth. Based on the experimental results, they proposed a model describing the observed kinetics of the PHB formation and consumption. In the model, they stated that provided that the sludge age was known and the PHB levels were measured, the maximum PHB content of the biomass (f_{PHB}) and the rate constant K_P for growth on PHB could directly be determined. They also claimed that the parameters K_P and f_{PHB} were properties of the sludge and therefore, would depend on the process conditions such as type of substrates and organisms, temperature and pH.

Majone et al. (1998), conducted batch experiments under anoxic and anoxic/aerobic conditions to investigate storage and subsequent use of stored products. A mixed culture selected under aerobic conditions was able to take up acetate and store it as PHB under anoxic conditions. PHB was produced until acetate was eliminated and then it was consumed at a slower rate than acetate. When acetate was depleted, NUR was also decreased sharply due to the shift from a readily available substrate like acetate to the slowly available PHB. The NUR on acetate in the presence of storage was 20 mg N/g VSS.hr while it dropped to 10-3 mg N/g VSS.hr in the "endogenous" phase when denitrification was on the stored PHB. It was observed that acetate uptake and PHB storage were quite faster under aerobic conditions with respect to the anoxic ones. Based on all observations it was assumed that the hydrolysis of the stored product was the rate limiting step of the "endogenous" metabolism and that the hydrolysis rate was not highly dependent on aerobic or anoxic conditions. It was further determined that all aerobic heterotrophs able to store were also able to denitrify.

CHAPTER 3 METHODS FOR THE ASSESSMENT OF ENDOGENOUS DECAY RATE AND INVESTIGATION OF DENITRIFICATION KINETICS FOR HYDROLYZED CARBON SOURCES

3.1 Assessment of Endogenous Decay Rate

3.1.1 Critical appraisal of the current practice

In the literature, two methods exist for the determination of aerobic endogenous decay rate coefficient. Both of these methods have been proposed by Marais and Ekama (1976), based on their batch aerobic digestion model. The first one involves the measurement of VSS while the second one is a respirometric method performed with OUR measurement. They concluded that both would give approximately similar values for b_H, but the second method would give more accurate results and was less laborious. Below, the theoretical basis of these two methods will be given.

3.1.1.1 Determination of b_H using volatile suspended solids

Total volatile solids (X_T) comprises, active heterotrophic biomass (X_H), endogenous residue solids concentration (X_E), and inert solids concentration (X_I). At time (t) in a batch aerobic digester,

$$X_{T(t)} = X_{H(t)} + X_{E(t)} + X_{I(t)} \quad (3.1)$$

Since X_I remains constant,

$$X_{I(t0)} = X_{I(t)}$$

Active biomass degrades according to a first order equation as below:

$$\frac{dX_H}{dt} = -b_H X_H \quad (3.2)$$

Equation (3.2) can be solved as:

$$X_{H(t)} = X_{H(0)}\, e^{-b_H t} \tag{3.3}$$

f_E units of X_E is generated with every unit of X_H that disappears

$$X_{E(t)} = f_E\, (X_{H(0)} - X_{H(t)}) \tag{3.4}$$

From (3.3)

$$X_{E(t)} = f_E\, (X_{H(0)} - X_{H(0)}\, e^{-b_H t}) \tag{3.5}$$

If $X_{H(t)}$ and $X_{E(t)}$ are substituted into equation (3.1) and rearranged:

$$X_{T(t)} = (1 - f_E)\, X_{H(0)}\, e^{-b_H t} + f_E\, X_{H(0)} + X_I \tag{3.6}$$

Then,

$$X_{T(t)} - f_E\, X_{H(0)} - X_I = (1 - f_E)\, X_{H(0)}\, e^{-b_H t} \tag{3.7}$$

As t approaches infinity (∞) $e^{-b_H t}$ approaches zero, so:

$$X_{T\infty} = f_E\, X_{H(0)} + X_I = C \tag{3.8}$$

where C is a constant value. Substituting for $f_E\, X_{H(0)} + X_I$ from equation (3.8) into equation (3.7):

$$X_{T(t)} - C = I = (1 - f_E)\, X_{H(0)}\, e^{-b_H t} \tag{3.9}$$

Equation (3.9) shows that if some constant concentration C is subtracted from each $X_{T(t)}$ value, the balance denoted as I would only be a function of X and t.

Since equation (3.9) characterizes an exponential function, it would plot linearly for lnI vs t. The slope defines b_H and the intercept on the I axis, I_0 gives a measure of the active mass

$$I_0 = (1 - f_E)\, X_{H(0)} \tag{3.10}$$

and

$$X_{H(0)} = \frac{I_0}{(1 - f_E)} \tag{3.11}$$

Since $X_{H(0)}$ is known, $X_{I(0)}$ can be determined from the condition at t=0, i.e.:

$$X_{T(0)} = X_{H(0)} + X_{I(0)} \tag{3.12}$$

Equation (3.9) provides the basis of the experimental procedure proposed by Marais and Ekama. In a batch test, a series of $X_{T(t)}$ values are obtained for a long experimental period such as 30 days. A value of C is estimated and subtracted from $X_{T(t)}$ and the balance plotted against ln $(X_{T(t)}$-C) vs time t. If C is too large, the plot curves downwards, if too small it curves horizantally. When the best straight line is obtained, the slope is given by:

$$b_H = \frac{\ln(X_{T(t)} - C) - \ln(X_{T(0)} - C)}{t_1 - t_2} \tag{3.13}$$

$X_{H(0)}$ and $X_{I(0)}$ can be obtained from equations (3.11) and (3.12) respectively.

It has been stated by the authors that, this method was not very reliable for the assessment of b_H due to the difficulties in measuring X_T accurately.

3.1.1.2 Determination of b_H using oxygen utilization rates

Biodegradation process during endogenous decay phase follows a first order mechanism (equation 3.2) and the concentration of the active heterotrophic biomass after a time period $X_{H(t)}$ can be computed as a function of the initial active heterotrophic biomass concentration $X_{H(0)}$ by equation (3.3). f_E is the fraction remaining as endogenous residue, the oxygen demand (OUR) exerted by the biomass during the phase of endogenous decay can be written as:

$$OUR_{(t)} = (1 - f_E)\, b_H\, X_{H(t)} \tag{3.14}$$

Substituting equation (3.3) into equation (3.14):

$$OUR_{(t)} = (1 - f_E)\, b_H\, X_{H(0)}\, e^{-b_H t} \tag{3.15}$$

Equation (3.15) can be written in a linear form as:

$$\ln OUR_{(t)} = \ln ((1 - f_E)\, b_H\, X_{H(0)}) - b_H t \qquad (3.16)$$

Plotting ln $OUR_{(t)}$ vs time t, the slope equals b_H. The intercept on the ln $OUR_{(t)}$ axis at t=0 gives:

$$OUR_{(t)} = (1 - f_E)\, b_H\, X_{H(0)} \qquad (3.17)$$

$X_{H(0)}$ can be solved for by the pre-determined b_H and $OUR_{(t)}$ values.

Based on equation (3.16), this method involves the measurement of OUR in a batch activated sludge system undergoing endogenous respiration. The experimental period is around 10 to 20 days.

The method outlined above was carried out by using activated sludge cultures acclimated to meat processing effluents, leather tanning effluents, and domestic wastewaters. The results will be demonstrated in Chapter 5. As will also be mentioned in Sections 5.1.1.1, 5.1.1.2, and 7.1.1 the most obvious deficiencies associated with the current procedure can be summarized as follows:

- Imprecise measurements due to the low initial electron acceptor utilization rates (in a range of 8 to 2 mg/l.hr) associated with endogenous respiration
- Observation of scattered data usually exhibiting cyclic variations with remarkably low coefficients of determination (r^2)
- The inability to differentiate OUR values associated with endogenous respiration and hydrolysis of adsorbed particulate organic matter

Since the application of the current practice led to results with insufficient accuracy and reliability, an alternative method was proposed to overcome the major drawbacks experienced with the current practice.

3.1.2 Conceptual basis of the proposed method

The proposed method was based on offsetting the observed deficiencies of the current method. For this reason, the major goal was to avoid

- Low OUR measurements associated with endogenous respiration
- Interference of slowly biodegradable substrate

It was therefore, decided to shift OUR measurements to the growth phase i.e., to replace $b_H X_H$ with $\mu_H X_H$. During the growth phase according to Monod kinetics OUR can be expressed as:

$$OUR = \frac{1-Y_H}{Y_H} \hat{\mu}_H \frac{S_s}{K_s + S_s} X_H + (1-f_E) b_H X_H \quad (3.18)$$

Maximum growth conditions prevail in the presence of adequate amount of readily biodegradable substrate, which might be expressed as below:

$$OUR = \frac{1-Y_H}{Y_H} \hat{\mu}_H X_H + (1-f_E) b_H X_H \quad (3.19)$$

Equation (3.19) gives a measure of $\hat{\mu}_H X_H$.

The proposed method aims to reflect the variation of X_H by providing a constant unlimited growth medium, which would ensure a constant $\hat{\mu}_H$ level. The experimental process involves running of an aerobic "main reactor" and an aerobic "feed reactor" in parallel. The main reactor contains heterotrophic biomass, which undergoes endogenous respiration during the whole experimental period. The feed reactor, on other hand, is put into operation whenever (preferably at daily intervals) seeded with the biomass transferred from the main reactor. To ensure maximum growth conditions, the feed reactor is fed with a synthetic solution (Table 4.1), representing readily biodegradable substrate, of fixed quantity and composition together with the mixed liquor of a pre-selected volume, transferred from the main reactor. OUR in the feed reactor is monitored long enough to detect the corresponding initial plateau. The initial OUR (OUR_I) in the feed reactor at time zero (t_0) can be written as:

$$OUR_{1(t0)} = \frac{1-Y_H}{Y_H} \hat{\mu}_H X_{H(0)} + (1-f_E) b_H X_{H(0)} \quad (3.20)$$

The procedure outlined above is repeated after a time period t by transferring the pre-selected volume of mixed liquor to a second batch feed reactor and adding the same amount of substrate. The initial OUR value after time t ($OUR_{1(t)}$) can then be expressed as:

$$OUR_{1(t)} = \frac{1-Y_H}{Y_H}\,\hat{\mu}_H\,X_{H(t)} + (1-f_E)\,b_H\,X_{H(t)} \tag{3.21}$$

Obviously, a lower initial OUR value is observed at time t due to the gradually decreasing activity of the biomass in the main reactor. The concentration of the heterotrophic active biomass in the main reactor can be expressed as a function of the initial active biomass concentration, as previously described by equation (3.3):

$$X_{H(t)} = X_{H(0)}\,e^{-b_H t}$$

Thus, the general expression for OUR_1 at any time instant t can be expressed in terms of the initial active biomass concentration $X_{H(0)}$:

$$OUR_{1(t)} = \left[\frac{1-Y_H}{Y_H}\,\hat{\mu}_H + (1-f_E)\,b_H\right] X_{H(0)}\,e^{-b_H t} \tag{3.22}$$

Writing the above equation in linear form:

$$\ln OUR_{1(t)} = \ln\left[\frac{1-Y_H}{Y_H}\,\hat{\mu}_H + (1-f_E)\,b_H\right] X_{H(0)} - b_H\,t \tag{3.23}$$

is obtained. The slope of this equation yields the aerobic endogenous respiration rate coefficient b_H.

In the same manner, a main anoxic reactor may be run in parallel to an anoxic feed reactor and the same procedure could be carried out for the determination of anoxic endogenous rate coefficient b_{HD}. The general expression for initial nitrate utilization rate at time t ($NUR_{1(t)}$) can be written as:

$$NUR_{1(t)} = \left[\frac{1-Y_{HD}}{2.86Y_{HD}}\,\hat{\mu}_{HD} + \frac{(1-f_E)}{2.86}\,b_{HD}\right] X_{HD(t)} \tag{3.24}$$

Since,

$$X_{HD(t)} = X_{HD(0)}e^{-b_{HD}t}$$

b_{HD} can readily be computed by the following expression

$$\ln NUR_{1(t)} = \ln\left[\frac{1-Y_{HD}}{2.86Y_{HD}}\hat{\mu}_{HD} + \frac{(1-f_E)}{2.86}b_{HD}\right]X_{HD(0)} - b_{HD}t \qquad (3.25)$$

It should be noted that nitrite accumulation should be taken into consideration in the determination of the electron acceptor demand under anoxic conditions as discussed in section 2.2.3.

3.2 Investigation of Denitrification Kinetics for Hydrolyzed Carbon Sources

In this study, primary sludge is considered as an example of hydrolyzed carbon sources. The major components for domestic primary sludge can be listed as volatile fatty acids (VFA's), carbohydrates, alcohols, peptones, and amino acids. Although these components can be assessed individually, the readily biodegradable organic matter content of the primary sludge may also be determined by respirometric analysis. In this study, the denitrification rates and the readily biodegradable fraction of COD was determined in wastewater and primary sludge by the application of the methods discussed in sections 3.2.1.2 and 3.2.1.1 respectively. These methods were also used for the determination of the amount of readily biodegradable substrate introduced to aerobic and anoxic batch feed reactors for the determination of b_H and b_{HD}.

3.2.1 Critical appraisal of the current practice

Ekama et al. (1986) proposed three methods for the determination of readily biodegradable COD (S_s) in the influent. These are:

1. Flow-through activated sludge system method
2. Aerobic batch reactor method
3. Anoxic batch reactor method

Since batch systems were utilized throughout this study, the first method was not applicable and no description will be provided regarding this method.

3.2.1.1 Aerobic batch reactor method

In this test, a pre-selected volume of wastewater or centrifuged primary sludge with a known total COD is mixed in an aerated batch reactor with a pre-selected volume of mixed liquor with known VSS concentration and the reactor contents are stirred

continuously. Samples for OUR measurement are withdrawn from this mixture, starting from the time of initial mixing until about 4 to 5 hours every 5 to 10 minutes. Selection of F/M ratio is very critical for the accurate estimation of S_s. Normally, the initial OUR plateau should be observed for 1 to 3 hours depending on the S_s fraction whereafter the OUR decreases sharply and levels off at a second plateau (Figure 3.1). The initial OUR plateau is due to the utilization of S_s together with the hydrolysis of particulate biodegradable COD. A constant initial OUR is experienced because the concentration of S_s is not limiting. This enables the heterotrophs to grow at a maximum rate ($\hat{\mu}_H$) according to Monod kinetics. If the F/M is too low, the shape of the OUR curve is tall and narrow which results in very quick utilization of S_s. In this case, only a limited number of OUR measurements can be taken which might not assure a reliable initial high OUR. If the F/M is too high, the shape is low and wide and the time when S_s is completely exhausted is quite difficult to assess. Ekama et al. recommend the setting of F/M at around 1.2 times the estimated active fraction of the VSS (f_a) to achieve the ideal step change in OUR i.e.:

F/M = (1 to 1.5) f_a

They also claim that the active fraction of the VSS is a function of the sludge age (θ_x) of the plant from which the sludge is obtained and can be estimated roughly by:

$f_a = 1.41\ (\theta_x)^{-0.53}$ for raw sewage

$f_a = 1.57\ (\theta_x)^{-0.43}$ for settled sewage

They noted that the above relationships were solely for giving some guidance for estimating the F/M of a batch test and should not be used for estimating the active fraction for any other purposes.

After the application of the above procedure, the influent readily biodegradable COD concentration is given by:

$$S_{S0} = \left(\frac{1}{1-Y_H}\right) \Delta O \left(\frac{V_{ml} + V_{ww}}{V_{ww}}\right) \qquad (3.26)$$

where

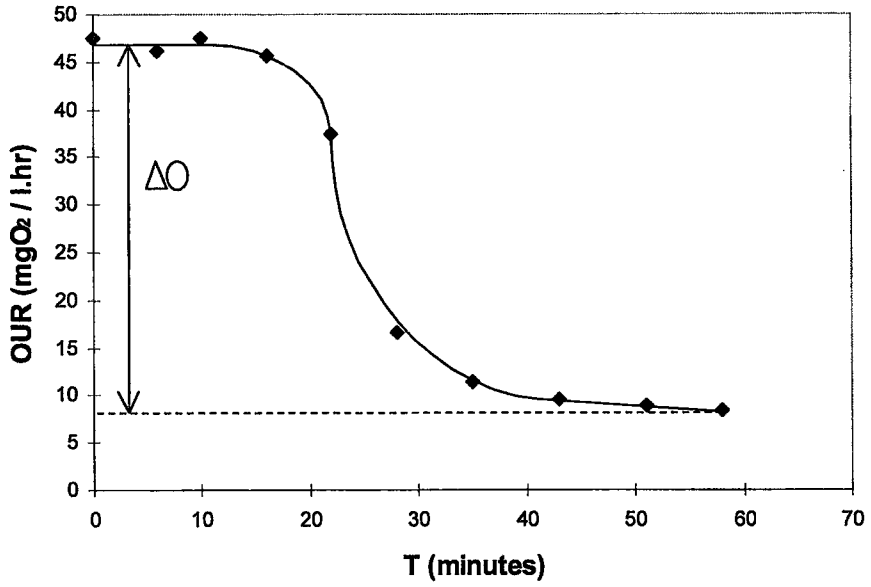

Figure 3.1 Example OUR profile for the illustration of aerobic S_s determination

ΔO = mass of oxygen utilized in S_s consumption per litre of batch mixture (Figure 3.1)

V_{ml} = volume of mixed liquor

V_{ww} = volume of wastewater

$(V_{ml}+V_{ww})/V_{ww}$ is a term used for volumetric correction to convert the amount of S_s measured in the test batch reactor to the amount of S_s actually present in the wastewater.

This test was applied to domestic wastewaters and primary sludges prior to the denitrification experiments. Applications were also carried out for the determination of S_s fed to the aerobic feed reactors in the b_H experiments. An example calculation will be illustrated in Section 7.1.2 with the data obtained from experimental set 9.

3.2.1.2 Anoxic batch reactor method

The basis of the anoxic batch reactor method is nearly identical to the aerobic batch reactor method. The only difference is the measurement of nitrate utilization rate instead of oxygen utilization rate, since nitrate would serve as the electron acceptor under anoxic conditions. Therefore, during the application of the test, nitrate is added externally at the start and the nitrate concentration is monitored for a period of about 4 to 5 hours. Initially, nitrate concentration will decrease at a constant rapid rate due to the utilization of readily biodegradable COD together with the hydrolysis of the

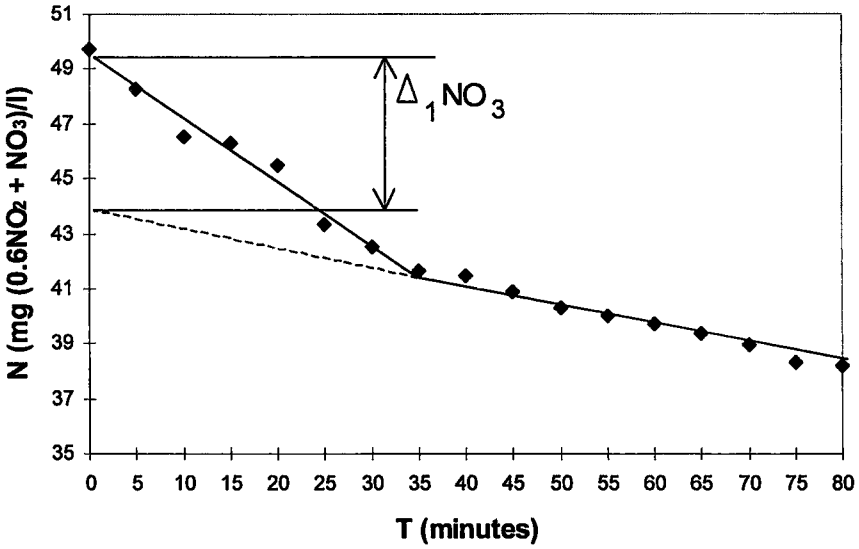

Figure 3.2 Example NUR profile for the illustration of anoxic S_s determination

particulate biodegradable COD. The initial high rate of denitrification is similar to the initial high OUR. The constant rate of denitrification is also indicated by the linearity. During this linear phase, because the concentration of S_s is high enough, the heterotrophic growth occurs at maximum conditions in accordance with Monod kinetics. When S_s is depleted, a decrease in the denitrification rate is observed with a flatter linear slope. This rate is associated with the utilization of readily biodegradable COD generated by the hydrolysis of particulate biodegradable COD. The second rate is again analogous to the second OUR plateau observed in the aerobic batch test (Figure 3.2).

To calculate S_s, the same data as for the aerobic batch test are required i.e., the volume and COD concentration of the wastewater (or primary sludge), the volume and the VSS concentration of the mixed liquor and $\Delta_1 NO_3$ which is the difference between the nitrate concentrations of the intercepts with the vertical axis of straight lines drawn through the initial rapid and second slower rates of denitrification (Figure 3.2). S_s in the influent is given by:

$$S_{S0} = (\frac{2.86}{1-Y_H})\,\Delta_1 NO_3\,(\frac{V_{ww}+V_{ml}}{V_{ww}}) \qquad (3.27)$$

It should be stated that in the application of this method during the present experimental study, nitrate correction ($0.6NO_2^-$-N+NO_3^--N) was used instead of reflecting sole nitrate nitrogen concentrations to account for nitrite accumulation and

thus, to avoid higher denitrification rates which would be observed without this correction.

The above procedure was applied to domestic wastewater, primary sludge and to acetate reactors to assess the rates of denitrification. It was also performed for the assessment of S_s introduced to anoxic feed reactors during b_{HD} experiments. An example calculation will again be illustrated in Section 7.1.2 for the results obtained from experimental set 9.

In the literature, biological, chemical, physical, and physico-chemical methods exist for the determination of readily biodegradable substrate but it is believed that the biological determination is safest (ASM2, 1995). It is also known that the application of aerobic and anoxic batch test results do not necessarily give the same results. This fact will be discussed in detail in section 7.1.2.

CHAPTER 4 EXPERIMENTAL APPROACH

4.1 Experimental Set-up

Acclimation periods were experienced prior to conducting experiments towards the assessment of kinetic parameters. First acclimation studies were started with biomass already acclimated to synthetic wastewater comprising glucose and soy medium. Due to the similarity in composition, domestic wastewater was chosen as the first type of wastewater to be acclimated. For this purpose, 3 and 4 l batch type glass cylindrical reactors were used. Reactors were operated in fill and draw pattern. Aerobic and anoxic cycles (each lasting for one day) were employed since subsequent experimental procedures for the determination of kinetic constants would require biomass acclimated to both media. During aerobic cycles, air flow originating from a diffuser was provided to maintain a dissolved oxygen concentration around 7-8 mg/l which would also enable circulation within the reactor to prevent settling. During anoxic cycles, on the other hand, nitrate was provided externally to comply with a C/N ratio of 5:1. Reactors were covered with stretch foils to avoid air intrusion. Magnetic stirrers were used for mixing purposes. Sludge age was selected as 15 days to allow for more sludge production within the system. This sludge age corresponded to a food to microorganism (F/M) ratio around 0.2 with an approximate VSS value of 1000 mg/l. Reactors were operated at room temperature. Daily COD removal efficiencies were determined as well as total suspended solids (SS) and volatile suspended solids (VSS) concentrations to monitor reactor stability.

Domestic wastewaters were obtained from Tuzla Industrial District (for the first year) and Ataköy Wastewater Treatment Plant (for the following year). Various parameters (COD_{total}, $COD_{filtered}$, $COD_{settled}$, TKN, ammonia-nitrogen, total phosphorus, pH, alkalinity, total suspended solids, volatile suspended solids) were monitored for wastewater characterization. No pH adjustment was required prior to reactor feeding. At the end of the week, reactors were fed with a synthetic wastewater, theoretically representing domestic wastewater, as a substitute for the weekend. Buffer and mineral needs were satisfied with Solution A and Solution B, respectively. The compositions of synthetic wastewater and buffer and mineral solutions are presented in Tables 4.1 and 4.2. Meat processing effluents were obtained from a factory producing delicatessen products. Wastewater was analyzed for the above mentioned parameters. No pH adjustment was again required due to the similarity of meat processing effluent characteristics to domestic wastewaters. Synthetic wastewater was provided together with buffer and mineral solutions at the end of the week for feeding purposes. Leather tanning effluents were obtained from Tuzla Industrial District. Biomass was transferred from batch reactors acclimated to leather tanning effluents and operated in fill and draw pattern with daily aerobic/anoxic cycles. Chromium and sulphur were monitored in addition to the parameters stated above. Chemical pre-treatment was usually required due to high concentrations of chromium and sulphur.

4.2 Determination of Kinetic Constants

4.2.1 Endogenous decay rate coefficient

The theoretical basis of the conventional method for the assessment of b_H as proposed by Marais and Ekama (1976) is outlined in Section 3.1.1.2. The experimental procedure involves the measurement of oxygen utilization rates (OUR) in a batch digestion system during 10 to 20 days. Experimental start-up is initiated by aerating tap water to saturation before being mixed with the biomass. Nitrification inhibitor was added to the tap water to avoid any oxygen consumption due to nitrification. Usually, biomass contents of two acclimation reactors were combined and added to the batch digestion reactor to achieve a high concentration of

Table 4.1 The composition of synthetic solution (Henze, 1992; Sözen, 1995)

	Experimental COD	Amount/l	mg COD
Acetic Acid	1000 mg/ml	10 ml	10000
Propionic Acid	1290 mg/ml	3.1 ml	4000
Ethanol	1190 mg/ml	1.68 ml	2000
Glutamic Acid	1105 mg/ml	3.62 ml	4000
Glucose	880 mg/ml	4.54 ml	4000
Total			24000 mg COD/l

Table 4.2 The composition of buffer and mineral solutions (O'Connor, 1972)

Solutions	Substance	Concentration (g/l)
Solution A	K_2HPO_4	320
	KH_2PO_4	160
Solution B	$MgSO_47H_2O$	15
	$FeSO_47H_2O$	0.5
	$ZnSO_47H_2O$	0.5
	$MnSO_43H_2O$	0.5
	$CaCl_2$	2.0

VSS. Right after the mixing of biomass and tap water, pH was controlled around 7 by adding phosphate buffer. Immediately, aliquots were withdrawn for OUR analysis from the magnetically stirred reactor. For sampling, a 50 ml glass vessel was used. Then, the oxygen probe was inserted into the vessel on the magnetic stirrer to record the rate of oxygen utilization by the oxygen meter. The mouth of the probe was compatible with the size of the vessel to prevent air inflow. This procedure of sample withdrawal was repeated three to four times a day. Batch digestion reactor was aerated continuously during the experimental period to avoid shortage of oxygen and provide complete mixing of the reactor contents. Each day evaporation losses were made up with distilled water and reactor walls were cleaned with a brush to avoid wall growth. The theoretical procedure suggests the measurement of OUR until the rates are decreased to 10 % of the initial value. However, this was practically not possible since the initial OUR values were around 8 mg/l and it was beyond the sensitivity of the oxygen meter to measure and monitor OUR values less than 2 mg/l. For this reason, OUR measurements were continued for 7 to 10 days after which accurate measurement of OUR was not possible.

For the assessment of nitrate utilization rate (NUR) during endogenous respiration phase, an equal amount of biomass was provided, as in the b_H test, for the purpose of direct comparison. Initially, tap water was bubbled with nitrogen gas to supply oxygen free conditions. Phosphate buffer was again added to achieve a pH value

around 7. A glass flask was used as the anoxic batch reactor with piping for sampling, nitrogen gas inflow and air outflow. Nitrate was added externally as potassium nitrate solution to comply with a C:N ratio of 5:1. Immediately after mixing of reactor contents and biomass, a sample was withdrawn from the sampling port with simultaneous nitrogen intrusion. Samples were filtered with Whatman GF/C filters (1.2 μm pore size) before being analyzed by the autoanalyzer system for nitrite and nitrate-nitrogen. Sampling procedure was repeated three to four times a day accompanied with nitrogen bubbling to avoid air intrusion. The batch test continued for three to four days usually after which nitrate- nitrogen was depleted in the batch reactor.

The theoretical basis of the method proposed for the assessment of aerobic and anoxic heterotrophic endogenous decay coefficients was stated in Section 3.1.2. In this framework, two reactors, namely main and feed reactors, were operated simultaneously. The main reactor undergoes endogenous respiration while growth occurs in the feed rector due to the constant amount of readily biodegradable substrate provided every time the reactor is put into operation. For the determination of aerobic endogenous respiration rate coefficient, an aerobic main reactor of 4 l was started with an approximate VSS concentration around 1000 mg/l. An incubator was employed for temperature control. pH was maintained around 7 and evaporation losses were made up with distilled water everyday as in the conventional method. Nitrification inhibitor was again added. The aerobic feed reactor, on the other hand, was operated everyday. The 500 ml reactor was inoculated with the same volume of mixed liquor (200 ml) transferred from the main reactor. 2 ml of synthetic solution with a corresponding COD value of 50 mg was added which yielded an initial OUR rate in the range of 40-50 mg/l.hr. 2 ml buffer and 0.5 ml mineral solutions to comply with a C:N:P ratio of 100:5:1 were also fed to the system. The feed reactor was brought to a final volume of 500 ml by 255 ml aerated tap water. A dissolved oxygen concentration of 7-8 mg/l was maintained in both main and feed reactors. OUR was monitored in the feed reactor for 60 to 90 minutes by withdrawing samples every 5 to 10 minutes.

In the same way, for the assessment of anoxic endogenous respiration rate coefficient, a 5 l batch anoxic main reactor was used. 100 mg/l nitrate-nitrogen was externally added to the main reactor. A 500 ml flask was used as the anoxic feed

reactor. Both main and feed reactors were equipped with a rubber stopper with piping for sampling, nitrogen gas inflow, and air outflow. The feed reactor was operated everyday and inoculated with 250 ml mixed liquor transferred from the main reactor, 2 ml synthetic solution, 2 ml buffer solution, 0.5 ml mineral solution and 195 ml tap water. The amount of nitrate-nitrogen added to the feed reactor was selected to avoid the need for external nitrate addition to the feed reactor and the necessity of dilution since the range of measurement of total oxidized nitrogen was 0 to 50 mg/l. Mixed liquor samples of 10 ml were withdrawn from the feed reactor during 2-2.5 hours for every 5-10 minutes. Whatman GF/C filter papers were used for filtering samples prior to the analysis of nitrite and nitrate-nitrogen. Nitrogen gas was purged during sampling to avoid air intrusion to both main and feed reactors and continuous magnetic stirring was provided.

4.2.2 Readily biodegradable organic matter

In the literature, three methods have been proposed by Ekama et al. (1986) for the assessment of readily biodegradable content of wastewaters for which the theoretical basis was explained in Sections 3.2.1.1 and 3.2.1.2.

Aerobic batch reactor method involves monitoring of OUR in a reactor operated with a pre-selected F/M ratio to give an optimum shape of OUR plateau as described previously. Reactor contents include wastewater (of known total COD), nitrification inhibitor, and tap water if necessary for final volume adjustment. After being aerated to saturation, the contents were mixed with biomass of known VSS concentration on a magnetic stirrer and samples were withdrawn immediately for OUR analysis by the oxygen meter. Sampling from the aerated batch reactor was repeated after the dissolved oxygen concentration in the glass vessel decreased to around 2 mg/l. The whole procedure was ended when a lower second plateau was observed. Anoxic batch reactor method was applied in similar conditions. Nitrate was added as an electron acceptor to comply with a C:N ratio of 5:1 to the batch reactor equipped with rubber stopper and piping for sampling and nitrogen and air flow, in addition to wastewater of known COD strength, and tap water when necessary. Before biomass (of known VSS) was added to the reactor, all contents were bubbled with nitrogen gas to supply oxygen free conditions. An immediate sample was followed by samples withdrawn at 5 minute intervals for the first hour and 10 minute intervals for

the following hours. Nitrogen gas was purged continuously during the whole experimental period. C:N:P ratio of 100:5:1 was satisfied with buffer and mineral solutions when necessary. Samples for nitrate and nitrite-nitrogen were filtered through Whatman GF/C filters before being transferred to the autoanalyzer.

For primary sludge samples obtained from the domestic wastewater treatment plant at Ataköy/İstanbul, centrifugation of sludge was performed for five minutes at 10000 rpm, prior to assessing the readily biodegradable organic matter by the aerobic batch reactor method. Biomass was seeded from fill and draw reactors acclimated to domestic wastewater and operated under 24 hr aerobic/ 24 hr anoxic conditions for a sludge age of 15 days, for aerobic and anoxic batch reactors. Before anoxic batch tests, sludge was either centrifuged or filtered through Whatman GF/C (1.2 μm) or membrane (0.45 μm) filters. The filtrate and centrifugate were refrigerated at 5°C until they were used. When acetate was employed for comparison, 100 % glacial acetic acid was added to the reactors. No pH adjustment was necessary.

4.2.3 Maximum specific growth rate

The method for the assessment of maximum specific growth rate ($\hat{\mu}_H$) was adopted from Kappeler and Gujer (1992). Accordingly, a batch test procedure with centrifuged wastewater was carried out with a very small amount of biomass. COD/VSS ratio was chosen around 4. The batch test was initiated with aerating wastewater to saturation and adding nitrification inhibitor. Biomass was finally added to the aerated and magnetically stirred mixture and OUR samples were withdrawn and analyzed as explained before. $\hat{\mu}_H$ was calculated by equation (4.1) as proposed by Kappeler and Gujer:

$$\ln \frac{OUR}{OUR_0} = (\hat{\mu}_H - b_H)t \qquad (4.1)$$

To be able to determine the active fraction of biomass, a $\hat{\mu}_H$ test was conducted in parallel to an experiment conducted for the assessment of readily biodegradable substrate at a relatively lower F/M ratio. The active biomass fraction can be assessed according to expression (4.2) as proposed by Sözen (1995). An example calculation will be demonstrated in section 5.2.

$$f_a = \frac{Y_H}{1 - f_x Y_H} \frac{OUR_1}{\hat{\mu}_H X_T} \quad (4.2)$$

4.3 Methods of Analysis

The analysis of basic wastewater parameters was performed in accordance with Standard Methods (1995). For the determination of SS and VSS, samples were filtered through Whatman GF/C (1.2 μm) filters.

A CHEM LAB autoanalyzer system was used for the measurement of total oxidized nitrogen and nitrite-nitrogen. Total oxidized nitrogen was reduced to nitrite by the method of hydrazine-reduction and nitrite-nitrogen was determined by the colorimetric method using sulphanilamide solution. Dissolved oxygen concentration was measured with a WTW OXI DIGI 550 oxygen meter connected to a Rang Hilger W+W Recorder 600.

CHAPTER 5 EXPERIMENTAL RESULTS

Experimental studies for the assessment of endogenous decay rate were conducted in two experimental periods. First period involves experiments based on the conventional method proposed by Marais and Ekama (1976). It was applied to domestic and industrial wastewaters, including meat processing and leather tanning effluents. In the second period of the experimental study, the method presented in the context of this thesis was tested for domestic wastewaters. Besides endogenous carbon, primary sludge was also studied as a carbon source for denitrification. The performance of primary sludge was compared with acetate, which is considered as a well-defined external carbon source.

In all experimental sets, the electron acceptor utilization rates under anoxic conditions will be expressed as nitrite plus nitrate-nitrogen concentration ($0.6NO_2^-$-N + NO_3^--N). The principles associated with nitrite-nitrogen correction were discussed in section 2.2.2.

5.1 Experimental Studies for the Assessment of Endogenous Decay Rate

5.1.1 Experiments based on the conventional method

All experiments in this section were conducted according to the method proposed by Marais and Ekama (1976) which was described in section 3.1.1.2. In some of the experimental sets, the method suggested by Kristensen et al. (1992) was employed for the comparison of electron acceptor utilization rates in aerobic and anoxic media.

5.1.1.1 Meat processing effluents

Meat processing effluents were fed to 3 - 4 l batch reactors operated in daily aerobic and anoxic cycles. Sludge age was maintained as 15 days. After an acclimation period of seven weeks, reactors were subjected to endogenous decay. The characteristics of meat processing effluents used during the acclimation period and experimental set 1 are summarized in Table 5.1.

In experimental set 1, aerobic sludge was provided from the biological treatment unit of a meat-processing factory, operated as a sequencing batch reactor. b_H test was conducted in a 2 l aerobic reactor with an initial F/M ratio of 0.02. Figures 5.1a to 5.1d show the b_H results obtained from experimental set 1. From these figures, it can be clearly seen that, b_H values vary with the duration of the experimental period i.e., for 40 days b_H was found as 0.02 1/day, for 20 days as 0.05 1/day, for about 10 days as 0.05 1/day and for 6 days it was calculated as 0.16 1/day.

Experimental set 2 was performed by activated sludge cultures obtained from 3 - 4 l batch acclimation reactors. Biomass concentration in the b_H test reactor was 1270 mg VSS/l. In order to assess an η_E factor for endogenous respiration, a 1 l anoxic batch reactor was operated in parallel, with an equal amount of biomass. Results obtained from experimental set 2 are illustrated in Figures 5.2a and 5.2b with the b_H value as 0.12 1/day and NUR_E value as 24.1 mg N/l.day. According to these results η_E was computed as:

$$\eta_E = 2.86 \frac{24.1\, mg\ N/l.day}{24hr/day * 3.5\, mg\ O_2/l.hr} = 0.82$$

Table 5.1 Characterization of meat processing effluents

Experimental Set	COD (mg/l) Total	COD (mg/l) Filtered	pH	TKN (mg/l)	Total P (mg/l)	SS (mg/l)	VSS (mg/l)
1 Acclimation period	325	90	7.06	17	14	275	173
Week 1	490	270	7.1	23	15	430	265
Week 3	325	170	7.1	21	11	-	-
Week 5	940	350	6.5	35	17	-	-
Week 7	370	185	7.0	18	12	-	-
Mean	360.0	169.0	7.0	22.8	13.8	352.5	219.0
Std deviation	78.0	67.5	0.3	7.2	2.4	109.6	65.1

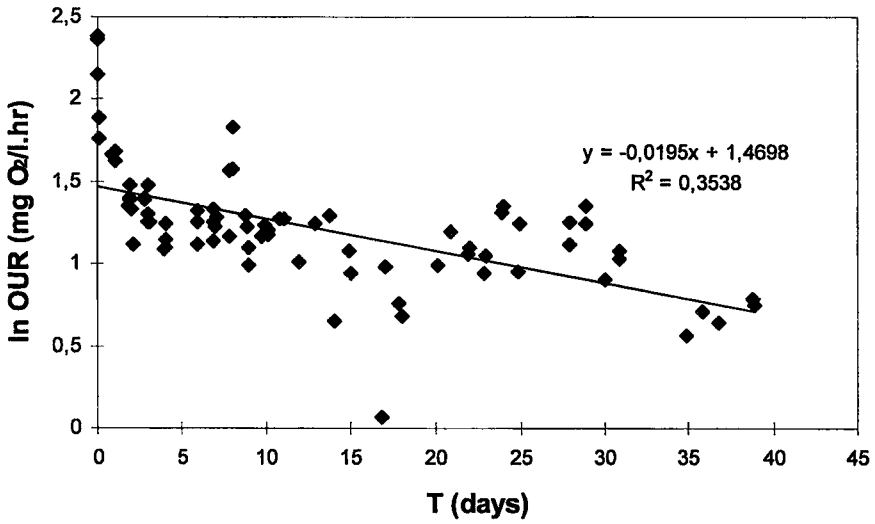

Figure 5.1a Results of b_H experiment for meat processing effluents- experimental set 1- experimental duration of 40 days

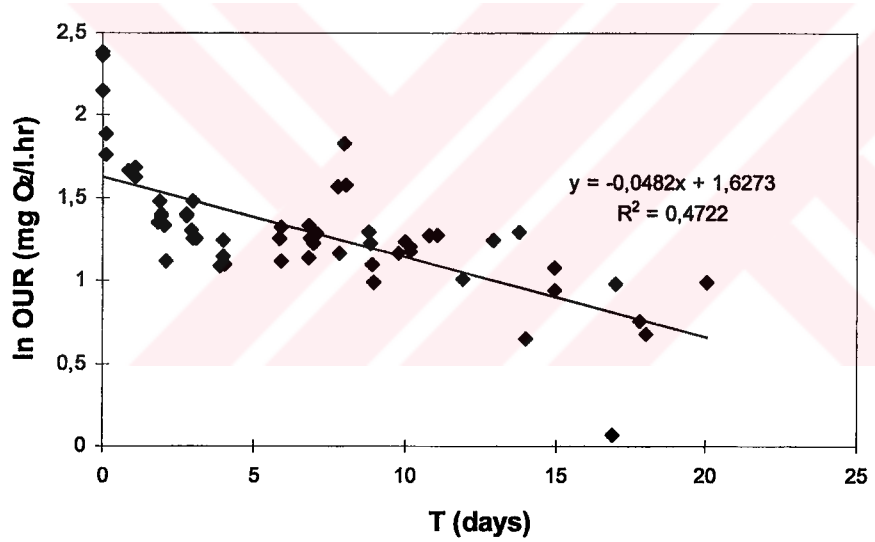

Figure 5.1b Results of b_H experiment for meat processing effluents- experimental set 1- experimental duration of 20 days

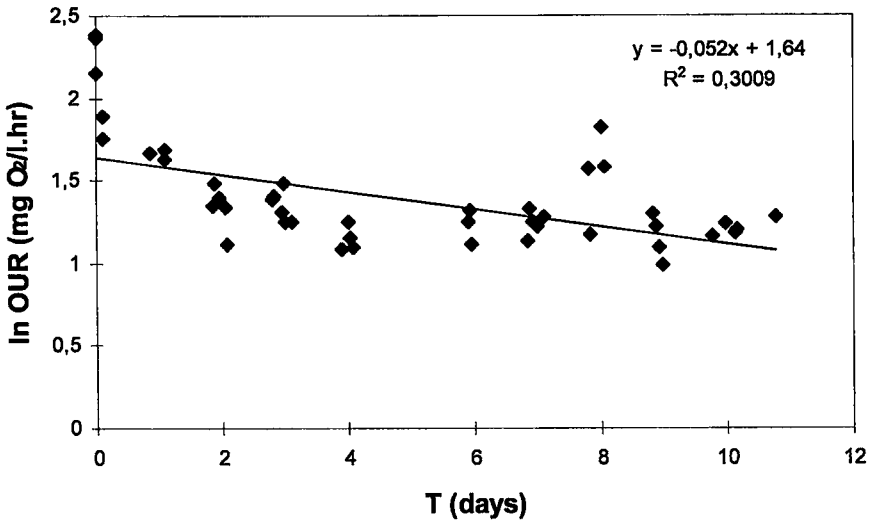

Figure 5.1c Results of b_H experiment for meat processing effluents- experimental set 1- experimental duration of 12 days

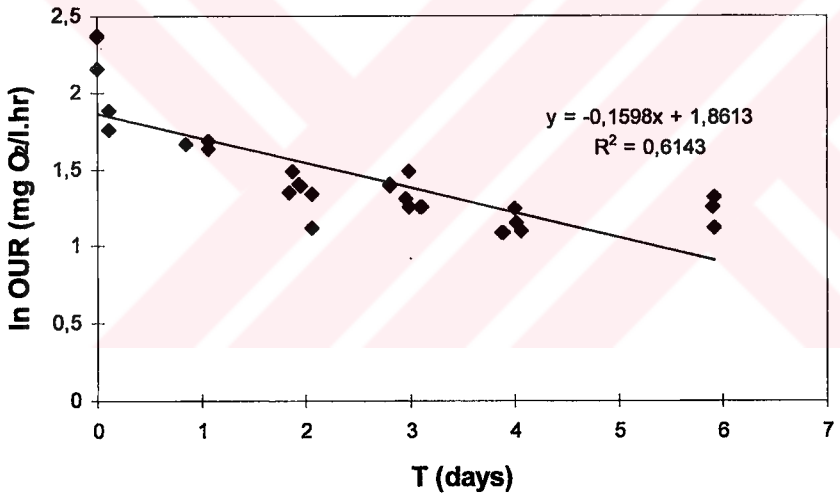

Figure 5.1d Results of b_H experiment for meat processing effluents- experimental set 1- experimental duration of 6 days

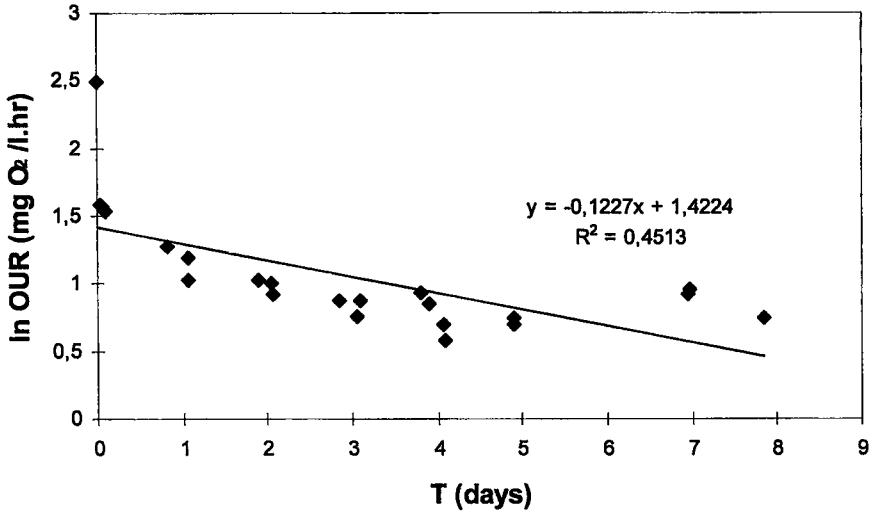

Figure 5.2a Results of b_H experiment for meat processing effluents- experimental set 2

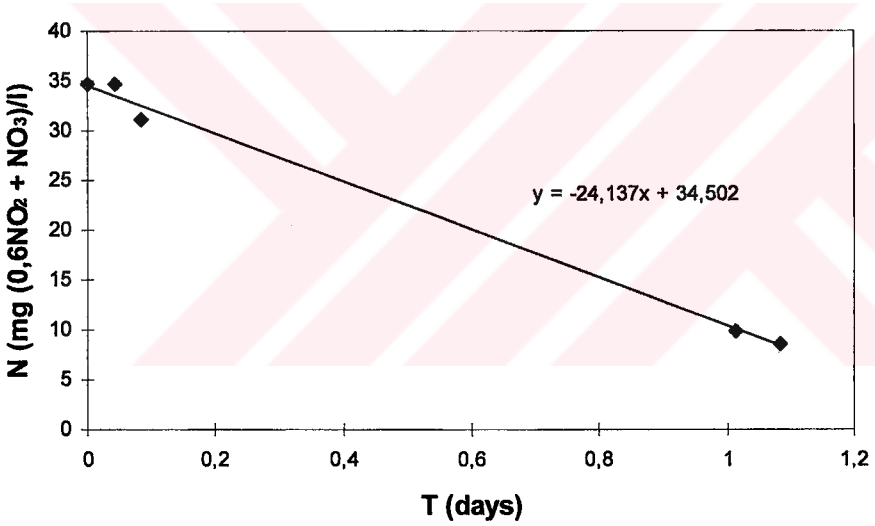

Figure 5.2b Determination of nitrate utilization rate for meat processing effluents- experimental set 2

5.1.1.2 Leather tanning effluents

As in the case of meat processing effluents, leather tanning effluents were also fed to 3 - 4 l batch reactors operated in daily aerobic and anoxic cycles with a sludge age of 15 days. After an acclimation period of about two months, reactors were subjected to endogenous decay.

Sludge utilized in experimental set 3 was obtained from a fill and draw reactor acclimated to leather tanning effluents and operated in daily aerobic/anoxic cycles with a sludge age of 15 days. b_H test reactor with 1 l volume contained 3460 mg VSS.

The same features as in the case of meat processing effluents were observed in the third experimental set as can be seen from Figures 5.3a, 5.3b, 5.3c, and 5.3d. b_H value was calculated as 0.05 1/day for an experimental duration of 30 days, as 0.06 1/day for 20 days, as 0.08 1/day for 10 days, and as 0.2 1/day for a time period of about 5 days. It should also be noted that the coefficient of determination is remarkably low in these cases.

The aim of the fourth experimental run was to compare aerobic and anoxic electron acceptor utilization rates, therefore, an aerobic reactor was operated in parallel to an anoxic reactor, both undergoing endogenous decay. Sludge was originated from 3 - 4 l acclimation reactors. Both reactors contained 4620 mg VSS. In the fourth experimental run, b_H was calculated as 0.12 1/day and the corresponding electron acceptor utilization rate (NUR_E) was 34.6 mg N/l.day as shown in Figures 5.4a and 5.4b. From these values, η_E was computed as 0.82.

5.1.1.3 Domestic wastewaters

An acclimation period of one year was experienced prior to the experiments conducted for the assessment of endogenous decay kinetics for domestic wastewaters. 3 - 4 l cylindrical batch reactors were operated in a fill and draw pattern with daily aerobic and anoxic cycles. Sludge age was adjusted to 15 days corresponding to an approximate F/M ratio of 0.2 with a VSS value around 1000 mg/l. Since the acclimation period was quite long, characterization values will be presented in average monthly values of major selected parameters as in Table 5.2.

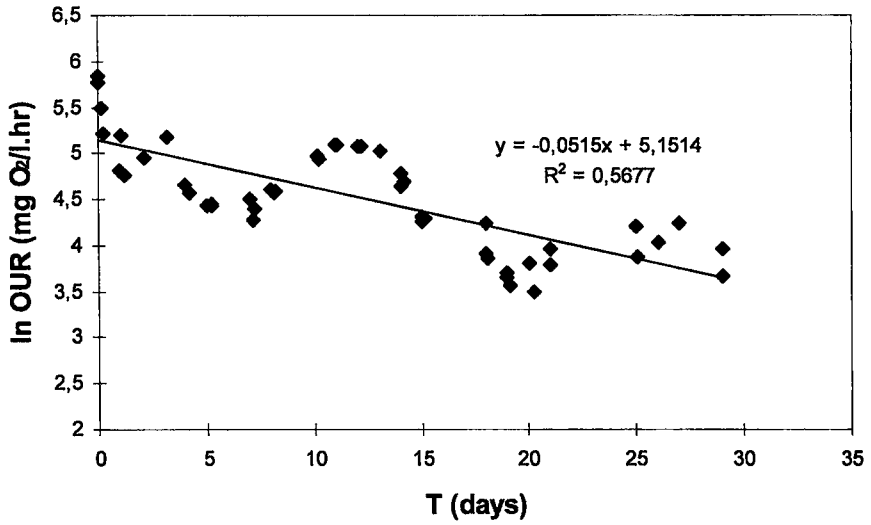

Figure 5.3a Results of b_H experiment for leather tanning effluents – experimental set 3 – experimental duration of 30 days

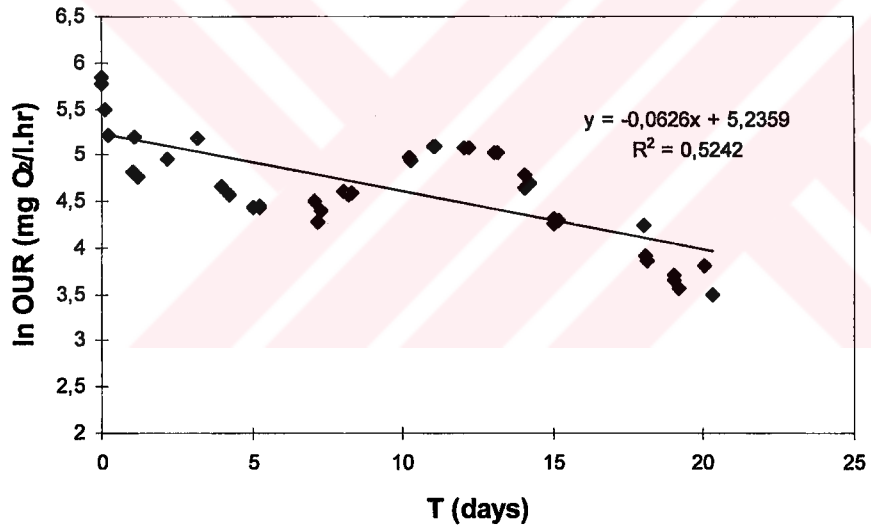

Figure 5.3b Results of b_H experiment for leather tanning effluents – experimental set 3 – experimental duration of 20 days

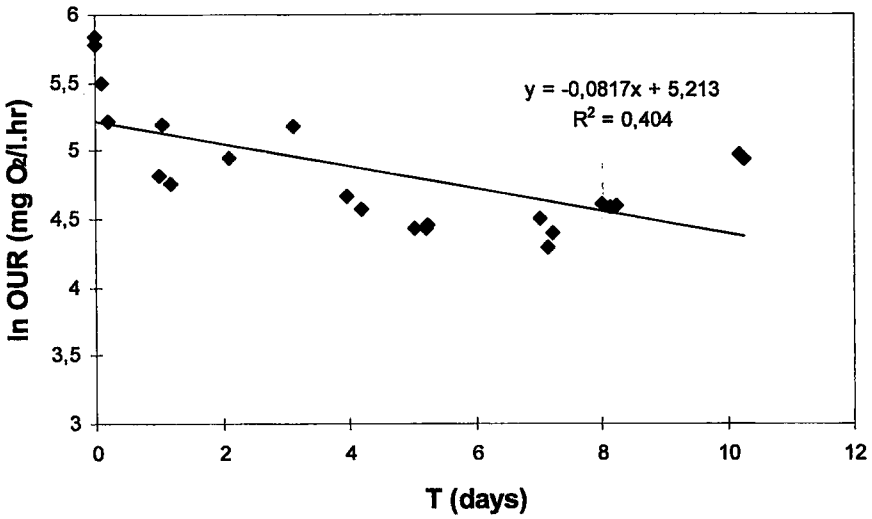

Figure 5.3c Results of b_H experiment for leather tanning effluents – experimental set 3 – experimental duration of 10 days

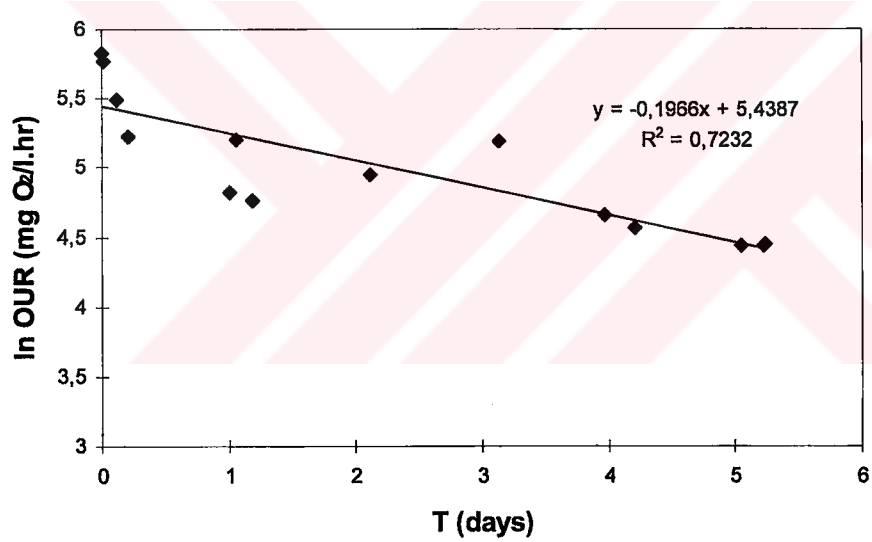

Figure 5.3d Results of b_H experiment for leather tanning effluents – experimental set 3 – experimental duration of 5 days

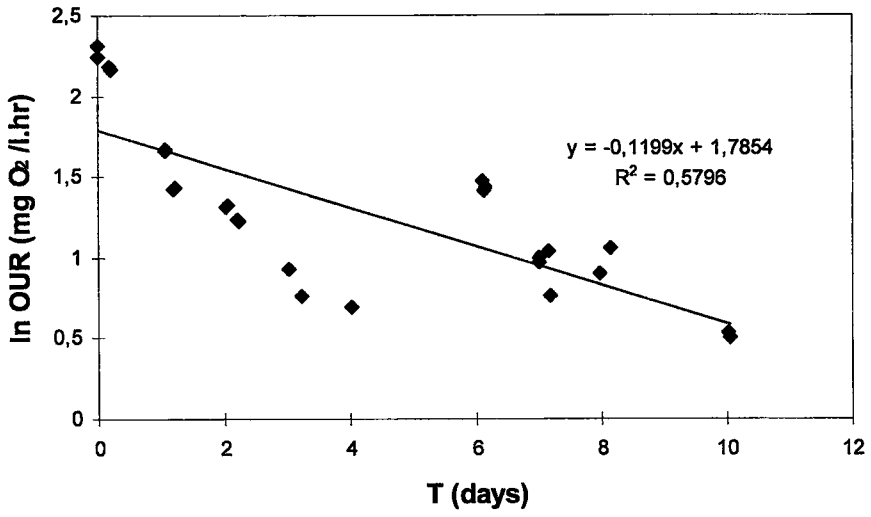

Figure 5.4a Results of b_H experiment for leather tanning effluents – experimental set 4

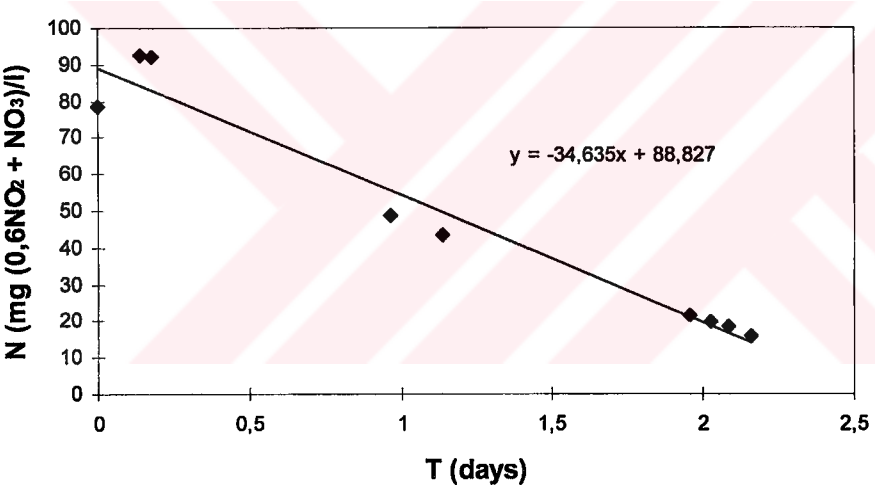

Figure 5.4b Determination of nitrate utilization rate for leather tanning effluents – experimental set 4

Table 5.2 Monthly average values of selected parameters for domestic wastewaters used for acclimation purposes-I

Month	COD (mg/l)		pH	Total P (mg/l)	TKN (mg/l)	Ammonia-N (mg/l)	Alkalinity (mg/l) (as $CaCO_3$)
	Total	Filtered					
1	160	80	7	4	24	15	210
2	205	89	7.2	8	35	21	200
3	240	60	7.1	3	22	12	190
4	275	120	7	5	40	23	-
5	270	120	6.8	5	32	28	-
6	240	120	7	8	45	32	-
7	335	180	7.3	8	45	30	-
8	350	125	7	12	63	40	220
9	260	120	6.8	7	31	16	
10	220	110	7.2	4	35	20	190
11	360	150	7.5	7	42	26	260
12	325	90	7.1	10	31	17	-
Mean	270.0	113.7	7.1	6.8	37.1	23.3	211.7
Std Dev	62.2	31.9	0.2	2.7	11.0	8.2	26.4

Experimental set 5 was conducted both in aerobic and anoxic media with the aim of measuring electron acceptor consumption rates. For the assessment of aerobic endogenous respiration coefficient, b_H test was performed in a 2 l reactor with 3080 mg VSS.

Figures 5.5a and 5.5b show the b_H results and electron acceptor utilization profiles obtained from experimental set 5. b_H value was evaluated as 0.09 1/day and NUR_E was assessed as 29.0 mg N/l.d. η_E was calculated as 0.58.

Experimental sets 6 and 7 were performed similarly in aerobic and anoxic media. In set 6, a 2 l reactor with a VSS amount of 5120 mg was involved with an anoxic 1 l reactor with the same amount of VSS. In experimental set 7, again a 2 l aerobic reactor with volatile suspended solids amount of 3630 mg was used in parallel to a 1 l anoxic reactor with the same VSS content.

Figures 5.6a, 5.6b, 5.7a, and 5.7b illustrate the results obtained from experimental sets 6 and 7. b_H values evolved from these two sets are very similar being 0.15 1/day from set 6 and 0.14 1/day from set 7. In the same way, nitrate utilization rates obtained from sets 6 and 7 were 36.3 mg N/l.d and 30.9 mg N/l.d respectively. Corresponding η_E values are 0.86 and 0.82.

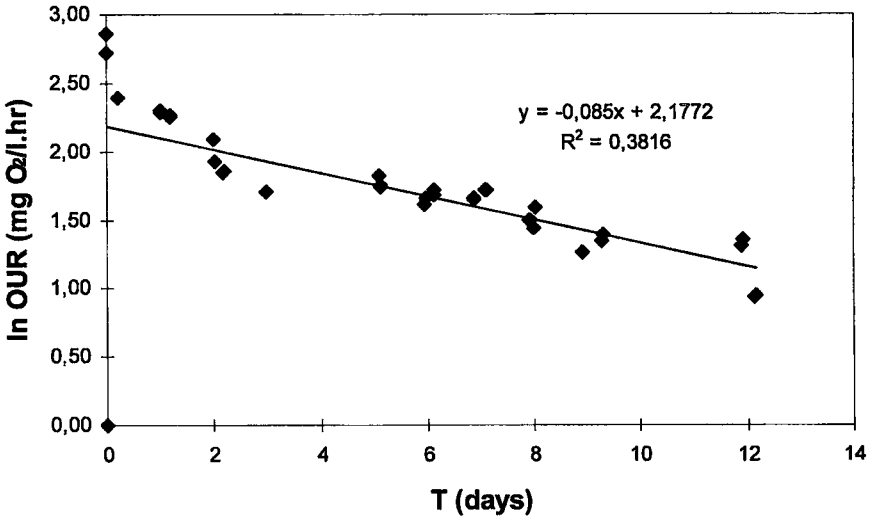

Figure 5.5a Results of b_H experiment for domestic wastewaters- experimental set 5

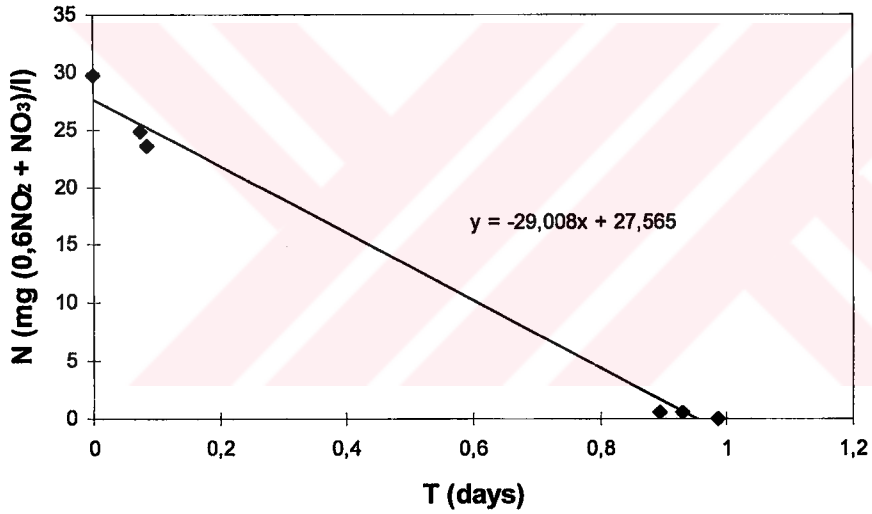

Figure 5.5b Determination of nitrate utilization rate for domestic wastewaters- experimental set 5

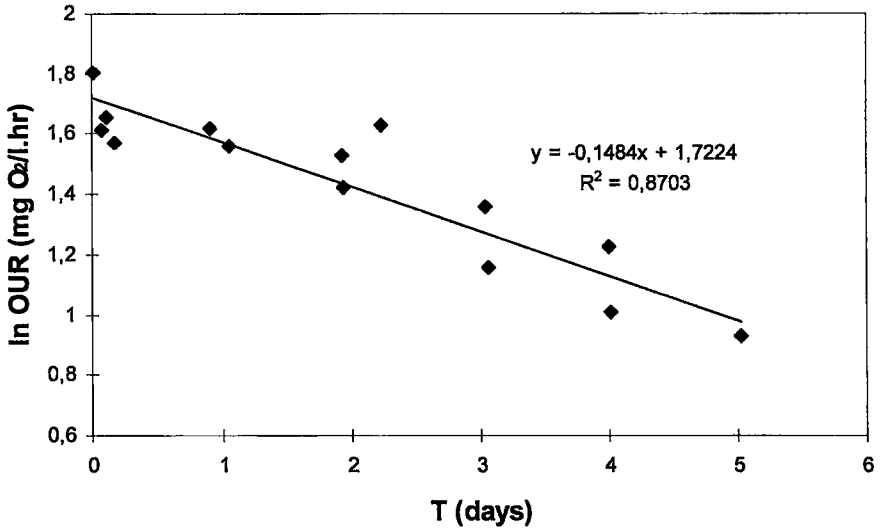

Figure 5.6a Results of b_H experiment for domestic wastewaters- experimental set 6

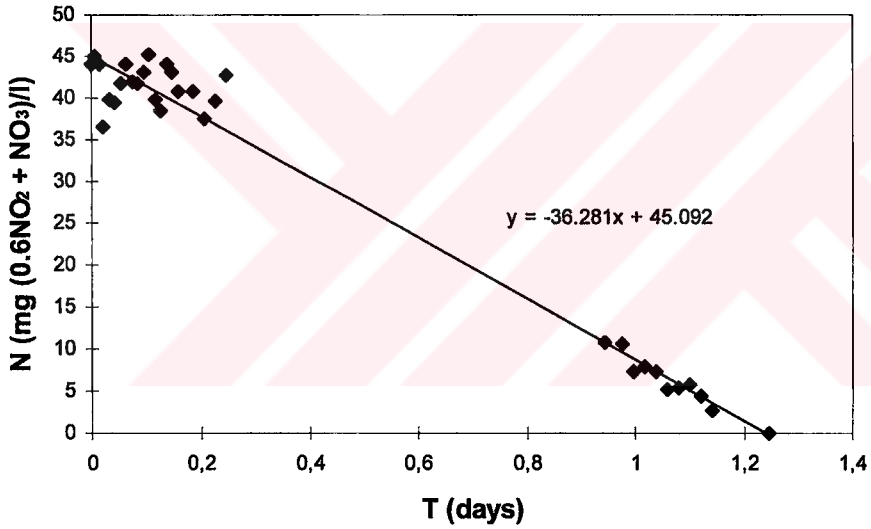

Figure 5.6b Determination of nitrate utilization rate for domestic wastewaters- experimental set 6

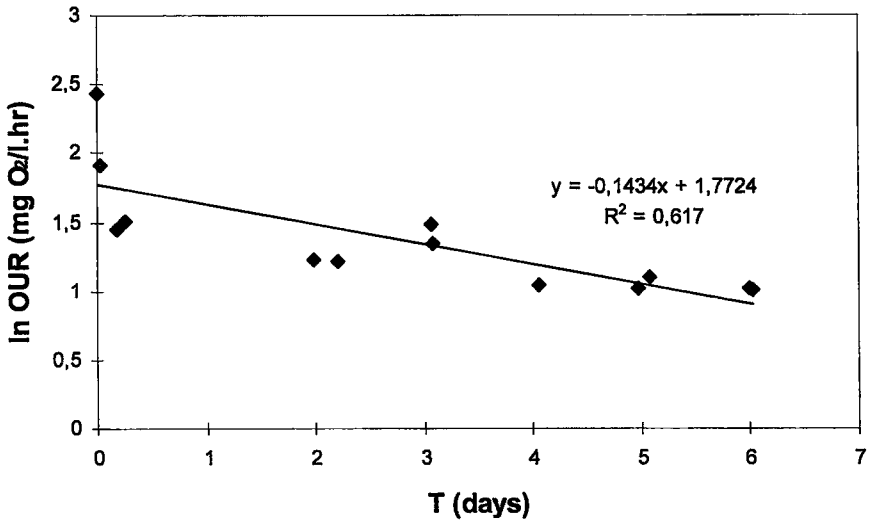

Figure 5.7a Results of b_H experiment for domestic wastewaters- experimental set 7

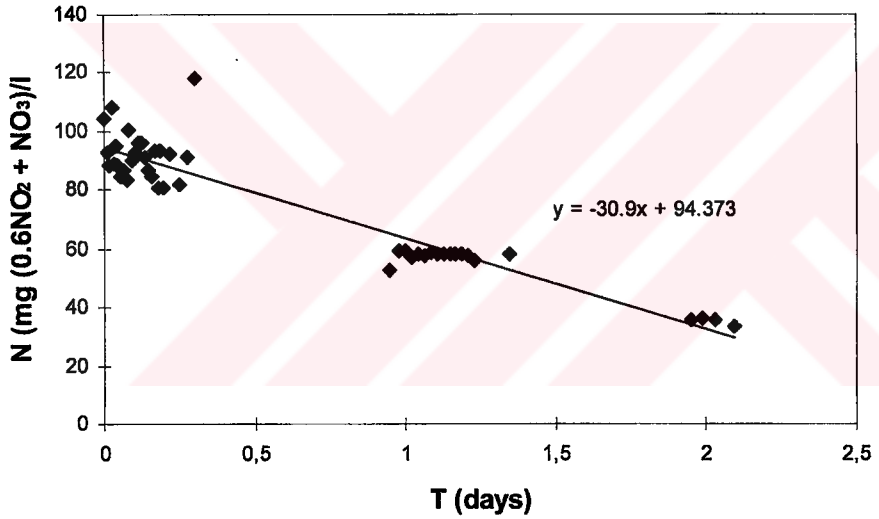

Figure 5.7b Determination of nitrate utilization rate for domestic wastewaters- experimental set 7

5.1.2 Experiments based on the proposed method

Results of the experiments based on the conventional method for the determination of endogenous decay coefficient in some instances led to unsatisfactory and misleading results especially in case of industrial wastewaters. Based on this observation, an alternative method was developed as described in Section 3.1.2. The practical application of this method was carried out for domestic wastewaters, as will be illustrated in the following section.

5.1.2.1 Domestic wastewaters

Biomass subjected to endogenous decay was originated from 4 l fill and draw reactors acclimated to domestic wastewaters. The reactors were operated aerobically one day and anoxically on the other, in a sequential basis. Sludge age was maintained as 15 days.

The characterisation of domestic wastewaters used for feeding purposes during an experimental period of about one year is given in Table 5.5. Since this period is quite long, selected parameters are again illustrated in the form of monthly average values.

Six sets of experiments were performed for the determination of aerobic and anoxic endogenous respiration rate coefficients. First five sets were conducted at 20 ± 1°C whereas the temperature for the final set was held at 10 ± 1°C, in a cooling incubator.

In all sets based on the proposed method, feed and main reactors were operated. The feed reactor consisted of the synthetic solution representing the readily biodegradable and the constant volume of biomass transferred daily from the main reactor. The initial F/M ratio was selected around 0.2. On the other hand, the main reactor undergoing endogenous respiration, contained only biomass acclimated to domestic wastewaters. OUR and NUR profiles obtained from the feed reactors, for sets 8 to 13, will be illustrated in **Appendix A**.

In experimental set 8, initial VSS amount was 5720 mg in 4 l aerobic and 4 l anoxic main reactors. During the experimental period, 200 ml of mixed liquor was transferred to the 500 ml feed reactor everyday. OUR and NUR profiles were monitored in aerobic and anoxic feed rectors which illustrated the decreased biomass activity due to endogenous metabolism.

Table 5.3 Monthly averages of selected parameters for domestic wastewaters used for acclimation purposes-II

Month	COD (mg/l)		pH	Total P (mg/l)	TKN (mg/l)	Ammonia-N (mg/l)	Alkalinity (mg/l) (as $CaCO_3$)
	Total	Filtered					
1	340	160	7.5	9	45	31	220
2	320	130	7	6	30	15	180
3	240	120	6.9	7	36	24	-
4	275	135	7.4	8	70	40	260
5	265	180	7.2	7	42	32	-
6	255	185	7.3	13	46	21	-
7	315	125	7.1	9	30	18	-
8	230	135	7.2	6	40	28	-
9	240	110	7.1	10	40	23	-
10	230	110	7	5	42	28	-
11	265	180	7.1	5	38	20	-
12	245	150	7.3	6	35	15	160
Mean	268.3	143.3	7.2	7.6	41.2	24.6	205
Std Dev	37.3	27.2	0.2	2.4	10.4	7.5	44.4

Figures A.1a to A.8a show the oxygen utilization rates recorded in the feed reactors. Figures A.1b to A.8b exhibit nitrite plus nitrate-nitrogen ($0.6NO_2^-$-N + NO_3^--N) profiles besides sole nitrite concentrations. The purpose of such an illustration was to show the insignificance of nitrite accumulation during endogenous respiration. Thus, nitrite profiles will not be presented for experimental sets of 9 to 13. Figures A.1c, to A.7d show the rates for the first and second phases of the NUR profiles. For the following sets, i.e. 9 to 13, the magnitude of the denitrification rates will again be presented in the electron acceptor consumption profiles. Figures 5.8a and 5.8b show the determination of aerobic and anoxic endogenous decay coefficients using the previous profiles obtained from feed reactors. b_H and b_{HD} were assessed as 0.1 1/day as 0.05 1/day respectively, for the eighth set.

In experimental set 9, 4300 mg VSS was maintained in 4 l aerobic and 5 l anoxic reactors. Figures A.9a to A.17a show the decreasing trend of OUR values during the whole course of the experimental period. Figures A.9b to A.16b illustrate nitrate utilization profiles as well as calculated denitrification rates. b_H value was computed as 0.09 1/day and b_{HD} as 0.05 1/day which can be seen from Figures 5.9a and 5.9b respectively.

In experimental set 10, 3000 mg VSS was maintained in aerobic and anoxic main reactors. OUR profiles observed in the feed reactors during the experimental period

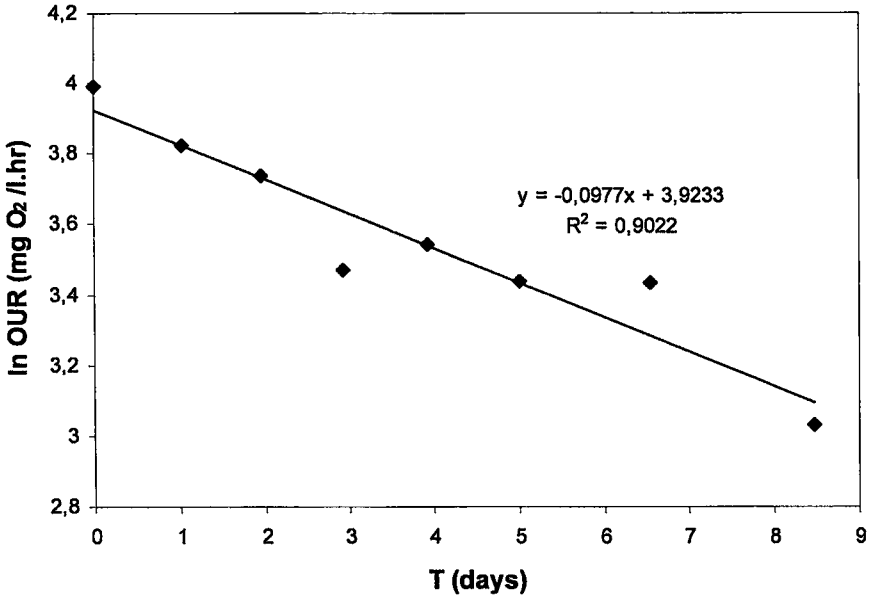

Figure 5.8a Determination of b_H value for domestic wastewaters - set 8

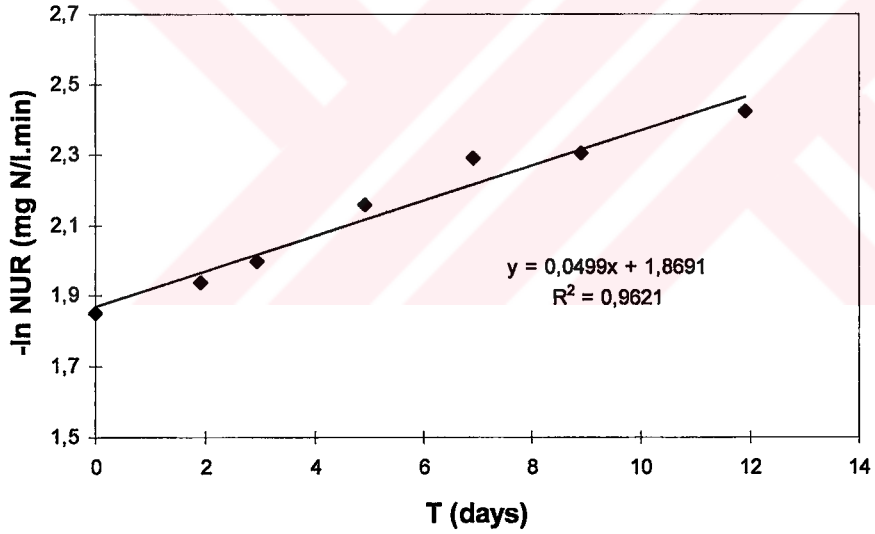

Figure 5.8b Determination of b_{HD} value for domestic wastewaters -set 8

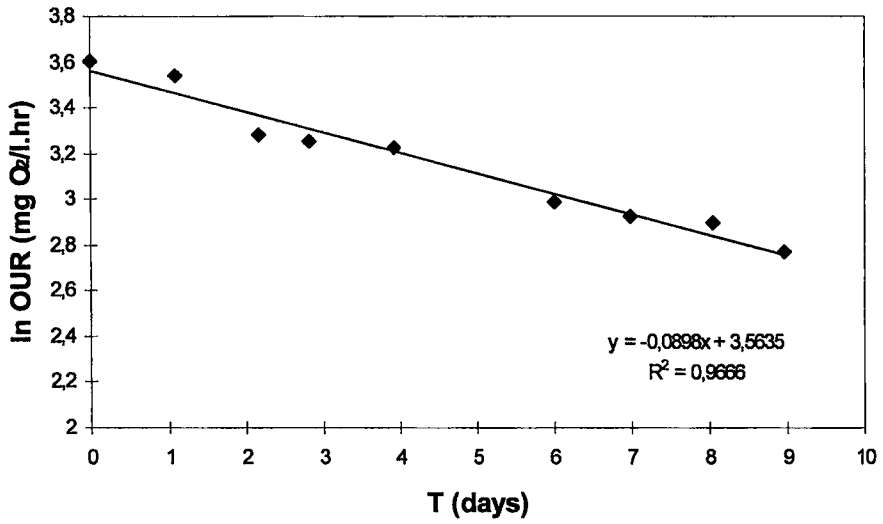

Figure 5.9a Determination of b_H value for domestic wastewaters-set 9

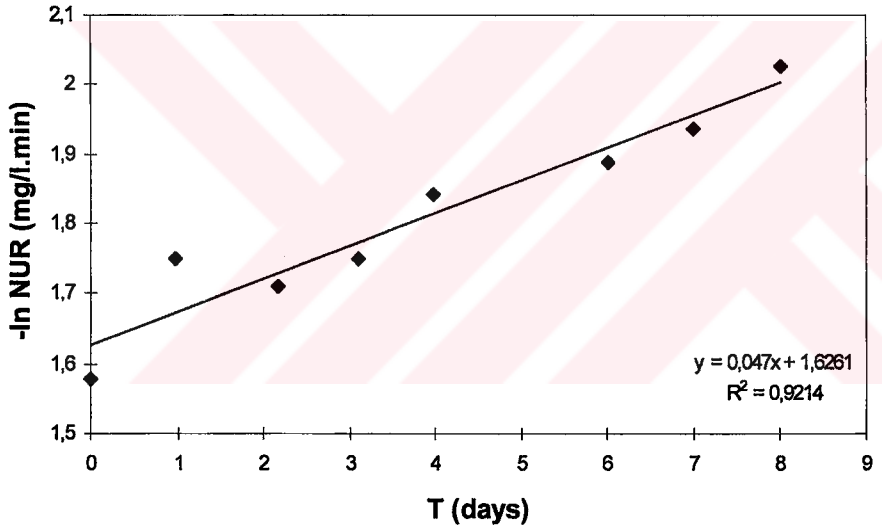

Figure 5.9b Determination of b_{HD} value for domestic wastewaters -set 9

for set 10 are shown in Figures A.18a to A.26a. Nitrate utilization profiles and denitrification rates are presented in Figures A.18b to A.26b. Figures 5.10a and 5.10b give the computed b_H and b_{HD} values as 0.07 1/day and 0.04 1/day respectively.

Experiment 11 was started with a VSS amount of 5200 mg both in aerobic and anoxic main reactors. OUR values versus time were plotted in Figures A.27a to A.35a. The rates of denitrification can be spotted in Figures A.27b to A.35b. The evaluation of daily data led to a b_H value of 0.08 1/day and a b_{HD} value of 0.06 1/day as seen in Figures 5.11a and 5.11b.

4 l aerobic and 5 l anoxic main reactors contained 4700 mg VSS each at the start of the experimental set 12. OUR profiles obtained from this set are displayed in Figures A.36a to A.43a. Denitrification rates are shown in Figures A.36b to A.43b. b_H and b_{HD} results obtained from set 12 can be listed as 0.06 1/day and 0.04 1/day respectively as shown in Figures 5.12a and 5.12b.

Experimental set 13 was conducted at 10 ± 1°C, i.e. at a much lower temperature from the previous sets. The initial volatile suspended solids amount in both aerobic and anoxic main reactors were 5055 mg. Oxygen utilization rate profiles can be seen in Figures A.44a to A.53. Denitrification rates on the other hand, are shown in Figures A.44b to A.52b. Figures 5.13a and 5.13b present the calculated values of b_H and b_{HD} as 0.04 1/day and 0.04 1/day respectively.

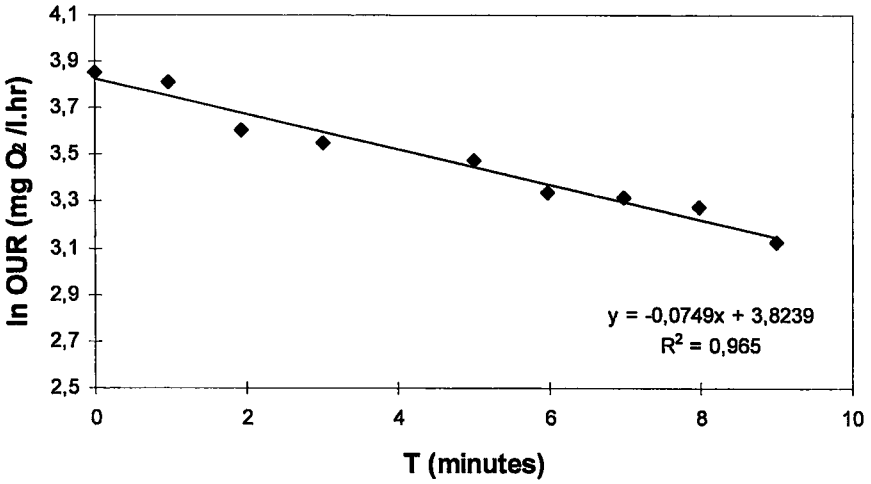

Figure 5.10a Determination of b_H value for domestic wastewaters - set 10

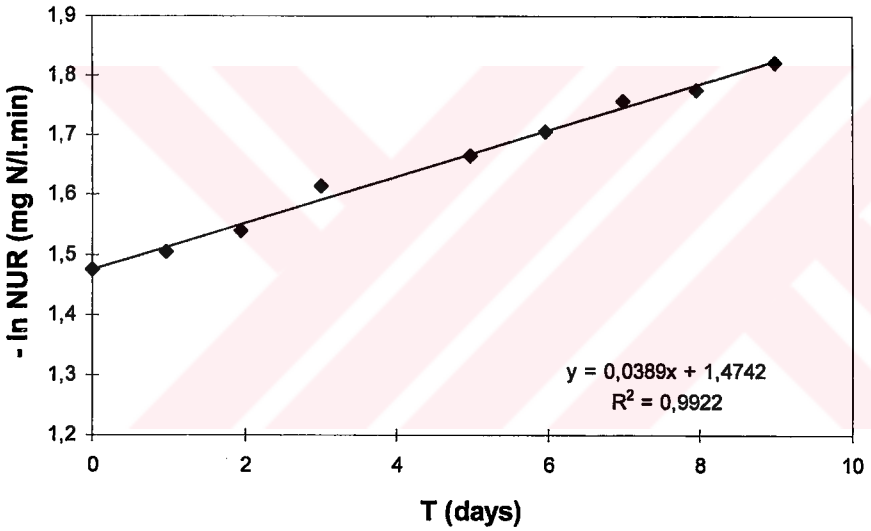

Figure 5.10b Determination of b_{HD} value for domestic wastewaters- set 10

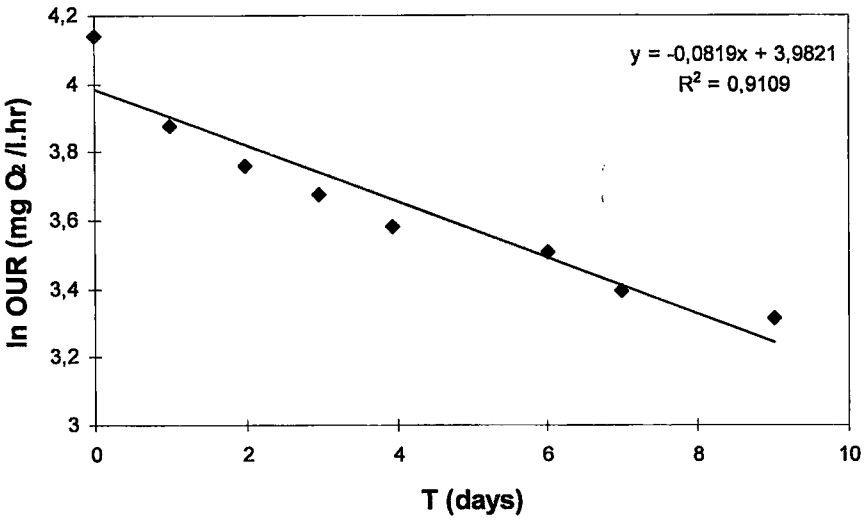

Figure 5.11a Determination of b_H value for domestic wastewaters - set 11

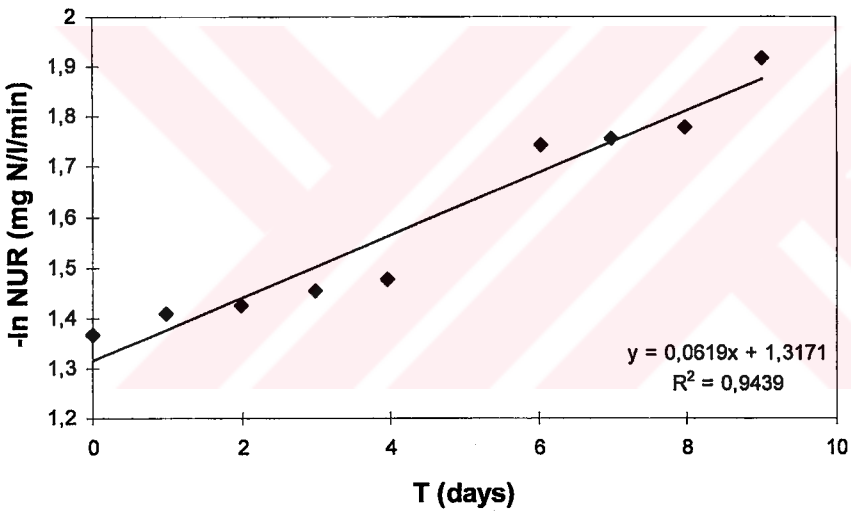

Figure 5.11b Determination of b_{HD} value for domestic wastewaters - set 11

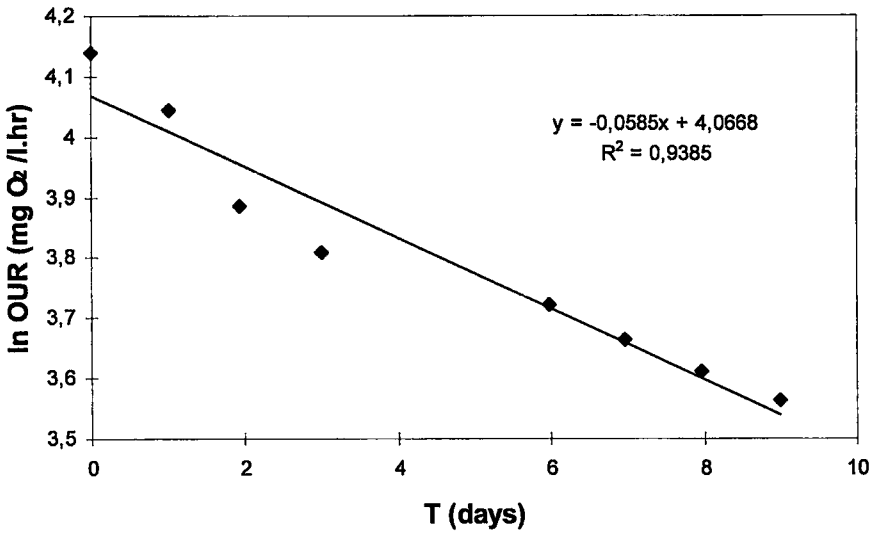

Figure 5.12a Determination of b_H value for domestic wastewaters - set 12

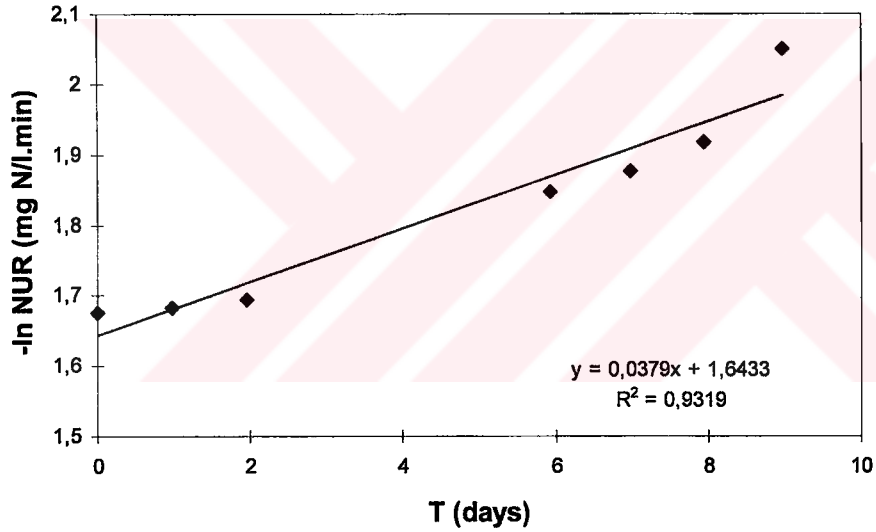

Figure 5.12b Determination of b_{HD} value for domestic wastewaters - set 12

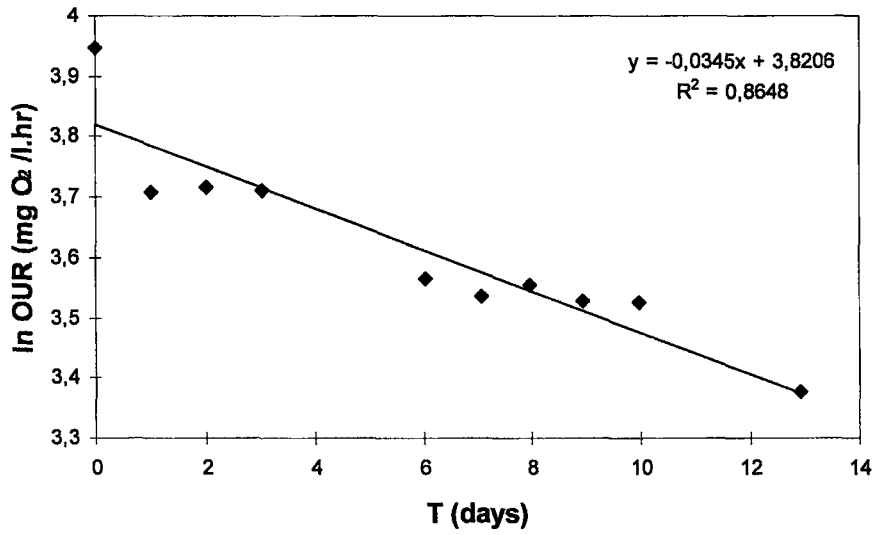

Figure 5.13a Determination of b_H value for domestic wastewaters - set 13

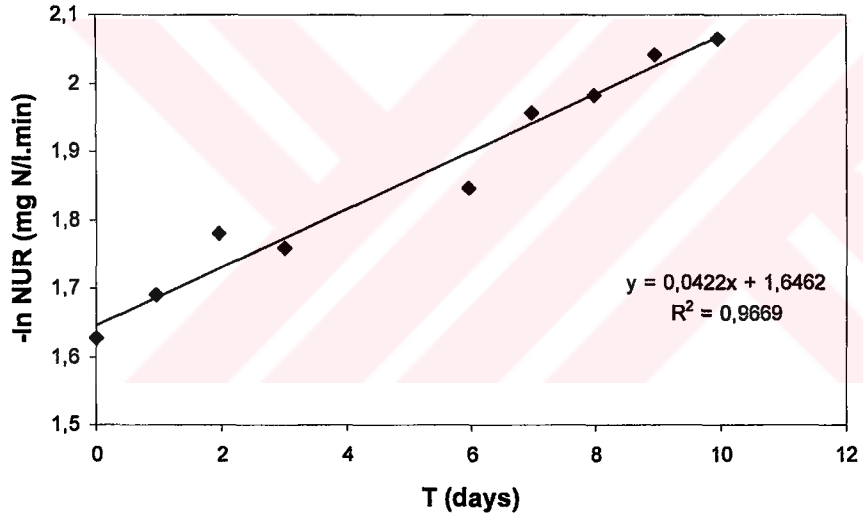

Figure 5.13b Determination of b_{HD} value for domestic wastewaters - set 13

5.2 Experimental Studies for the Investigation of Denitrification Kinetics Using Hydrolyzed Carbon Sources

In this experimental period, domestic primary sludge was investigated as a carbon source for denitrification. The primary sludge samples were obtained from a domestic wastewater treatment plant at Ataköy/Istanbul over a period of two months. Sludge was withdrawn from the underflow line of the primary clarifier where wastewater and sludge hydraulic retention times were 17 and 1.5 hours respectively. Table 5.4 shows total, C_{T1}, and filtered, S_{T1}, COD results for wastewater and primary sludge. For primary sludge, C_{T1} denotes total centrifuged COD while, S_{T1} is for the COD assessed by filtering through 0.45 μm membrane filter. The readily biodegradable COD content of the sludge was determined by the aerobic respirometric method proposed by Ekama and Marais (1986) as outlined in section 3.2.1.1. Figures 5.14a, 5.14b, 5.15, 5.16a, 5.16b, 5.17a, 5.17b, 5.18a, 5.18b, 5.19, 5.20, and 5.21 show OUR versus time profiles obtained from experimental sets 15 to 24 for raw wastewater and centrifuged primary sludge.

Table 5.4 depicts the initial F/M ratios for OUR experiments and S_S values determined from the OUR profiles. First, it was intended to investigate raw wastewater as a potential carbon source for denitrification besides primary sludge, but as the S_S fraction in the wastewater was lower than expected, only one experimental set was conducted for comparison purposes. Thus, the sources of COD employed were primary sludge and acetate, the latter considered as one of the best examples of readily biodegradable substrate. Denitrification experiments were conducted for equivalent S_S concentrations of substrates in parallel batch tests.

In order to determine the fraction of active biomass, two experiments were performed simultaneously, i. e., for the assessment of readily biodegradable COD at a relatively low F/M ratio, under aerobic conditions according to Ekama and Marais (1986) and for the assessment of aerobic maximum growth rate ($\hat{\mu}_H$), at a high F/M ratio, according to Kappeler and Gujer (1992). Activity coefficient was determined according to expression (4.2) as previously described in Section 4.2.3.

Table 5.4 COD values for domestic primary sludge and raw wastewater

Experimental Set	Primary Sludge C_{TI}[a] (mg COD/l)	Primary Sludge S_{TI}[b] (mg COD/l)	Wastewater C_{TI} (mg COD/l)	Wastewater S_{TI} (mg COD/l)
14	715	-	265	110
15	2490	-	545	120
16	2300	1030	500	125
17	1460	280	450	190
18	1000	625	290	130
19	1120	680	310	210
22	420	265	320	75
23	685	395	180	90
24	1825	710	-	-

[a] Centrifuged primary sludge
[b] Filtered through 0.45 μm membrane filter

Table 5.5 Initial F/M ratios in OUR experiments and S_S values determined from OUR profiles for raw wastewater (WW) and centrifuged primary sludge (CPS)

Experimental Set	Initial F/M		S_S (mg COD/l)	
	WW	CPS	WW	CPS
15	1.58	1.60	10	520
16	-	1.5	-	480
17	0.69	0.68	15	100
18	1.42	1.46	35	290
19	0.29	0.31	35	255
22	-	0.11	-	115
23	-	0.14	-	210
24	-	0.13	-	370

Table 5.6 Characterization results for raw wastewater, digester sludge, and primary sludge for experimental set 14

	pH	Total TKN (mg/l)	Total P (mg/l)	Solids SS (mg/l)	Solids VSS (mg/l)	Alk as $CaCO_3$ (mg/l)
Raw wastewater	7.79	44	6	170	90	200
Digester sludge	7.31	-	-	-	-	-
Primary sludge	6.98	820	42	5620	3670	445

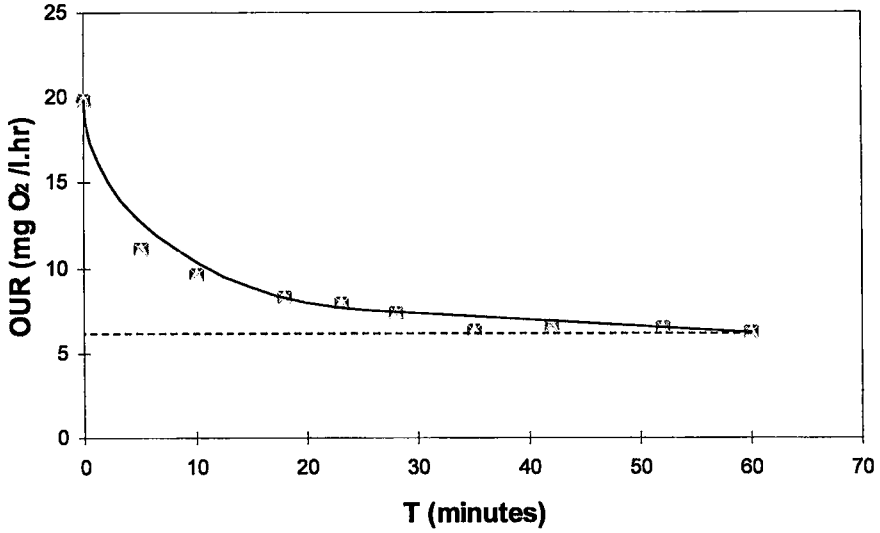

Figure 5.14a Determination of the S_s content of raw wastewater : OUR values versus time - experimental set 15

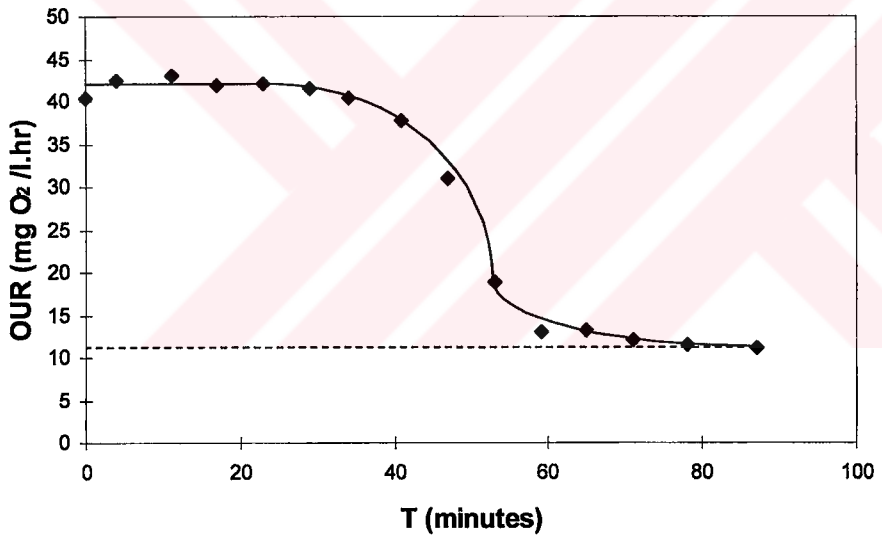

Figure 5.14b Determination of the S_s content of primary sludge : OUR values versus time - experimental set 15

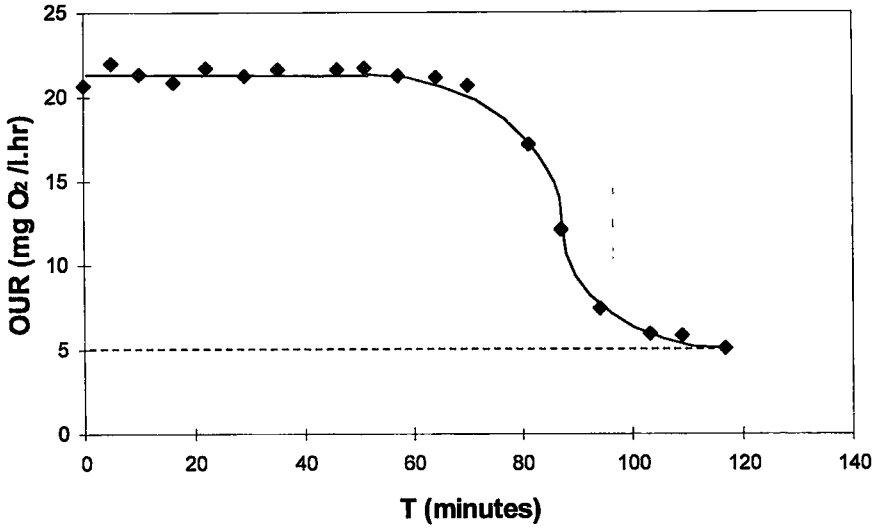

Figure 5.15 Determination of the S_s content of primary sludge: OUR values versus time - experimental set 16

$$f_a = \frac{Y_H}{1 - f_x Y_H} \frac{OUR_1}{\hat{\mu}_H X_T} \tag{4.2}$$

In this expression, Y_H was assumed as 0.45 mg VSS/mg COD as proposed for domestic wastewaters according to Task Group Model No 1. $\hat{\mu}_H$ was already computed as 3.5 1/day. The value of the first OUR plateau observed in the readily biodegradable organic matter test was 152 mg O_2/l.hr and the initial VSS concentration in the 500 ml aerobic reactor was 2715 mg/l. Hence, the activity coefficient (f_a) was computed as 0.52. Since sets 14 to 24 were conducted in two months time, the activity coefficient was assumed to be constant during this period. In Chapter 7, denitrification rates will be expressed in terms of active biomass.

In experimental set 14, it was intended to compare raw wastewater, primary sludge, and digester sludge as carbon sources for denitrification. The total (centrifuged) and filtered COD in the digester sludge were 840 and 185 mg/l. Each reactor was inoculated with 430 mg of VSS. F/M ratios in three anoxic reactors, namely, centrifuged primary sludge (CPS), digester sludge and raw wastewater were 0.39, 0.37 and 0.55 respectively. Sludge and wastewater samples were analysed for basic parameters, which are shown in Table 5.6.

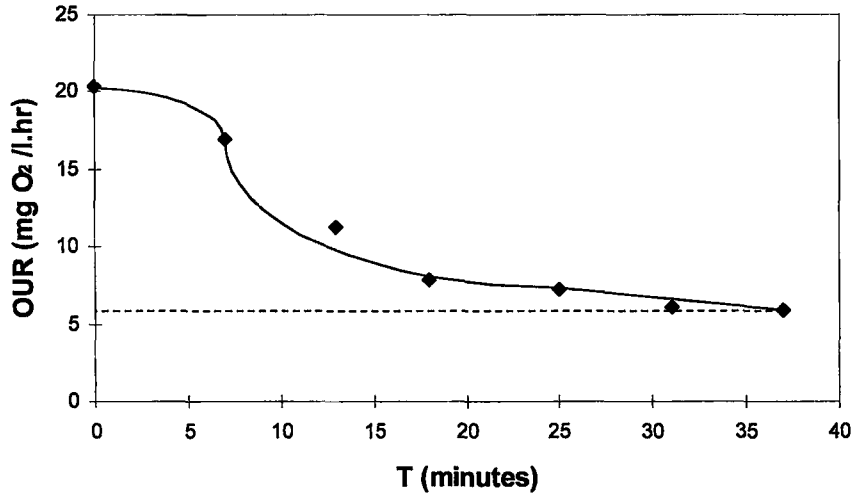

Figure 5.16a Determination of the S_s content of raw wastewater : OUR values versus time - experimental set 17

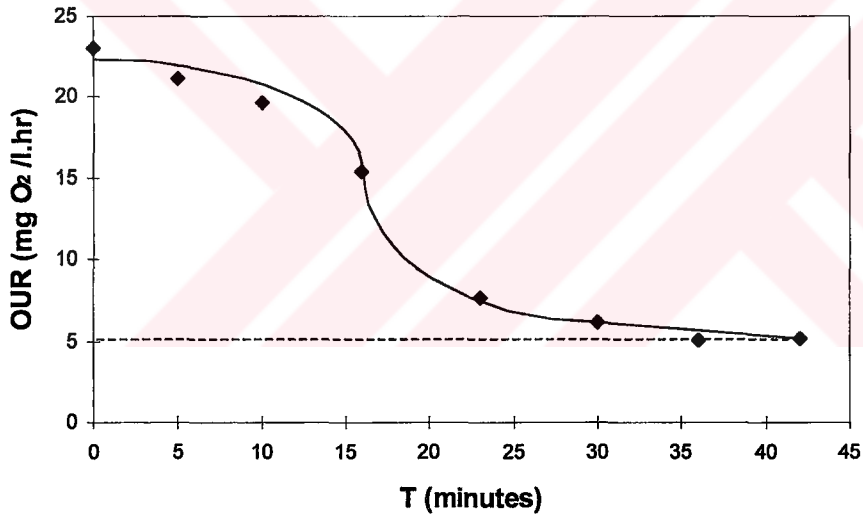

Figure 5.16b Determination of the S_s content of primary sludge : OUR values versus time - experimental set 17

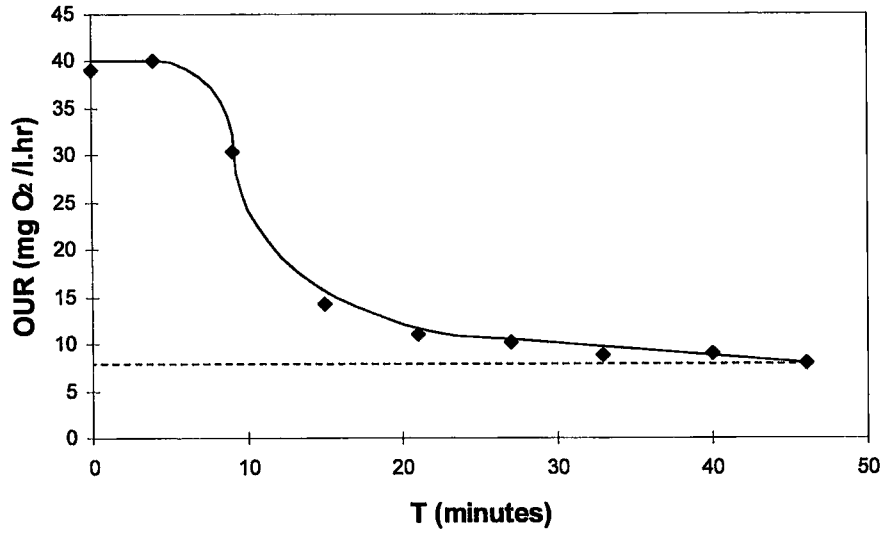

Figure 5.17a Determination of the S_s content of raw wastewater : OUR values versus time - experimental set 18

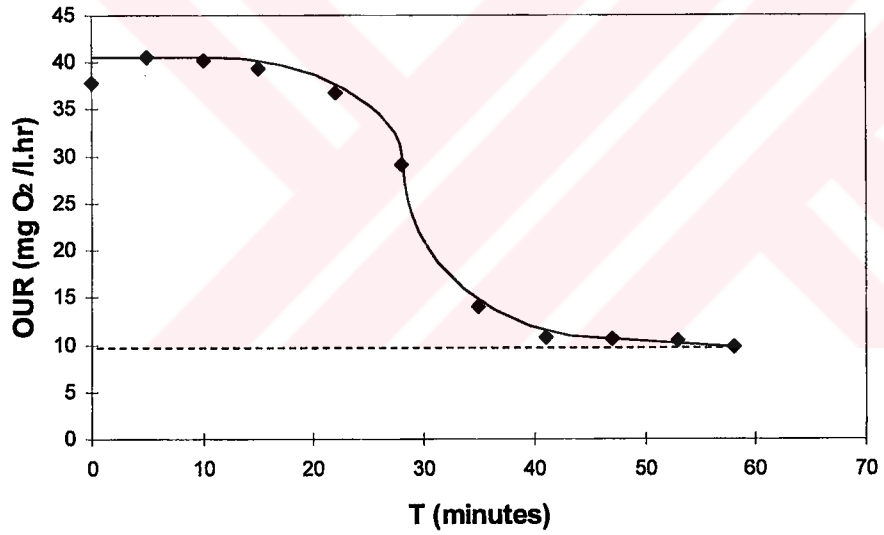

Figure 5.17b Determination of the S_s content of primary sludge : OUR values versus time - experimental set 18

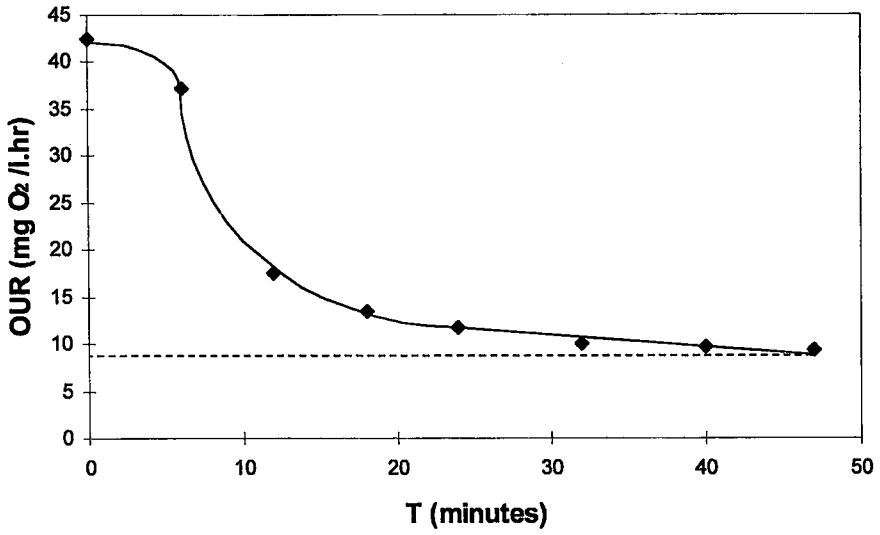

Figure 5.18a Determination of the S_s content of raw wastewater : OUR values versus time - experimental set 19

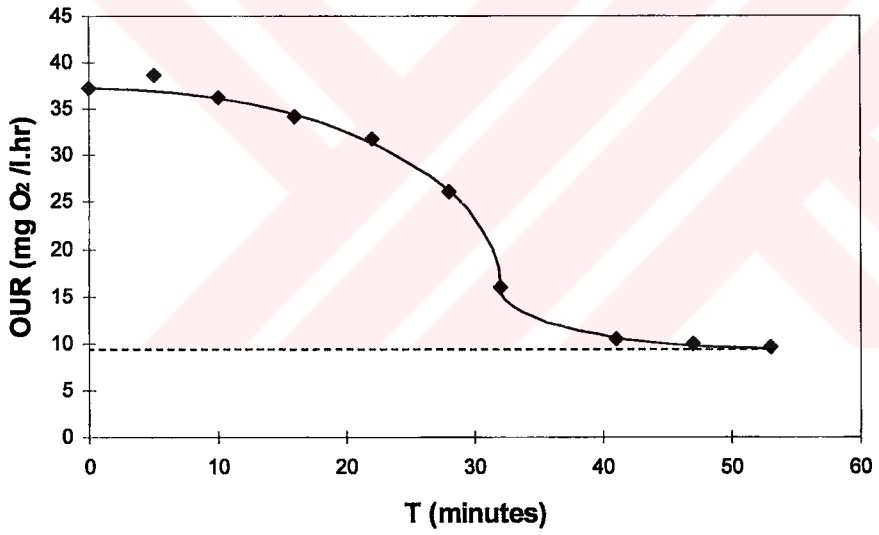

Figure 5.18b Determination of the S_s content of primary sludge : OUR values versus time - experimental set 19

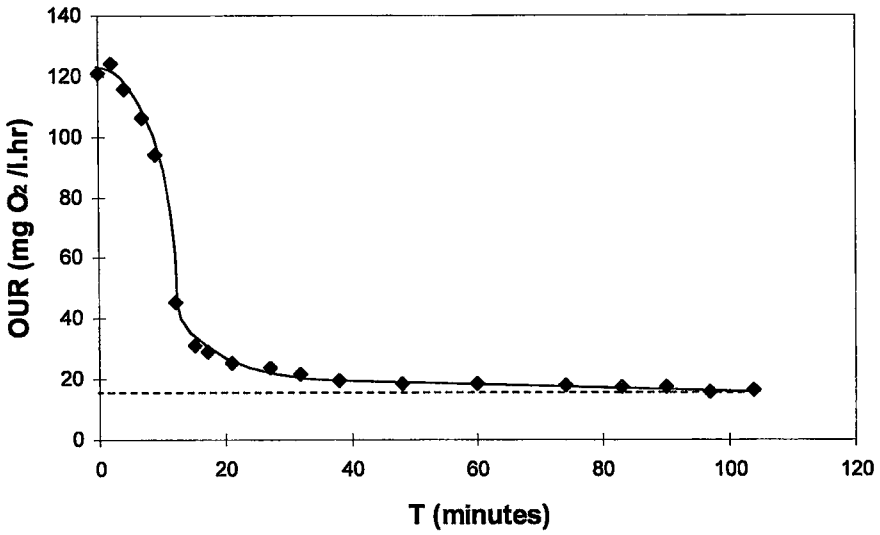

Figure 5.19 Determination of the S_s content of primary sludge : OUR values versus time - experimental set 22

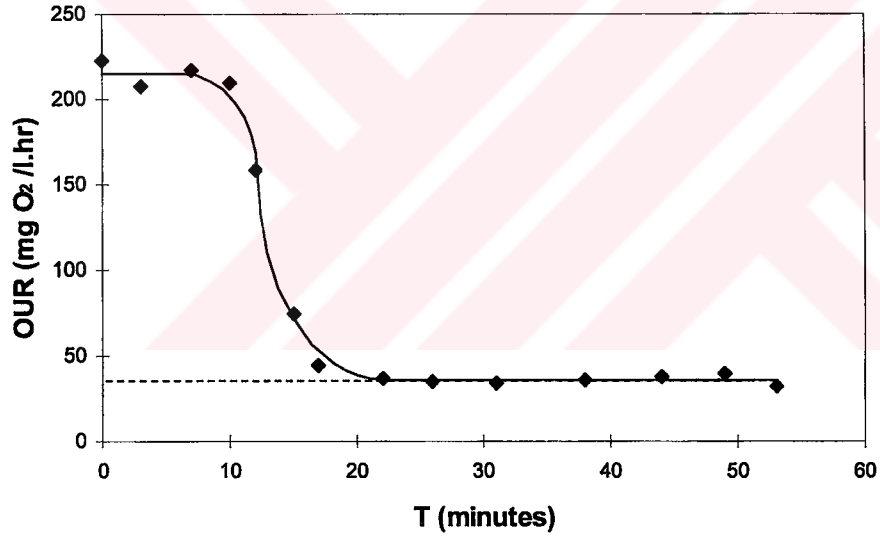

Figure 5.20 Determination of the S_s content of primary sludge : OUR values versus time - experimental set 23

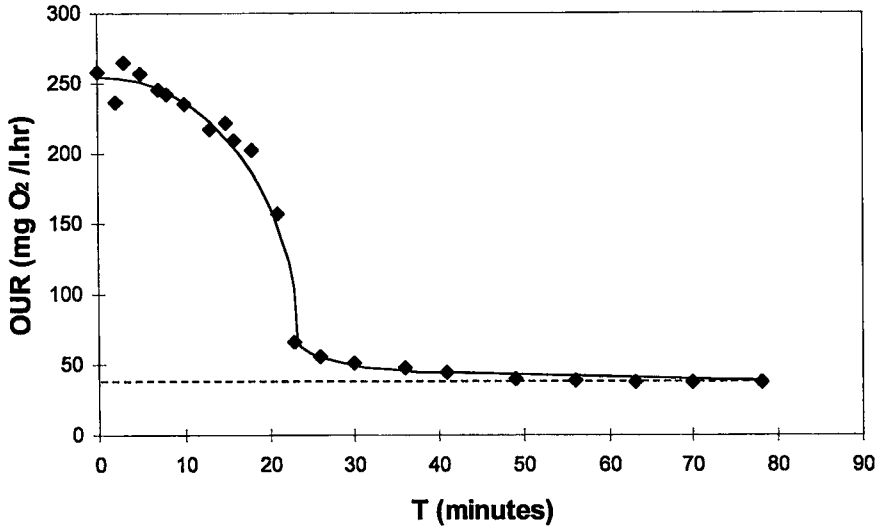

Figure 5.21 Determination of the S_s content of primary sludge: OUR values versus time - experimental set 24

Figures 5.22a to 5.22c show electron acceptor utilization rates for raw wastewater, primary sludge, and digester sludge. The highest rate was observed for centrifuged primary sludge followed by the digester sludge and raw wastewater, which can be listed as 0.14 mg N/l.min, 0.05 mg N/l.min and 0.03 mg N/l.min. The rates associated with the second phases are also depicted in these figures.

In experimental set 15, the objective was to compare the denitrification rates observed for centrifuged primary sludge (CPS) and acetate, both containing equivalent amounts of readily biodegradable COD of 100 mg/l. F/M ratios in CPS and acetate reactors were 0.8 and 0.16 respectively. The denitrification rates during the first phase of the electron acceptor utilization profile were 0.31 mg N/l.min for centrifuged primary sludge and 0.19 mg N/l.min for acetate, i.e., primary sludge was consumed much more rapidly than acetate (Figures 5.23a and 5.23b). Denitrification rates corresponding to the second phase of the electron acceptor utilization profile are also shown in these figures.

Denitrification rates of centrifuged primary sludge (CPS), filtered primary sludge (FPS), and acetate were compared in experimental set 16. The initial S_S concentration in all reactors was 120 mg COD/l. Initial F/M ratios in CPS, FPS, and acetate reactors were 0.61, 0.3, and 0.13 respectively. The electron acceptor utilization profiles are presented in Figures 5.24a to 5.24c. As can be seen from the

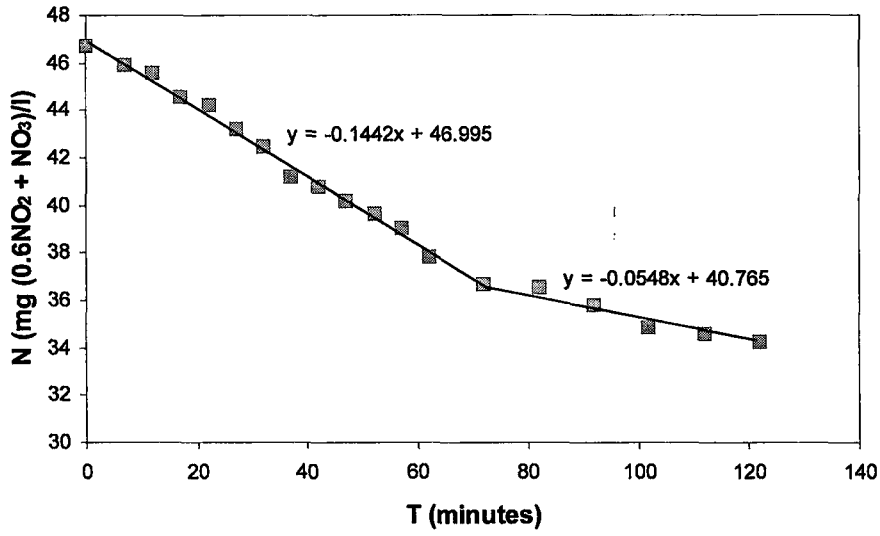

Figure 5.22a Determination of nitrate utilization rate: Centrifuged primary sludge - experimental set 14

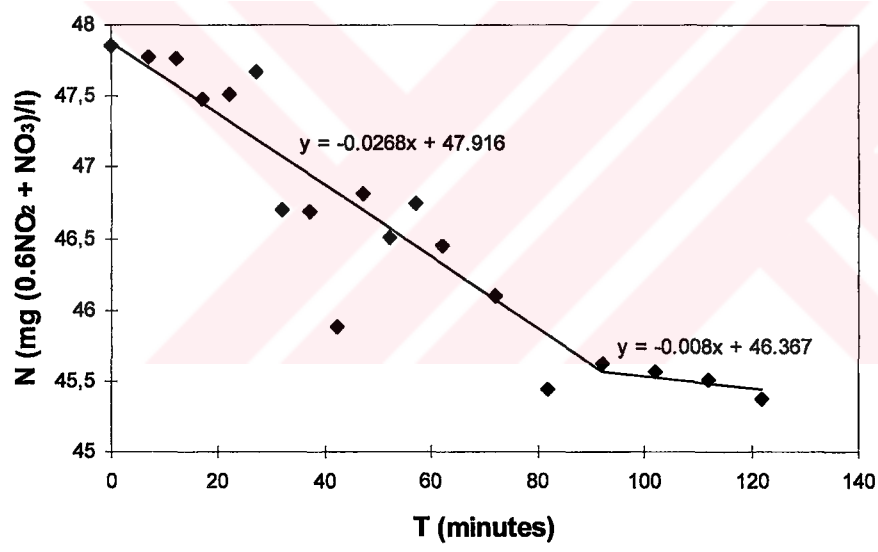

Figure 5.22b Determination of nitrate utilization rate: Raw wastewater - experimental set 14

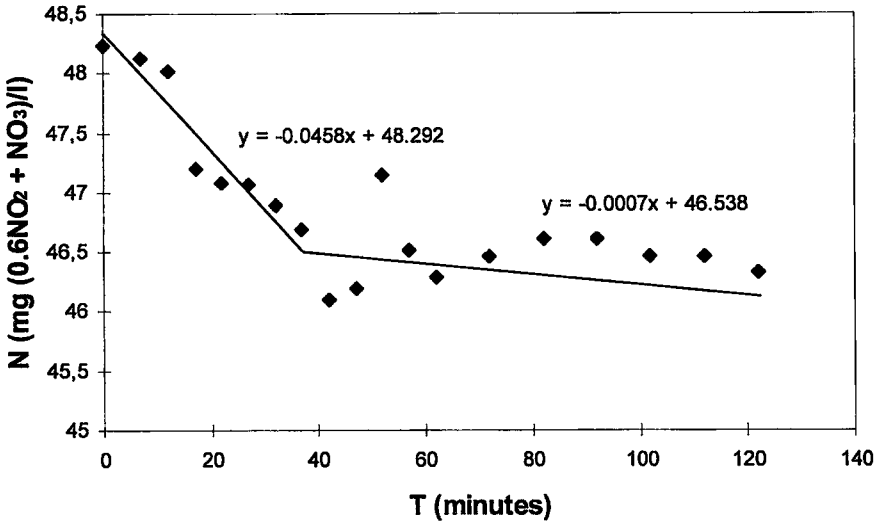

Figure 5.22c Determination of nitrate utilization rate: Centrifuged sludge digester effluent - experimental set 14

figures, the highest rate was observed in the CPS reactor as 0.37 mg N/l.min, second, in the FPS reactor as 0.33 mg N/l.min and the slowest rate was observed in the acetate reactor as 0.25 mg N/l.min. The rates for the second phases are also shown in these figures.

In experimental set 17, denitrification rates for CPS, FPS, and wastewater were compared for S_s concentration of 15 mg COD/l. F/M ratios in CPS, FPS and wastewater reactors were 1.21, 0.23, and 1.59 respectively. Results of this set are illustrated in Figures 5.25a to 5.25c. Similar rates of denitrification were observed for the first phase, as, 0.09 mg N/l.min, 0.08 mg N/l.min., and 0.07 mg N/l.min for CPS, raw wastewater, and FPS reactors respectively.

In the following sets including set 18, it was decided to filter primary sludge since higher denitrification rates were obtained so far possibly due to biomass interference. In experimental set 18, denitrification rates were compared for FPS and acetate reactors, both containing initial S_S concentration of 250 mg/l. F/M ratios were 0.75 and 0.35 for FPS and acetate reactors. Observed denitrification rates were 0.29 mg N/ l.min for FPS and 0.30 mg N/ l. min. for acetate (Figures 5.26a and 5.26b). As can be seen from the figures, only one phase could be observed in both reactors during the 120 minutes of experimental period due to higher levels of carbon involved.

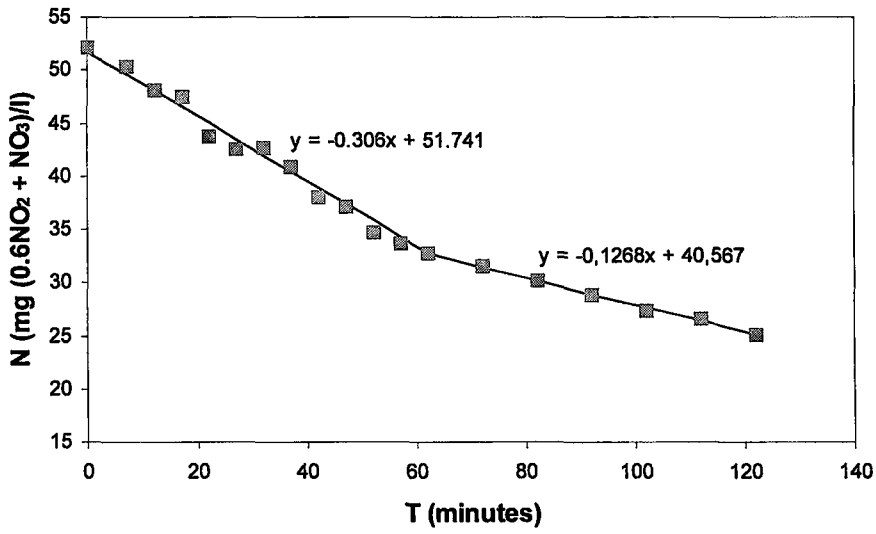

Figure 5.23a Determination of nitrate utilization rate: Centrifuged primary sludge - experimental set 15

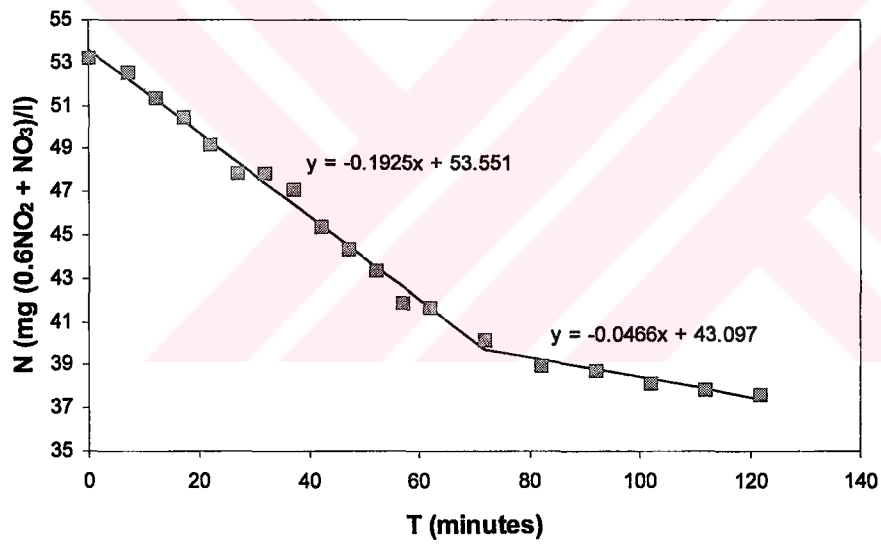

Figure 5.23b Determination of nitrate utilization rate: Acetate - experimental set 15

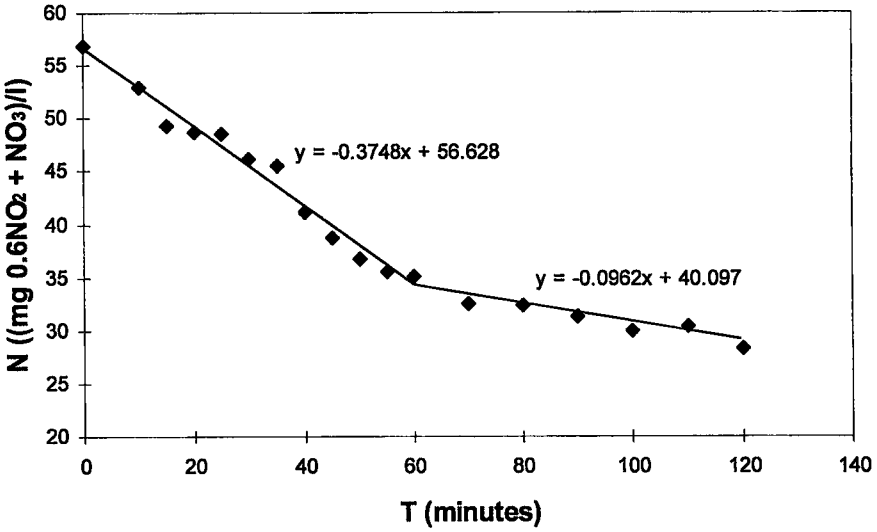

Figure 5.24a Determination of nitrate utilization rate: Centrifuged primary sludge - experimental set 16

In experimental set 19, an initial S_s concentration of 230 mg COD/l was tested. F/M ratios were 0.94 and 0.36 for FPS and acetate reactors. The denitrification rates obtained for acetate and FPS were 0.27 mg N/l.min and 0.23 mg N/l.min respectively (Figures 5.27a and 5.27b).

In experimental set 20, a comparison was made between denitrification rates of acetate and the synthetic waste whose composition was given in Table 4.1, for an initial S_S concentration of 100 mg COD/l. The initial F/M ratio in both reactors was 0.37. Acetate was consumed at almost the same rate (0.09 mg N/ l.min) with the synthetic waste (0.08 mg N/ l. min.) as can be seen in Figures 5.28a and 5.28b.

In experimental set 21, acetate was tested for two initial S_S concentrations, as, 250 mg/l and 500 mg/l. F/M ratios in the reactors were 0.21 and 0.42. Figures 5.29a and 5.29b show that the lower concentration of COD was consumed at a faster rate (0.52 mg N/l.min.) than the higher concentration (0.46 mg N/l.min.).

In experimental set 22, 100 mg/l of initial S_s concentration was selected for the comparison of acetate and FPS. The initial F/M ratios in acetate and FPS reactors were 0.16 and 0.36 respectively. Figures 5.30a and 5.30b illustrate the rates of denitrification observed in both cases. In case of FPS, the observed rate was 0.19 mg N/l.min whereas for acetate it was 0.20 mg N/l.min.

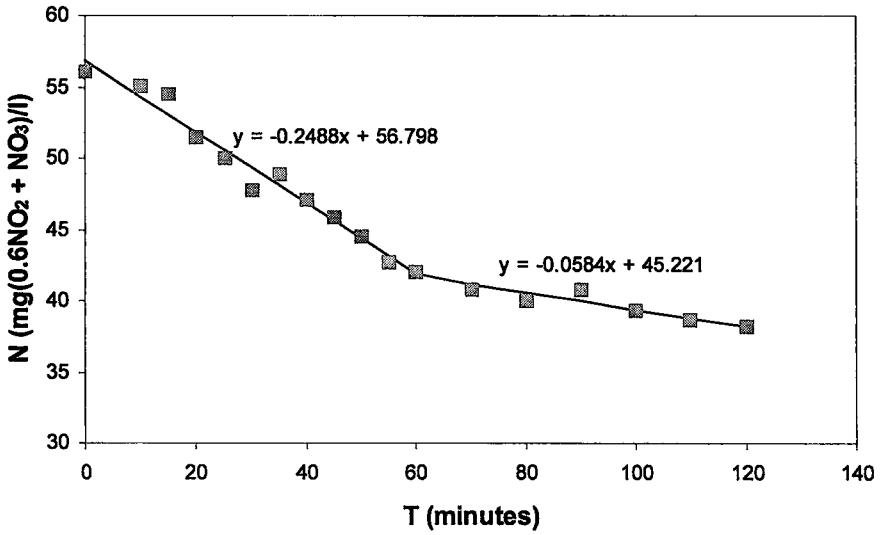

Figure 5.24b Determination of nitrate utilization rate: Acetate - experimental set 16

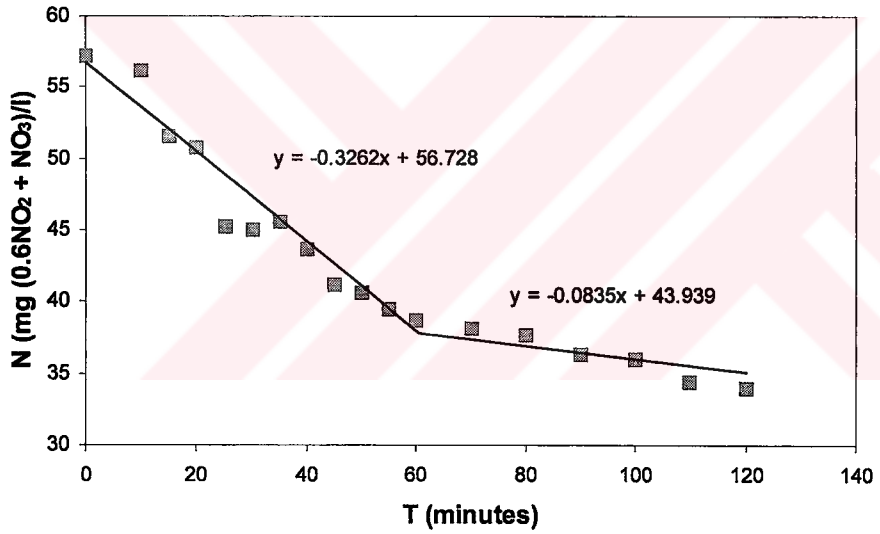

Figure 5.24c Determination of nitrate utilization rate: Filtered primary sludge - experimental set 16

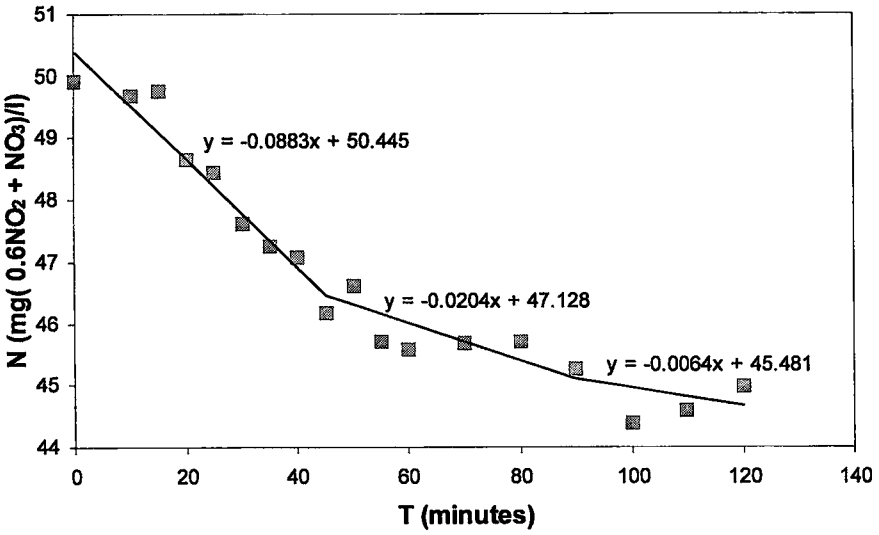

Figure 5.25a Determination of nitrate utilization rate: Centrifuged primary sludge - experimental set 17

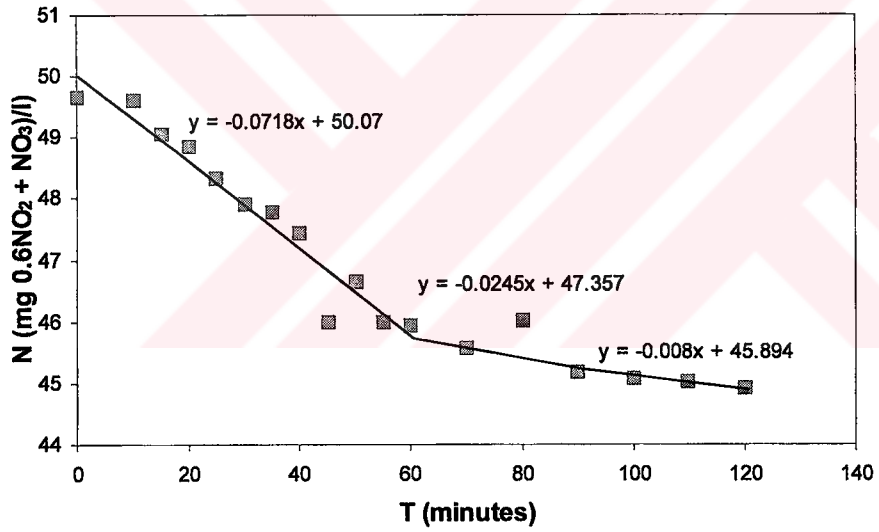

Figure 5.25b Determination of nitrate utilization rate: Filtered primary sludge - experimental set 17

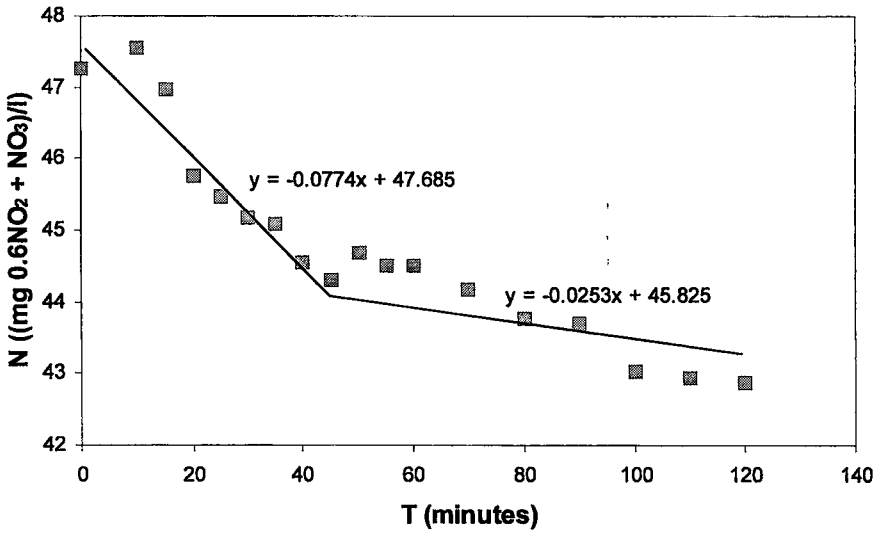

Figure 5.25c Determination of nitrate utilization rate: Raw wastewater - experimental set 17

The denitrification rates were investigated for acetate and FPS, both containing 175 mg/l of readily biodegradable COD, in experimental set 23. F/M ratios in acetate and FPS reactors were 0.14 and 0.27 respectively. Nitrate utilization rates obtained for FPS and acetate were 0.42 mg N/l.min. and 0.43 mg N/l.min. as shown in Figures 5.31a and 5.31b.

In experimental set 24, 50 mg COD/l of S_S was chosen for comparison. Initial F/M ratios in FPS and acetate reactors were 0.28 and 0.14 respectively. Denitrification rates assessed for both FPS and acetate were 0.02 mg N/l.min. (Figures 5.32a and 5.32b).

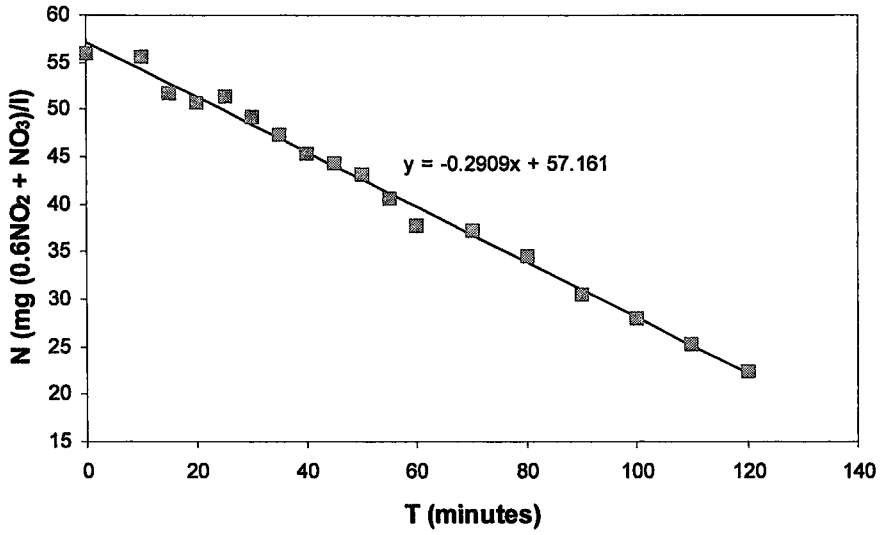

Figure 5.26a Determination of nitrate utilization rate: Filtered primary sludge - experimental set 18

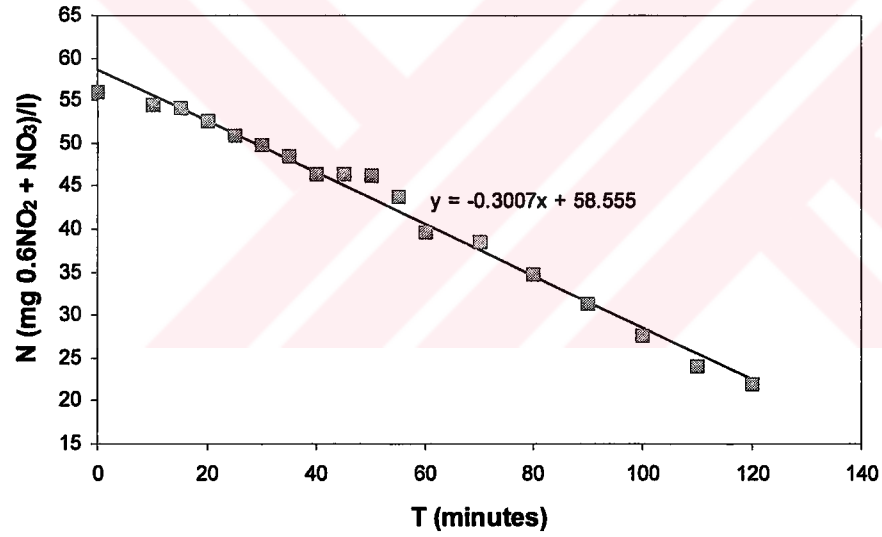

Figure 5.26b Determination of nitrate utilization rate: Acetate - experimental set 18

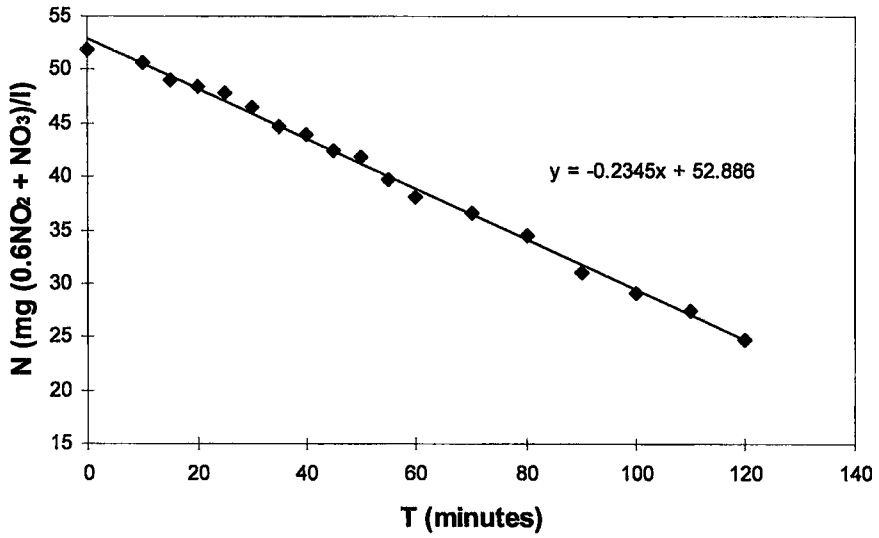

Figure 5.27a Determination of nitrate utilization rate: Filtered primary sludge - experimental set 19

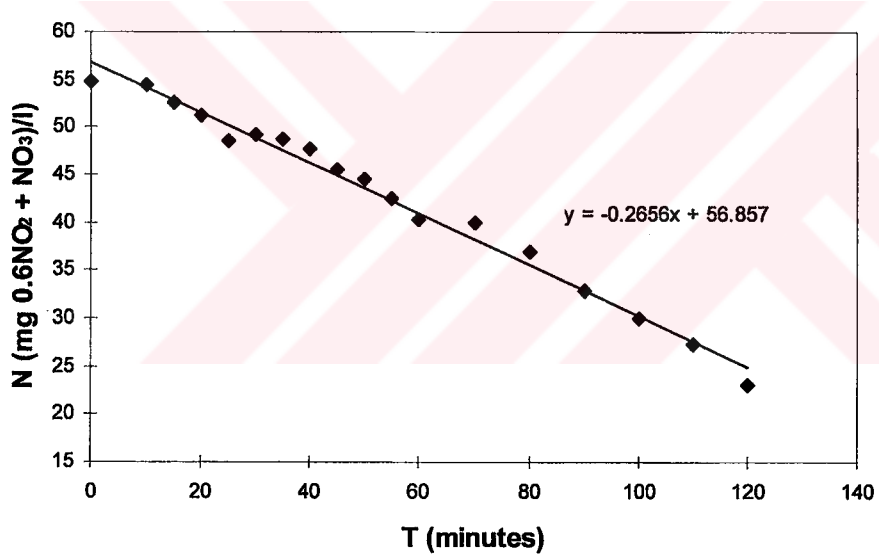

Figure 5.27b Determination of nitrate utilization rate: Acetate - experimental set 19

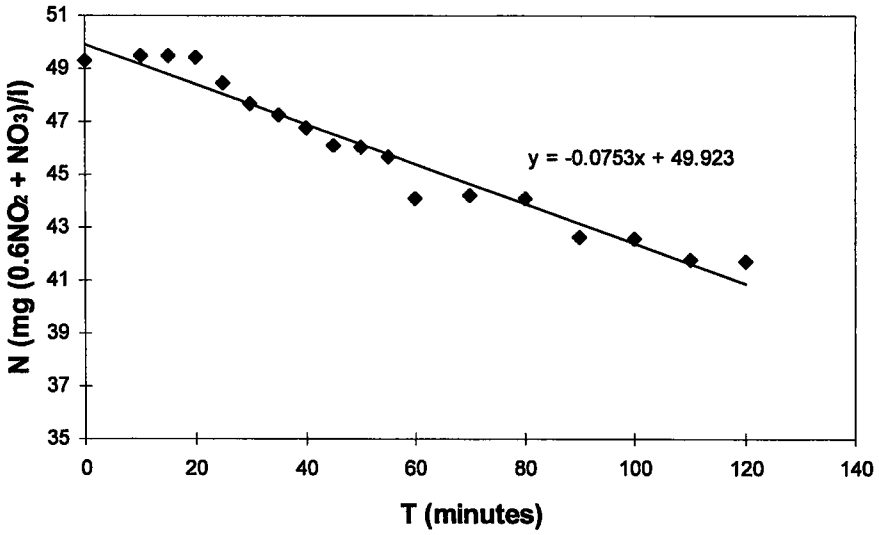

Figure 5.28a Determination of nitrate utilization rate: Synthetic waste - experimental set 20

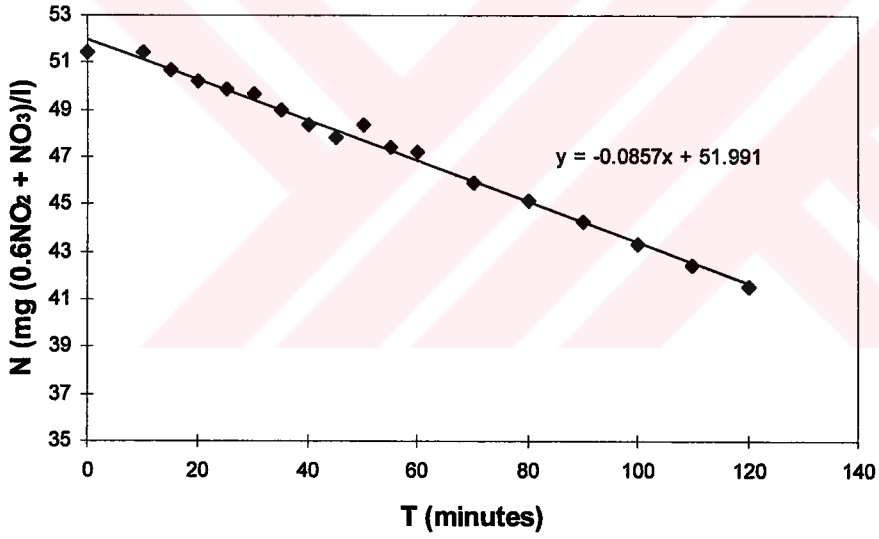

Figure 5.28b Determination of nitrate utilization rate: Acetate - experimental set 20

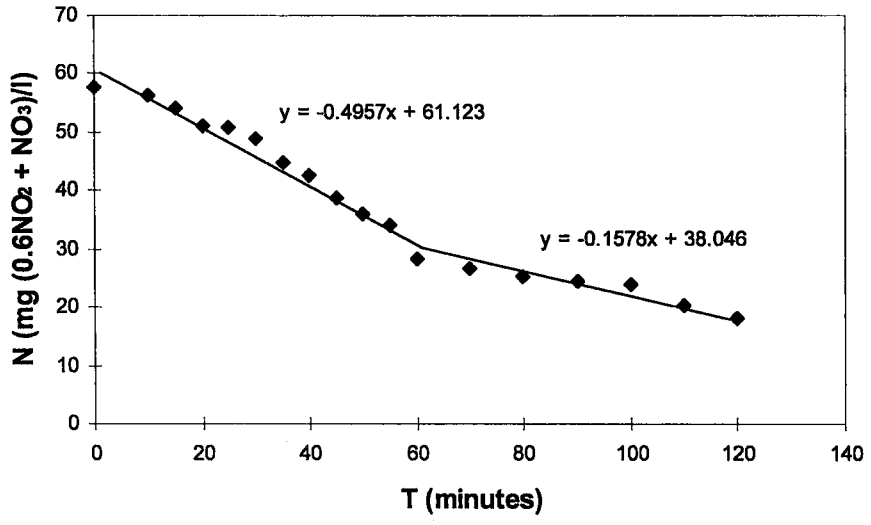

Figure 5.29a Determination of nitrate utilization rate: Acetate - 250 mg/l - experimental set 21

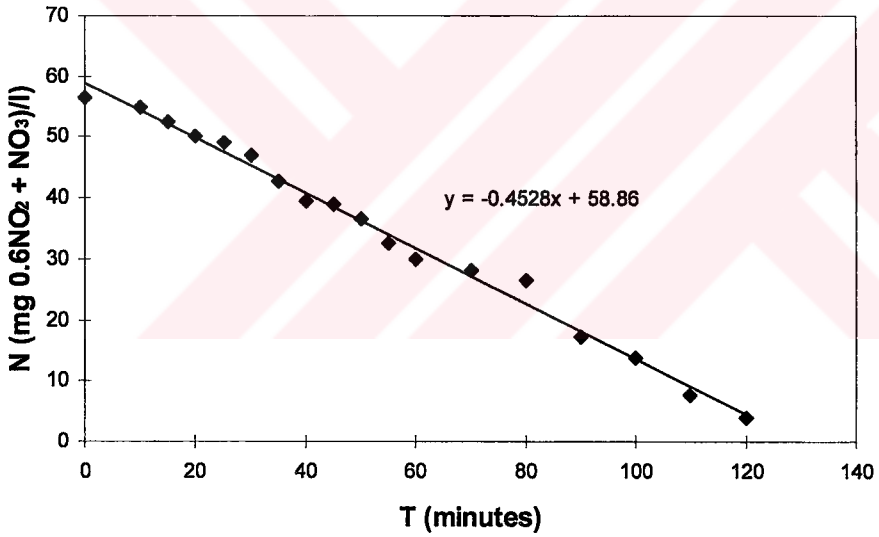

Figure 5.29b Determination of nitrate utilization rate: Acetate - 500 mg/l - experimental set 21

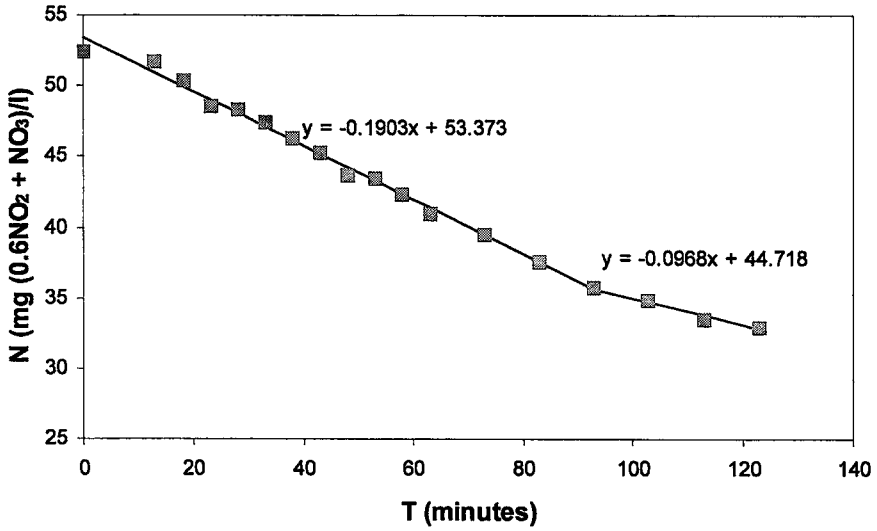

Figure 5.30a Determination of nitrate utilization rate: Filtered primary sludge - experimental set 22

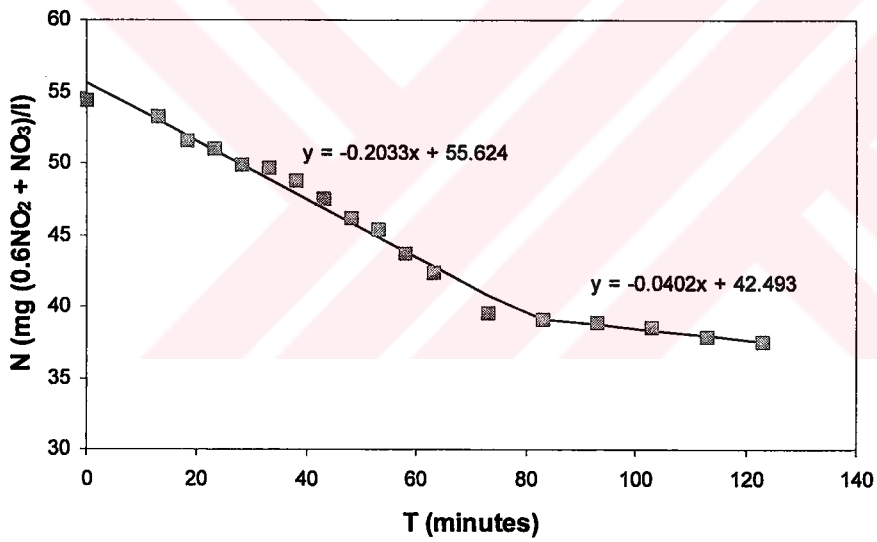

Figure 5.30b Determination of nitrate utilization rate: Acetate - experimental set 22

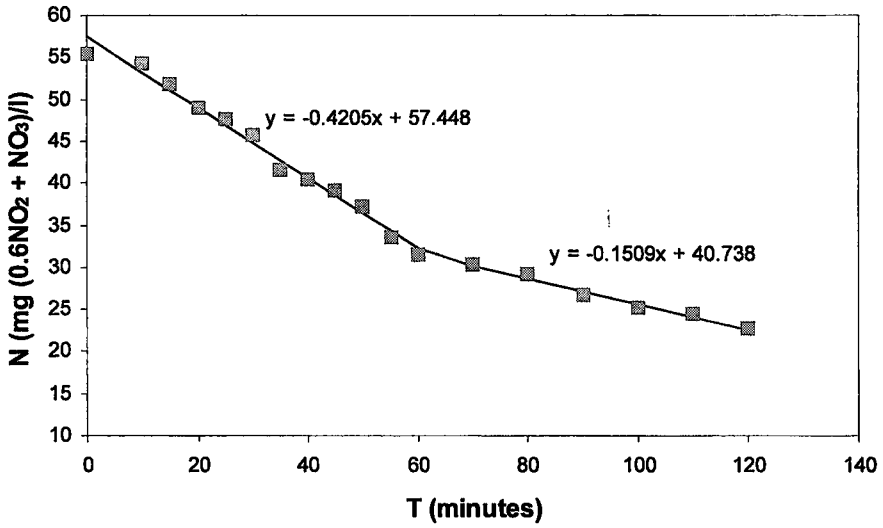

Figure 5.31a Determination of nitrate utilization rate: Filtered primary sludge - experimental set 23

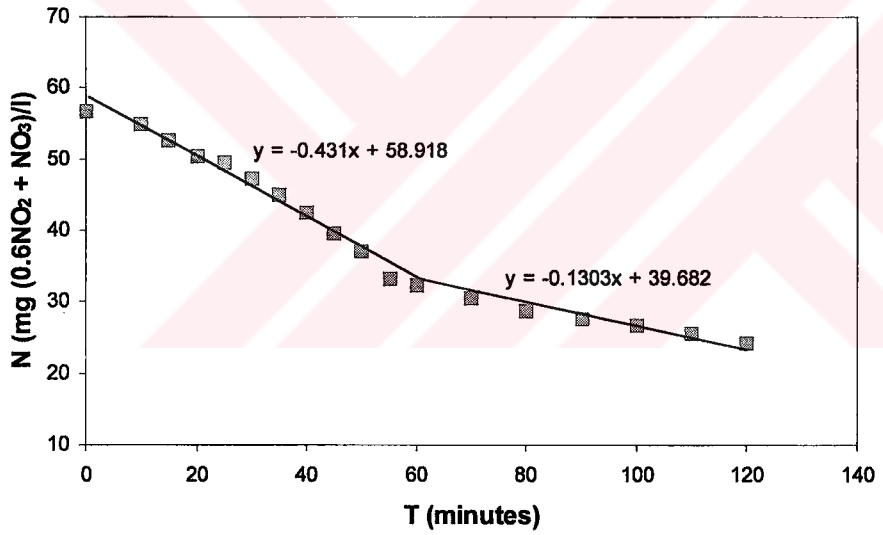

Figure 5.31b Determination of nitrate utilization rate: Acetate - experimental set 23

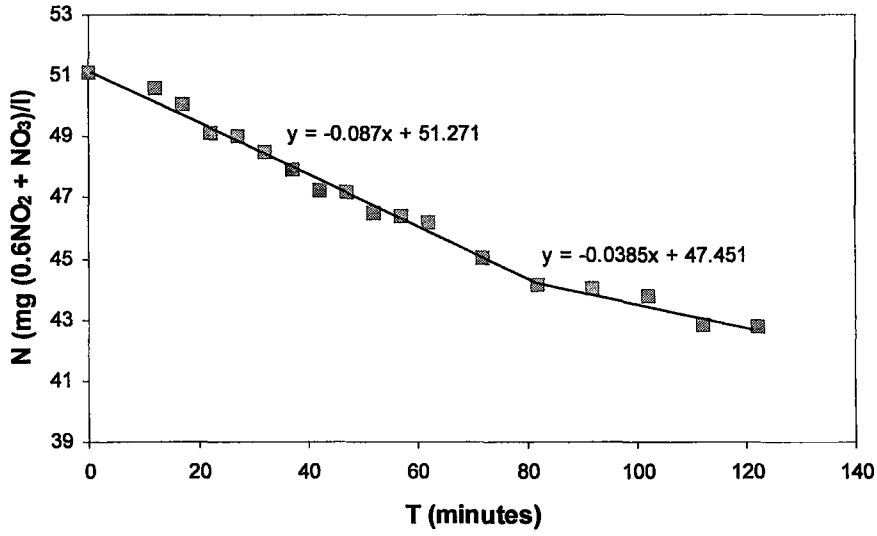

Figure 5.32a Determination of nitrate utilization rate: Filtered primary sludge - experimental set 24

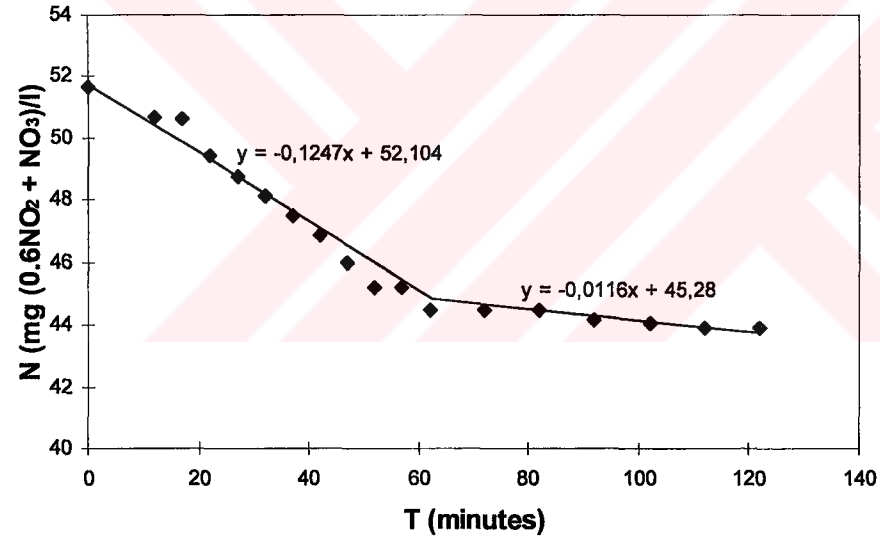

Figure 5.32b Determination of nitrate utilization rate: Acetate - experimental set 24

CHAPTER 6 SIMULATION OF EXPERIMENTAL DATA FOR DENITRIFICATION KINETICS USING EXTERNAL AND HYDROLYZED CARBON SOURCES

In this chapter, experimental data obtained from parallel anoxic batch tests for primary sludge and acetate will be simulated by using two models, namely Endogenous Decay Model (EDM) and, a more recent one, Activated Sludge Model No 3 (ASM3). First, it is intended to provide information about the process kinetics of both models. Second, sensitivity analysis will be performed for notable stochiometric and kinetic parameters of EDM and ASM3. Finally, the results of experimental data simulation will be presented.

The electron acceptor concentration will be expressed as S_{NO} for model simulation purposes, which includes NO_3^--N + NO_2^--N, as defined in EDM and ASM3.

6.1 Description of Process Kinetics in EDM

As previously explained in Section 2.2.3, processes involved in EDM are growth, hydrolysis and endogenous respiration. Among these processes, growth and decay exhibit electron acceptor (which is nitrate-nitrogen under anoxic conditions) consumption whereas hydrolysis is a mechanism which converts slowly biodegradable particulate substrate (X_S) into the readily biodegradable form without energy consumption. Within the context of this study, based on the composition of filtered primary sludge, X_S will be substituted with S_H representing hydrolyzable COD. Table 6.1 illustrates process kinetics and stochiometry for denitrification by matrix representation for the system specified in section 5.2.

Electron acceptor consumption profiles play a significant role for the mechanistic understanding of energy consuming biological processes. Figure 6.1 depicts a schematized S_{NO} versus time profile. This profile consists of three subsequent linear phases with decreasing rates in order. The first phase characterizes electron acceptor (S_{NO}) consumption mainly due to growth on the soluble readily biodegradable

Table 6.1 System-specific simplified matrix of EDM

j ↓	Component i→ Process Expressed as→	1 S_S COD	2 S_{NO} N	3 X_P COD	4 S_H COD	5 X_H COD	Process rate equation, ρ_j,all $\rho_j \geq 0$
1	Hydrolysis	1			-1		$k_{hs}\eta_h \frac{S_H/X_H}{K_{XS}+S_H/X_H} X_H \frac{S_{NO}}{K_{NO}+S_{NO}}$
2	Anoxic growth		$-\frac{1-Y_{HD}}{2.86Y_{HD}}$			1	$\hat{\mu}_H\eta_g \frac{S_S}{K_S+S_S} X_H \frac{S_{NO}}{K_{NO}+S_{NO}}$
3	Anoxic endogenous respiration		$-\frac{1-f_{EX}}{2.86}$	f_{EX}		-1	$b_H\eta_E X_H$

organic matter (S_S). Maximum growth conditions prevail during this phase provided that S_S is much greater in magnitude than the half-saturation coefficient K_S in accordance with Monod expression. After the depletion of S_S, heterotrophic microorganisms start to grow on the portion of S_S formed by the hydrolysis of the hydrolyzable soluble substrate (S_H). This rate is slower than the rate in the first phase since hydrolysis acts as the rate-limiting step. When the exogenous substrate is depleted, heterotrophic biomass starts to consume its own metabolism for energy requirements. Thus, the final phase of S_{NO} profile is due to the electron acceptor demand associated with endogenous respiration. In EDM, η factor is introduced for each phase to account for the reduced rates of each process under anoxic conditions. By definition it has been stated that η could either represent some part of heterotrophic microorganisms which perform denitrification or may as well be a factor for all heterotrophic organisms performing denitrification at a reduced rate.

6.1.1 Sensitivity analysis for EDM

In this section, the effect of stochiometric and kinetic parameters on the electron acceptor consumption profile was investigated. For this purpose, the data for filtered primary sludge in experimental set 24 was used for EDM simulation. The simulation was performed by using AQUASIM computer program developed by Swiss Federal Institute for Environmental Science and Technology. The individual effect of each parameter was assessed for lower and higher values of the selected parameter while keeping the other parameters constant. The parameters of interest are, Y_{HD}, $\hat{\mu}_H$, K_S, k_{hs}, K_{XS}, and b_H. Table 6.2 depicts the range considered for the selected parameters in addition to the value of each parameter, which fits the model simulation.

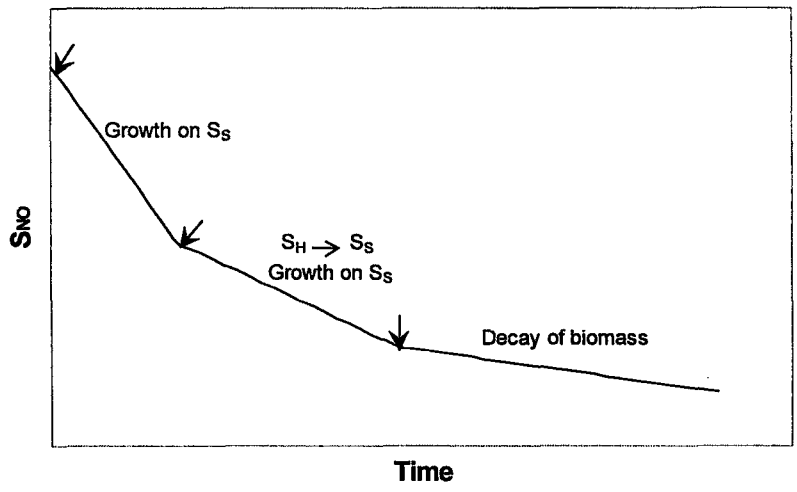

Figure 6.1 Schematic illustration of dominant processes in an S_{NO} versus time profile as described in EDM

As can be seen from Figure 6.2, the S_{NO} versus time profile is very sensitive to changes in Y_{HD}. +0.1 and –0.1 unit changes result in slower and faster depletion of S_{NO} respectively. The duration of the first phase is approximately the same in all cases.

As seen in Figure 6.3, the first phase lasts longer for the lower value of $\hat{\mu}_H$ since S_S is depleted much slower in that case. For the high value of $\hat{\mu}_H$, first phase lasts shorter due to faster depletion of S_S. The second phase proceeds slightly faster due to the greater magnitude of $\hat{\mu}_H$.

In relation to the growth expression in EDM, an increase in K_S would result in a decrease in the rate of S_S utilization. This effect would lead to a shifted S_{NO} profile with a lower rate as also can be seen in Figure 6.4. The variation of K_S would also affect the rate of the second phase due to the formation of S_S by the hydrolysis of S_H.

Table 6.2 Selected range of parameters for the sensitivity analysis performed for EDM

Parameter	Range	Fitted value	Unit
Y_{HD}	0.55-0.75	0.65	g COD/g COD
$\hat{\mu}_H$	4-7	6	1/d
K_S	2-20	5	g COD/m3
k_{hs}	1-4	3	g COD/g CODd
K_{XS}	0.01-0.1	0.01	g COD/g COD
b_H	0.1-0.3	0.2	1/d

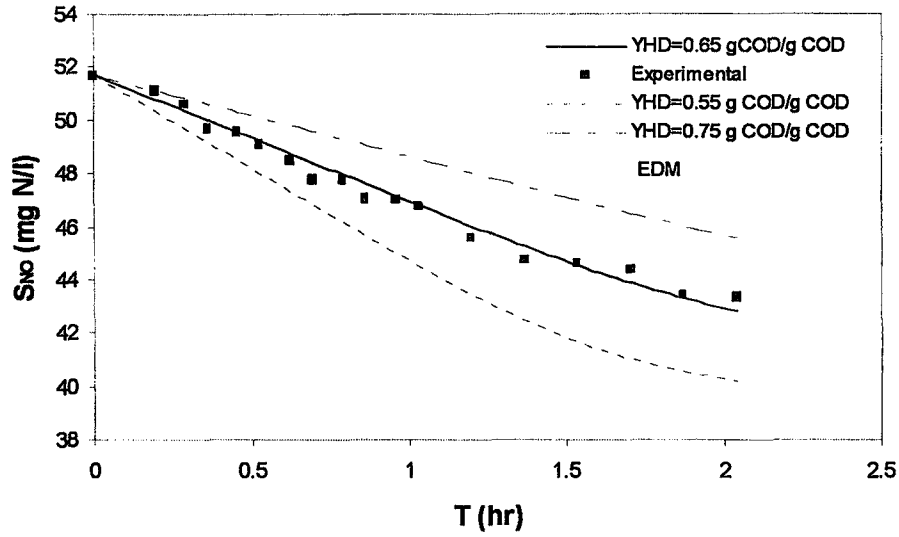

Figure 6.2 The effect of Y_{HD} on S_{NO} versus time profile for experimental set 24 for filtered primary sludge in EDM

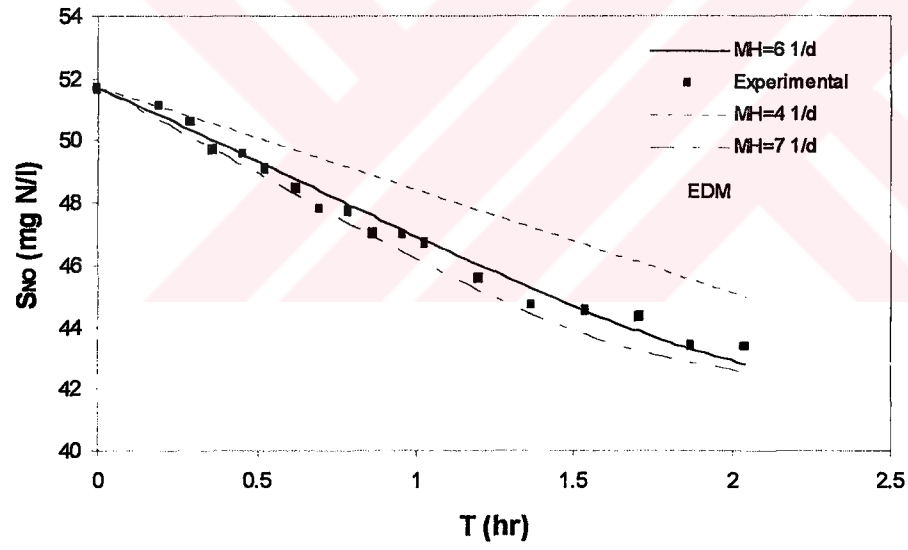

Figure 6.3 The effect of $\hat{\mu}_H$ on S_{NO} versus time profile for experimental set 24 for filtered primary sludge in EDM

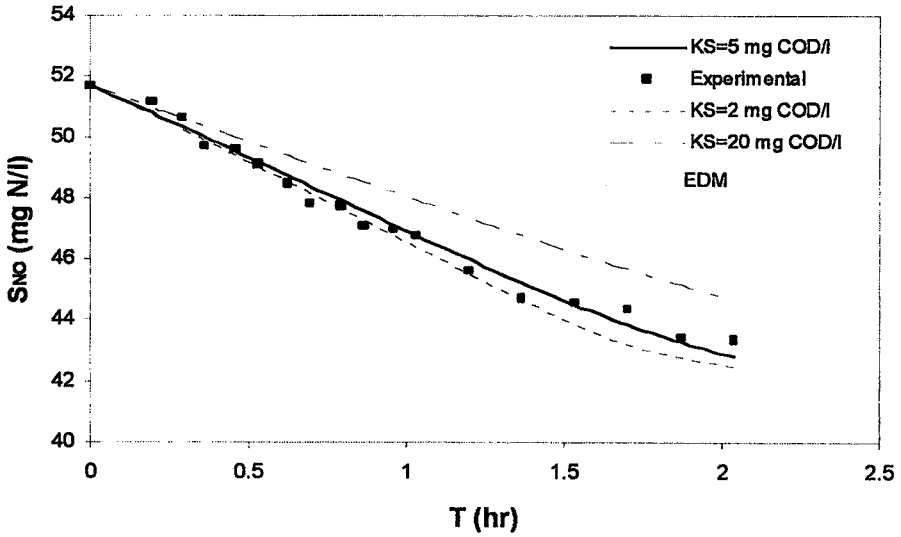

Figure 6.4 The effect of K_S on S_{NO} versus time profile for experimental set 24 for filtered primary sludge in EDM

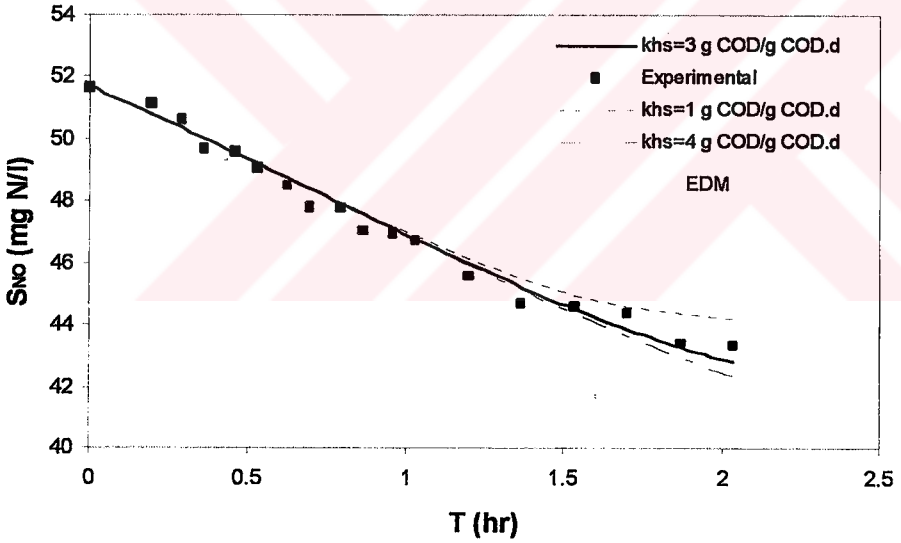

Figure 6.5 The effect of k_{hs} on S_{NO} versus time profile for experimental set 24 for filtered primary sludge in EDM

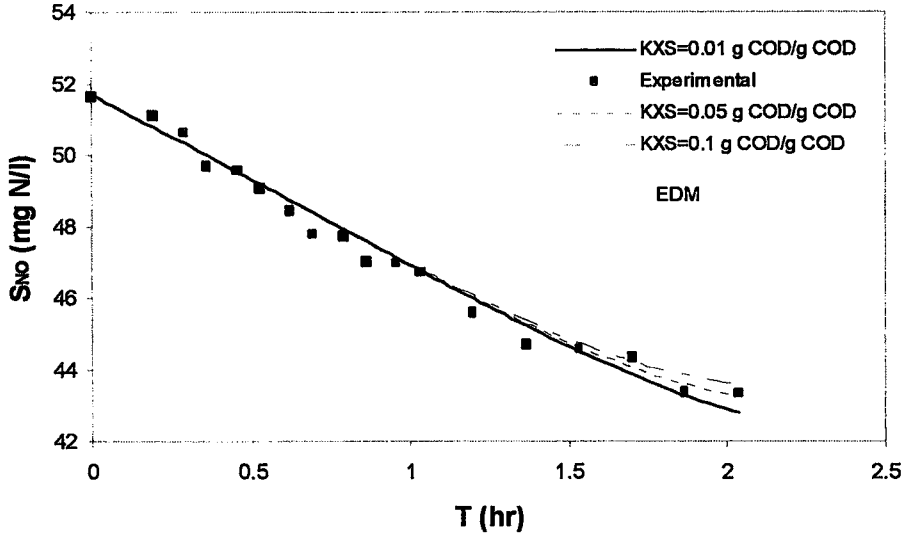

Figure 6.6 The effect of K_{XS} on S_{NO} versus time profile for experimental set 24 for filtered primary sludge in EDM

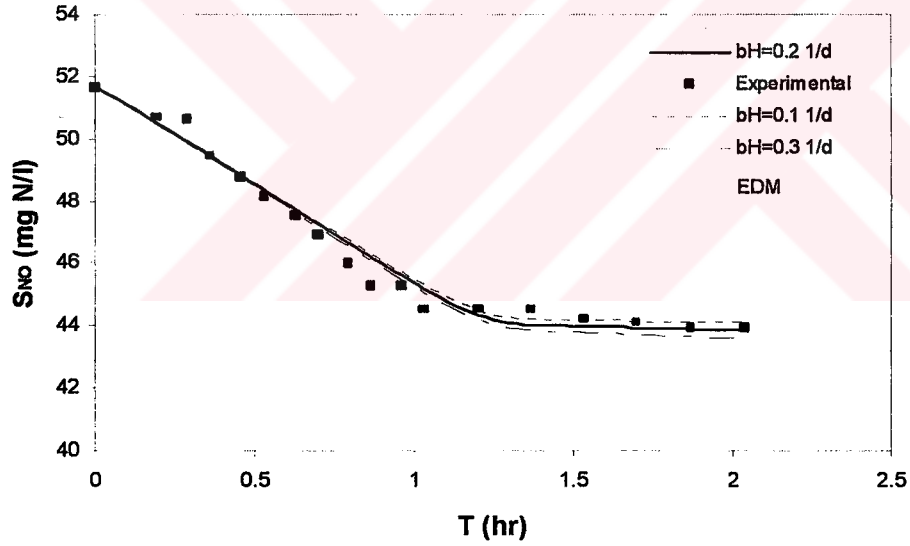

Figure 6.7 The effect of b_H on S_{NO} versus time profile for experimental set 24 for acetate in EDM

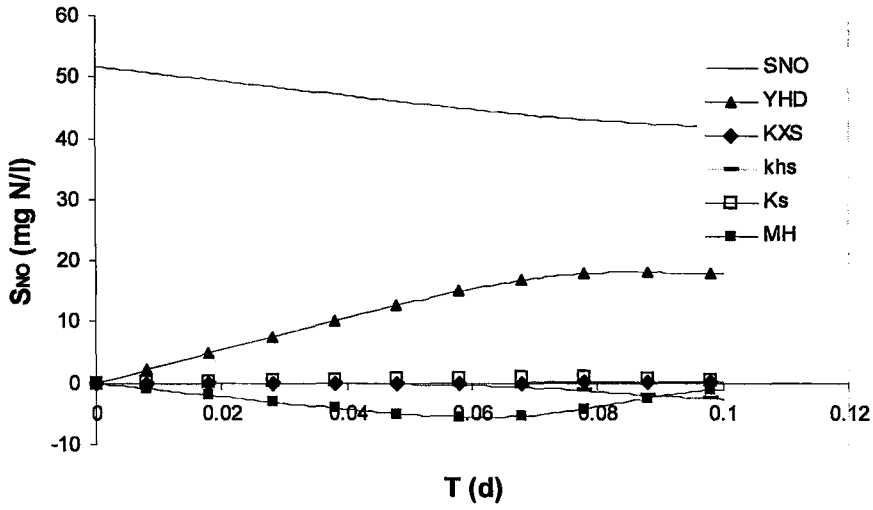

Figure 6.8 Sensitivity analysis obtained for EDM for the data for filtered primary sludge in experimental set 22, using Aquasim computer program

From Figure 6.5 it can be seen that the hydrolysis of S_H is effective during the second phase. The rate of S_{NO} consumption in the second phase is faster when k_{hs} is increased and vice versa. It is also apparent from the figure that the duration of the first phase is constant in all cases because the portion of S_S produced by hydrolysis does not contribute to the S_{NO} consumption in the first phase.

The higher values of K_{XS} used for simulation resulted in higher rates in the S_{NO} profile due to the increased overall rate of hydrolysis as shown in Figure 6.6. The saturation function may be turned to a first order reaction with respect to S_H for high values of K_{XS} and low values of S_H.

To illustrate the effect of b_H on the S_{NO} versus time profile, the data obtained for acetate in set 22 was used, since endogenous decay phase was not observed in the batch test for filtered primary sludge. As Figure 6.7 illustrates, the effect of b_H becomes visible through the end of the first phase of the S_{NO} profile. A remarkably higher rate is observed during the second phase for the higher value of b_H which is also shifted to the right.

Figure 6.8 shows the results of the sensitivity analysis performed by using Aquasim computer program, for the results of experimental set 24 for filtered primary sludge. Among the parameters considered, Y_{HD} exerts a significant impact on the whole S_{NO} versus time profile while $\hat{\mu}_H$ is effective to a less extent mid-way through the first phase until almost the end of the second phase.

6.1.2 Simulation of experimental data by EDM

Initial experimental conditions form the vital part of model inputs. Among these, initial COD fractionation is assessed according to model definitions. EDM states that the readily biodegradable COD, S_{S1}, content of the filtered domestic primary sludge should be determined by respirometric analysis. The soluble inert COD, S_{I1}, and the soluble hydrolyzable fraction, S_{H1}, are the remaining constituents for domestic sludge. Thus, COD components can be defined for filtered primary sludge by expression (6.1) as below:

$$S_{T1}=S_{S1}+S_{H1}+S_{I1} \qquad (6.1)$$

Table 6.3 COD fractionation for acetate (AA) and filtered primary sludge (FPS) reactors in accordance with EDM

Experimental Set	AA (mg COD/l)	FPS (mg COD/l)			
	$S_{S1}=S_{T1}$	S_{T1}	S_{S1}	S_{H1}	S_{I1}
15	100	-	-	-	-
16	120	260	120	110	30
22	100	230	100	105	25
23	175	330	175	120	35
24	50	95	50	35	10

Table 6.4 Selected and default values of kinetic and stochiometric parameters for EDM

Parameter	Unit	Default (20°C)	Acetate	FPS	Reference for Default Value
Y_{HD}	gCOD/gCOD	0.54	0.58	0.62[a],0.64[b], 0.65[c], 0.66[d]	ASM3
f_{EX}	dimensionless	0.2	0.2	0.2	ASM1, ASM3
k_{hs}	gCOD/gCODd	3.1	-	3	Orhon et al., 1999
K_{XS}	gCOD/gCOD	0.2	-	0.01	Orhon et al., 1999
η_g	dimensionless	0.8	0.5	0.5	ASM1
η_h	dimensionless	0.4	0.4	0.4	ASM1
η_E	dimensionless	0.8-1.0	0.5	0.5	Kristensen et al.,1992
K_S	gCOD/m^3	20, 2	2	5	ASM1, ASM3
K_{NO}	gNO$_3$-N/m^3	0.5	0.5	0.5	ASM1, ASM3
$\hat{\mu}_H$	1/d	6, 2	6	6,6.5[e]	ASM1, ASM3
b_H	1/d	0.24,0.2	0.2	0.2	ASM1, ASM3

[a,b,c,d] Y_{HD} values for runs 22, 23, 24, and 16 respectively

[e] $\hat{\mu}_H$ value for run 16

In this study, S_{S1} was determined by respirometric analysis as shown in section 5.2. S_{I1} was assumed as 10 % of the total soluble COD, S_{T1} (Sözen et al., 1998). S_{H1} was determined according to expression (6.1). The COD fractionation of filtered primary sludge assessed according to EDM is presented in Table 6.3

S_{NO} versus time profiles obtained from experimental sets 15, 16, 22, 23, and 24, as presented in section 5.2, were simulated for EDM. These were the sets where the second phase of the experimentally obtained electron acceptor consumption profile was observed in parallel batch tests for acetate and filtered primary sludge. Similar to sensitivity analysis, AQUASIM computer program was used for model simulation.

The kinetic and stochiometric parameters used in EDM simulation for acetate and filtered primary sludge are given in Table 6.2 together with default values at 20°C.

The results of EDM simulation for acetate and filtered primary sludge for experimental sets 15 to 24 are shown in Figures 6.9 to 6.26.

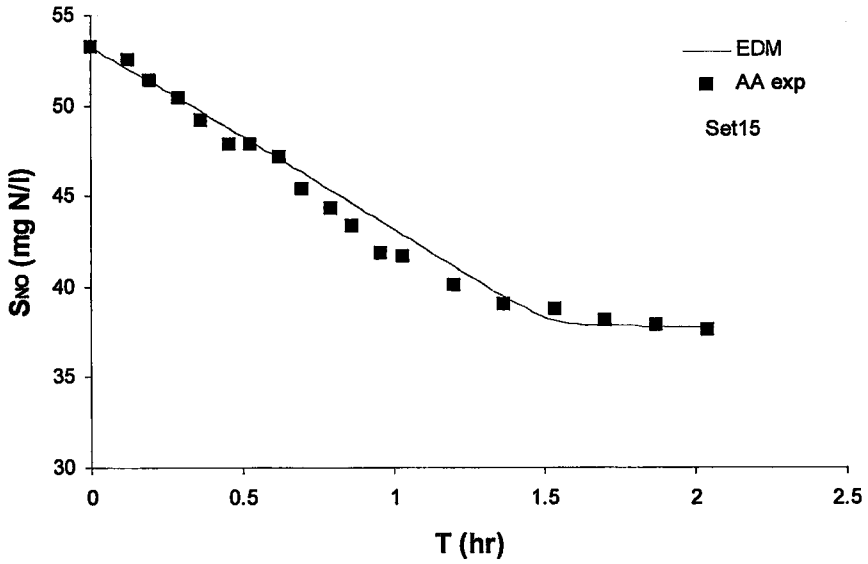

Figure 6.9 Experimental data and S_{NO} versus time profile obtained by EDM simulation for acetate (AA) for experimental set 15

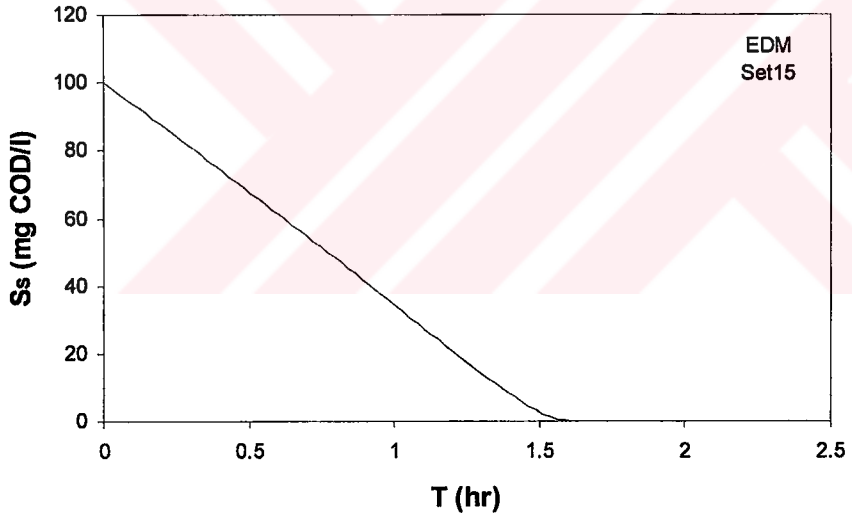

Figure 6.10 S_S versus time profile obtained by EDM simulation for acetate for experimental set 15

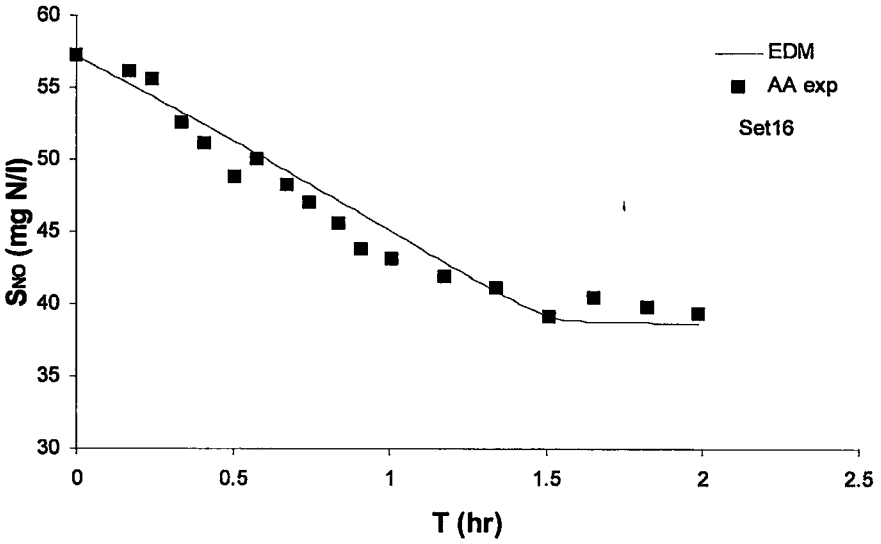

Figure 6.11 S_{NO} versus time profile obtained by EDM simulation for acetate (AA) for experimental set 16

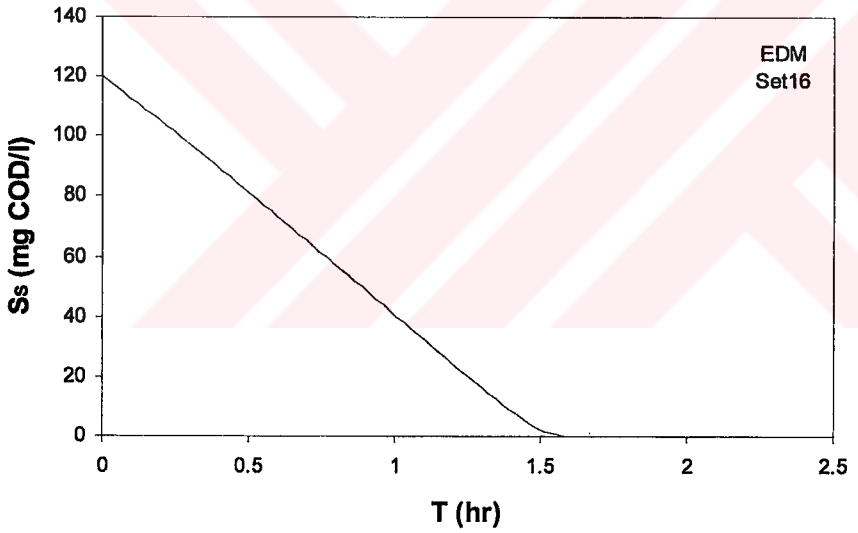

Figure 6.12 S_S profile obtained by EDM simulation for acetate for experimental set 16

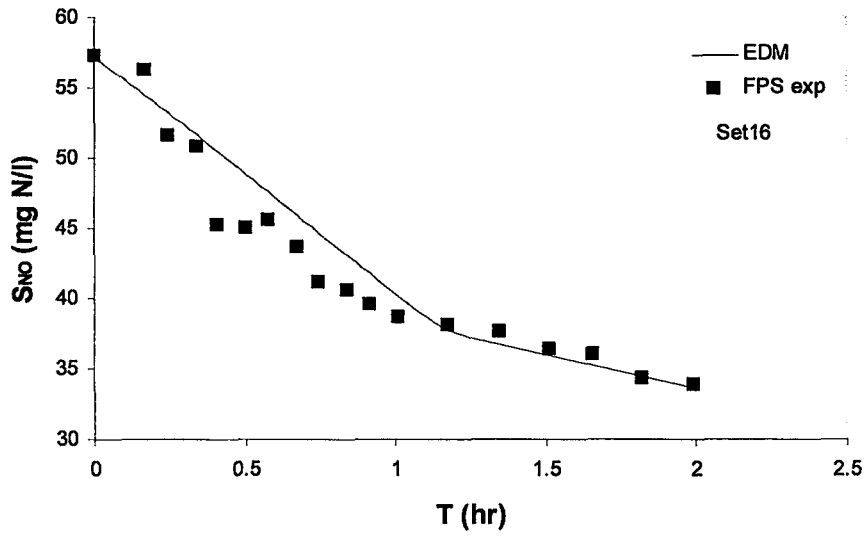

Figure 6.13 S_{NO} versus time profile obtained by EDM simulation for filtered primary sludge (FPS) for experimental set 16

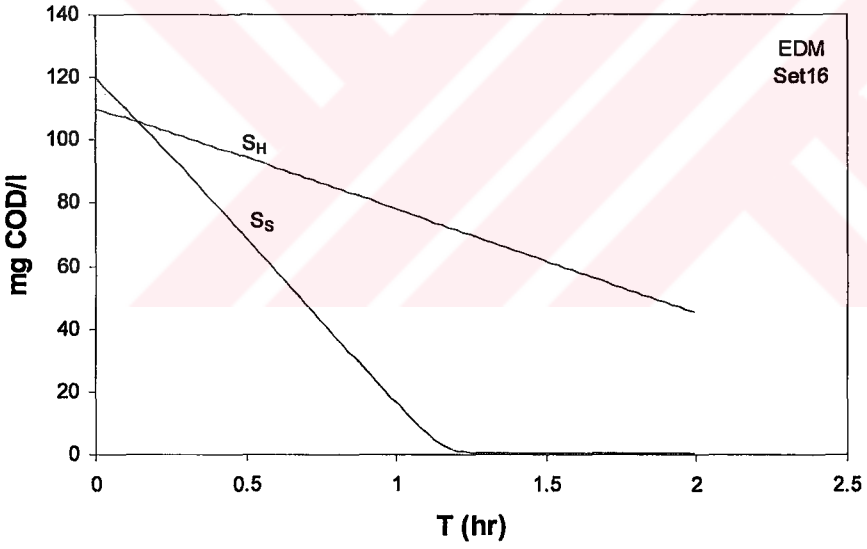

Figure 6.14 S_S and S_H versus time profiles obtained by EDM simulation for filtered primary sludge for experimental set 16

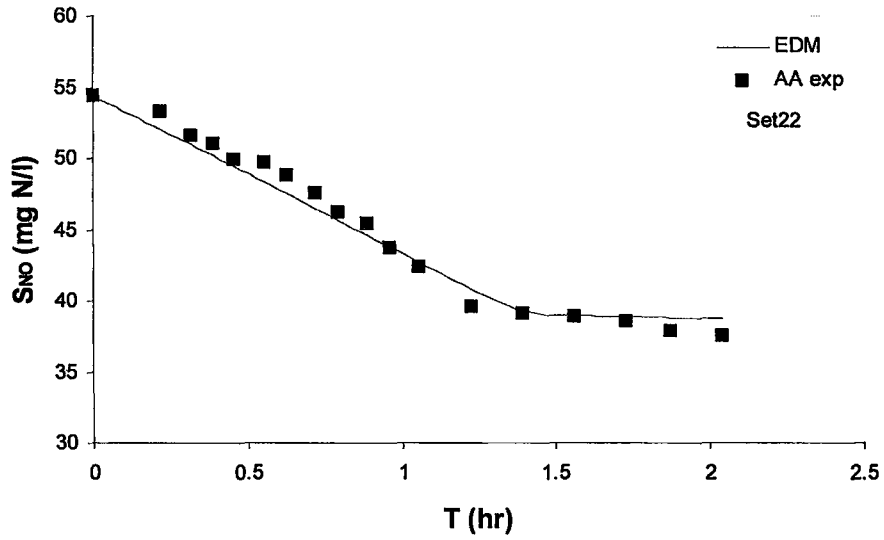

Figure 6.15 S_{NO} versus time profile obtained by EDM simulation for acetate (AA) for experimental set 22

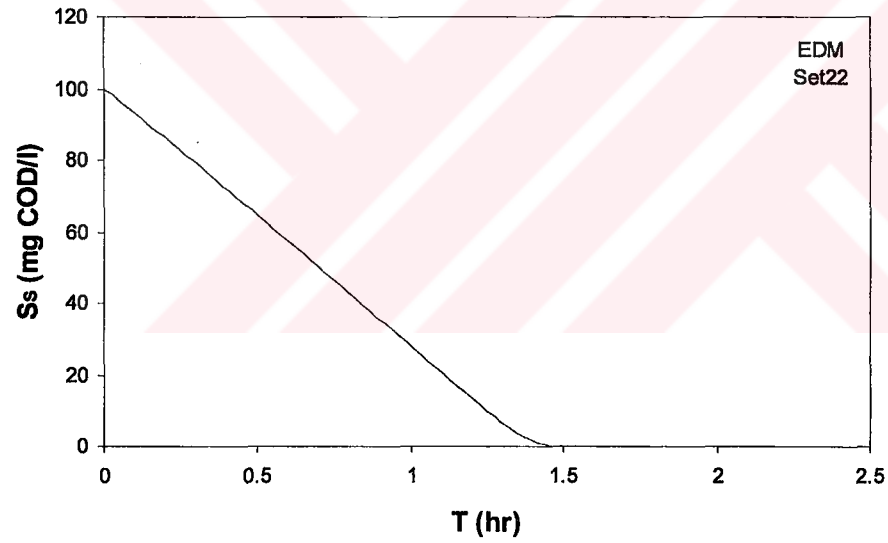

Figure 6.16 S_S versus time profile obtained by EDM simulation for acetate for experimental set 22

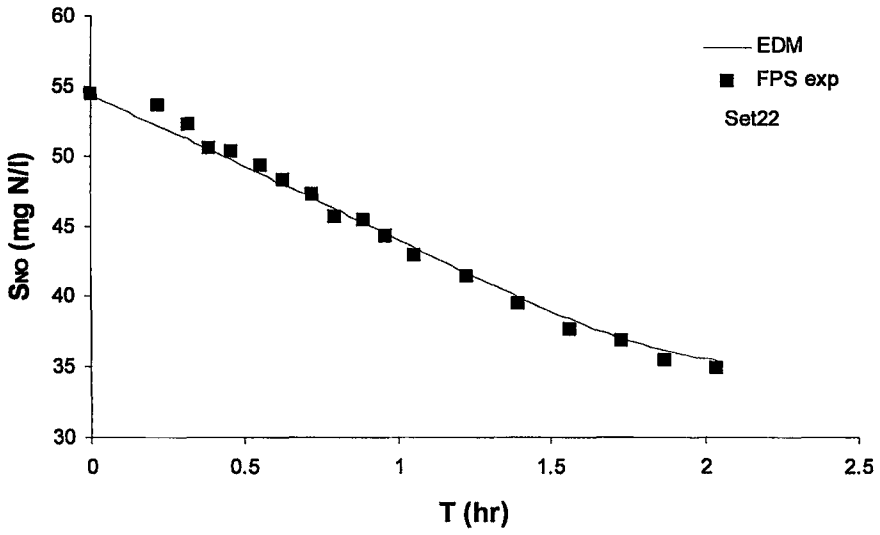

Figure 6.17 S_{NO} versus time profile obtained by EDM simulation for filtered primary sludge (FPS) for experimental set 22

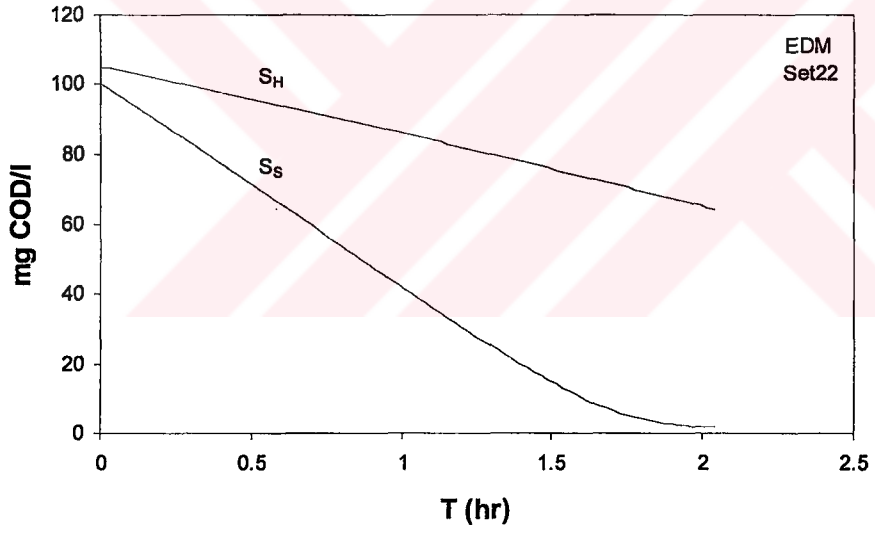

Figure 6.18 S_S and S_H versus time profiles obtained by EDM simulation for filtered primary sludge for experimental set 22

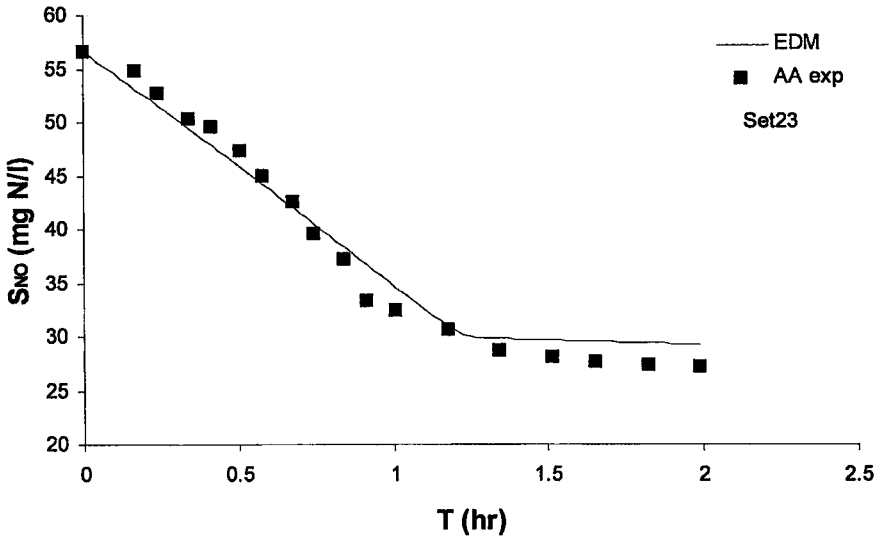

Figure 6.19 Experimental data and S_{NO} versus time profile obtained by EDM simulation for acetate (AA) for experimental set 23

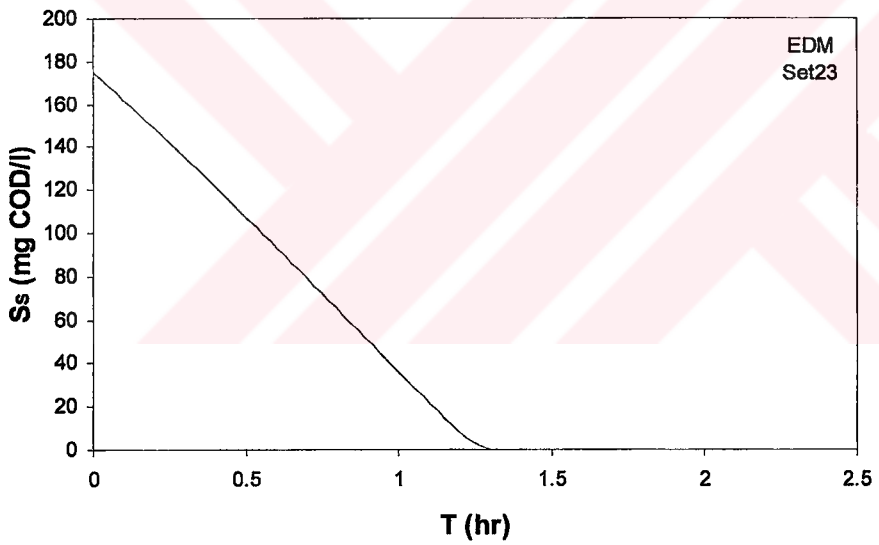

Figure 6.20 S_S versus time profile obtained by EDM simulation for acetate for experimental set 23

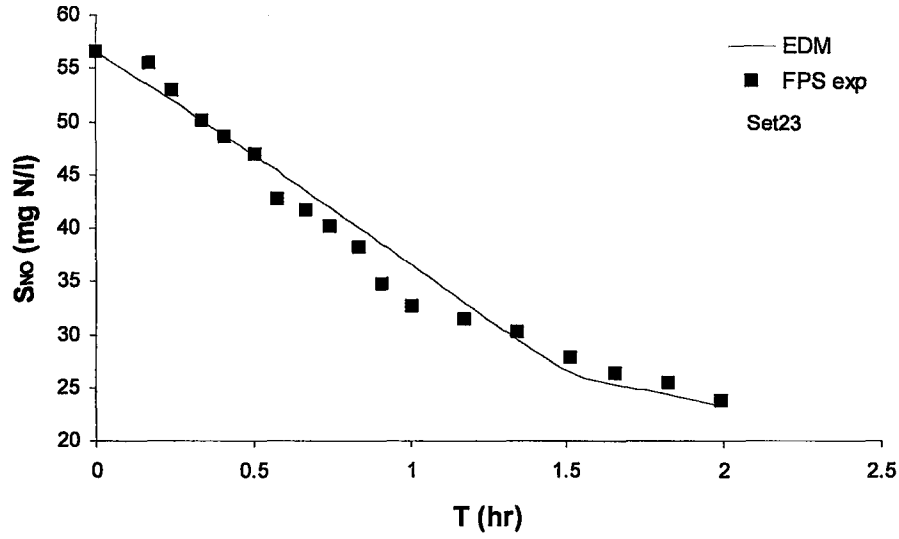

Figure 6.21 Experimental data and S_{NO} versus time profile obtained by EDM simulation for filtered primary sludge (FPS) for experimental set 23

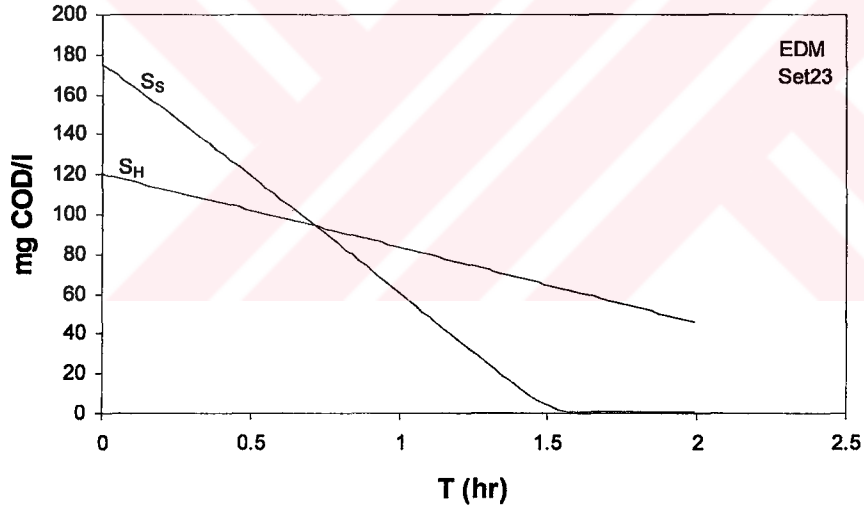

Figure 6.22 S_S and S_H versus time profiles obtained by EDM simulation for filtered primary sludge for experimental set 23

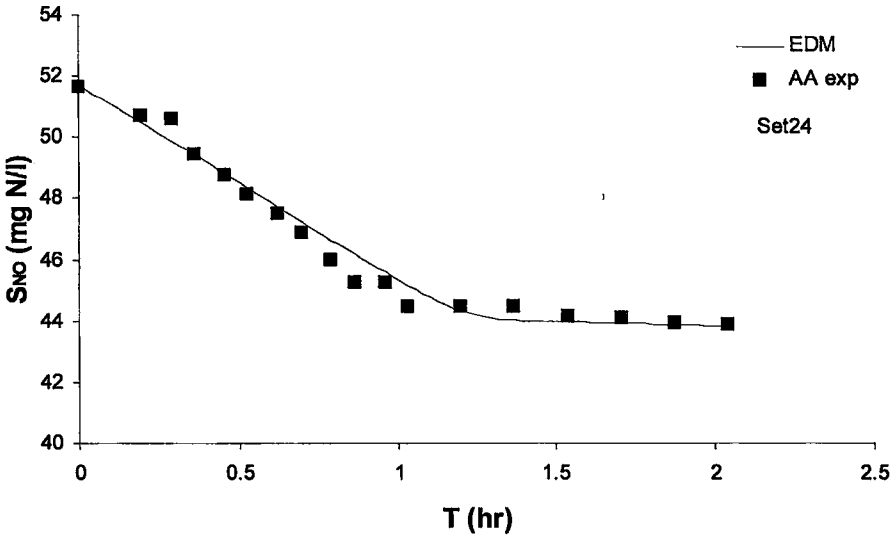

Figure 6.23 Experimental data and S_{NO} versus time profile obtained by EDM simulation for acetate (AA) for experimental set 24

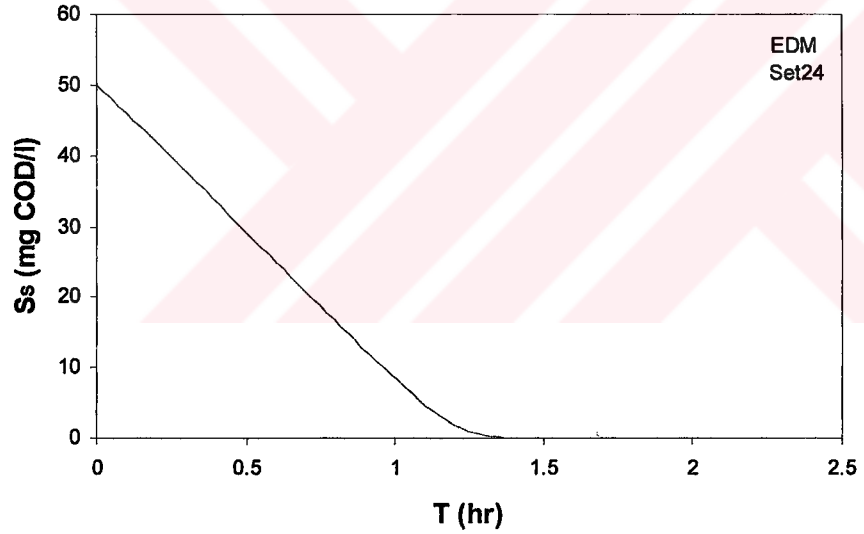

Figure 6.24 S_S versus time profile obtained by EDM simulation for acetate for experimental set 24

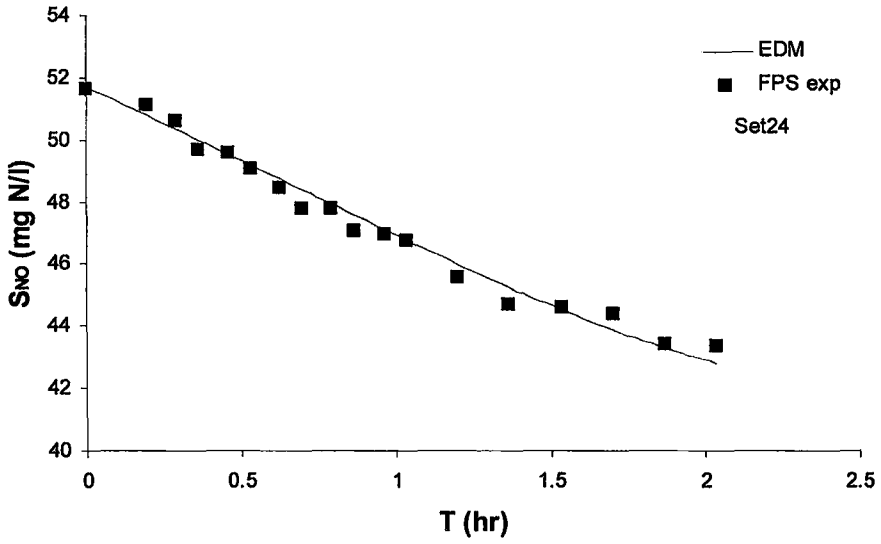

Figure 6.25 Experimental data and S_{NO} versus time profile obtained by EDM simulation for filtered primary sludge (FPS) for experimental set 24

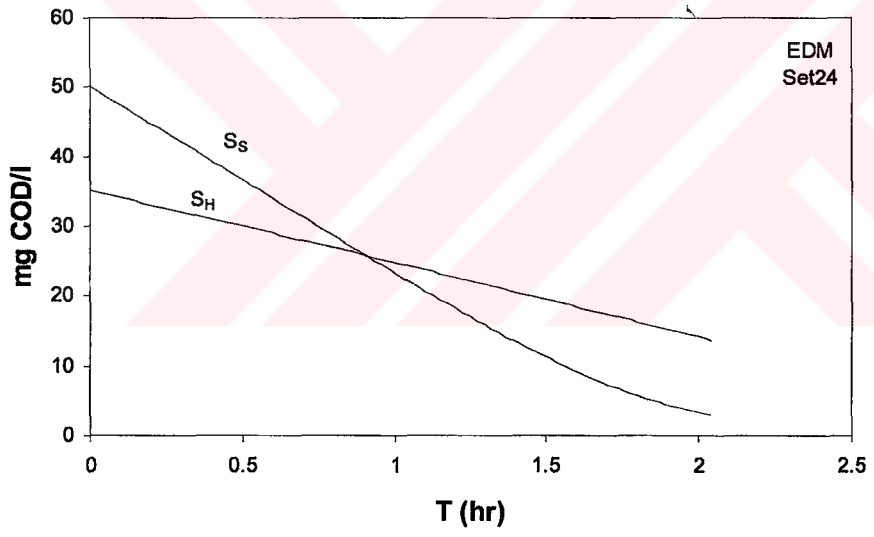

Figure 6.26 S_S and S_H versus time profiles obtained by EDM simulation for filtered primary sludge for experimental set 24

6.2 Description of Process Kinetics in ASM3

Activated Sludge Model No 3 (ASM3) has recently been introduced by Gujer et al. (1999). Its main objective is stated as offsetting the drawbacks of formerly used models by introducing mechanisms, namely storage and respiration of storage products. These processes have not been included in the prior model structures such as EDM and ASM1. Storage process involves the conversion of S_S into the form of cell internal storage products referred as X_{STO}, which includes polyhydroxyalkanoates (PHA), glycogen, etc. It is defined as an energy consuming process. The kinetic expression for storage involves the Monod kinetic expression. Growth occurs on the stored products and is defined by a saturation function. ASM3 introduces respiration of storage products as another energy consuming process, which involves the decay of storage products, analogous to endogenous respiration.

This model assumes that X_S is converted to S_S at a comparably higher rate as compared to growth on X_{STO}, thus, in contrast to EDM, hydrolysis is not a rate-limiting mechanism.

Table 6.5 illustrates the matrix representation for ASM3. It should be noted that, this matrix constitutes only the processes and components involved in the simulation studies.

Table 6.5 System-specific simplified matrix of ASM3

j ↓	Component i→ Process Expressed as→	1 S_S COD	2 S_{NO} N	3 X_P COD	4 X_H COD	5 X_{STO} COD	Process rate equation, ρ_j,all $\rho_j \geq 0$
1	Anoxic storage of COD	-1	$-\frac{1-Y_{STOD}}{2.86}$			Y_{STOD}	$k_{STO}\eta_D \frac{S_S}{K_S+S_S} X_H \frac{S_{NO}}{K_{NO}+S_{NO}}$
2	Anoxic growth		$-\frac{1-Y_{HD}}{2.86Y_{HD}}$		1	$-\frac{1}{Y_{HD}}$	$\hat{\mu}_H\eta_D \frac{X_{STO}/X_H}{K_{STO}+X_{STO}/X_H} X_H \frac{S_{NO}}{K_{NO}+S_{NO}}$
3	Anoxic endogenous respiration		$-\frac{1-f_{EX}}{2.86}$	f_{EX}	-1		$b_{HD}X_H \frac{S_{NO}}{K_{NO}+S_{NO}}$
4	Anoxic respiration of X_{STO}		$-\frac{1}{2.86}$			-1	$b_{STOD}X_{STO} \frac{S_{NO}}{K_{NO}+S_{NO}}$

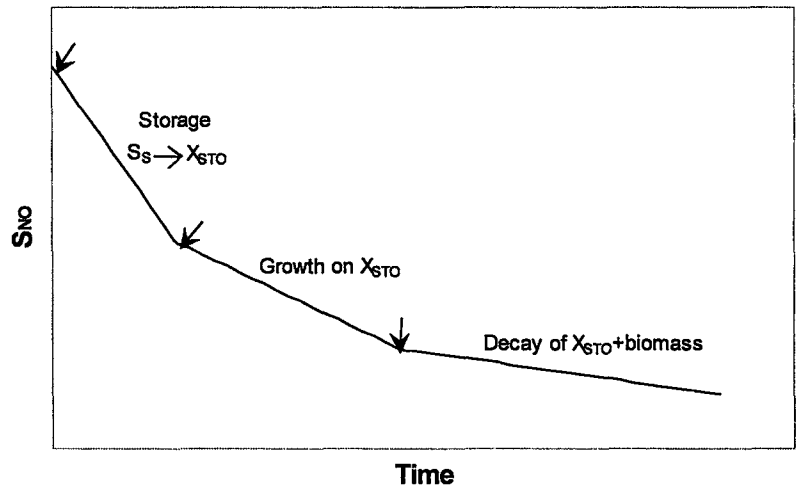

Figure 6.27 Schematic illustration of dominant processes in an S_{NO} versus time profile as described in ASM3

Figure 6.27 shows a schematized S_{NO} consumption profile. Similar to Figure 6.1, it is obtained by running AQUASIM simulation program by using default values as initial conditions for ASM3. The first phase is associated mainly with the electron acceptor (S_{NO}) consumption due to storage of S_S in the form of X_{STO}. At the end of this phase, while S_S is depleted completely, X_{STO} concentration reaches its peak concentration. Since the rate of storage is envisaged faster than the rate of growth, storage does not act as a rate-limiting step. During the second phase, S_{NO} consumption is mostly due to the growth of heterotrophic biomass on storage products. In this phase, growth is dominant among the processes of endogenous respiration and respiration of storage products. When X_{STO}/X_H ratio in the saturation function becomes limiting, the growth process proceeds slower or may even stop. At this point, the third phase starts. During this phase, anoxic endogenous decay and anoxic respiration of X_{STO} contribute to the S_{NO} consumption. Since anoxic respiration is the sole mechanism for the consumption of X_{STO}, the depletion of X_{STO} would only occur after a period of days, which is not practically observed throughout a batch test. After then, endogenous respiration will take role in the consumption of S_{NO}.

Figure 6.28 depicts the COD flow during storage, growth, and respiration of storage products. In the figure, *f* indicates the fraction of X_{STO} used for growth while *(1-f)* denotes the remaining fraction of X_{STO} consumed for the respiration of storage products.

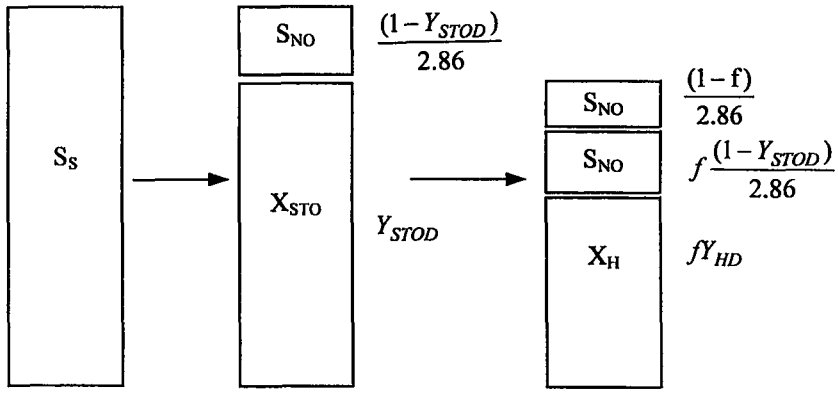

Figure 6.28 COD flow in ASM3 during processes of storage, growth, and respiration of storage products

According to ASM3, the rate of S_{NO} utilization during storage, growth and anoxic respiration of X_{STO} can be written as below:

$$\frac{dS_{NO}}{dt} = \frac{1-Y_{STOD}}{2.86}\frac{dS_S}{dt} + \frac{1-Y_{HD}}{2.86} f \frac{dX_{STO}}{dt} + \frac{1-f}{2.86}\frac{dX_{STO}}{dt} \qquad (6.2)$$

Since dX_{STO}/dt can be written as:

$$\frac{dX_{STO}}{dt} = Y_{STOD}\frac{dS_S}{dt} \qquad (6.3)$$

Expression (6.2) can be reorganized as:

$$\frac{dS_{NO}}{dt} = \frac{1-fY_{STOD}Y_{HD}}{2.86}\frac{dS_S}{dt} \qquad (6.4)$$

Equation (6.4) states that the anoxic biomass yield can be expressed as a product of anoxic storage yield and anoxic heterotrophic growth yield, thus reduced by the Y_{STOD} coefficient. Furthermore, the anoxic biomass yield is proportional to the fraction of storage products utilized for growth .

It should also be emphasized that, with the exception of hydrolysis, each process defined in ASM3 has a counterpart under anoxic conditions. Biomass yield is also adapted for anoxic storage and anoxic heterotrophic yields as Y_{STOD} and Y_{HD} respectively.

6.2.1 Sensitivity analysis for ASM3

For ASM3, sensitivity analysis was performed for the recently introduced parameters namely, Y_{STOD}, k_{STO}, K_{STO}, and b_{STOD} besides $\hat{\mu}_H$. The other stochiometric and kinetic parameters exhibit similar effects as stated in section 6.1.1. Table 6.6 presents the range considered for model simulation besides the fitted value of each parameter.

Figure 6.29 shows the significant effect of Y_{STOD} on the S_{NO} versus time profile. The lower value of Y_{STOD} used for simulation (0.63 g COD/g COD) affects the S_{NO} versus time profile such that less percentage of S_S is converted to X_{STO} resulting in the depletion of X_{STO} in a shorter time. As a consequence, the first phase in the electron acceptor utilization profile lasts shorter.

Figure 6.30 shows the effect of $\hat{\mu}_H$ on the S_{NO} versus time profile. The increased rate of growth on X_{STO} leads to faster depletion of S_{NO} starting from almost the middle of the first phase. It should also be noted that, $\hat{\mu}_H$ does not exert a significant effect on the S_{NO} profile as in EDM.

k_{STO} has a major effect on the electron acceptor utilization profile due to its direct effect on storage. The slower the rate of storage is, the slower S_{NO} is consumed. In such a case, the duration of the first phase also lasts longer. Figure 6.31 shows that the use of the default value of k_{STO} (5 g COD/g CODd) results in slower conversion of S_S to X_{STO}, thus only a single phase is observed throughout the experimental period. For an increased value of k_{STO}, the first phase lasts shorter and the electron acceptor is depleted faster.

Table 6.6 Selected range of parameters for sensitivity analysis performed for ASM3

Parameter	Range	Fitted value	Unit
Y_{STOD}	0.63-0.85	0.8	g COD/g COD
$\hat{\mu}_H$	4-7	6	1/d
k_{STO}	5-20	16	g COD/g CODd
K_{STO}	0.1-2	1	g COD/g COD
b_{STOD}	0.01-0.3	0.1	1/d

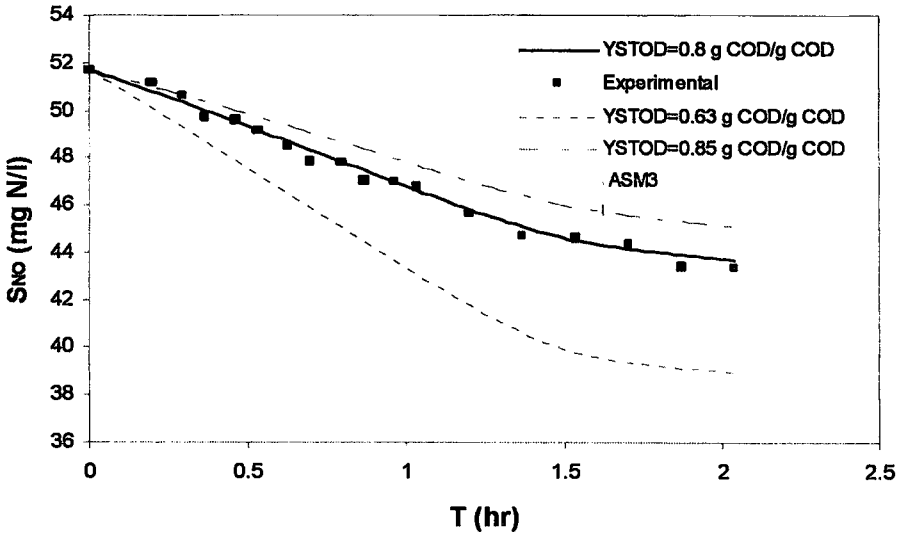

Figure 6.29 The effect of Y_{STOD} on S_{NO} versus time profile for experimental set 24 for filtered primary sludge in ASM3

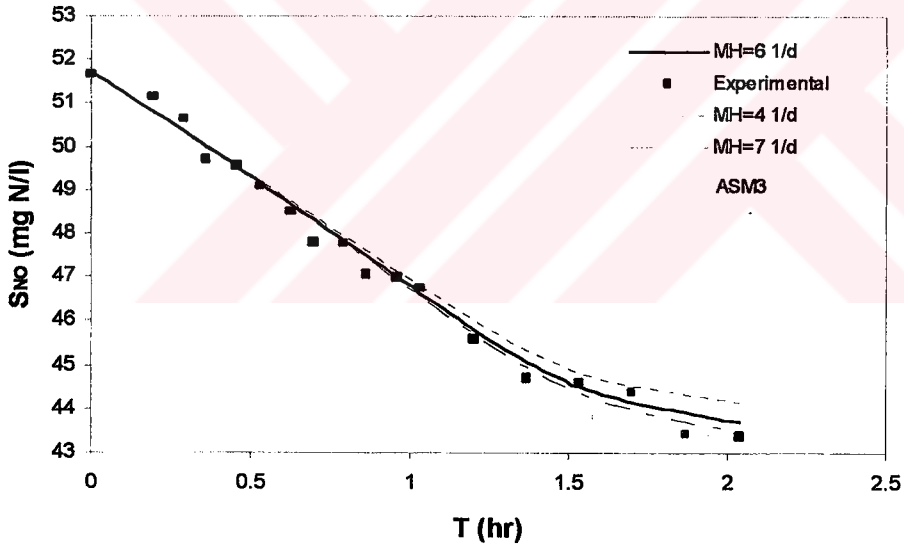

Figure 6.30 The effect of $\hat{\mu}_H$ on S_{NO} versus time profile for experimental set 24 for filtered primary sludge in ASM3

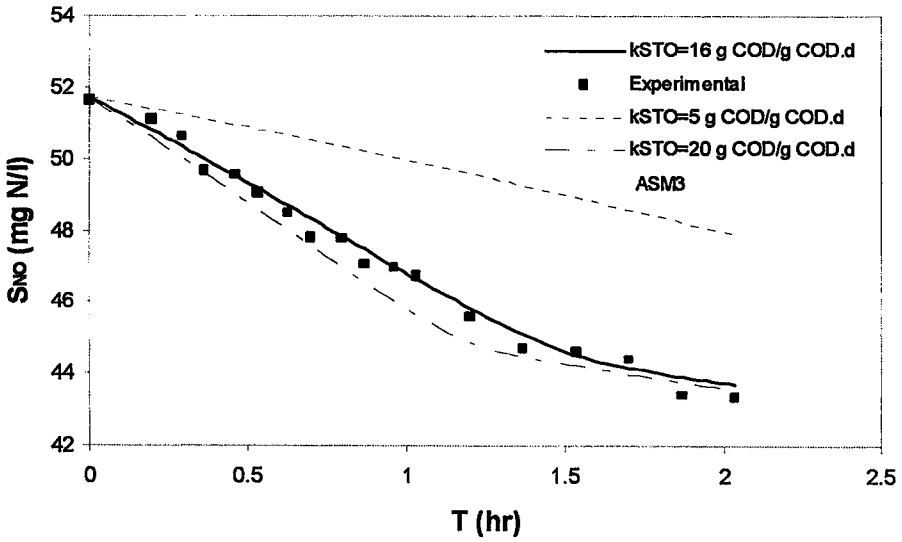

Figure 6.31 The effect of k_{STO} on S_{NO} versus time profile for experimental set 24 for filtered primary sludge in ASM3

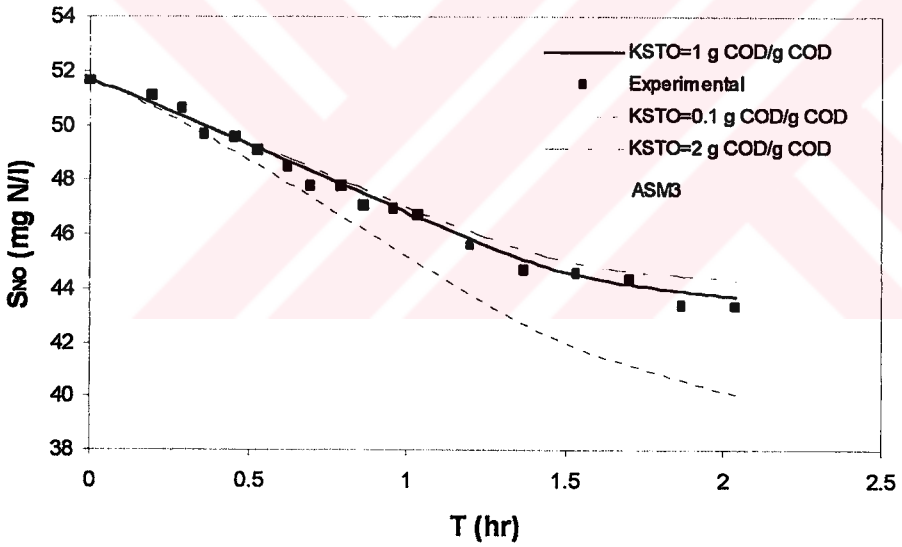

Figure 6.32 The effect of K_{STO} on S_{NO} versus time profile for experimental set 24 for filtered primary sludge in ASM3

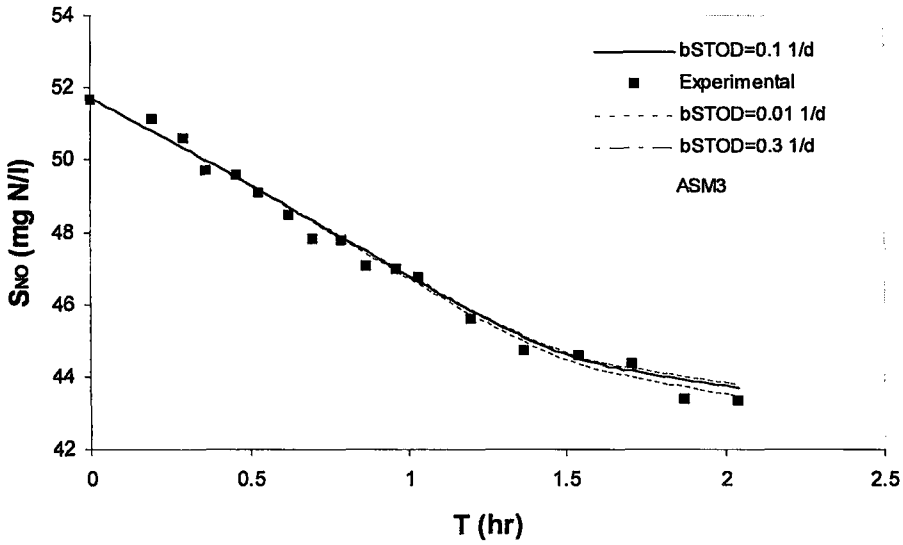

Figure 6.33 The effect of b_{STOD} on S_{NO} versus time profile for experimental set 22 for filtered primary sludge in ASM3

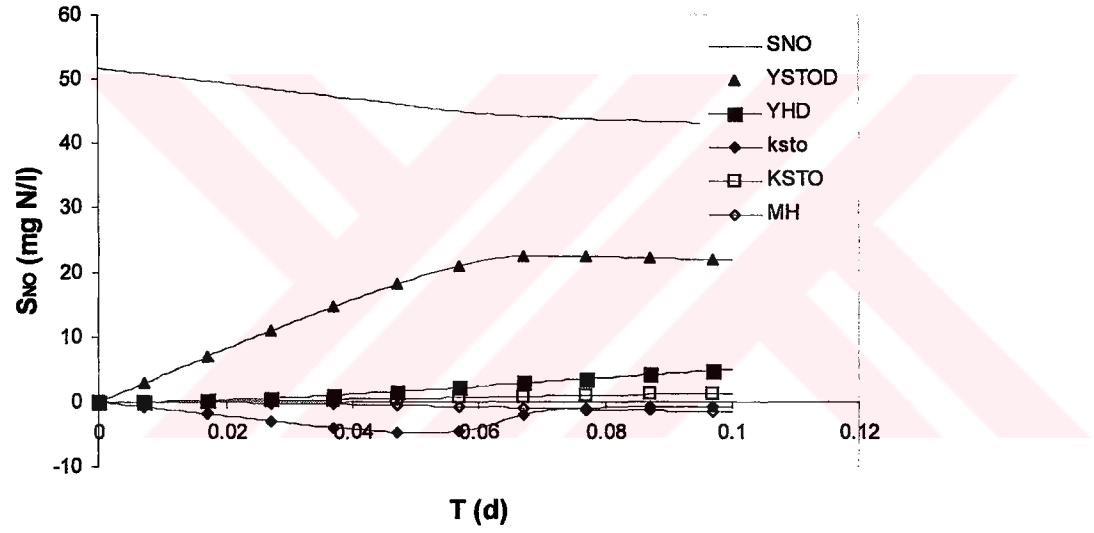

Figure 6.34 Sensitivity analysis obtained for ASM3 by using data for filtered primary sludge in experimental set 22, using Aquasim computer program

The effect that K_{STO} exerts on the S_{NO} profile becomes more pronounced for its greater variations in magnitude as Figure 6.32 shows. The default value of K_{STO} (1 g COD/g COD) leads to a profile compliant with the experimental data. The use of a lower value for K_{STO} results in a higher rate of S_{NO} consumption, due to its presence in the denominator of the half-saturation function associated with the growth process in ASM3.

As Figure 6.33 shows, b_{STOD} does not exert any significant effect on the S_{NO} versus time profile even for big variations in its magnitude.

The results of the sensitivity analysis obtained by Aquasim computer program are depicted in Figure 6.34. Y_{STOD}, k_{STO}, and Y_{HD} can be listed in decreasing order, for the influence these parameters exert on the electron acceptor utilization profile. $\hat{\mu}_H$ and K_{STO} behave similarly but, they exert opposite effects on the rate of S_{NO} consumption as the figure shows.

6.2.2 Simulation of experimental data by ASM3

Initial COD fractionation was assessed according to the definition in ASM3. The model states that the total filtered COD (0.45μm membrane filters) is composed of readily biodegradable and inert fractions of COD as shown in expression (6.5):

$$S_{TI}=S_{SI}+S_{II} \qquad (6.5)$$

S_{II} was determined by the same assumption in EDM. Table 6.7 shows the initial COD fractions used in ASM3 simulation for acetate and filtered primary sludge.

Similar to section 6.1.2, S_{NO} profiles obtained from experimental sets 15, 16, 22, 23, and 24 were simulated for ASM3. Figures 6.35 to 6.52 present the simulation studies conducted for ASM3 by using data obtained from parallel batch tests of acetate and filtered primary sludge. The values of kinetic and stochiometric parameters used for model simulation of acetate and filtered primary sludge, as stated in ASM3 can be seen in Table 6.8.

Table 6.7 Initial COD fractions in acetate (AA) and filtered primary sludge (FPS) reactors in accordance with ASM3

Experimental Set	AA (mg COD/l)	FPS (mg COD/l)		
	$S_{SI}=S_{TI}$	S_{TI}	S_{SI}	S_{II}
15	100	-	-	-
16	120	260	230	30
22	100	230	205	25
23	175	330	295	35
24	50	95	85	10

Table 6.8 Selected and default values of kinetic and stochiometric parameters for ASM3

Parameter	Unit	Default (20°C)	Acetate	FPS
Y_{HD}	gCOD/gCOD	0.54	0.58	0.62[a],0.64[b], 0.65[c], 0.66[d]
Y_{STOD}	gCOD/gCOD	0.8	0.63	0.78[e],0.8
f_{EX}	dimensionless	0.2	0.2	0.2
η_D	dimensionless	0.6	0.5	0.5
k_{STO}	gCOD/gCODd	5	12	16[f,g],17[h],,20[i]
K_{STO}	gCOD/gCOD	1	1	1
K_S	gCOD/m^3	2	2	5
K_{NO}	gNO_3N/m^3	0.5	0.5	0.5
$\hat{\mu}_H$	1/d	2	6	6,6.5[j]
b_{HD}	1/d	0.1	0.1	0.1
b_{STOD}	1/d	0.1	0.1	0.1

[a,b,c,d] Y_{HD} values for runs 22, 23, 24, and 16 respectively
[e] Y_{STOD} value for run 23
[f,g,h,i] k_{STO} values for runs 22, 24, 23and 16 respectively
[j] $\hat{\mu}_H$ value for run 16

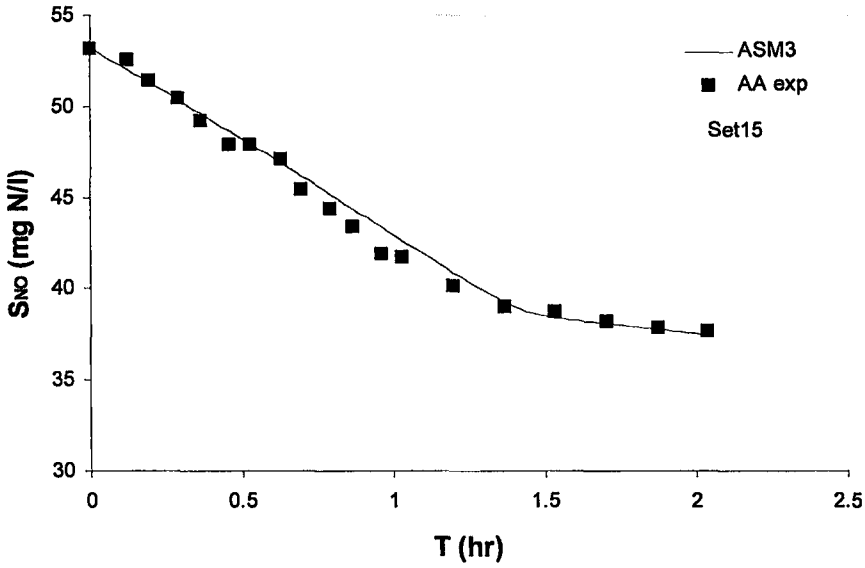

Figure 6.35 Experimental data and S_{NO} versus time profile obtained by ASM3 simulation for acetate (AA) for experimental set 15

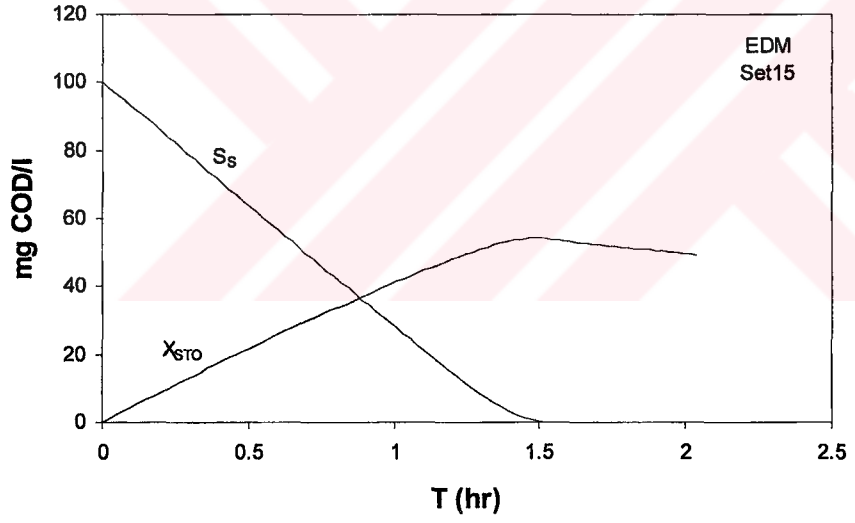

Figure 6.36 S_S and X_{STO} versus time profiles obtained by ASM3 simulation for acetate for experimental set 15

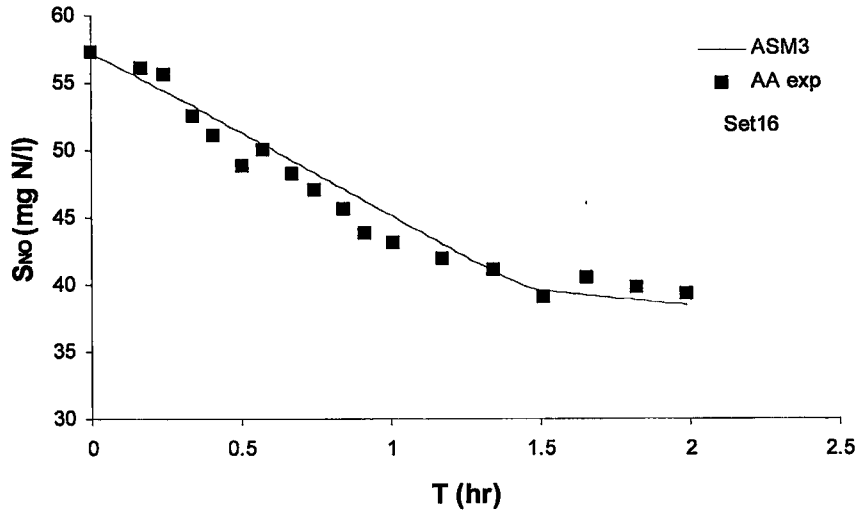

Figure 6.37 Experimental data and S_{NO} versus time profile obtained by ASM3 simulation for acetate (AA) for experimental set 16

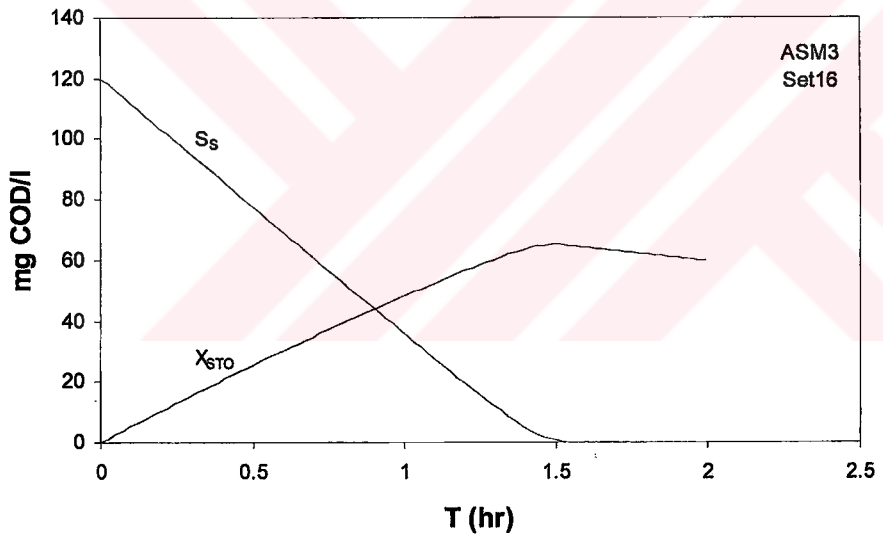

Figure 6.38 S_S and X_{STO} versus time profiles obtained by ASM3 simulation for acetate for experimental set 16

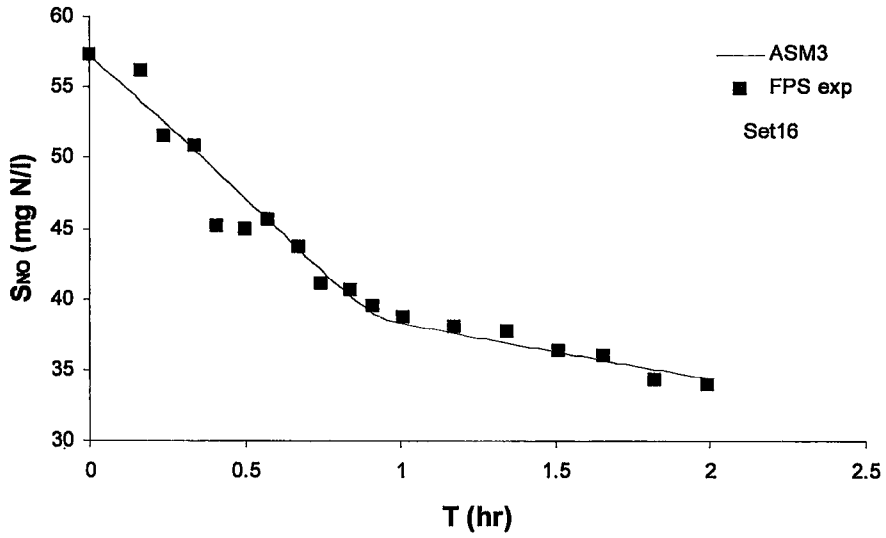

Figure 6.39 Experimental data and S_{NO} versus time profile obtained by ASM3 simulation for filtered primary sludge (FPS) for experimental set 16

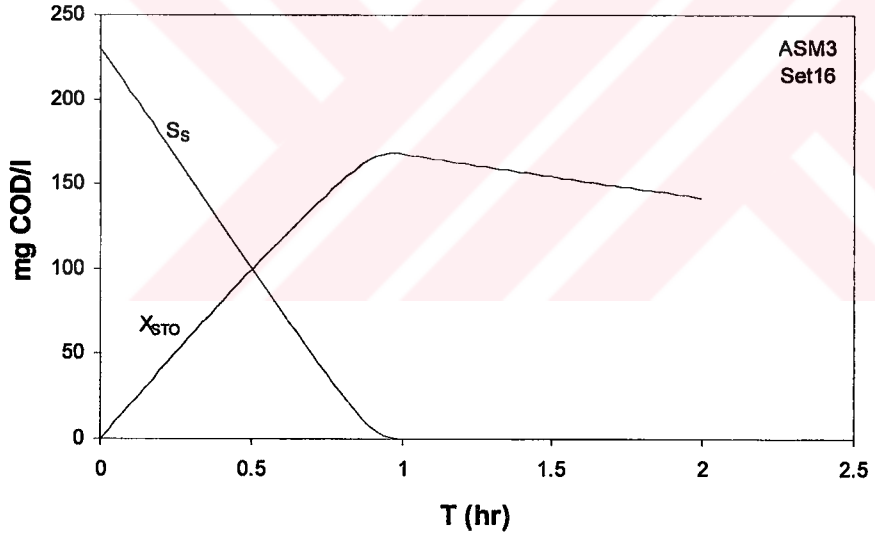

Figure 6.40 S_S and X_{STO} versus time profiles obtained by ASM3 simulation for filtered primary sludge for experimental set 16

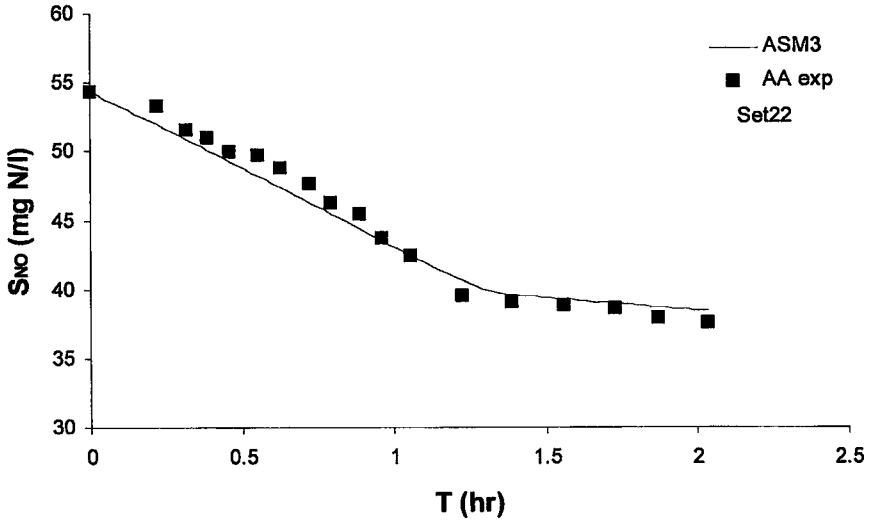

Figure 6.41 Experimental data and S_{NO} versus time profile obtained by ASM3 simulation for acetate (AA) for experimental set 22

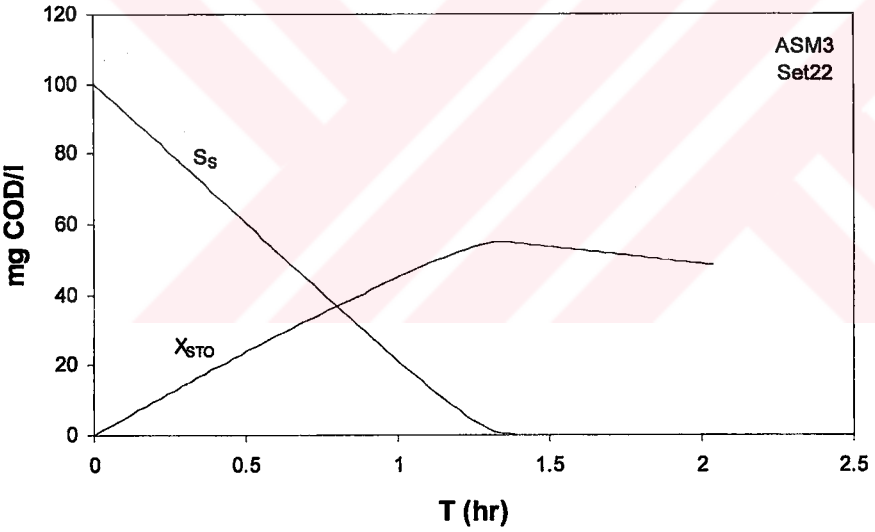

Figure 6.42 S_S and X_{STO} versus time profiles obtained by ASM3 simulation for acetate for experimental set 22

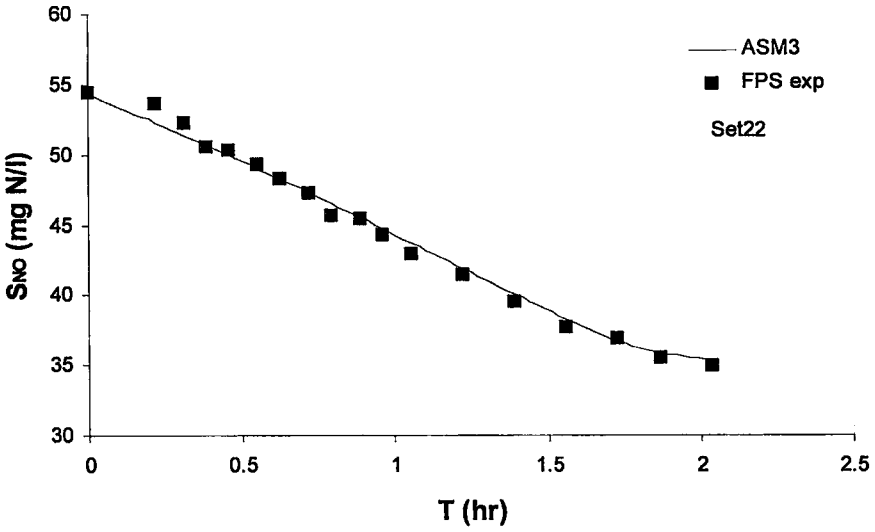

Figure 6.43 Experimental data and S_{NO} versus time profile obtained by ASM3 simulation for filtered primary sludge (FPS) for experimental set 22

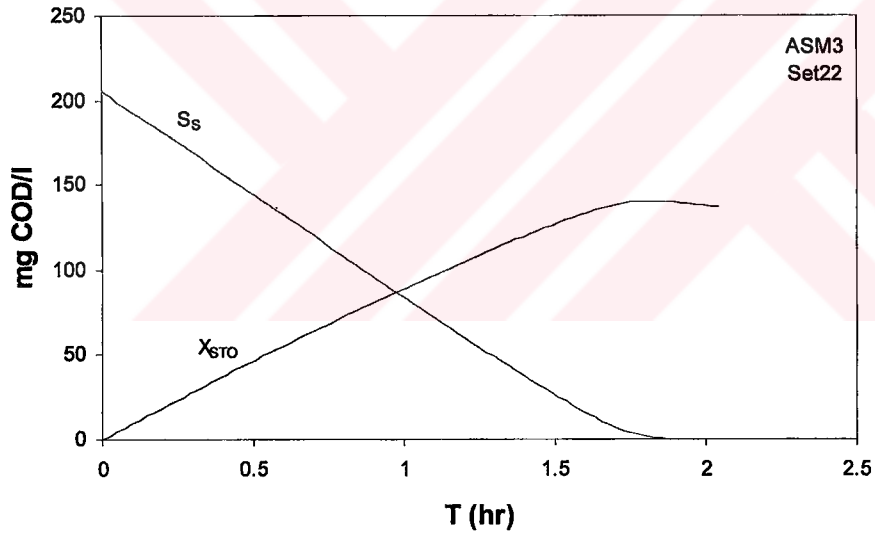

Figure 6.44 S_S and X_{STO} versus time profiles obtained by ASM3 simulation for filtered primary sludge for experimental set 22

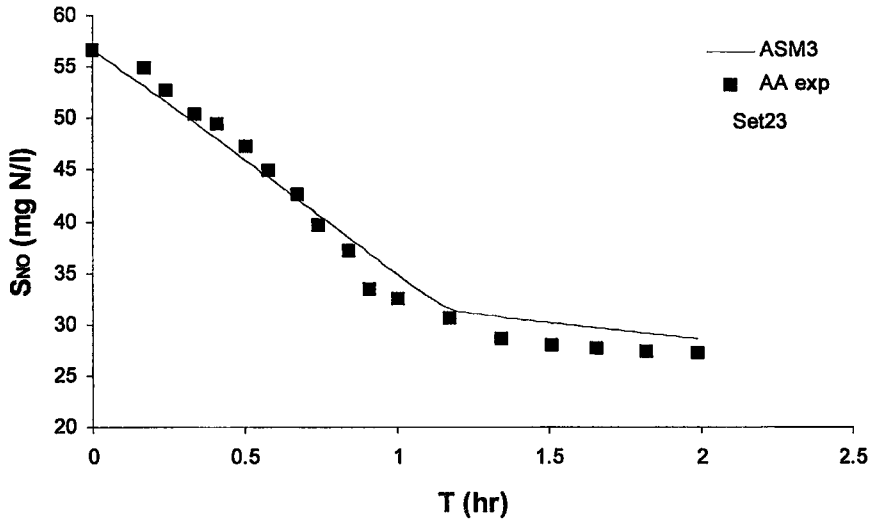

Figure 6.45 Experimental data and S_{NO} versus time profile obtained by ASM3 simulation for acetate (AA) for experimental set 23

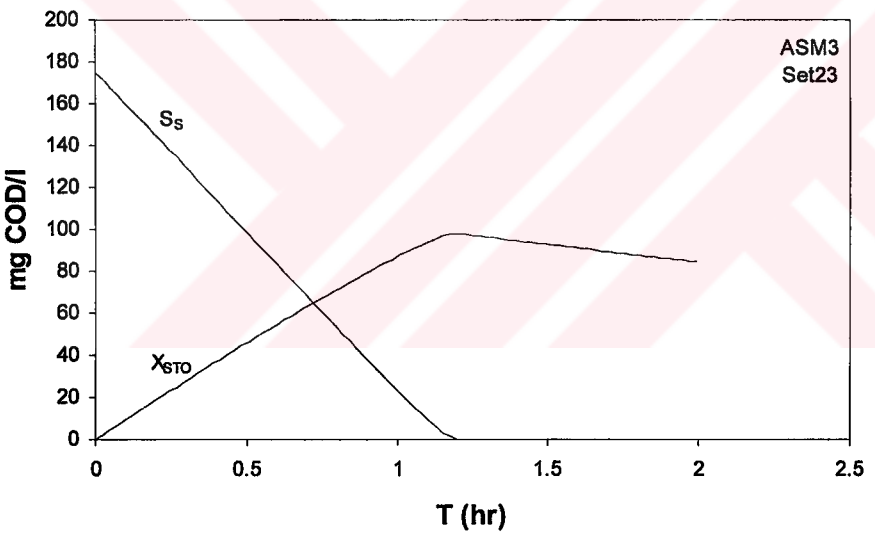

Figure 6.46 S_S and X_{STO} versus time profiles obtained by ASM3 simulation for acetate for experimental set 23

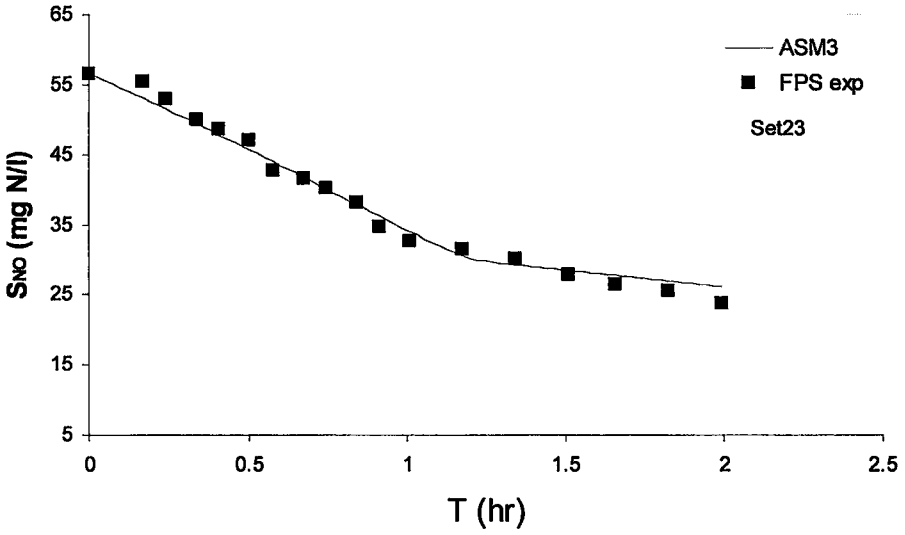

Figure 6.47 Experimental data and S_{NO} versus time profile obtained by ASM3 simulation for filtered primary sludge (FPS) for experimental set 23

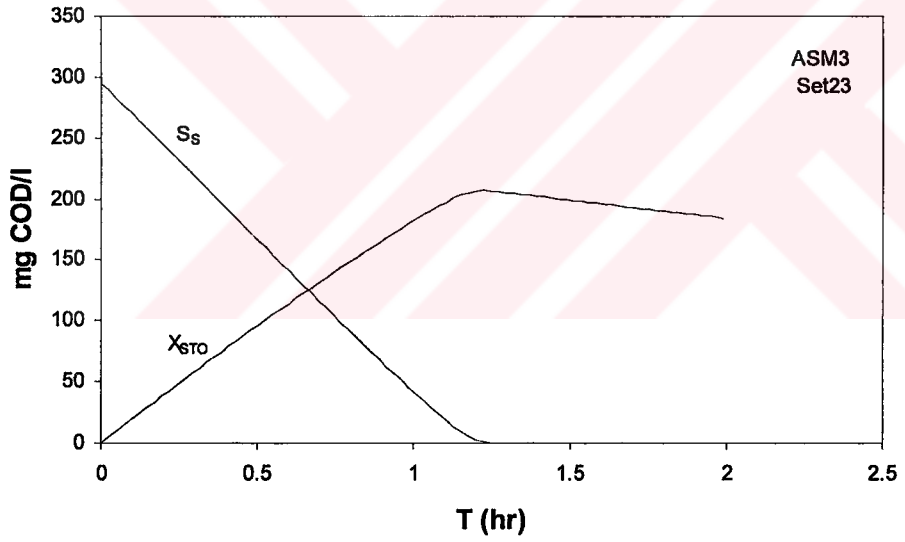

Figure 6.48 S_S and X_{STO} versus time profiles obtained by ASM3 simulation for filtered primary sludge for experimental set 23

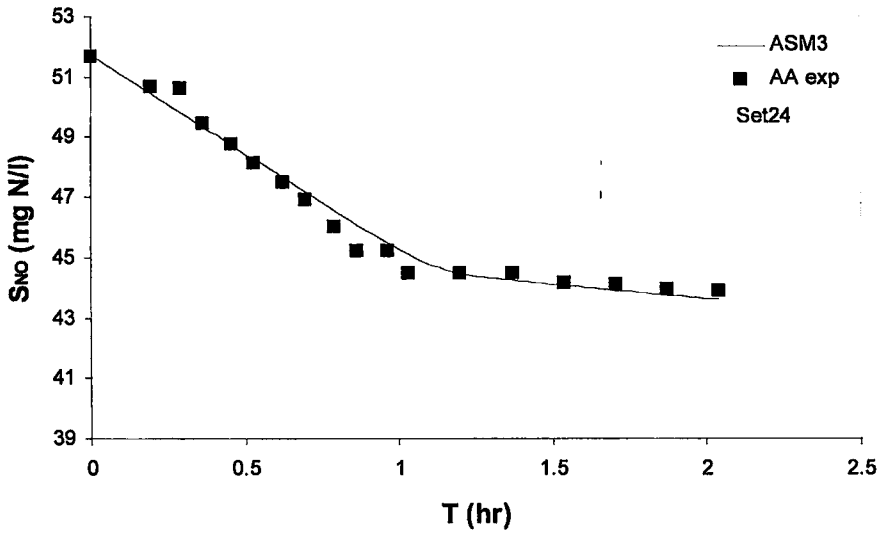

Figure 6.49 Experimental data and S_{NO} versus time profile obtained by ASM3 simulation for acetate (AA) for experimental set 24

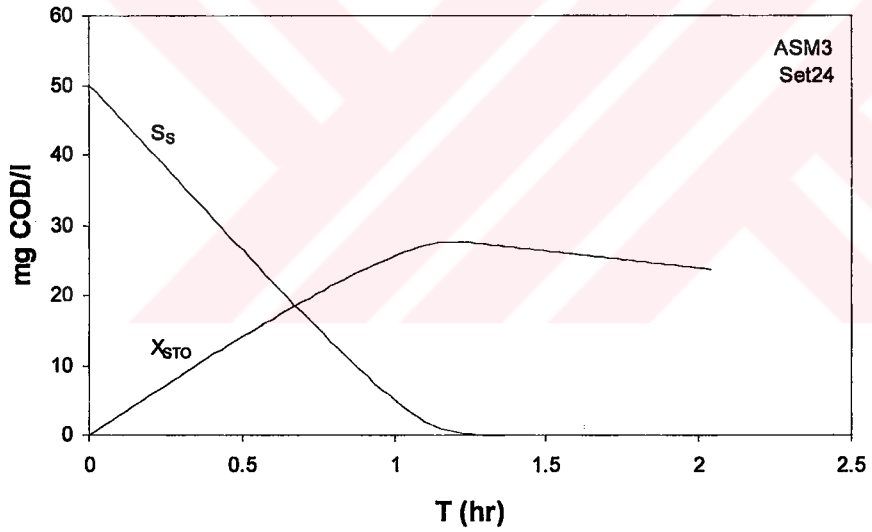

Figure 6.50 S_S and X_{STO} versus time profiles obtained by ASM3 simulation for acetate for experimental set 24

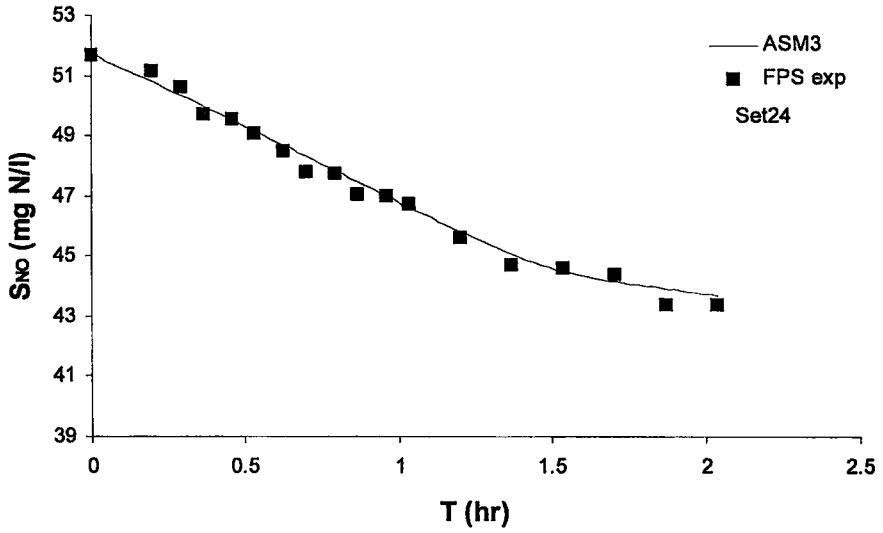

Figure 6.51 Experimental data and S_{NO} versus time profile obtained by ASM3 simulation for filtered primary sludge (FPS) for experimental set 24

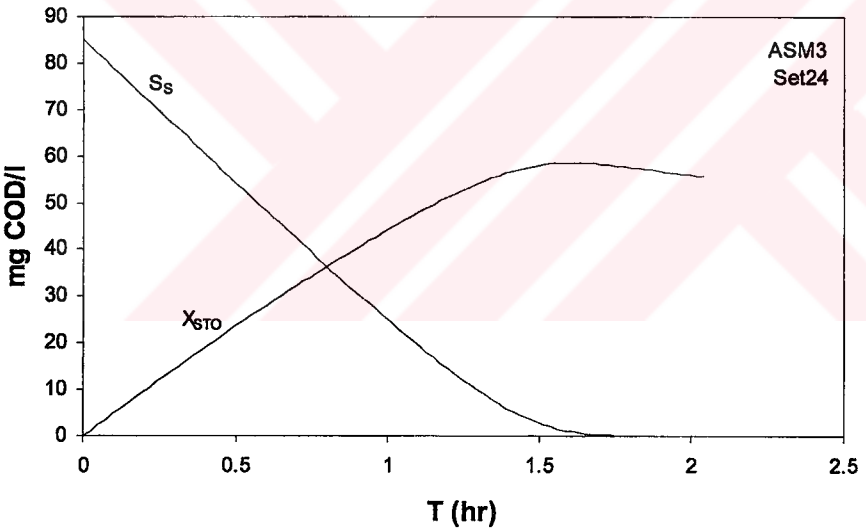

Figure 6.52 S_S and X_{STO} versus time profiles obtained by ASM3 simulation for filtered primary sludge for experimental set 24

CHAPTER 7 EVALUATION OF RESULTS

7.1 Evaluation of Results for the Assessment of Endogenous Decay Rate

7.1.1 Results obtained by the conventional method

Similar characteristics were observed in the batch digestion tests, performed for meat processing and leather tanning effluents. Both cases resulted in the observation of scattered data usually exhibiting cyclic variations. As previously indicated in sections 5.1.1.1 and 5.1.1.2, the value of b_H obtained varied according to the duration of the experimental period considered i.e. for meat processing effluents in experimental set 1 b_H was 0.02 1/day for 40 days, 0.05 1/day for 20 days, 0.05 1/day for 10 days, and 0.16 1/day for 6 days whereas for leather tanning effluents in experimental set 3 b_H could be calculated as 0.05 1/day for 30 days, 0.06 1/day for 20 days, 0.08 1/day for 10 days, and 0.2 1/day for 5 days. These inaccurate test results can be mainly attributed to:

- the analytical limitations associated with oxygen measurements with considerably low magnitudes in a range of 2 - 8 mg/l.hr
- interference of adsorbed particulate organic matter

Although the data obtained from batch aerobic digestion tests conducted for domestic wastewaters do not exhibit such scattered features, the coefficient of determination was not high enough to indicate a great percentage of accuracy. Table 7.1 summarizes the results for b_H and the related coefficient of determination (r^2), endogenous nitrate utilization rate (NUR_E), and η_E values for experimental sets 2, 4, 5, 6, and 7.

Table 7.1 Summary of results for experimental sets 2, 4, 5, 6, and 7

Experimental Set	Wastewater Type	b_H (1/day)	r^2	NUR_E (mg/l.day)	η_E
2	Meat processing	0.12	0.45	24.1	0.82
4	Leather tanning	0.12	0.58	34.6	0.83
5	Domestic	0.09	0.38	29.0	0.58
6	Domestic	0.15	0.87	36.3	0.86
7	Domestic	0.14	0.62	30.9	0.82

As can be seen from Table 7.1 the coefficients of determination, r^2, for meat processing and leather tanning effluents are quite low. In the same way, experimental set 5 conducted for domestic wastewaters, led to a remarkably low r^2 value around 0.4. From these results, it can be concluded that the conventional method for the assessment of aerobic endogenous decay coefficient is not very reliable in terms of accuracy and consistency.

7.1.2 Results obtained by the proposed method

The alternative approach for the assessment of aerobic and anoxic endogenous decay rate coefficient was based on avoiding

- low oxygen utilization rates (usually between 2 - 8 mg/l.hr) which could not be measured sensitive enough by the oxygen meter
- interference of slowly biodegradable substrate which would produce different results according to the portion of the data considered as previously described in Sections 5.1.1.1, 5.1.1.2, and 7.1.1.

Therefore, a constant unlimited growth medium was provided by the addition of easily biodegradable substrate as described in Sections 3.1.2 to ensure OUR and NUR levels high enough to be measured accurately by the respirometric instruments. Figures 7.1a and 7.1b illustrate the decreasing biomass activity experienced in aerobic and anoxic feed reactors throughout the experimental period in set 10. As can be seen from Figure 7.1a the initial OUR plateau values are between 47 mg/l.hr and 27 mg/l.hr, all of which can be measured on an accurate analytical basis.

The concentration of easily biodegradable substrate introduced to both aerobic and anoxic feed reactors was 50 mg/l as described in Section 4.2.1. To be able to assess the percent recovery of the readily biodegradable substrate fed to the reactors, the following procedure proposed by Ekama and Marais (1986) was applied:

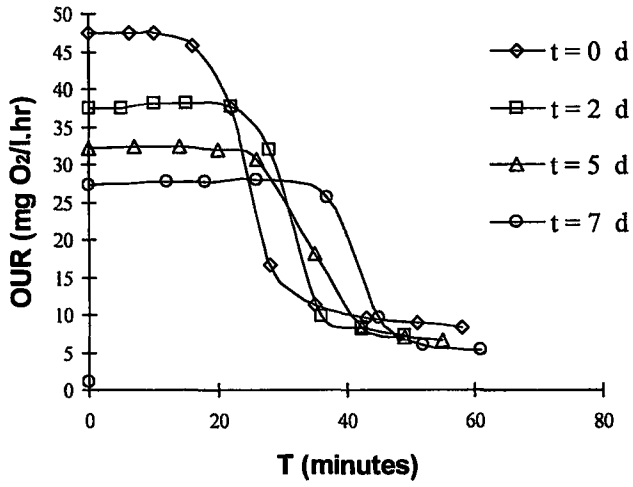

Figure 7.1a The effect of decreasing biomass activity on the OUR profile – experimental set 10

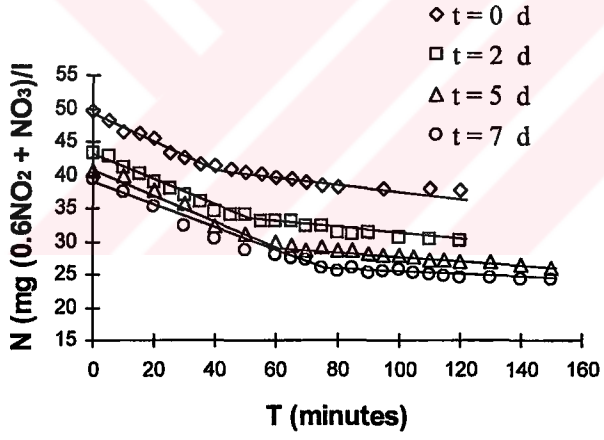

Figure 7.1b The effect of decreasing biomass activity on the NUR profile – experimental set 10

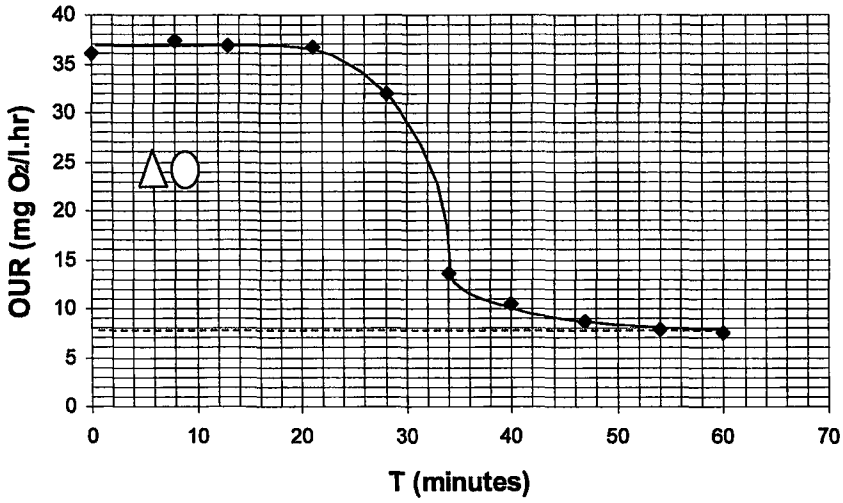

Figure 7.2a OUR profile obtained in the feed reactor - experimental set 9 - initial day

Figures 7.2a and 7.2b show oxygen utilization (OUR) and nitrate utilization rate (NUR) profiles obtained in aerobic and anoxic feed reactors respectively, on the initial day in experimental set 9.

In Figure 6.2a, ΔO specifies the area between the OUR curve and the dashed line. By the help of the gridlines, the number of squares was counted as 474.25. From Figure 7.2a it can be seen that one square corresponds to 1 mg O_2/l.hr * 2 minutes. If a unit conversion is done:

474.25 squares * 1 mg O_2/l.hr * 2min * 1hr/60 min = 15.81 mg/l

Since

$$S_s = \frac{\Delta O}{1 - Y_H} \tag{3.26}$$

and Y_H can be assumed as 0.67 mg cell COD/mg COD for domestic wastewaters according to ASM1, S_s can be computed as

$$S_s = \frac{15.81}{1 - 0.67} = 48 \text{ mg COD/l}$$

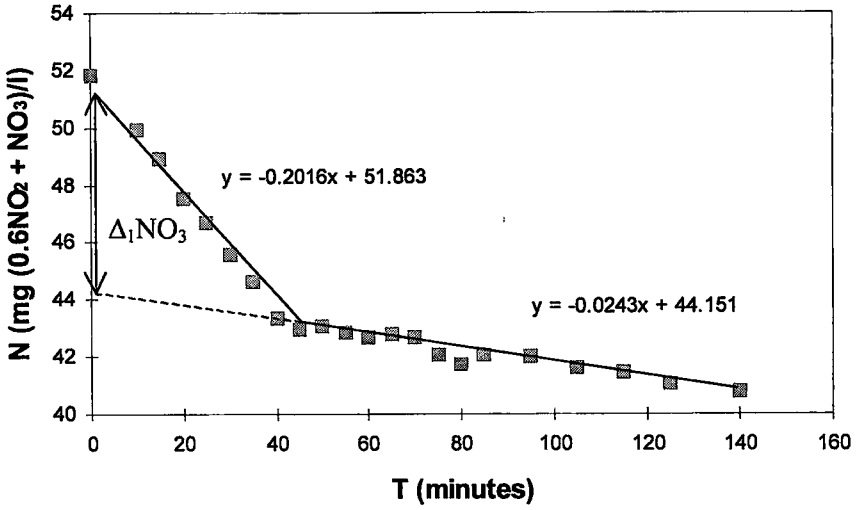

Figure 7.2b NUR profile obtained in the feed reactor - experimental set 9 - initial day

In Figure 7.2b, Δ_1NO_3 is the difference between the y intercepts of growth and endogenous respiration lines. Since the equations of both lines are known it can be computed as

$\Delta_1NO_3 = (51.863 - 44.151) = 7.712$ mg N/l

As previously explained S_s equals

$$S_s = \frac{2.86}{1 - Y_H} \Delta_1 NO_3 \qquad (3.27)$$

In this case S_S can be calculated with the same Y_H assumption as

$$S_s = \frac{2.86}{1 - 0.67} 7.712 = 67 \text{ mg COD/l}$$

As can be seen from this demonstration, the amount of S_s in the anoxic feed reactor was calculated to be greater as compared to the amount of S_s calculated in the aerobic feed reactor.

The amount of readily biodegradable substrate fed to aerobic and anoxic feed reactors in experimental sets 8 through 13 was calculated according to the procedure proposed by Ekama and Marais and the results are tabulated in Tables 7.2 to 7.7. It can be seen that, in most cases the anoxic S_s calculated is found to be greater. This is mainly attributed to the fact that the same Y_H was assumed for aerobic and anoxic

cases (equations 3.26 and 3.27) resulting in a smaller numerical value in the denominator which leads to a greater magnitude of anoxic S_s. Orhon et al. (1996) provided the conceptual proof that the yield coefficient is significantly lower for the anoxic growth on the basis of energetics of the related metabolic processes. The same conclusion was also stated by Stouthamer et al. (1982) from aerobic and anoxic yield studies with *Pseudomonas denitrificans*, as denitrification was about 40% less efficient than aerobic respiration. Thus, it can be concluded that the current method does not seem to be very accurate for the determination of anoxic S_s and the aerobic batch test method is likely to produce more accurate results. However, it should also be noted that no other biological methods exist for the determination of readily biodegradable substrate and none will be provided within the context of this study.

Table 7.2 Calculated values of aerobic and anoxic S_s seeded to the feed reactors in experimental set 8

Experimental Set	Day	Aerobic S_s (mg COD/l)	Anoxic S_s (mg COD/l)
8	0	40	41
	1	43	-
	2	40	38
	3	37	45
	4	45	-
	5	38	61
	6	46	-
	7	-	52
	8	57	-
	9	-	59
	12	-	50

Table 7.3 Calculated values of aerobic and anoxic S_s seeded to the feed reactors in experimental set 9

Experimental Set	Day	Aerobic S_s (mg COD/l)	Anoxic S_s (mg COD/l)
9	0	48	67
	1	39	37
	2	45	69
	3	46	67
	4	43	57
	6	45	69
	7	46	63
	8	41	65
	9	42	-

Table 7.4 Calculated values of aerobic and anoxic S_s seeded to the feed reactors in experimental set 10

Experimental Set	Day	Aerobic S_s (mg COD/l)	Anoxic S_s (mg COD/l)
10	0	50	44
	1	48	59
	2	48	61
	3	48	65
	5	47	80
	6	49	68
	7	47	80
	8	56	78
	9	55	85

Table 7.5 Calculated values of aerobic and anoxic S_s seeded to the feed reactors in experimental set 11

Experimental Set	Day	Aerobic S_s (mg COD/l)	Anoxic S_s (mg COD/l)
11	0	61	67
	1	49	72
	2	51	72
	3	49	76
	4	48	72
	6	49	72
	7	43	82
	8	-	79
	9	43	-

Table 7.6 Calculated values of aerobic and anoxic S_s seeded to the feed reactors in experimental set 12

Experimental Set	Day	Aerobic S_s (mg COD/l)	Anoxic S_s (mg COD/l)
12	0	51	55
	1	50	50
	2	40	-
	3	42	-
	6	43	-
	7	43	89
	8	47	95
	9	47	85

Table 7.7 Calculated values of aerobic and anoxic S_s seeded to the feed reactors in experimental set 13

Experimental Set	Day	Aerobic S_s (mg COD/l)	Anoxic S_s (mg COD/l)
13	0	69	58
	1	55	53
	2	54	54
	3	54	56
	6	54	63
	7	60	57
	8	58	52
	9	56	56
	10	51	65
	13	58	-

Table 7.8 Mean and standard deviation for calculated values of aerobic and anoxic S_s (experimental sets 8 to 13)

Experimental Set	Mean for Aerobic S_s (mg COD/l)	Mean for Anoxic S_s (mg COD/l)	Std Deviation for Aerobic S_s (mg COD/l)	Std Deviation for Anoxic S_s (mg COD/l)
8	43.25	49.43	6.41	8.70
9	43.89	61.75	2.85	10.74
10	49.79	68.89	3.38	13.16
11	49.13	74.00	5.62	4.75
12	45.38	74.8	3.96	20.74
13	56.9	57.11	4.98	4.37

Table 7.8 gives mean and standard deviation values of aerobic and anoxic S_s. From the table it can be seen that for aerobic S_s, mean ranges between 43.3 and 56.9 mg COD/l while the range for mean for anoxic S_s is higher which is between 49.4 and 74.8 mg COD/l. The standard deviation for aerobic S_s has the range of 2.9 and 6.4 mg COD/l. It can be observed that standard deviation is higher for anoxic S_s with a minimum of 4.4 mg COD/l for the 13^{th} set and a maximum of 20.7 mg COD/l for the 12^{th} experimental run.

As mentioned earlier in Chapter 5, the proposed method was only applied to domestic wastewaters within the context of this thesis. Table 7.9 shows the results obtained for aerobic and anoxic endogenous decay rate coefficients at 20 ± 1 °C and 10 ± 1 °C.

Table 7.9 Experimental results obtained for b_H and b_{HD} values at 20±1°C and 10±1°C

Experiment No	Temperature (°C)	b_H (1/d)	b_{HD} (1/d)
1	20± 1	0.10	0.05
2	20± 1	0.09	0.05
3	20± 1	0.08	0.04
4	20± 1	0.08	0.06
5	20± 1	0.06	0.04
6	10± 1	0.04	0.04

The arithmetic mean of aerobic and anoxic endogenous decay rate coefficient for five sets at 20 ± 1°C are 0.08 1/day and 0.05 1/day respectively. The standard deviation for the measured values of b_H and b_{HD} were calculated as 0.01 and 0.01 which are quite low indicating a good level of consistency. The ratio of anoxic and aerobic coefficients is 0.6. At 10 ± 1°C only one set of experiment was performed which led to a value of 0.04 1/day at both aerobic and anoxic media with a ratio of 1.

7.1.2.1 Comparison of the results with the literature

The results obtained for b_H and b_{HD} are quite consistent with each other as indicated by the low standard deviation values. b_H values in the literature, either assumed for mathematical modeling or experimentally determined, were submitted in Chapter 2 in Table 2.4. From the table it can be seen that b_H values group around 0.1 - 0.4 1/day at 22 °C, 0.24 1/day at 20 °C, and 0.05 - 0.12 1/day between 10 – 15 °C. A comparison for 20 °C shows that the b_H value of 0.08 1/day is markedly lower than the reported values in the literature. This difference can be due to the following reasons:

- Limitations of the currently available respirometric procedure
- Interference of adsorbed organic particulate matter
- Variations in wastewater characteristics

A comparison for b_{HD} is not possible due to the lack of data in the literature.

As previously mentioned in Section 2.2.3, η_E is a factor used for the comparison of electron acceptor utilization rates during the phase of endogenous respiration. Kristensen et al. (1992) reported η_E values in the range of 0.79 - 1.07. In this study η_E was found as 0.6 which is again lower than the reported value. In the study conducted by Kristensen et al., a limited amount of electron acceptor was supplied

within a short experimental period. However, according to Warner et al. (1983), it would normally take 8 - 12 hours for the adsorbed COD to be utilized before the OUR reaches the value associated with endogenous respiration. This fact might lead to the conclusion that the currently available respirometric procedure may, in fact, not characterize the real endogenous respiration phase. Such high values of η_E may be due to the presence of substrate associated with the hydrolysis of particulate organic matter.

7.2 Evaluation of Results for Denitrification Kinetics Using External and Hydrolyzed Carbon Sources

In this section, experimental and model simulation results submitted in Chapters 5 and 6 will be evaluated. As also mentioned in section 5.2, filtered primary sludge (FPS) was investigated experimentally as a carbon source for denitrification. Its performance was tested against acetate, considered as one of the best examples of readily biodegradable substrate. The comparison of denitrification rates was performed for equivalent S_S concentrations of both substrates in parallel batch tests. Evaluation of experimental results, for the investigation of denitrification rates associated with the readily biodegradable substrate, will be based on respirometric principles adopted in Endogenous Decay Model (EDM). The evaluation of model simulation results on the other hand, will cover the compliance of the experimental data with the model simulation as well as the analysis of processes and parameters associated with EDM and ASM3.

7.2.1 Evaluation of experimental results

7.2.1.1 Denitrification rates

Table 7.10 shows the rates of denitrification obtained as well as pre-selected initial S_S concentrations. In section 5.2 the rates were expressed as mg N/l.min. In this chapter denitrification rates will be expressed in terms of active biomass as mg N/g X_H.hr. Here, N denotes the corrected nitrogen concentration as ($0.6NO_2^-$-N + NO_3^--N).

As can be seen from the table, denitrification rates associated with the utilization of readily biodegradable organic matter (k_1) are between 45.7 and 56.3 mg N/g X_H.hr for cenrifuged primary sludge, between 29.1 and 46.8 mg N/g X_H.hr for filtered primary sludge, and between 30.3 and 48.4 mg N/g X_H.hr for acetate, for the initial S_s concentration range of 15 and 500 mg/l. In this table the active biomass concentration is expressed as VSS.

Table 7.10 Denitrification rates for centrifuged primary sludge (CPS), filtered primary sludge (FPS), and acetate (AA) for experimental sets 15 to 24.

Experimental	S_s	k_1 (mg N/g X_H.hr)			k_2 (mg N/g X_H.hr)		
Set	(mg COD/l)	**CPS**	**FPS**	**AA**	**CPS**	**FPS**	**AA**
15	100	56.0		35.3	23.2		8.5
16	120	45.7	39.7	30.3	11.7	10.2	7.1
17	15	56.3	45.8	49.3*	13.0	15.6	16.1*
18	250	-	46.8	48.4	-	-	-
19	230	-	41.4	48.9	-	-	-
20	100	-	32.3**	36.8	-	-	-
21	250/500	-	-	47.3/43.2	-	-	15.1/-
22	100	-	34.7	37.1	-	17.7	7.3
23	175	-	39.9	40.9	-	14.3	12.4
24	50		29.1	41.7		12.9	3.9

* Wastewater
** Synthetic waste

Table 7.10 also reveals that denitrification rates for centrifuged primary sludge are relatively higher than the rates obtained for filtered primary sludge, possibly due to the interference of biomass present in the centrifuged sludge. Therefore, it is more reliable to make a comparison between rates of denitrification for filtered primary sludge and acetate for performance evaluation. For almost all S_s concentrations tested, the rates are very similar indicating that primary sludge performs almost as good as acetate as a carbon source. This finding is in good agreement with most of the research results (Barnard, 1984; Rabinowitz and Oldham, 1985; Lotter and Murphy, 1986; Comeau et al. 1987; Pitman et al. 1992; Lee et al. 1995; Lie et al. 1997).

Figures 7.3a and 7.3b are drawn to establish a relationship between the denitrification rate k_1 and the readily biodegradable organic matter concentration S_s. In Figure 7.3a, the data for 15 mg S_s/l (45.8 mg N/g X_H.hr) and in Figure 7.3b the data for 120 mg/l S_s (30.3 mg N/g X_H.hr) were discarded due to possible erratic experimental results.

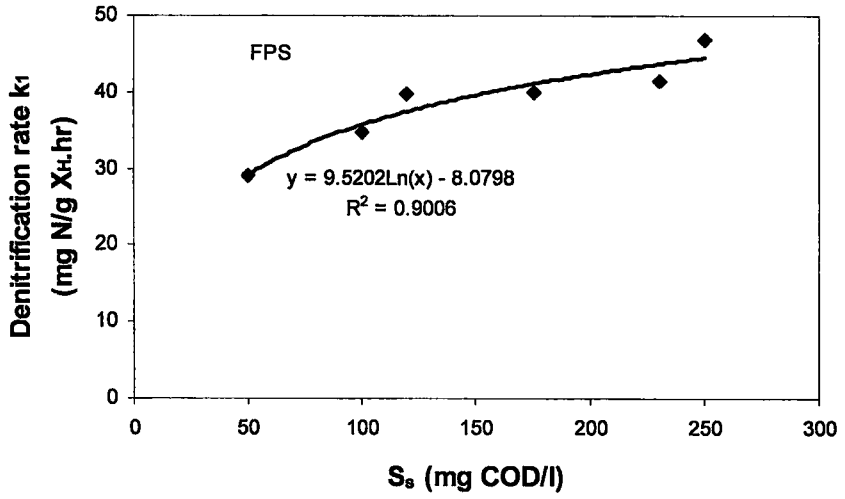

Figure 7.3a Relationship between readily biodegradable organic matter (S_s) and denitrification rate (k_1) for filtered primary sludge (FPS)

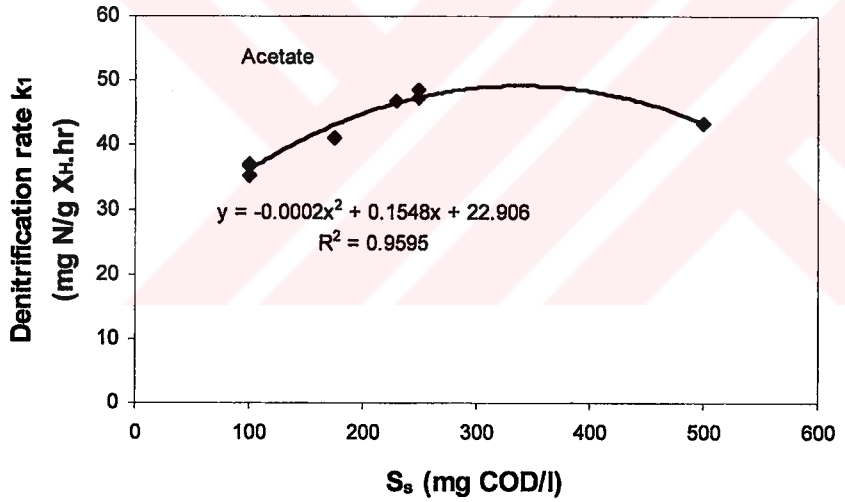

Figure 7.3b Relationship between readily biodegradable organic matter (S_s) and denitrification rate (k_1) for acetate

According to Monod kinetic model, the specific nitrate utilization rate should reach a maximum after experiencing a linear trend and becomes independent of carbon concentration at high levels. The data shown in Figure 7.3a have a logarithmic trend rather than a linear one which is also supported by the high coefficient of determination ($r^2 = 0.9006$). Excluding the denitrification rate for S_S concentration of 50 mg/l, the remaining rates accumulate in a narrow range i.e. between 34.7 and 46.8 mg N/g X_H. Thus, it can be deduced that carbon was not limiting for denitrification above S_S concentration of 100 mg COD/l. On the other hand, the data for acetate in Figure 7.3b fits a polynomial trend with a coefficient of determination equal to 0.9595. Similar to filtered primary carbon, the rates obtained for S_S concentrations of 230 to 250 mg/l pile up in a small range indicating no carbon limitation under these circumstances. However, for 500 mg/l of S_S concentration, the decrease observed in the rate of denitrification may address substrate inhibition.

Table 7.11 summarizes denitrification rates (k_1) on acetate and filtered primary sludge (FPS) found in the literature. As the table also indicates, not all authors used the same unit to express k_1. Some of them used total oxidized nitrogen concentration (N_{OX}-N) and some used only nitrate-nitrogen (NO_3^--N) for the amount of nitrogen removed. Also, for heterotrophic microorganisms, either suspended solids (SS) or volatile suspended solids (VSS) parameters were used.

From Table 7.11, a broad range of rates can be seen. For laboratory scale batch systems, the rates of denitrification on acetate are between 2.1 mg N_{OX}-N /(g VSS.hr) and 49 mg NO_3-N/(g SS.hr) whereas for FPS the range is between 3.5 mg N_{OX}-N /(g VSS.hr) and 9 mg N_{OX}-N /(g SS.hr). For pilot plant and full-scale systems, the observed ranges are lower. For pilot plants, for acetate the rates change between 1.5 and 4.5 mg N_{OX}-N /(g VSS.hr) while for FPS, a similar range is observed from 0.2 mg NO_3^--N/(g SS.hr) to 4.1 mg N_{OX}-N /(g VSS.hr). For full-scale systems, acetate was denitrified at 2 mg N_{OX}-N /(g VSS.hr) and the range for FPS is between 2-2.6 mg NO_3^--N/(g VSS.hr) at 10 ° C.

Table 7.11 Denitrification rates (k_1) on acetate (AA) and filtered primary sludge (FPS) as reported in the literature

Mode of Operation	Denitrification Rate, k_1 AA	FPS	Unit	Reference
Lab-scale (batch)	12.1		mg NO_3^--N/ g VSS.hr	Lee et al. (1995)
Lab-scale (batch)	27		mg N_{OX}-N / g VSS.hr	Akunna et al (1993)
Lab-scale (batch)	2.1-2.4	3.5-3.6	mg N_{OX}-N / g VSS.hr	Isaacs and Henze (1995)
Pilot plant (CSTR)	1.5-3.2	1.2-4.1	mg N_{OX}-N / g VSS.hr	Isaacs and Henze (1995)
Full-scale (CSTR)	-	2-2.6 (10°C)	mg NO_3^--N/ g VSS.hr	Brinch et al. (1994)
Lab-scale (batch)	-	9	mg N_{OX}-N / g SS.hr	Hatziconstantinou et al. (1996)
Pilot plant (CSTR)	4.5	1.5[a]	mg N_{OX}-N / g VSS.hr	Isaacs et al. (1994)
Lab-scale (SBR)	7-7.2	1.25-10	mg NO_3^--N / g VSS.hr	Abufayed and Schroeder (1986)
Lab-scale (CSTR)	19	-	mg N_{OX}-N / g SS.hr	Fass et al. (1994)
Pilot plant (CSTR)	-	0.2-2	mg NO_3^--N / g SS.hr	Christensen et al. (1977)
Lab-scale (batch)	49[b],76[c]	-	mg NO_3^--N / g SS.hr	Lee and Welander (1996)
Full-scale (CSTR)	2	-	mg N_{OX}-N / g VSS.hr	Nyberg et al. (1992)
Lab-scale (CSTR)	20	-	mg NO_3^--N / g VSS.hr	Majone et al. (1998)
Lab-scale (batch)	3.8	-	mg NO_3^--N / $kgCOD_{tot}$.hr	Engeler et al. (1998)
Lab-scale (batch)	2.2-2.5	-	mg NO_3^--N / g SS.hr	Gerber et al. (1987)

[a] Wastewater
[b] Apparent denitrification rate
[c] Maximum denitrification rate

A quick comparison of denitrification rates of the observed data and the data reported in the literature leads to the finding that, the observed rates are higher especially for FPS. However, it should be remembered that, in none of those studies, the microorganism concentration was expressed in terms of *active* biomass. Therefore, a

comparison of denitrification rates expressed in terms of active biomass with the rates reported in terms of SS or VSS would not be compatible. It could also be noted that since the activity coefficient (f_a) is less than one, the rate expression assumes a greater magnitude when it is divided by f_a.

For the sets used for modelling purposes (sets no 15, 16, 22, 23, 24), when the active biomass concentration is expressed in terms of COD, the experimental denitrification rates observed during the first phase of the electron acceptor utilization profile are in a range of 20.5 mg N/g X_H.hr and 28.2 mg N/g X_H.hr for acetate, while the range varies between 19.7 mg N/g X_H.hr and 27.0 mg N/g X_H.hr for FPS. In order to be able to compare these rates with the results of model simulation studies, the rate of S_{NO} utilization during growth phase, as previously given in Table 6.1 for EDM, can be rewritten for maximum growth conditions in terms of active biomass as below:

$$\frac{dS_{NO}}{dtX_H} = -\frac{1-Y_{HD}}{2.86Y_{HD}}\hat{\mu}_H\eta_g \qquad (7.1)$$

The magnitude of this expression can be assessed by using Y_{HD} and $\hat{\mu}_H$ values adopted for model simulation. Hence, for acetate, dS_{NO}/dtX_H assumes a value of 31.6 mg N/g X_H.hr and for FPD a range exists between 24.4 and 26.8 mg N/g X_H.hr, due to the varying values of Y_{HD} and $\hat{\mu}_H$ used for simulation. Based on these numerical values it can be stated that, denitrification rates determined either experimentally or by model simulation are consistent with each other.

k_2 values for acetate vary between 2.6 and 8.4 mg N/(g X_H (as COD).hr) for the sets used for modelling purposes. According to EDM, these rates would be associated with the use of endogenous carbon sources since acetate was depleted by the end of the first phase of the S_{NO} versus time profile. The rate of S_{NO} utilization during the phase of endogenous respiration in EDM, as previously given in Table 6.1, can be written in terms of active biomass as below:

$$\frac{dS_{NO}}{dtX_H} = -\frac{1-f_{EX}}{2.86} b_H \eta_E \qquad (7.2)$$

The values of f_{EX}, b_H and η_E used for model simulation are 0.2, 0.2 1/d and 0.5 respectively. Hence, dS_{NO}/dtX_H term equals to 1.2 mg N/g X_H.hr for acetate. Since experimental versus model compliance was succeeded, as can be seen in model simulation graphs, the discrepancy between model and experimental values for expression (7.2) can be regarded as insignificant.

In the literature there is still a debate about the source of carbon being utilized in the second phase of the electron acceptor utilization profile. Some researchers claim about the utilization of storage polymers (see section 2.3.4.3) while others submit data about the utilization of a pool of intermediate intracellular metabolite other than storage polymers (Goel et al., 1998). The rates of denitrification for acetate are reported to be in a range of 3 to 10 mg NO_3^-/(g VSS.hr) by Majone et al (1998). They also claim that a reduction in the concentration of stored polymers (PHB) was observed during that phase.

Domestic sewage is mainly composed of VFA's, carbohydrates, alcohols, peptones and amino acids, which are biodegradable at different rates (Majone et al., 1999). Since VFA's are regarded as readily biodegradable, the remaining constituents may represent the hydrolyzable soluble portion of the COD. In this context, k_2 values for FPS (10.17 to 17.67 mg N/g X_H.hr) could be associated with the utilization of hydrolyzable soluble COD since they are too high to be associated with endogenous respiration as also implied in the simulation studies associated with EDM.

7.2.1.2 Readily biodegradable substrate concentration

As mentioned in Section 7.2, comparison of denitrification rates for primary sludge and acetate were performed for a pre-selected concentration of readily biodegradable organic matter (S_s). Previously, S_S content of primary sludge was determined by an OUR test as explained in Section 3.1.2 and a theoretically equivalent amount of

Table 7.12 Comparison of experimental and theoretical values of S_s for experimental sets 15, 16, 22, 23, and 24.

Experimental Set	$S_{s(theo)}$ (mg COD/l)	$S_{s(exp)}$ (mg COD/l)		$S_{s(exp)} / S_{s(theo)}$	
		AA	**FPS**	**AA**	**FPS**
15	100	99	-	0.99	-
16	120	120	118	1.0	0.98
22	100	97	99	0.97	0.99
23	175	173	172	0.99	0.98
24	50	50	47	1.0	0.94

readily degradable organic matter ($S_{s(theo)}$) was provided for acetate and primary sludge. The amount of S_s utilized by the microorganisms was determined according to the procedure proposed by Ekama and Marais (1986) which was outlined in Section 3.2.3. Table 7.13 presents S_s values ($S_{s(exp)}$) calculated by the experimental data according to this procedure and the ratio of $S_{s(exp)}$ to $S_{s(theo)}$. The table constitutes the values obtained for sets 15, 16, 22, 23, and 24 where the second phase for denitrification could be observed for parallel sets of acetate and FPS. For the remaining sets (18, 19, 20, and 21) the second phase for denitrification could not be observed due to the inadequacy of the experimental period and/or the depletion of nitrate for C/N > 5. Y_{HD} values used for the calculation of S_S were adopted from the model simulation studies whose results were presented in Table 6.4.

Table 7.12 shows that $S_{s(exp)}$ values for acetate and FPS are quite close to $S_{s(theo)}$ values. The mean values for $S_{s(exp)}$ / $S_{s(theo)}$ ratios for acetate and FPS are 0.99 and 0.97 respectively, indicating the consistency of Y_{HD} values used for model simulation with the experimental data.

7.2.2 Evaluation of model simulation results

Although all model simulations were presented in Chapter 6, the results of experimental set 22 will be depicted again in the sections below for illustration purposes. In this set, denitrification rates were assessed for acetate and filtered primary sludge. The initial S_S concentration for both substrates was 100 mg/l in EDM. The S_S content for FPS was determined according to aerobic batch test method as described in section 3.2.1. However, due to the definition in ASM3, S_S was assigned as 205 mg COD/l for FPS, while for acetate the initial S_S was again adopted as 100 mg COD/l. Figure 7.4 depicts the experimental S_{NO} versus time profiles obtained for acetate and FPS on the same graph. As the figure shows, the profiles exhibit very similar trends.

7.2.2.1 Endogenous Decay Model (EDM)

The kinetic and stochiometric parameters used in EDM simulation for acetate and filtered primary sludge were given in Table 6.4 together with default values at 20°C. For acetate Y_{HD} value used was 0.58 g COD/g COD while for filtered primary sludge the range for Y_{HD} was between 0.62 and 0.66 g COD/g COD. Y_{HD} values used for simulation are lower than the Y_H values cited in the literature for acetate (0.75 g COD/g COD Majone et al. 1996; 0.70 g COD/g COD Beccari et al.) This finding is similar to the views stated by Stouthamer et al. (1982) and Orhon et al. (1996) claiming that the yield coefficient is significantly lower for the anoxic growth. The value of $\hat{\mu}_H$ used for the simulation of acetate and FPS was 6 1/d with the exception of set 16 for FPS where a $\hat{\mu}_H$ value of 6.5 1/d was used. These values are consistent with the default value of $\hat{\mu}_H$ in EDM stated for domestic wastewaters in which acetate forms a substantial fraction of S_S. The anoxic correction factor for growth, η_g, is used to account for the anoxic growth rate. The value of η_g (0.5) used for simulation agrees well with the suggested η_g value of 0.6 by Sözen et al. (1998), while it is relatively lower than the default value of 0.8 in Activated Sludge Model No 1 (Henze et al, 1987). Similarly, aerobic endogenous respiration rate is 50 % reduced by η_E value of 0.5.

Experimental S_{NO} versus time profiles obtained from run no 22 for acetate as shown in Figure 7.5 exhibit perfect fit with EDM. The utilization of S_S during the first phase

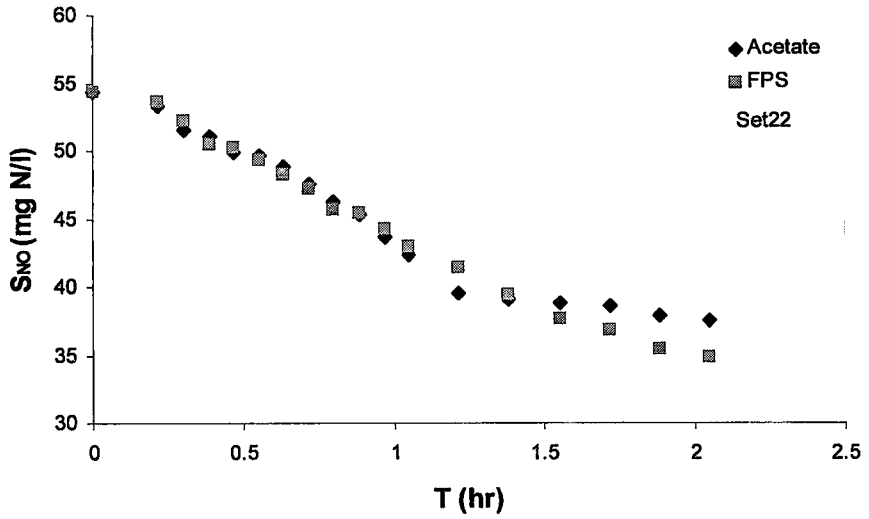

Figure 7.4 Experimental S_{NO} versus time profiles for acetate and filtered primary sludge (FPS) for experimental set 22

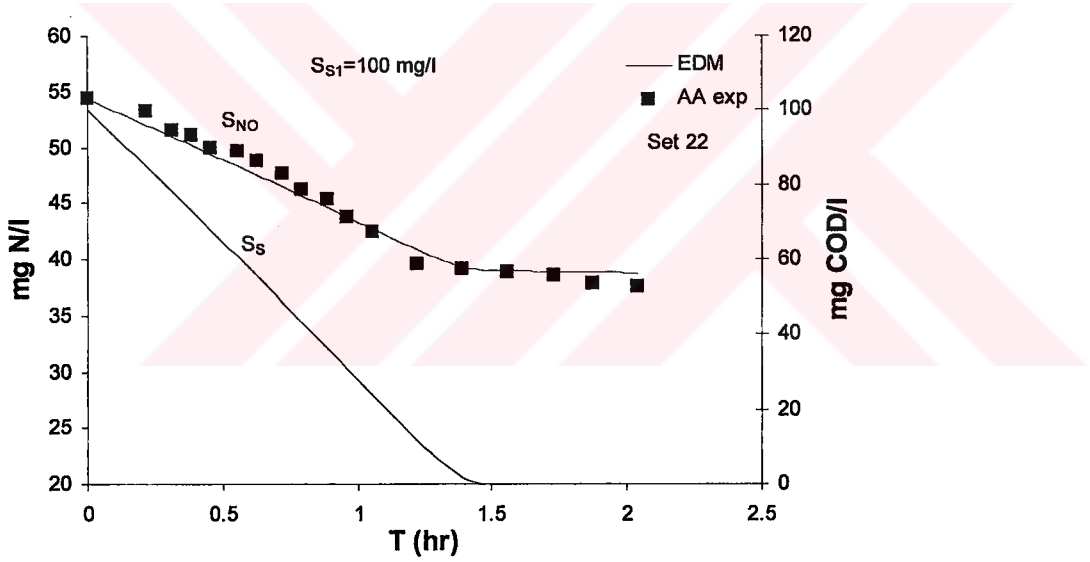

Figure 7.5 Model simulation for acetate (AA) for experimental set 22 based on EDM

is coupled with a high rate of S_{NO} consumption during the same period. The first phase is followed by a decreased rate of S_{NO} consumption due endogenous respiration.

Although sludge production should be evaluated for continuous systems, the sludge components monitored in the batch experimental system for acetate, in accordance with EDM, will be presented for an estimation of the behaviour of particulate COD components. Figures 7.6a and 7.6b show the change of the particulate COD fractions, defined in EDM, with time. Total particulate COD, active heterotrophic biomass and particulate inert COD concentrations are denoted as X_T, X_H, and X_P respectively. Since negligible amount of X_P was produced for two hours of experimental period, X_H and X_T followed the same trend during this time. The peak point in the X_T versus time profile was observed at t=1.56 hr where X_T was equal to 386 mg COD/l. X_T concentrations at t=2 hr and t=2.1 d were 385 mg COD/l and 330 mg COD/l respectively.

Similar to acetate, S_{NO} profiles obtained for filtered primary sludge consist of sequential phases with decreasing rates. S_S was depleted at the end of the first phase as can be seen in Figure 7.7. However, unlike acetate, the slope of the second phase is too high to be associated with endogenous respiration. This finding can be explained by the presence of hydrolyzable soluble COD (S_H) in the sludge besides S_S. Based on this fact, X_S in the conventional EDM matrix was substituted with S_H (see Table 6.1). This situation is validated by the good correlation of experimental data with the model simulation. A range of $\hat{\mu}_H$ (6-6.5 1/d) and Y_{HD} (0.62-0.66 g COD/g COD) values used for simulation can be explained by the variable content and/or fractions of filtered primary sludge components produced in a settling tank rather than a steady-state fermentor. From Figure 7.7 it can be seen that 64 % of S_H was left unused after 2 hours. The rates of hydrolysis used for simulation (k_{hs}=3 g COD/g CODd and K_{XS}=0.01 g COD/g COD) are similar to the rates reported as k_{hs}=3.1 g COD/g CODd and K_{XS}=0.2 g COD/g COD by Orhon et al. (1999).

7.2.2.2 Activated Sludge Model No 3

As previously stated in Section 6.2.2, for the experimental circumstances described in this study, S_{NO} profile is mostly sensitive to the changes in Y_{STOD}, k_{STO}, and Y_{HD}, among the other parameters considered. Since $\hat{\mu}_H$ (6 1/d) value used for acetate in

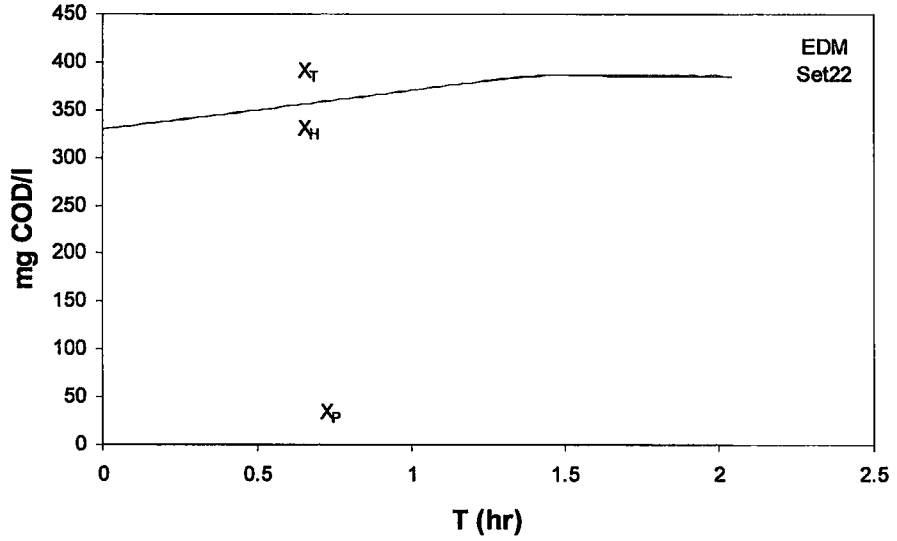

Figure 7.6a The change of X_H, X_P, and X_T with time for t=2 hr in EDM for acetate in experimental set 22

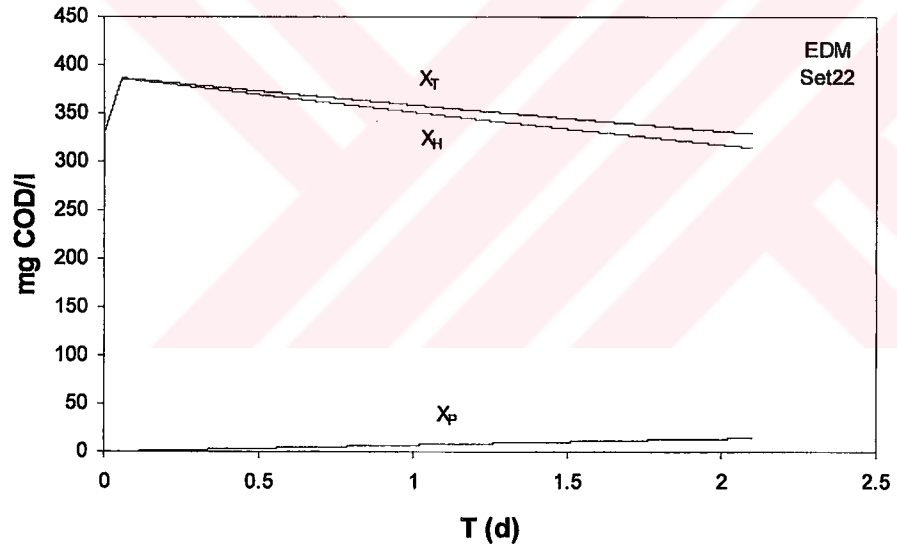

Figure 7.6b The change of X_H, X_P, and X_T with time for t=2.1 d in EDM for acetate in experimental set 22

endogenous decay model is compatible with the stated default value of 6 1/d and Y_{HD} (0.58 g COD/g COD) value is found to be reasonably lower than the default value of Y_H (0.67 g COD/g COD) in the model, $\hat{\mu}_H$ and Y_{HD} values were equally adopted in ASM3. Thus, simulation trials were based on various values of Y_{STOD} and k_{STO} while using the default values of ASM3 for the remaining parameters.

Figure 7.8 shows the S_{NO} versus time profile obtained for acetate using default values of Y_{STOD} and k_{STO} (Y_{STOD}=0.8 g COD/g COD; k_{STO}=5 g COD/g CODd). As can be seen from the figure, S_{NO} is depleted slower than the experimental profile with no substantial decrease in the consumption rate, which would lead to a slower second phase. The figure also shows that storage process still proceeds for the 2 hr experimental period. Since storage is an energy consuming process, the rate of storage was increased considerably (k_{STO}=12 g COD/g CODd) in the next trial. As Figure 7.9 shows, while two phases become apparent as a consequence of increased rate of storage, the rate of S_{NO} depletion is still slower than the experimental profile. Thus, Y_{STOD} was decreased to increase the overall rate of electron acceptor consumption. Figure 7.10 shows a profile compliant with the experimental data where the adopted Y_{STOD} and k_{STO} values were 0.63 g COD/g COD and 12 g COD/g CODd respectively.

The values of stochiometric and kinetic parameters used for model simulation of acetate were given in Table 6.4. b_{HD} values of 0.1 1/d for acetate are identical to the b_H value used in EDM (0.2 1/d) which is reduced by η_E factor of 0.5. b_{STOD} values are equal to b_{HD} values.

Figure 7.10 also presents S_S, and X_{STO} versus time profiles for acetate. The depletion of S_S corresponds to the end of the first phase in the S_{NO} versus time profile, as in EDM. At the same time, the peak point in the X_{STO} profile is observed due to the termination of storage process. The Y_{STOD} value of 0.63 practically means 63 % conversion of S_S to X_{STO}. The figure illustrates approximately 55 % conversion, which is slightly lower than 63 %. A stochiometric mass balance, starting from the initial time (t=0) till the time storage ceased (t=1.3 hr) reveals that, the remaining 8 % of X_{STO} was used for growth, assuming that the fraction of X_{STO} used for the anoxic respiration is negligible. However, the concentration of X_H formed by the utilization of the corresponding concentration of X_{STO} does not appear in the model output indicating that endogenous decay mechanism also participated during the first

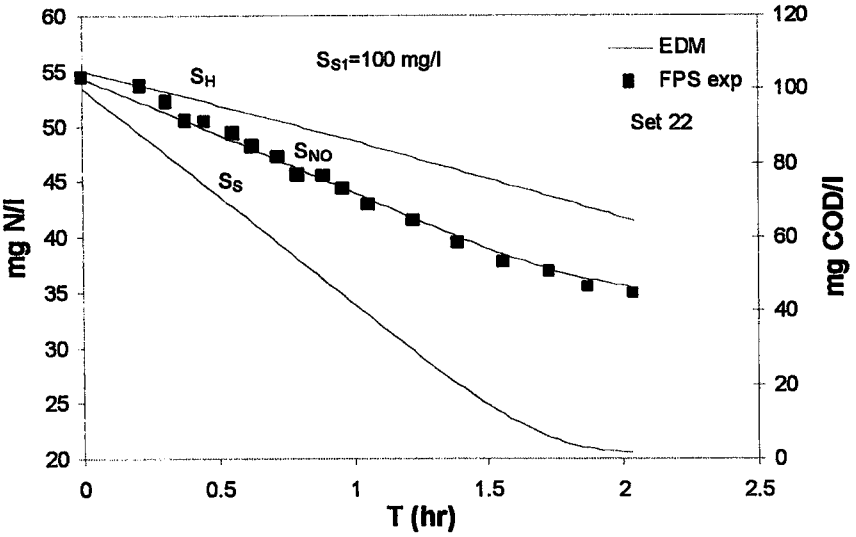

Figure 7.7 Model simulation for filtered primary sludge (FPS) for experimental set 22 based on EDM

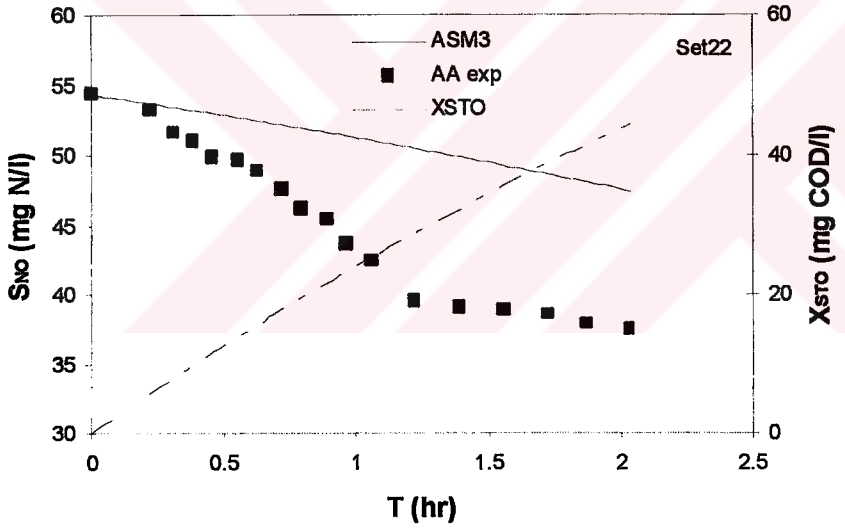

Figure 7.8 S_{NO} versus time profile obtained for acetate (AA) in experimental set 22 using default values of Y_{STOD} (0.8 g COD/g COD) and k_{STO} (5 g COD/g CODd) in ASM3

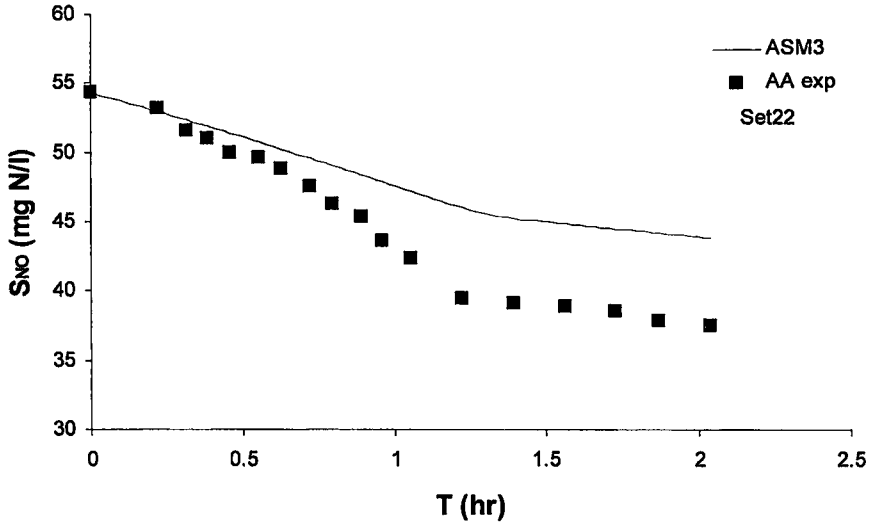

Figure 7.9 S_{NO} versus time profile obtained for acetate (AA) in experimental set 22 using Y_{STOD} (0.8 g COD/g COD) and k_{STO} (12 g COD/g CODd) in ASM3

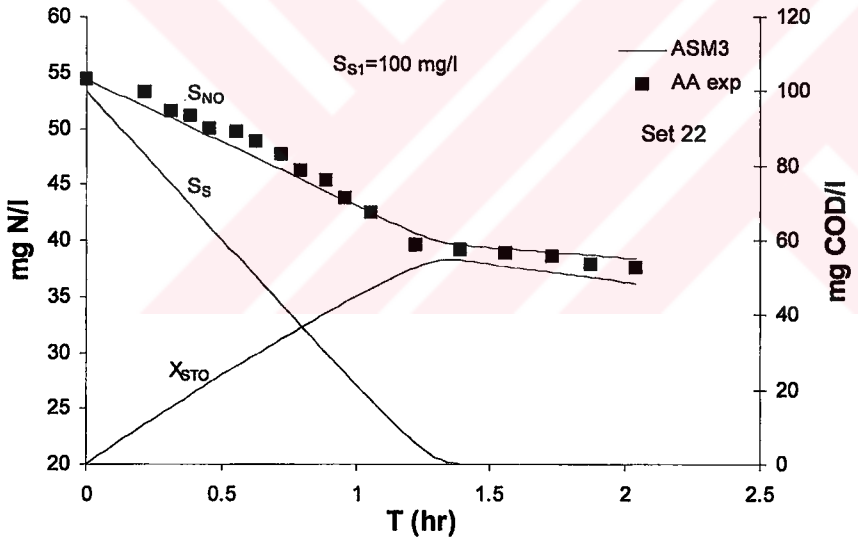

Figure 7.10 S_{NO}, S_S, and X_{STO} versus time profiles for acetate (AA) in experimental set 22 for ASM3

phase of the electron acceptor profile. From a stochiometric mass balance it was found that, the percent contribution of storage, growth, and endogenous respiration processes to the S_{NO} consumption were 89 %, 8 %, and 3 % respectively. Thus, storage was the dominant mechanism during the initial phase of the electron acceptor utilization profile.

Considering the experimental circumstances associated with this study, the total particulate COD, X_T, would be composed of the active heterotrophic biomass, X_H, cell internal storage products, X_{STO}, and inert particulate organic material, X_P in accordance with ASM3. As Figures 7.11a and 7.11b show, X_P concentration was negligible within two hours of experimental period. The peak point in the X_T versus time profile was reached at t=1.37 hr where X_T concentration was 388 mg COD/l. At t=2 hr, X_T concentration was 385 mg COD/l which is quite close to the X_T value (385 mg COD/l) for acetate in EDM due to the presence of X_{STO} fraction during this time period. At the end of two days, X_T concentration was equal to 310 mg/l which is lower than the concentration of X_T (X_T=330 mg COD/l) produced in EDM for acetate for the same time duration. After storage process is completed, a decreasing trend is observed in the X_{STO} profile. Following the depletion of X_{STO}, the difference between the concentrations of X_T becomes more pronounced due to the difference between net yield (See equation 6.4) defined in ASM3 (Y_{STOD}*Y_{HD}=0.63*0.58=0.37 g X_H/g S_S) and in EDM (Y_{HD}=0.58 g X_H/g S_S). Hence, X_T concentration in ASM3 was observed to be lower as compared to EDM.

As previously described in section 6.2.2, ASM3 defines the total soluble COD (filtered through 0.45 m) as the sum of S_S and S_I fractions. Thus, the soluble hydrolyzable fraction, S_H, defined in EDM is included within the content of S_S in ASM3. If a numerical evaluation is done, in EDM, the COD fractions were assessed as S_S=100 mg COD/l and S_H=105 mg COD/l while in ASM3 S_S was equal to 205 mg COD/l for experimental set 22 (Table 6.8).

Figure 7.12 shows the S_{NO} versus time profile obtained when Y_{HD} and $\hat{\mu}_H$ values were adopted as in EDM while the same Y_{STOD} and k_{STO} values were considered as in acetate. The default values of ASM3 were used for the remaining parameters. Due to the increased concentration of S_S by definition, a single phase was observed which was slightly faster than the experimental data. The X_{STO} profile illustrates that the storage process still proceeded. Since the model profile did not exhibit a two-phase

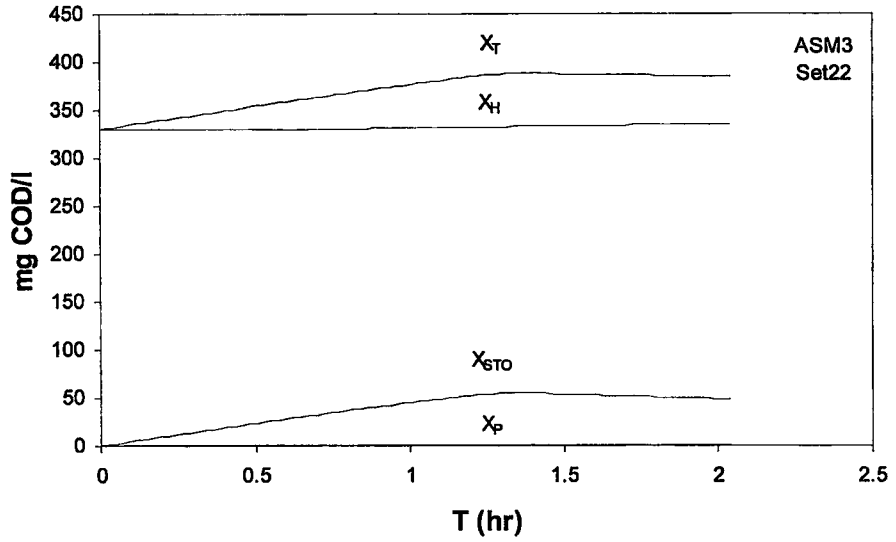

Figure 7.11a The change of X_H, X_{STO}, X_P, and X_T with time for t=2 hr in ASM3 for experimental set 22

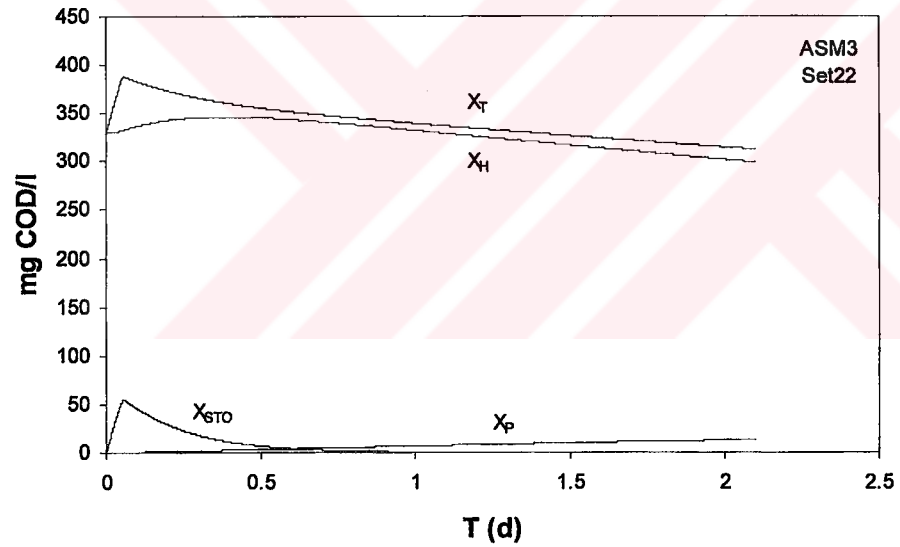

Figure 7.11b The change of X_H, X_{STO}, X_P, and X_T with time for t=2.1 d in ASM3 for experimental set 22

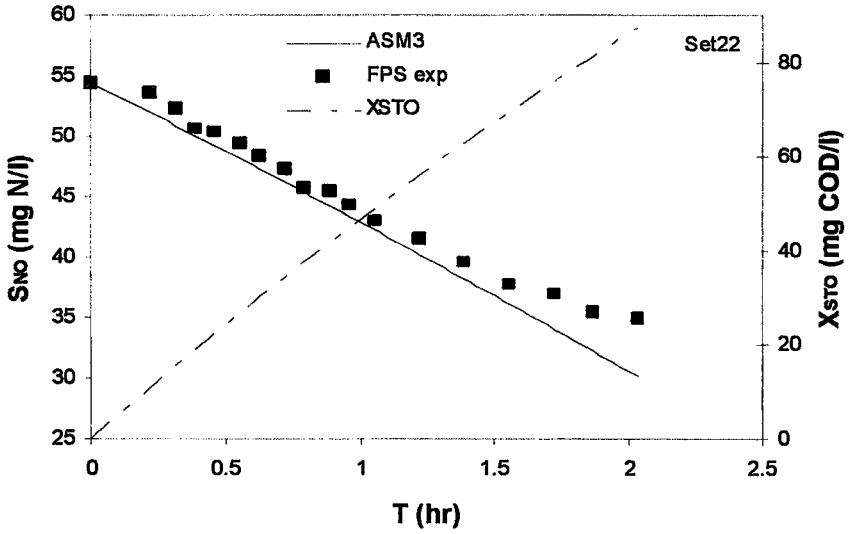

Figure 7.12 S_{NO} versus time profile obtained for filtered primary sludge (FPS) in experimental set 22 using Y_{STOD} (0.63 g COD/g COD) and k_{STO} (12 g COD/g CODd) in ASM3

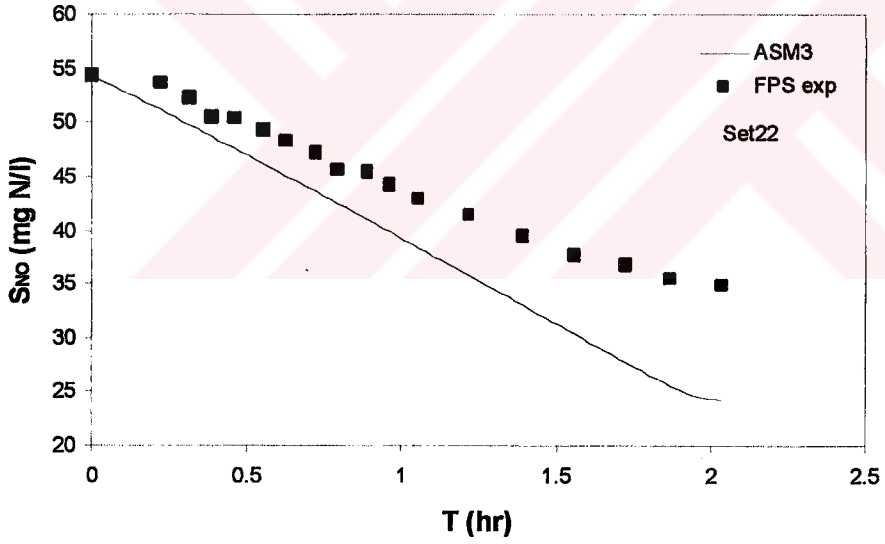

Figure 7.13 S_{NO} versus time profile obtained for filtered primary sludge (FPS) in experimental set 22 using Y_{STOD} (0.63 g COD/g COD) and k_{STO} (16 g COD/g CODd) in ASM3

trend, model versus experimental data fit was not established. Similar to acetate, observation of a second phase would be possible by increasing the storage rate. When k_{STO} was increased to 16 g COD/g CODd, a second phase appeared through the end of the S_{NO} versus time profile similar to the experimental data. However, increased rate of storage resulted in a faster proceeding electron acceptor utilization profile, as seen in Figure 7.13. In order to decrease the rate, Y_{STOD} value was increased to 0.8 g COD/g COD. Figure 7.14 shows the perfect fit of model simulation and experimental profiles using Y_{STOD} and k_{STO} values of 0.8 g COD/g COD and 16 g COD/g CODd respectively.

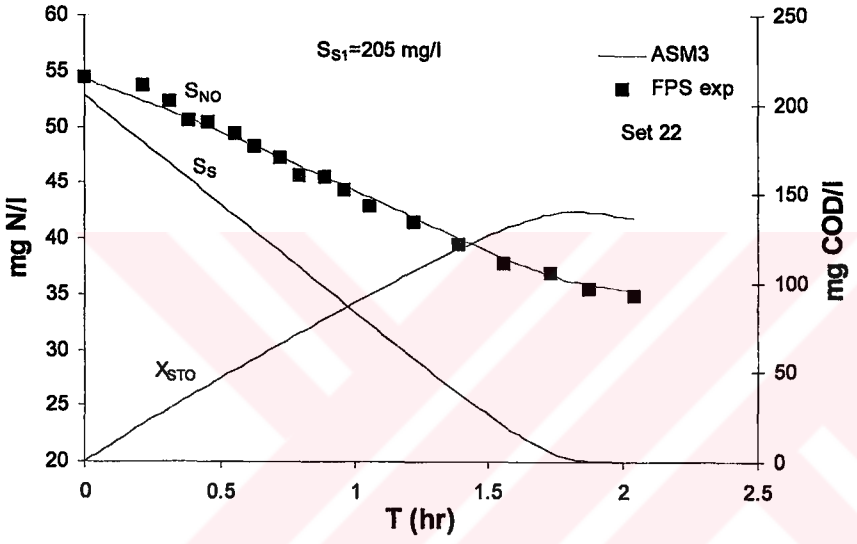

Figure 7.14 S_{NO}, S_S, and X_{STO} versus time profiles for filtered primary sludge (FPS) in experimental set 22 for ASM3

The kinetic and stochiometric parameters used in ASM3 simulation for FPS were given in Table 6.9. $\hat{\mu}_H$, Y_{HD}, and K_S values were identical to the values adopted in EDM. As the table presents, the remaining stochiometric and kinetic parameters, except for Y_{STOD} and k_{STO}, are the same as in acetate.

Similar to acetate, the end of the first phase in the S_{NO} versus time profile occurred at the point of depletion of S_S where X_{STO} reached to the peak point (Figure 7.14). The X_{STO} profile illustrates approximately 70 % conversion of S_S to X_{STO} although Y_{STOD} value addresses 80 % conversion. A stochiometric mass balance shows that 10 % of X_{STO} was used for growth neglecting the fraction of X_{STO} used for anoxic respiration. Since the concentration of X_H formed by the use of 10 % of X_{STO} was not reflected in the X_H profile, it was deduced that endogenous respiration was one of the processes

contributing to S_{NO} utilization. The percent contribution of storage, growth, and endogenous respiration processes during the first phase of the electron acceptor profile were 79 %, 16 %, and 5 % respectively. When these figures are compared to the values of percent contribution of each process assessed for acetate in set 22, it can be seen that while the percentage of S_{NO} utilization for storage process is lower (89 % vs 79 %), a higher percentage of S_{NO} was used for growth for FPS (8 % vs 16 %).

CHAPTER 8 CONCLUSIONS AND SUGGESTIONS FOR FURTHER WORK

8.1 Assessment of Heterotrophic Endogenous Respiration Rate

The first part of the experimental studies was oriented towards the assessment of heterotrophic endogenous respiration rate, b_H. The method proposed by Marais and Ekama (1976) was applied for b_H determination for domestic, meat processing and leather tanning effluents. The obtained experimental data were usually scattered, especially in case of industrial effluents they exhibited cyclic variations. The statistical analysis of the data yielded a low percentage of consistency. Furthermore, the value of b_H obtained varied according to the duration of the experimental period considered. The above observations were attributed to the analytical limitations associated with the recent oxygen meter technology in measuring oxygen utilization rates as low as 2-8 mg/l.hr as well as the interference of adsorbed particulate organic matter initially present, leading to higher electron acceptor consumption rates associated with hydrolysis rather than endogenous degradation.

The information obtained from the conventional method of assessment indicates that the numerical values obtained for b_H and η_E can not be regarded as accurate and reliable.

The deficiencies observed with the conventional method have led to the search of an alternative method for the assessment of heterotrophic endogenous respiration rate. The basic idea was to avoid the interferences and shortcomings associated with the conventional method. Hence, the proposed method aims to shift OUR measurements to the growth phase by providing a constant unlimited growth medium, which would ensure a constant $\hat{\mu}_H$ level. The method would also enable the determination of anoxic endogenous respiration coefficient for which no alternative methods of assessment exists in the literature. The method was applied to domestic wastewaters. Five experimental sets were conducted at 20 ± 1°C and one experiment was performed at 10 ± 1°C. Based on these results the following conclusions can be drawn:

1. The arithmetic mean of the b_H value obtained at the end of five experimental runs was 0.08 1/day whereas an arithmetic average of 0.05 1/day was obtained for b_{HD} at 20 ± 1°C

2. At 10 ± 1°C, a value of 0.04 1/ day was obtained for both b_H and b_{HD} at the end of one experimental run

3. The statistical analysis of the experimental data indicates a high percentage of consistency between results obtained within each experimental set and among individual sets

4. At 20 ± 1°C an η_E value of 0.6 was assessed which yields to the practical conclusion that the anoxic digester tank volume has to be almost twice the volume of the aerobic tank to achieve the same treatment efficiency

The values of b_H and η_E obtained in this study are appreciably lower than the values reported in the literature. This may either be attributed to the variations in wastewater characteristics or to the above mentioned limitations of the current method.

Substantial improvement in the generation of data reliably usable in modeling was achieved by the implementation of the proposed method for the assessment of heterotrophic endogenous decay rate under aerobic and anoxic conditions. During the course of this study, the method was applied only for domestic wastewaters. It should be emphasized that further experimental work is required both on domestic and industrial wastewaters at various temperatures to support the results of this study.

8.2 Investigation of Denitrification Kinetics Using Hydrolyzed Carbon Sources

Primary sludge was employed as a hydrolyzed carbon source for the investigation of denitrification kinetics. In order to assess the performance of primary sludge as a carbon source, denitrification rates obtained with primary sludge were compared with the rates obtained with acetate, which is accepted as a well-defined external carbon source. For this purpose, batch experiments were conducted for equivalent initial S_S concentrations of both substrates in parallel tests.

Filtered primary sludge and acetate yielded similar denitrification rates (k_1) indicating that primary sludge proved to be as efficient as acetate. This observation

agrees well with most of the literature findings. It should also be noted that observed denitrification rates for both filtered primary sludge and acetate were relatively higher than literature values. This might be due to the expression of denitrification rates on the active biomass (X_H) basis rather than volatile suspended solids (VSS) as reported in the literature.

The experimental data obtained from denitrification tests were simulated using two models, namely, Endogenous Decay Model (EDM) and Activated Sludge Model No 3 (ASM3). The compliance of experimental data with the model simulations was investigated on the basis of the processes and parameters associated with both models.

The experimental electron acceptor utilization profiles, for both acetate and filtered primary sludge were found to be compliant with the model simulation of EDM. The maximum growth rate ($\hat{\mu}_H$) and anoxic yield (Y_{HD}) values for acetate were obtained as 6 1/d and 0.58 g COD/g COD respectively. A range of $\hat{\mu}_H$ (6-6.5 1/d) and Y_{HD} (0.62-0.66 g COD/g COD) values used for filtered primary sludge could be explained by the variable content and/or fractions of filtered primary sludge components produced in a settling tank rather than a steady-state fermentor. $\hat{\mu}_H$ values considered for acetate and filtered primary sludge, both of which contain acetate, are consistent with each other. These values can also be regarded as compatible with the default value reported in EDM for domestic wastewaters in which acetate, again, forms a substantial fraction of S_S. Y_{HD} values adopted in the model are reasonably lower than the default value of Y_H (0.67 g COD/g COD), stated in EDM for domestic wastewaters.

During simulation of EDM for the data obtained for filtered primary sludge, it was noticed that denitrification rates observed during the second phase of the electron acceptor utilization profile (k_2) for filtered primary sludge were found to be too high to be associated with endogenous respiration. This finding is justified by the presence of hydrolyzable soluble COD fraction, S_H, besides the readily biodegradable portion, S_S, in the structure of the primary sludge and validated by the good correlation of experimental data with the model simulation.

The experimental results' compliance with the model simulation run with a range of meaningful parameter values show that the processes and parameters within the structure of EDM are proficient in explaining the behaviour of acetate and filtered primary sludge as carbon sources for denitrification.

Two new processes, namely storage and respiration of storage products, both of which consume energy, are introduced by ASM3. These processes were not involved in the former model structures including EDM. While an increased number of processes are considered in ASM3, the model simplifies the definition of the readily biodegradable content, S_S, by assessing this fraction simply by filtration instead of employing the respirometric analysis method as adopted in EDM. This definition brings the inclusion of the slowly hydrolyzable fraction, S_H, defined in EDM, within the content of S_S. Thus, the S_S content of systems composed of more than one fraction of COD, such as primary sludge, becomes greater in magnitude than the S_S fraction considered in EDM.

It was experimentally illustrated that, the electron acceptor utilization profiles for acetate and filtered primary sludge exhibited quite similar trends. However, during the simulation of ASM3, it became apparent that the model and experimental compliance could be provided by the use of different values of parameters associated with storage. For acetate, the anoxic storage yield (Y_{STOD}) was assessed as 0.63 g COD/g COD, while for filtered primary sludge, Y_{STOD} assumed values between 0.78 g COD/g COD and 0.8 g COD/g COD. Although Y_{STOD} value determined for filtered primary sludge is in good agreement with the default value of Y_{STOD} (0.8 g COD/g COD) as stated in ASM3, Y_{STOD} value for acetate was much lower. On the other hand, for acetate the storage rate was assessed as 12 g COD/g CODd and filtered primary sludge, the rates of storage (k_{STO}) varied between 16 and 20 g COD/g CODd respectively. Hence, the storage rates compliant with the experimental data were quite high for both cases, as compared with the default value for k_{STO} as 5 g COD/g COD. Based on these observations, it can be stated that, although acetate and primary sludge are similar in content, which is also reflected in similar experimental behaviour, the model parameters associated with storage do not exhibit the expected consistency as already observed in EDM, mainly due to the COD fractionation approach adopted in ASM3.

The model simulation studies for ASM3 have provided evidence that monitoring of the storage products should be an essential part of the experimental studies. Based on this consideration, an experimental database should be formed towards the assessment of kinetic and stochiometric parameters associated with storage. Another aspect worth investigating is the determination of the contents of released carbon, both for the optimization of processes generating carbon sources and the assessment of the individual effect of these components on the efficiency of nutrient removal.

REFERENCES

Abufayed, A. A. and Schroeder, E.D., 1986. Performance of SBR/Denitrification with a primary sludge carbon source, *Journal WPCF*, **58,** (5), 387-396.

Abufayed, A. A. and Schroeder, E.D., 1986. Kinetics and stochiometry of SBR/ Denitrification with a primary sludge carbon source, Journal WPCF, **58,** (5), 398-405.

Akunna, J. C., Bizeau, C. and Moletta, R., 1993. Nitrate and nitrite reductions with anaerobic sludge using various carbon sources: glucose, glycerol, acetic acid, lactic acid, and methanol, *Water Research*, **27,** (8), 1303-1312.

Alleman, J. E. and Irvine, R. L., 1980, Storage induced denitrification using sequencing batch reactor operation, *Water Research*, **14,** 1483-1488.

Anderson, B. C. and Mavinic, D. S., 1992. Assessment and application of kinetic reaction rates in pilot-scale semi-continuous aerobic sludge digestion, *Environmental Technology*, **13,** 115-128.

Barnard, J. L., 1975. Biological nutrient removal without the addition of chemicals, *Water Research*, **9,** 485.

Barnard, J. L. and Meiring, P. G. J., 1977. Sources of hydrogen donors and their effects on denitrification rates, *Progress in Water Technology*, **8,** (4-5), 577-588.

Barnes, D. and Bliss, P.J., 1983. Biological Control of Nitrogen in Wastewater Treatment, E&F. N. Spon, USA.

Beeftink, H. H., Van Der Heijden, R. T. J. M. and Heijnen, J. J., 1990. Maintenance requirements: energy supply from simultaneous endogenous respiration and substrate consumption, *FEMS Microbiology Ecology*, **73,** 203-210.

Bitton, G., 1994. Wastewater Microbiology, Wiley-Liss Inc., USA.

Brinch, P. P., Rindel, K. and Kalb, K., 1994. Upgrading to nutrient removal by means of internal carbon from sludge hydrolysis, *Water Science and Technology*, **29,** (12), 31-40.

Bundgaard, E., Andersen, K. and Henze, M., Process optimization by fermenter technology. (Reference available upon request)

Carley, B.N. and Mavinic, D. S., 1991. The effects of external carbon loading on nitrification and denitrification of a high ammonia landfill leachate, *Research Journal WPCF*, **63,** (1), 51-59.

Cech, J. S. and Chudoba, J., 1983. Influence of accumulation capacity of activated sludge microorganisms on kinetics of glucose removal, *Water Research*, **17**, (6), 659-666.

Christensen, M. H. and Harremoes, P., 1972, Biological denitrification in water treatment, Report 72-2, Department of Sanitary Engineering, Technical University of Denmark.

Christensen, M. H. and Harremoes, P., 1977. Biological denitrification of sewage: A literature review, *Progress in Water Technology*, **8**, (4-5), 509-555.

Christensen, M. H. and Harremoes, P., 1985. *Nitrification and Denitrification in Wastewater Treatment*, Topics in Wastewater Treatment, Edited by J. M. Sidwick, Oxford, Blackwell Scientific.

Christensson, M., Lie, E. and Welander, T., 1994. A comparison between ethanol and methanol as carbon sources for denitrification, *Water Science and Technology*, **30**, (6), 83-90.

Chudoba, J., Grau, P. and Ottova, V., 1973. Control of activated sludge filamentous bulking-ii. Selection of microorganisms by means of a selector, *Water Research*, **7**, 1389-1406.

Claus, G. and Kutzner, H. J., 1985. Denitrification of nitrate and nitric acid with methanol as carbon source, *Applied Microbiology and Biotechnology*, **22**, 378-381.

De Renzo, 1978, Nitrogen Control and Phosphorus Removal in Sewage Treatment, Noyes Data Corporation, USA.

Dold, P. L., Ekama, G. A. and Marais, G.v.R., 1980. A general model for the activated sludge process, *Progress in Water Technology*, **12**, 47-77.

Dold, P. L. and Marais, G.v.R., 1986. Evaluation of the general activated sludge model proposed by the IAWPRC task group, *Water Science and Technology*, **18**, (6), 63-89.

Eastman, J. A. and Ferguson, J.F., 1981. Solubilization of particulate organic carbon during the acid phase of anaerobic digestion, *Journal WPCF*, **53**, (3), 352-366.

Eilersen, A. M., Henze, and M., Kloft, L., 1995. Effect of volatile fatty acids and trimethylamine on denitrification in activated sludge, *Water Research*, **29**, (5), 1259-1266.

Ekama, G. A., Dold, P. L. and Marais, G.v.R., 1986. Procedures for determining influent COD fractions and the maximum specific growth rate of heterotrophs in activated sludge systems, *Water Science and Technology*, **18**, 91-114.

Elefsiniotis, P. and Oldham, W.K., 1994. Effect of HRT on acidogenic digestion of primary sludge, *Journal of Environmental Engineering*, **120**, (3), 645-660.

EPA Manual Nitrogen Control, 1975. Office of Technology Transfer, Washington D.C.

EPA Manual Nitrogen Control, 1993. Office of Research and Development, Cincinnati, Ohio, Office of Water, Office of Wastewater Enforcement and Compliance, Washington D.C.

Fass, S., Ganaye, V., Urbain, V., Manem, J. and Block, J.C., 1994. Volatile fatty acids as organic carbon sources in denitrification, *Environmental Technology*, **15**, 459-467.

Gerber, A., Mostert, E. S., Winter, C. T. and De Villiers, R.H., 1987. Interactions between phosphate, nitrate and organic substrate in biological nutrient removal processes, *Water Science and Technology*, **19**, Rio, 183-194.

Ghosh, S., Conrad, J. R. and Klass, D.L., 1975. Anaerobic acidogenesis of wastewater sludge, *Journal WPCF*, **47**, (1), 30-45.

Goel, R., Mino, T., Satoh, H. and Matsuo, T., 1998. Intracellular storage compounds, oxygen uptake rates and biomass yield with readily and slowly biodegradable substrates, *IAWQ 19th Biennial International Conference*, Vancouver, Canada, **2**, 77-84.

Grady, C. P. L. and Lim, H.C., 1980. Biological Wastewater Treatment, Marcel Dekker Inc., New York.

Gray, N. F., 1989. Biology of Wastewater Treatment, Oxford University Press, New York.

Gujer, W. and Zehnder, J.B., 1983. Conversion processes in anaerobic digestion, *Water Science and Technology*, **15**, 127-167.

Gujer, W., Henze, M., Mino, T. and Loosdrecht, M., 1999. Activated Sludge Model No 3, *Water Science and Technology*, **39**, (1), 183-193.

Hao, O.J., Kim, M.H. and Al-Ghusain, I., 1991. Alternating aerobic and anoxic digestion of waste activated sludge, *Journal of Chemical Technology and Biotechnology*, **52**, 457-472.

Hanel, K., 1988. Biological Treatment of Sewage by the Activated Sludge Process, Ellis Horwood Ltd., England.

Hatziconstantinou, G. J., Yannakopoulus, P. and Andreadakis, A., 1996. Primary sludge hydrolysis for biological nutrient removal, *Water Science and Technology*, **34**, (1-2), 417-423.

Henze, M., 1986. Nitrate versus oxygen utilization rates in wastewater and activated sludge systems, *Water Research*, **18**, 115-122.

Henze, M., 1989. The influence of raw wastewater biomass on activated sludge oxygen respiration rates and denitrification rates, *Water Research*, **21**, 603-607.

Henze, M., 1991. Capabilities of biological nitrogen removal processes from wastewater, *Water Science and Technology*, **23**, Kyoto, 669-679.

Henze, M., 1992. Characterization of wastewater for modeling of activated sludge processes, *Water Science and Technology*, **25**, (6), 1-15.

Henze, M., Grady, C.P.L. Jr., Gujer, W., Marais, G.v.R. and Matsuo, T., 1987. *Activated Sludge Model No. 1*, IAWPRC Task Group on Mathematical Modeling for Design and Operation of Biological Wastewater Treatment.

Henze, M., Gujer, W., Mino, T., Matsuo, T., Wentzel, M.C. and Marais, G.v.R., 1995. *Activated Sludge Model No. 2*, IAWPRC Task Group on Mathematical Modeling for Design and Operation of Biological Wastewater Treatment.

Henze, M., Harremoes P. and Jensen, O.R., 1977. Combined sludge denitrification of sewage utilizing internal carbon sources, *Water Science and Technology*, **8**, (4-5), 589-599.

Isaacs, S. H. and Henze, M., 1995. Controlled carbon source addition to an alternating nitrification-denitrification wastewater treatment process including biological p removal, *Water Research*, **29**, (1), 77-89.

Isaacs, S. H., Henze, M., Soeberg, H. and Kummel, M., 1994. External carbon source addition as a means to control an activated sludge nutrient removal process, *Water Research*, **28**, (3), 511-520.

Kappeler, J. and Gujer, W., 1992. Estimation of kinetic parameters of heterotrophic biomass under aerobic conditions and characterization of wastewater for activated sludge modeling, *Water Science and Technology*, **25**, (6), 125-139.

Kaspar, H. F. and Wuhrmann, K., 1978. Kinetic parameters and relative turnovers of some important catabolic reactions in digesting sludge, *Applied and Environmental Microbiology*, **36**, (1), 1-7.

Kristensen, G.H., Jorgensen, P. E. and Henze, M., 1992. Characterization of functional microorganism groups and substrate in activated sludge and wastewater by AUR, NUR and OUR, *Water Science and Technology*, **25**, (6), 43-57.

Kristensen, G.H., Jorgensen, P. E., Strube, R. and Henze, M., 1992. Combined pre-precipitation, biological sludge hydrolysis and nitrogen reduction-A pilot demonstration of integrated nutrient removal, *Water Science and Technology*, **26**, (5-6), 1057-1066.

Kappeler, J. and Gujer, W., 1992. Estimation of kinetic parameters of heterotrophic biomass under aerobic conditions and characterization of wastewater for activated sludge modeling, *Water Science and Technology*, **25**, (6), 125-139.

Kim, M. H. and Hao, O. J., 1990. Comparison of activated sludge stabilization under aerobic and anoxic conditions. *Research Journal WPCF*, **62**, (2), 160-168.

Kristensen, G.H., Jorgensen, P. E. and Henze, M., 1992. Characterization of functional microorganism groups and substrate in activated sludge and wastewater by AUR, NUR and OUR, *Water Science and Technology,* **25**, (6), 43-57.

Lamanna, C., (Editor) 1963. Endogenous metabolism with special reference to bacteria, *Annals of the New York Academy of Sciences*, **102**, (3), 515-793.

Lee, N. M. and Welander, T., 1996. The effect of different carbon sources on respiratory denitrification in biological wastewater treatment, *Journal of Fermentation and Bioengineering,* **82**, (3), 277-285.

Lee S., Koopman, B., Park, S. and Cadee, K., 1995. Effect of fermented wastes on denitrification in activated sludge, *Water Environment Research*, **67**, (7), 1119-1122.

Lie, E. and Welander, T., 1997. A method for determination of the readily fermentable organic fraction in municipal wastewater, *Water Science and Technology,* **34**, (6), 1269-1274.

Lilley I.D., Wentzel, M.C., Loewenthal, R. E. and Marais, G.v.R., 1990. Acid fermentation of primary sludge at 20°C, *Research Report*, W64, Dept. of Civil Eng., Univ. of Cape Town.

Loosdrecht, M. C. M., Pot, M. A. and Heijnen, J. J., 1997. Importance of bacterial storage polymers, *Water Science and Technology*, **35**, (1), 41-47.

Lotter, L. H. and Murphy, M., 1986. Volatile acid production in anaerobic digesters and primary sedimentation tanks: The effect of selected parameters on acid production, Laboratory and Technical Services Branch, City Health Department, Johannesburg.

Majone, M., Massanisso, P. and Ramadori, R., 1998. Comparison of carbon storage under aerobic and anoxic conditions, *IAWQ 19th Biennial International Conference*, Vancouver, Canada, **2**, 69-76.

Majone, M., Massanisso, Carucci, A., Lindrea, K. and Tandoi, V., 1996. Influence of storage on kinetic selection to control aerobic filamentous bulking, *Water Science and Technology*, **34**, (5-6), 223-232.

Majone, M., Dircks, K. and Beun, J. J., 1999. Aerobic storage under dynamic conditions in activated sludge processes. The state of the art, *Water Science and Technology*, **39**, (1), 61-73.

Manoharan, R., Liptak, S., Parkinson, P., Mavinic D. and Randall, C. W., 1989. Denitrification of a high ammonia leachate using an external carbon source, *Environmental Technology*, **10**, 701-706.

Marais, G.v.R. and Ekama, G.A., 1976. The activated sludge process Part 1 - Steady state behavior, *Water SA*, **2**, (4), 165-199.

Mc Carty et al., 1966. Task Groups 2610-0, Nutrients in water-nitrogen and phosphorus in water quality and treatment, *AWWA Annual Conference*, Florida.

Mc Carty, P. L., Beck, L., and Amant, P. ST., 1969. Biological denitrification of wastewaters by addition of organic materials, *Proceedings of the 24th Industrial Waste Conference,* Purdue, **2**, 1271-1285.

Mcclintock, S. A., Pattarkine, V. M. and Randall, C. W., 1992. Comparison of yields and decay rates for a biological nutrient removal process and a conventional activated sludge process, *Water Science and Technology*, **26**, (9-11), 2195-2198.

Monteith, H. D., Bridle, T.R. and Sutton, P.M., 1980. Industrial waste carbon sources for biological denitrification, *Progress in Water Technology*, **12**, 127-141.

Moser-Engeler, R., Udert, K., Wild, D. and Siegrist, H., 1998. Products from primary sludge fermentation and their suitability for nutrient removal, *IAWQ 19th Biennial International Conference,* Vancouver, Canada, **1**, 252-259.

Narkis, N., Rebhun, M. and Sheindorf, Ch., 1979. Denitrification at various carbon to nitrogen ratios, *Water Research*, **13**, 93-98.

Nicholls, H. A., Osborn, D. W. and Pitman, A. R., 1985. Biological phosphorus removal-johannesburg experience, *Proceedings of the Institute of Water Pollution Control Biennial Conference*, Durban, South Africa.

Nyberg, U., Aspegren, H., Andersson, B., Jansen, J. C. and Villadsen, I. S., 1992. Full-scale application of nitrogen removal with methanol as carbon source, *Water Science and Technology,* **26**, (5-6), 1077-1086.

O'Connor, J. T., 1972. Environmental engineering unit operations and unit processes laboratory manual, Association of Environmental Engineering Professors.

Orhon, D. and Artan, N., 1994. Modeling of Activated Sludge Systems, Technomic Publ., Lancaster.

Orhon, D., Sözen, S. and Artan, N., 1996. The effect of heterotrophic yield on the assessment of the correction factor for the anoxic growth, *Water Science and Technology,* **39**, (1), 87-95.

Orhon, D., Çokgör Ubay E. and Sözen, S., 1999. Experimental basis for the hydrolysis of slowly biodegradable substrate in different wastewaters, *Water Science and Technology,* **32**, (2), 476-488.

Osborn, D. W., Lotter, L. H., Pitman, A. R. and Nicholls, H.A., 1986. Enhancement of biological phosphate removal by altering process feed composition, Johannesburg City Council, *WRC Report*, No. 137/1/86, Water Research Commission South Africa.

Paskins, A. R., Jones, G. L. and Wheatland, A. B., 1978. Kinetics of denitrification in the activated sludge process, *Progress in Water Technology*, **10**, (1-2), 255-260.

Pitman, A. R. and Lotter, L.H., 1986. Volatile acid production in the activated sludge process, *Proceedings of the Symposium on Anaerobic Digestion*, Bloemfontein, South Africa.

Pitman A. R., Venter, S. L. V. and Nicholls, H.A., 1983. Practical experience with biological phosphorus removal plants in Johannesburg, *Water Science and Technology*, **15**, 233-259.

Pitman, A. R., 1995. Practical experiences with biological nutrient removal on full-scale wastewater treatment plants in South Africa, *Internationale Konferenz zur Vermehrten Biologischen Phosphorel.*

Pitman, A. R., Lotter, L.H., Alexander, W. V. and Deacon, S. L., 1992. Fermentation of raw sludge and elutriation of resultant fatty acids to promote excess biological phosphorus removal, *Water Science and Technology*, **25**, (4-5), 185-194.

Rabinowitz, B. and Oldham, W. K., 1985. The use of primary sludge fermentation in the enhanced biological p removal process, *International Conference for New Directives and Research in Waste Treatment and Residual Management*, University of British Columbia, Vancouver.

Ragazzi, M., Canziani, R., Bortone, G. and Rozzi, A., Kinetics of primary sludge hydrolysis. (Reference available upon request)

Reichert, P., 1994. Concepts underlying a computer program for the identification and simulation of aquatic systems, Swiss Federal institute for Environmental Science and Technology, CH-8600 Dubendorf, Switzerland.

Rodriguez, G.C., Gonzalez, O. and Gonzalez, S., 1998. Wastewater fermentation and nutrient removal in sequencing batch reactors, *IAWQ 19th Biennial International Conference,* Vancouver, Canada, **1**, 242-251.

Sarıkaya, H.Z., Orhon, D., San, H.A., Sözen, S., Demir, I., İnanç, B., Yüksel, E., Çokgör, E., Avcıoğlu, E. and Arıkan, O., 1997. Wastewater characterization in Tuzla wastewater treatment plant catchment basin, Final Report, Istanbul Technical University, Department of Environmental Engineering.

Skrinde, J. R. and Bhagat, S. K., 1982. Industrial wastes as biological carbon sources in denitrification, *Journal Water Pollution Control Federation*, **54**, 370-377.

Sollfrank, U. and Gujer, W., 1991. Characterization of the domestic wastewater for mathematical modeling of the activated sludge process, *Water Science and Technology*, **23**, (4-6), 1057-1066.

Sözen, S., 1995. Experimental evaluation of nitrification - denitrification kinetics, *Ph.D. Thesis*, Istanbul Technical University (in Turkish).

Sözen, S. and Orhon, D., 1999. The effect of nitrite correction on the evaluation of the rate of nitrate utilization under anoxic conditions, *Journal of Chemical Technology and Biotechnology*, **74**, 790-800.

Sözen, S., Çokgör Ubay E., Orhon, D. and Henze M., 1998. Respirometric analysis of activated sludge behaviour-II. Heterotrophic growth under aerobic and anoxic conditions, *Water Research*, **32**, (2), 476-488.

Spanjers, H., Vanrolleghem, P. A., Olsson, G. and Dold, P. L., 1998. Respirometry in control of the activated sludge process: Principles, *IAWQ Scientific and Technical Report No.7.*

Standard Methods for the Examination of Water and Wastewater, 1995. 19th Edn, American Public Health Association / American Water Works Association / Water Environment Federation, Washington DC, USA.

Stouthamer, A. H., Boogerd, F. C. and Van Verseveld, H. W., 1982. The bioenergetics of denitrification, *Antonie van Leeuwenhoek*, **48**, 545-553.

Tam, N. F. Y., Leung, G. L. W. and Wong, Y.S., 1994. The effects of external carbon loading on nitrogen removal in sequencing batch reactors, *Water Science and Technology*, **32**, (6), 73-81.

Tam, N. F. Y., Wong, Y. S. and Leung, G., 1992. Effect of exogenous carbon sources on removal of inorganic nutrient by the nitrification-denitrification process, *Water Research*, **26**, (9), 1229-1236.

Van Aalst-Van Leeuwen M.A., Pot, M. A., Van Loosdrecht M. C. M. and Heijnen, J.J., 1997. Kinetic modeling of poly (β-hydroxybutyrate) production and consumption by *Paracoccus pantatrophus* under dynamic substrate supply, *Biotechnology and Bioengineering*, **55**, (5), 773-782.

Warner, A.P.C., Ekama, G. A. and Marais, G.v.R., 1983. Anoxic-aerobic digestion of waste activated sludge, *Research Report*, W48, Dept. of Civil Eng., Univ. of Cape Town.

Warner, A.P.C., Ekama, G. A. and Marais, G.v.R., 1986. The activated sludge process-4, *Water Research*, **20**, (8), 943-958.

Winkler, M., 1984. Biological control of nitrogenous pollution in wastewater, *Topics in Enzyme and Fermentation Biotechnology*, **8**, Alan Wiseman (Editor), Ellis Horwood Limited.

Zoetemeyer, R. J., Van Den Heuvel, J. C. and Cohen, A., 1982. pH influence on acidogenic dissimilation of glucose in an anaerobic digestor, *Water Research*, **16**, 303-311.

APPENDIX A

ELECTRON ACCEPTOR UTILIZATION PROFILES IN FEED REACTORS

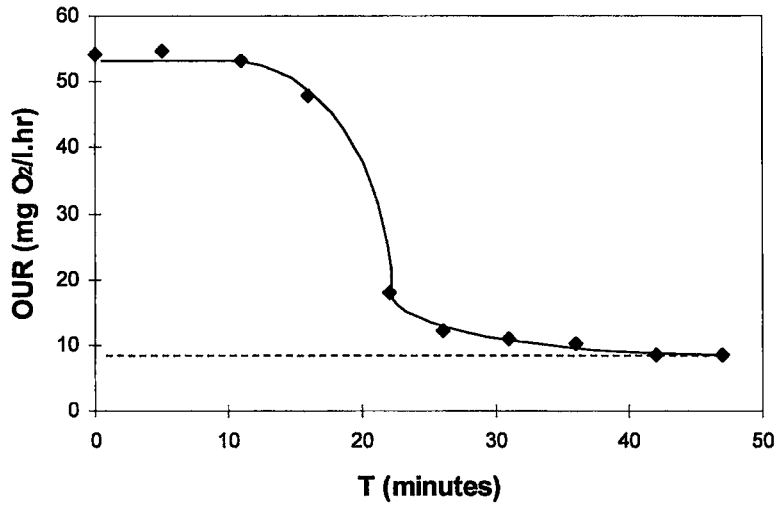

Figure A.1a OUR values versus time - b_H experiment - set 8 - initial day

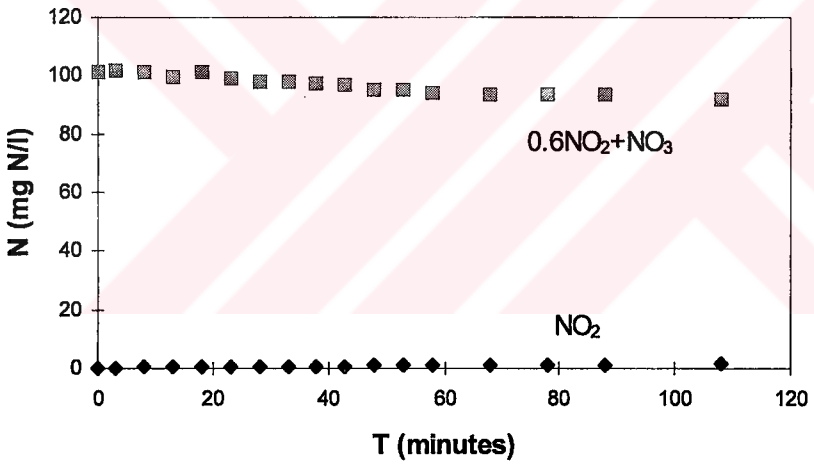

Figure A.1b $0.6NO_2$ –N+NO_3 –N and NO_2 –N concentrations versus time-b_{HD} experiment-set 8-initial day

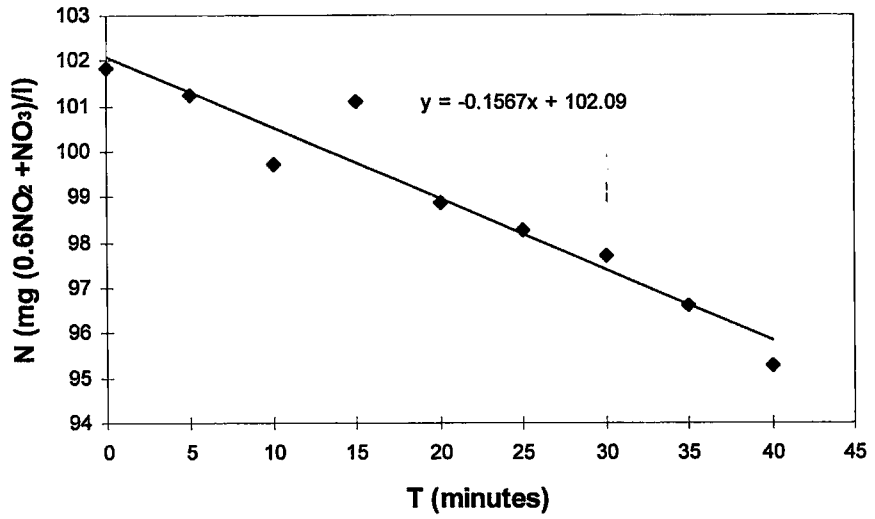

Figure A.1c Determination of nitrate utilization rate for the first phase - b_{HD} experiment - set 8 - initial day

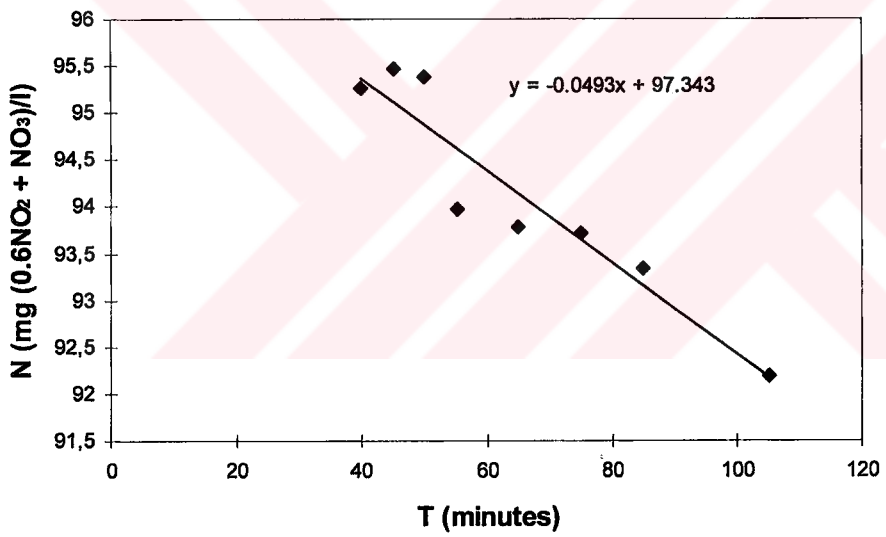

Figure A.1d Determination of nitrate utilization rate for the second phase – b_{HD} experiment – set 8 – initial day

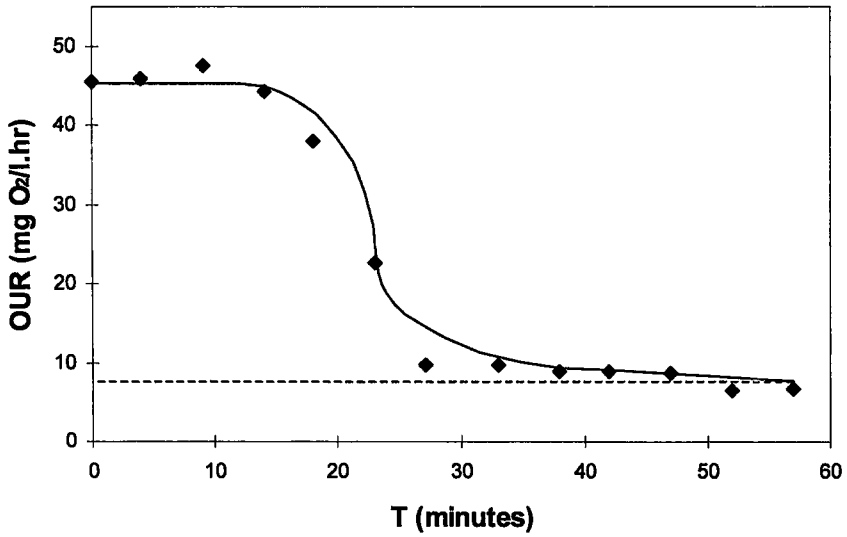

Figure A.2a OUR values versus time - b_H experiment - set 8 - day 1

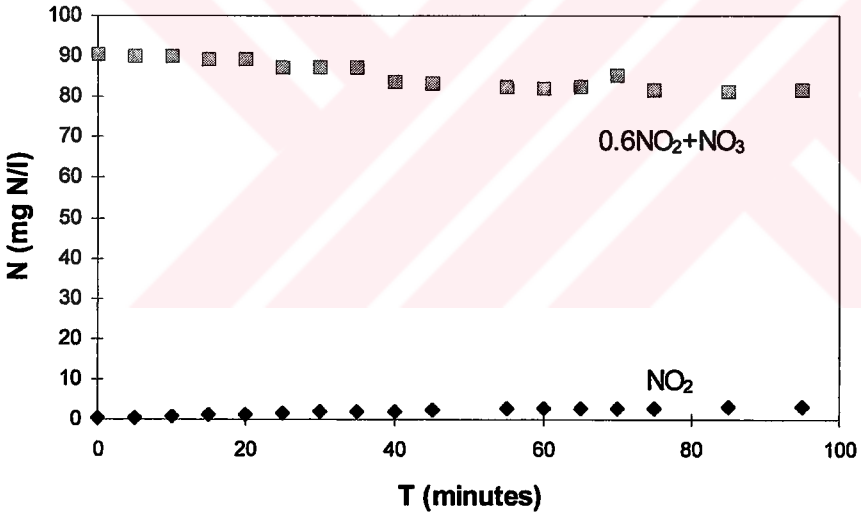

Figure A.2b $0.6NO_2$ –N+NO_3 –N and NO_2 –N concentrations versus time - b_{HD} experiment – set 8 - day 2

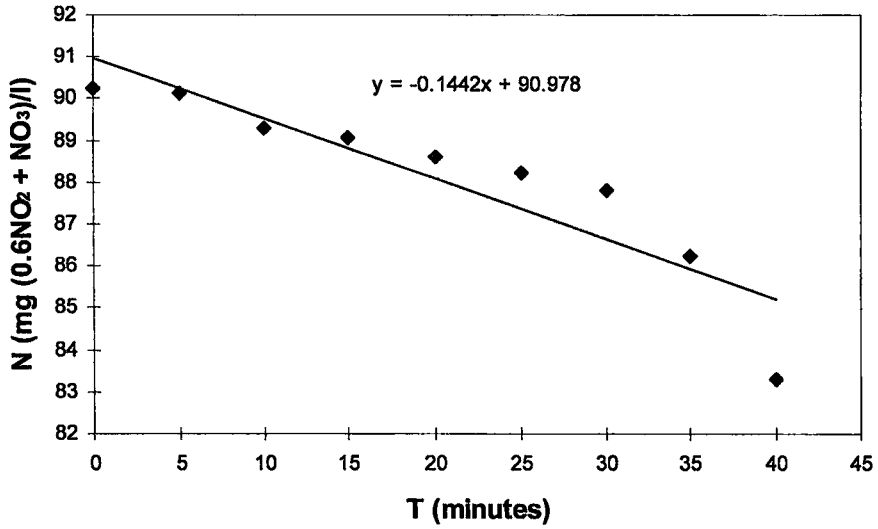

Figure A.2c Determination of nitrate utilization rate for the first phase - b_{HD} experiment - set 8 - day 2

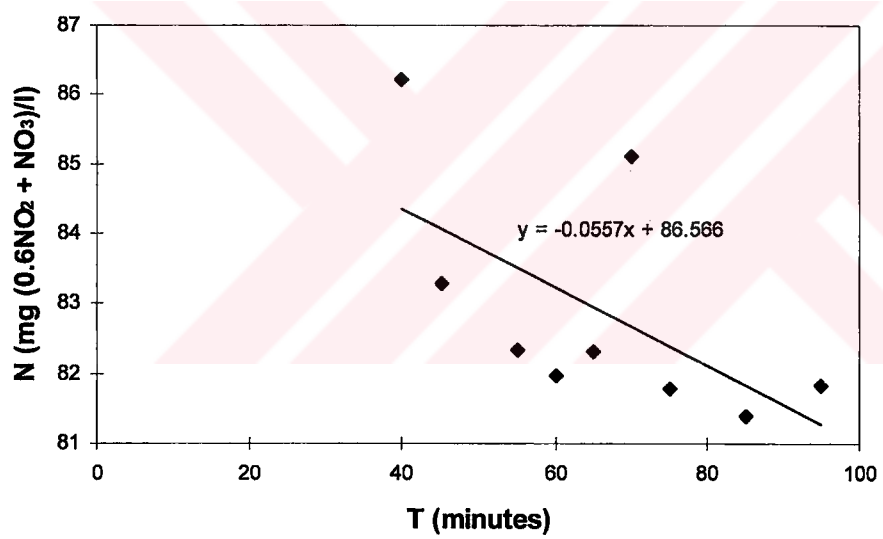

Figure A.2d Determination of nitrate utilization rate for the second phase - b_{HD} experiment - set 8 - day 2

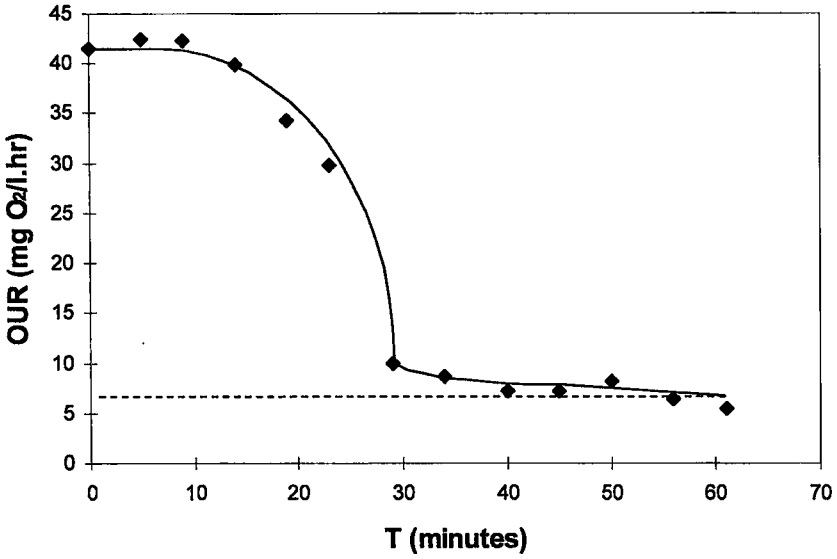

Figure A.3a OUR values versus time - b_H experiment - set 8 - day 2

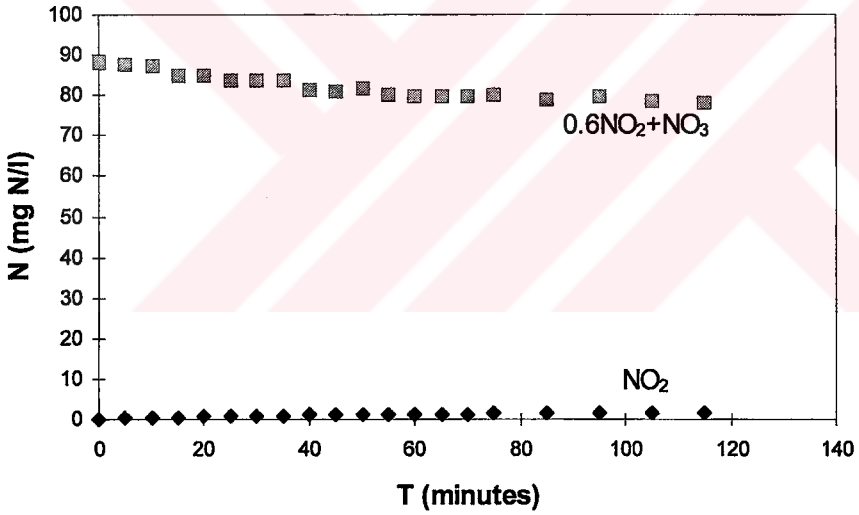

Figure A.3b $0.6NO_2$ –N+NO_3 –N and NO_2 –N concentrations versus time -b_{HD} experiment -set 8 -day 3

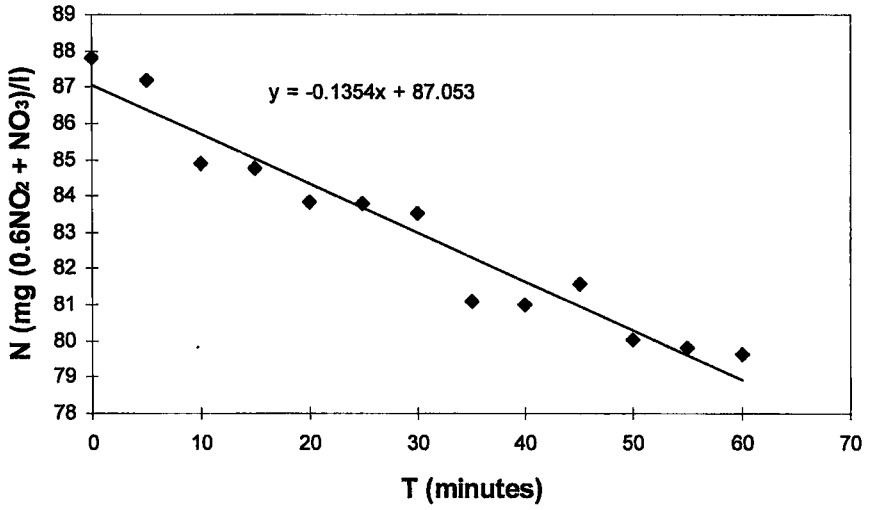

Figure A.3c Determination of nitrate utilization rate for the fist phase - b_{HD} experiment - set 8 - day 3

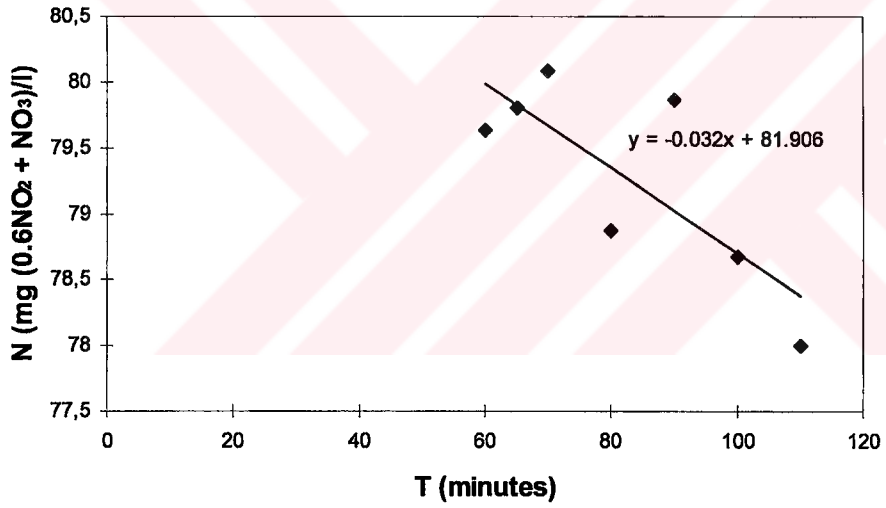

Figure A.3d Determination of nitrate utilization rate for the second phase - b_{HD} experiment - set 8 - day 3

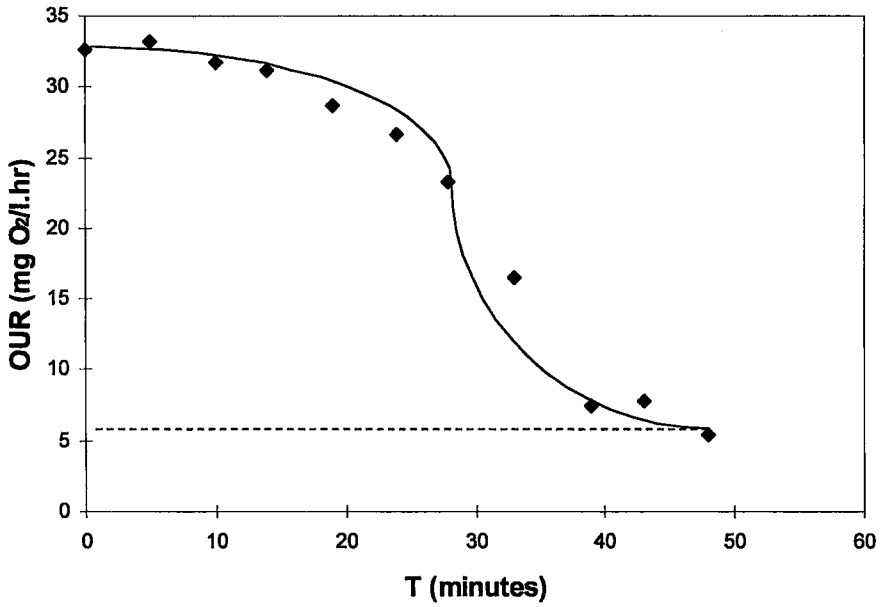

Figure A.4a OUR values versus time - b_H experiment - set 8 - day 3

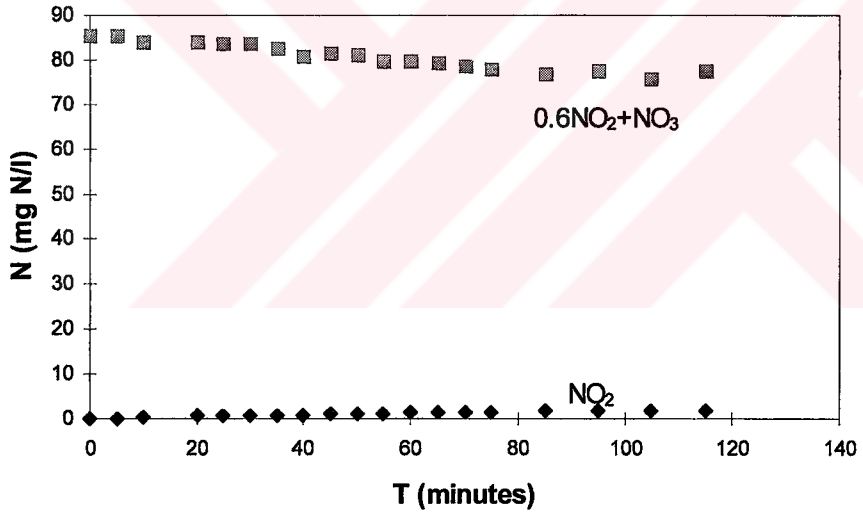

Figure A.4b $0.6NO_2$ –N+NO_3 –N and NO_2 –N concentrations versus time -b_{HD} experiment - set 8 -day 5

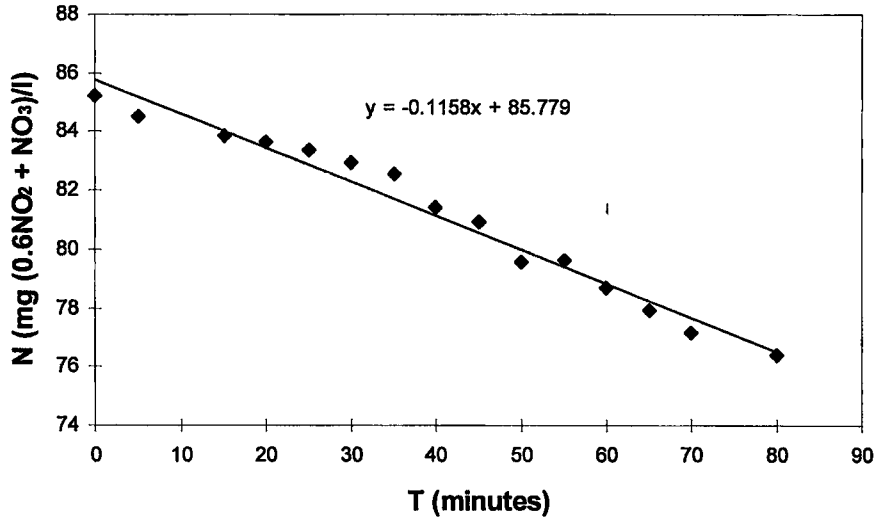

Figure A.4c Determination of nitrate utilization rate for the first phase - b_{HD} experiment - set 8 - day 5

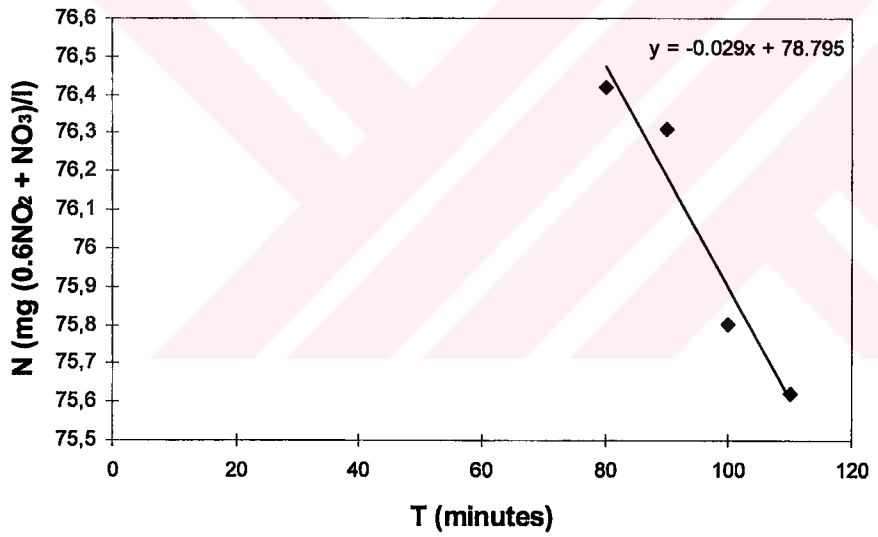

Figure A.4d Determination of nitrate utilization rate for the second phase - b_{HD} experiment - set 8 - day 5

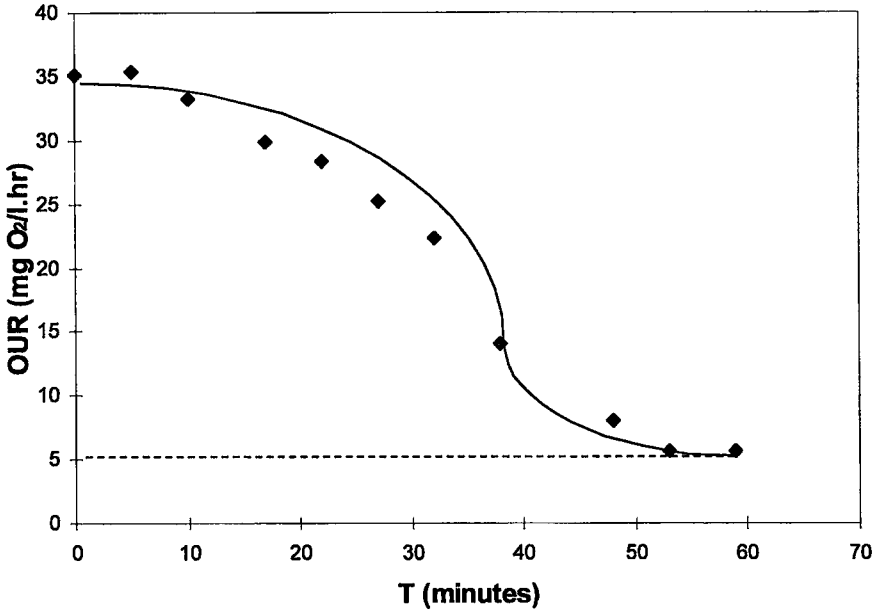

Figure A.5a OUR values versus time - b_H experiment - set 8 - day 4

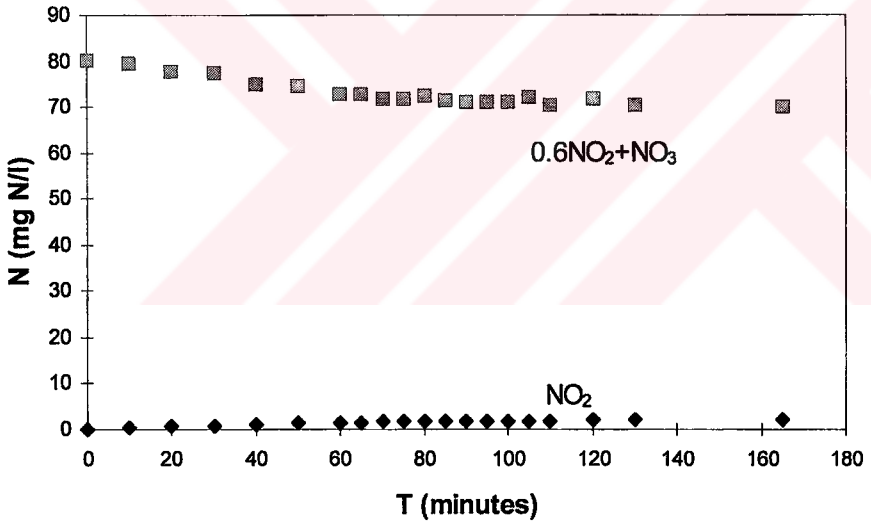

Figure A.5b $0.6NO_2$ –N+NO_3 –N and NO_2 –N concentrations versus time - b_{HD} experiment -set 8 -day 7

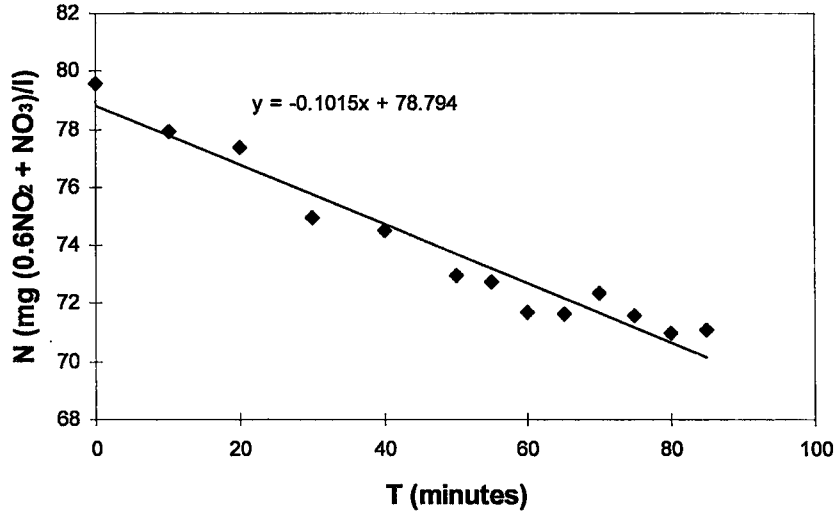

Figure A.5c Determination of nitrate utilization rate for the first phase - b_{HD} experiment - set 8 - day 7

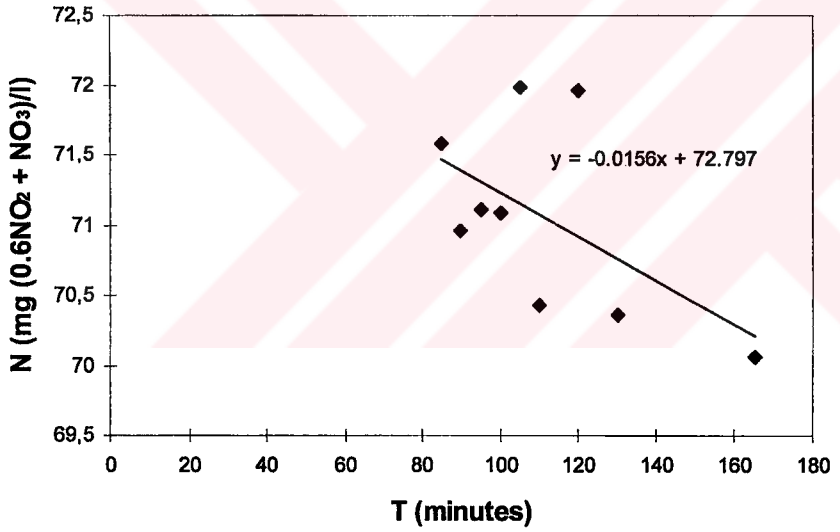

Figure A. 5d Determination of nitrate utilization rate for the second phase - b_{HD} experiment - set 8 - day 7

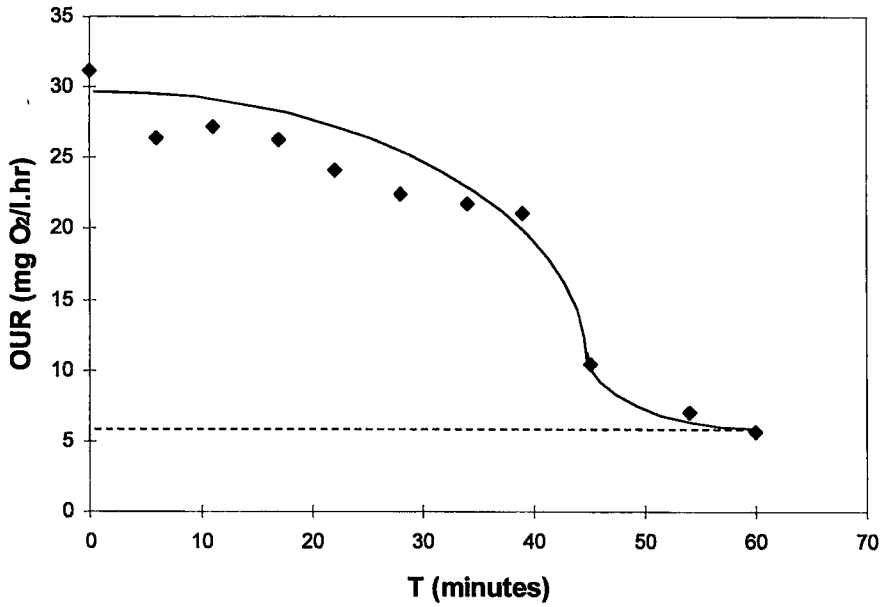

Figure A.6a OUR values versus time - b_H experiment -set 8 - day 5

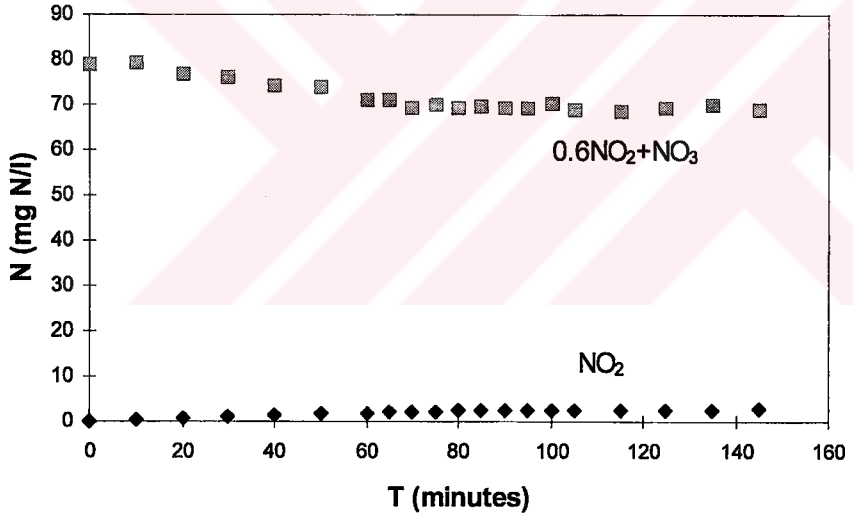

Figure A.6b 0.6 NO_2 -N +NO_3 -N and NO_2 -N concentrations versus time - b_{HD} experiment- set 8 -day 9

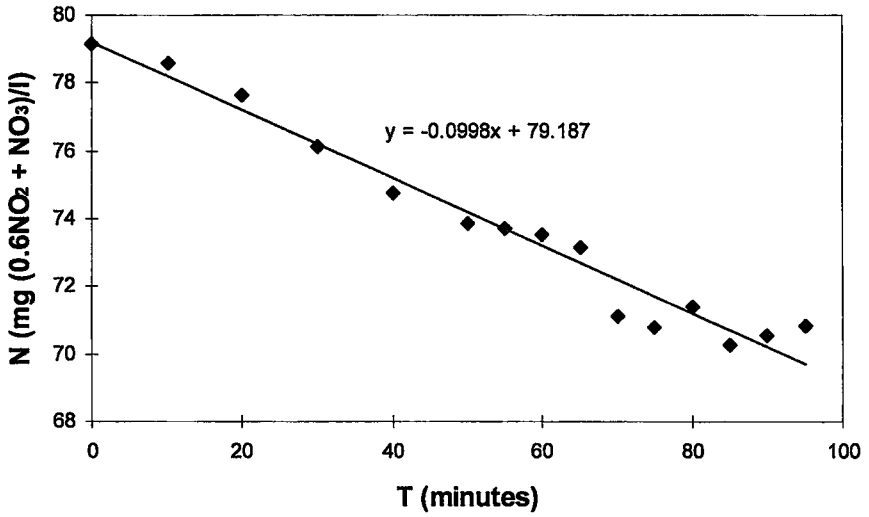

Figure A.6c Determination of nitrate utilization rate for the first phase - b_{HD} experiment - set 8 - day 9

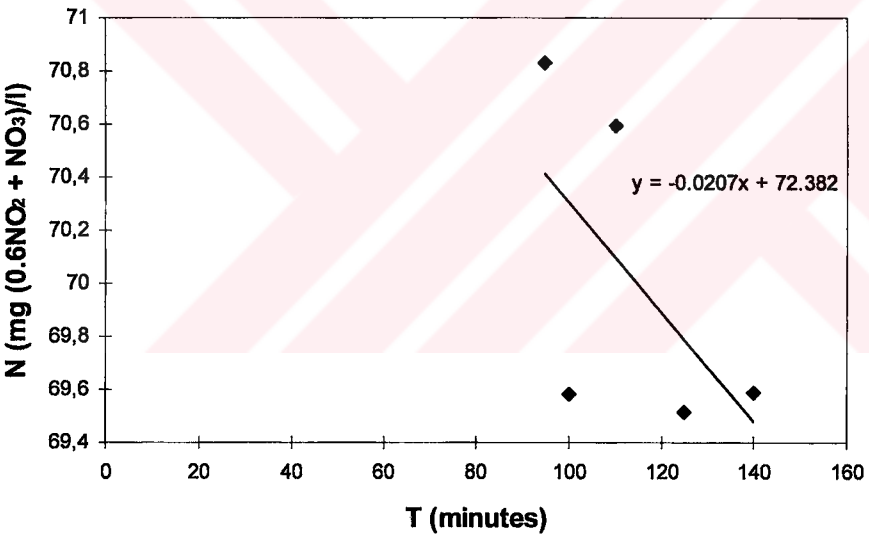

Figure A.6d Determination of nitrate utilization rate for the second phase - b_{HD} experiment - set 8 - day 9

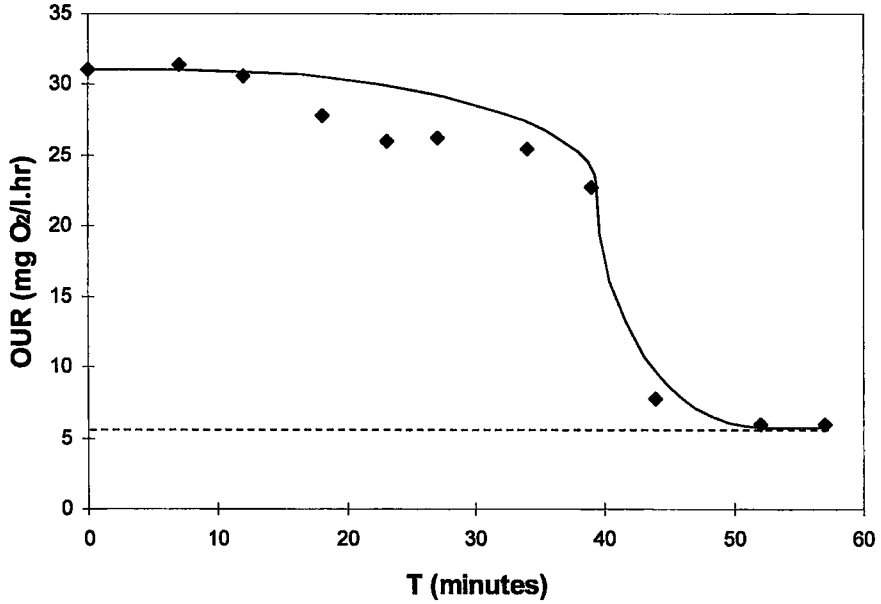

Figure A.7a OUR values versus time - b_H experiment - set 8 - day 6

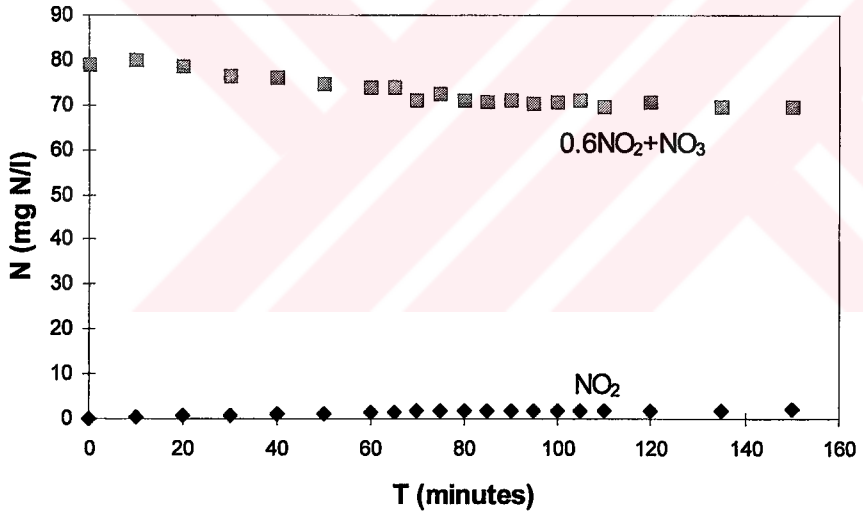

Figure A.7b 0.6 NO_2 -N +NO_3 -N and NO_2 -N concentrations versus time-b_{HD} experiment -set 8 -day 12

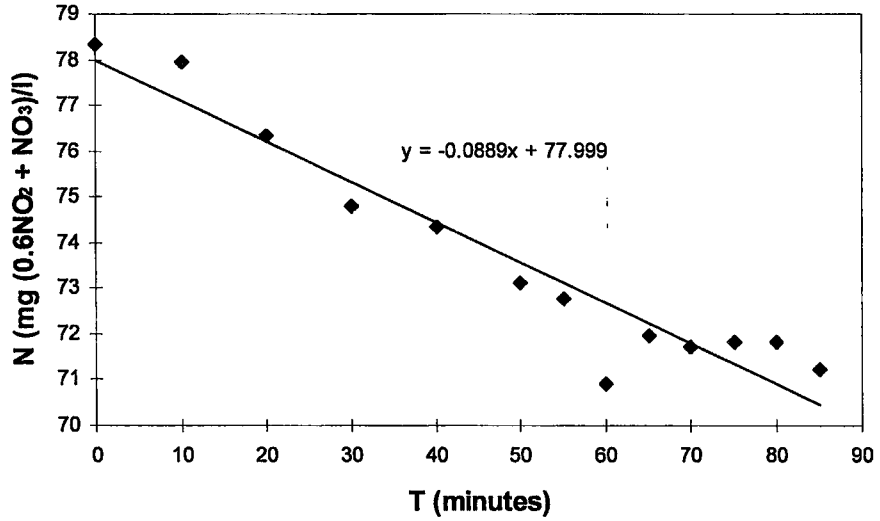

Figure A.7c Determination of nitrate utilization rate for the first phase - b_{HD} experiment - set 8 - day 12

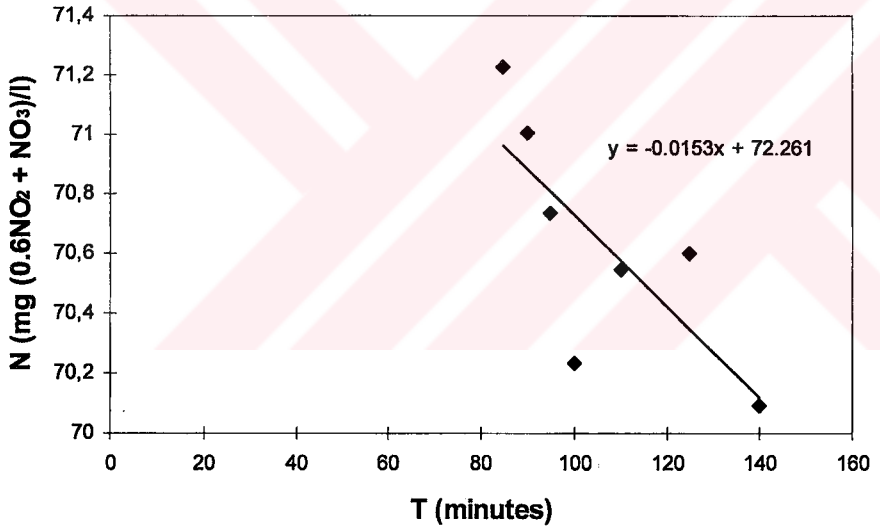

Figure A.7d Determination of nitrate utilization rate for the second phase - b_{HD} experiment - set 8 - day 12

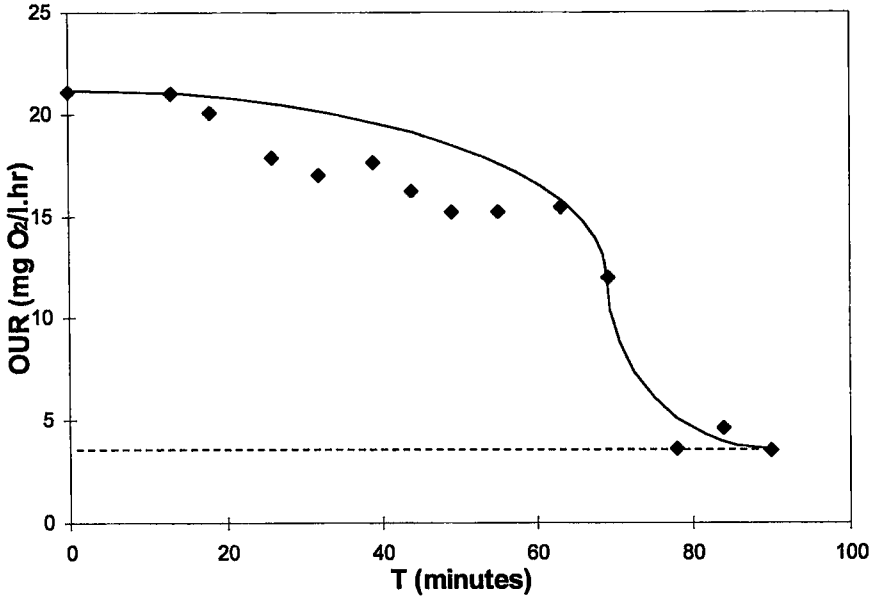

Figure A.8 OUR values versus time - b_H experiment – set 8 - day 8

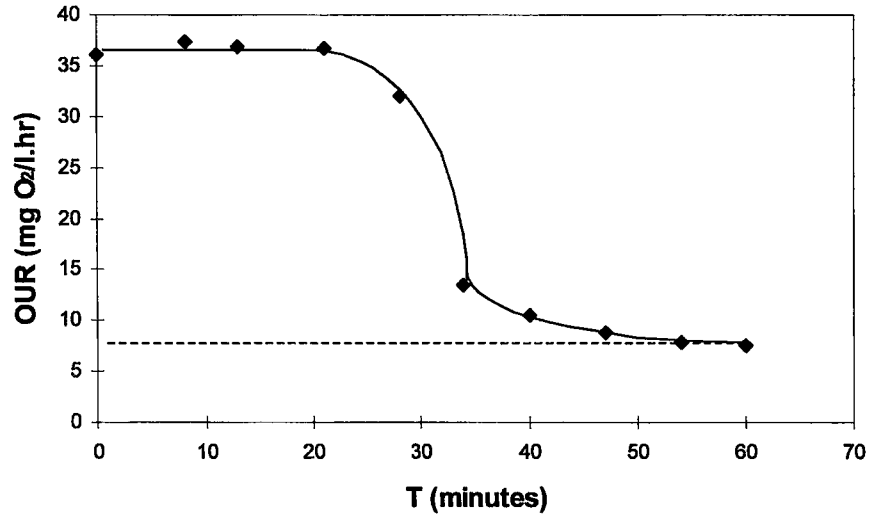

Figure A.9a OUR values versus time - b_H experiment - set 9 - initial day

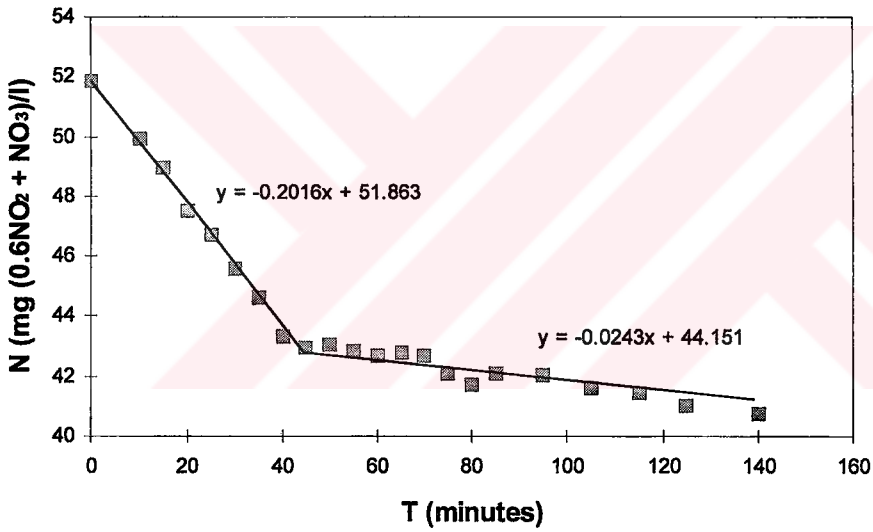

Figure A.9b $0.6NO_2^-$-N+NO_3^--N concentration versus time - b_{HD} experiment - set 9 - initial day

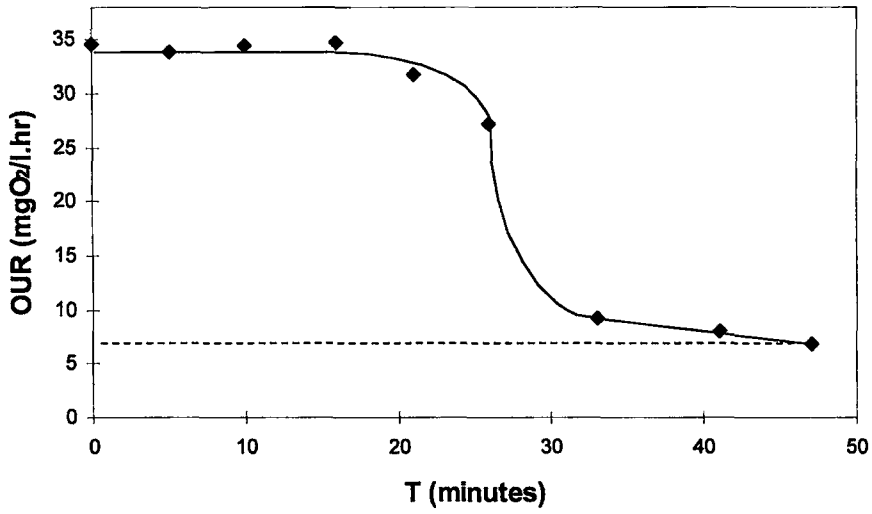

Figure A.10a OUR values versus time - b_H experiment - set 9 - day 1

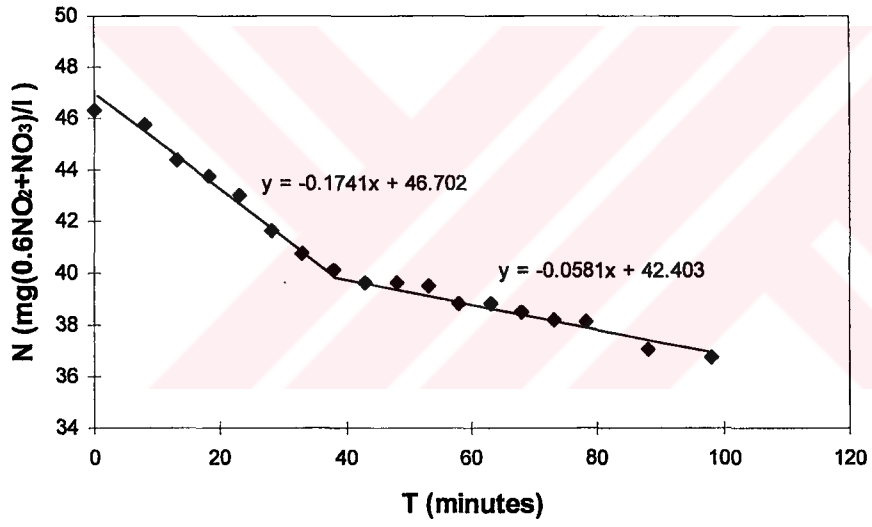

Figure A.10b $0.6NO_2^-$-N+NO_3^--N concentration versus time - b_{HD} experiment - set 9 - day 1

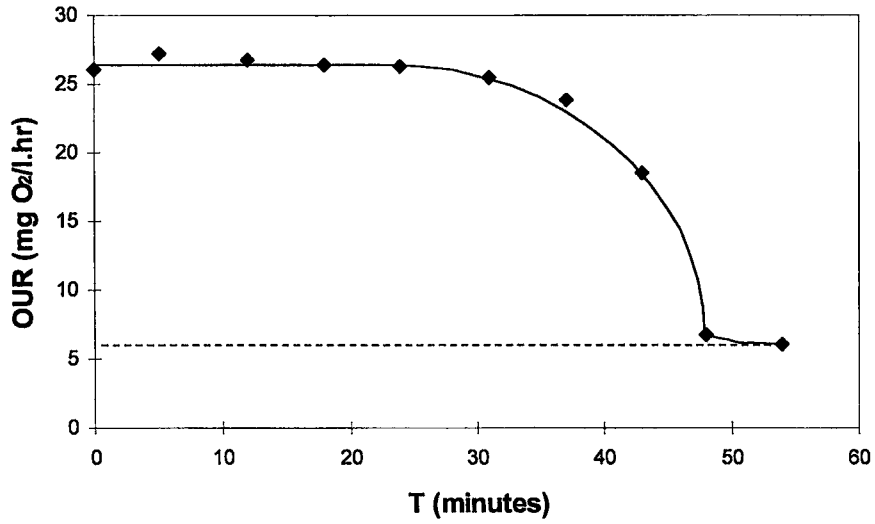

Figure A.11a OUR values versus time - b_H experiment - set 9 - day 2

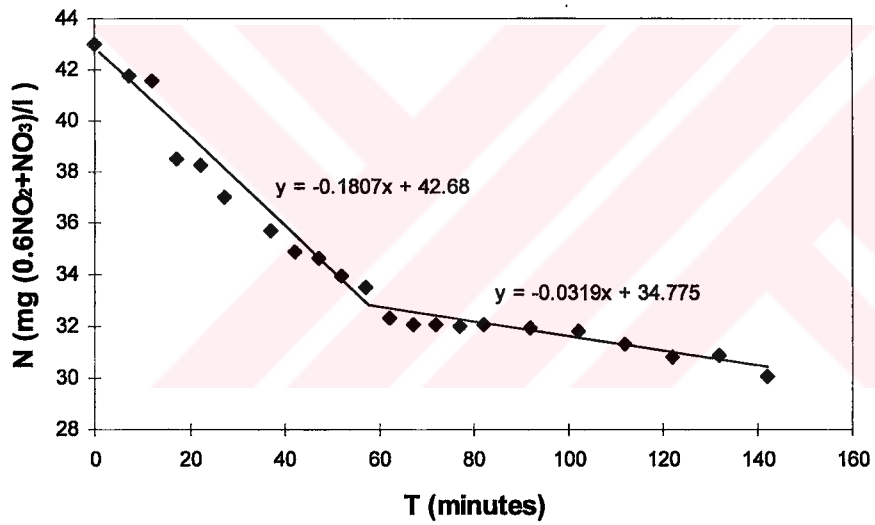

Figure A.11b $0.6NO_2^-$-N+NO_3^--N concentration versus time - b_{HD} experiment - set 9 - day 2

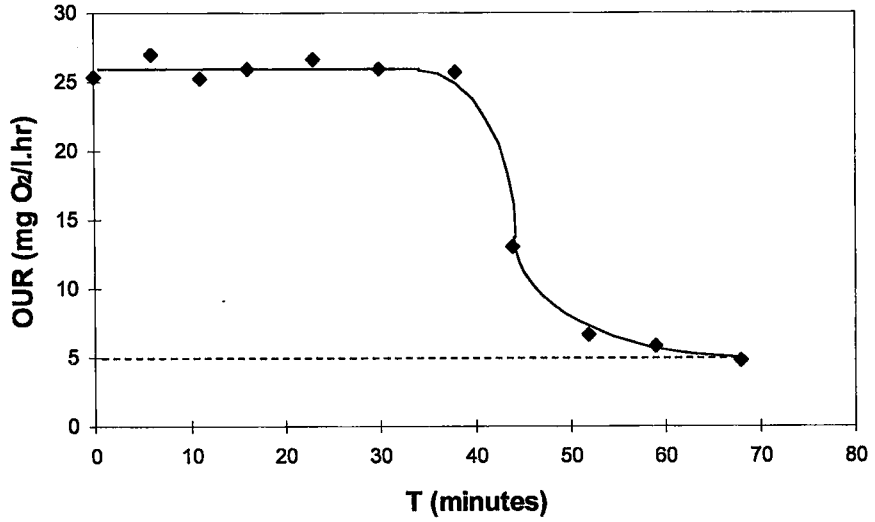

Figure A.12a OUR values versus time - b_H experiment - set 9 - day 3

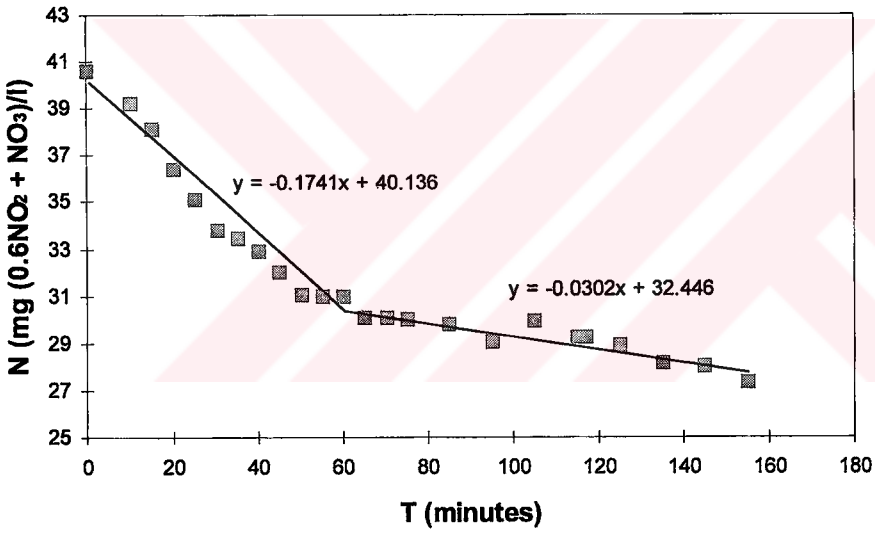

Figure A.12b $0.6NO_2^-$-N+NO_3^--N concentration versus time - b_{HD} experiment - set 9 - day 3

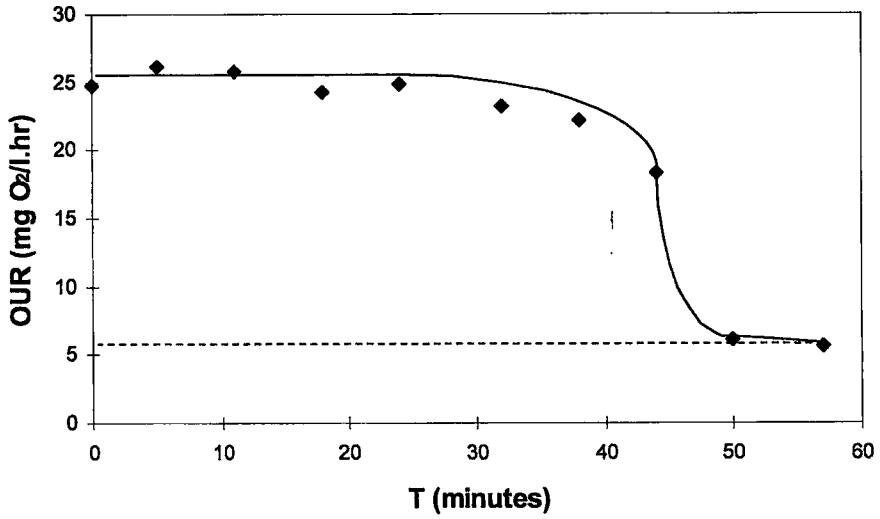

Figure A.13a OUR values versus time - b_H experiment - set 9 - day 4

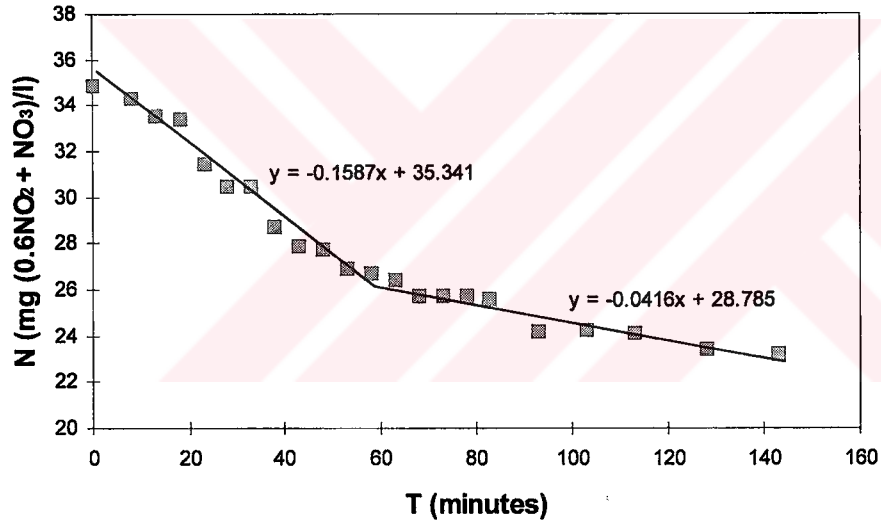

Figure A.13b $0.6NO_2^-$-N+NO_3^--N concentration versus time - b_{HD} experiment - set 9 - day 4

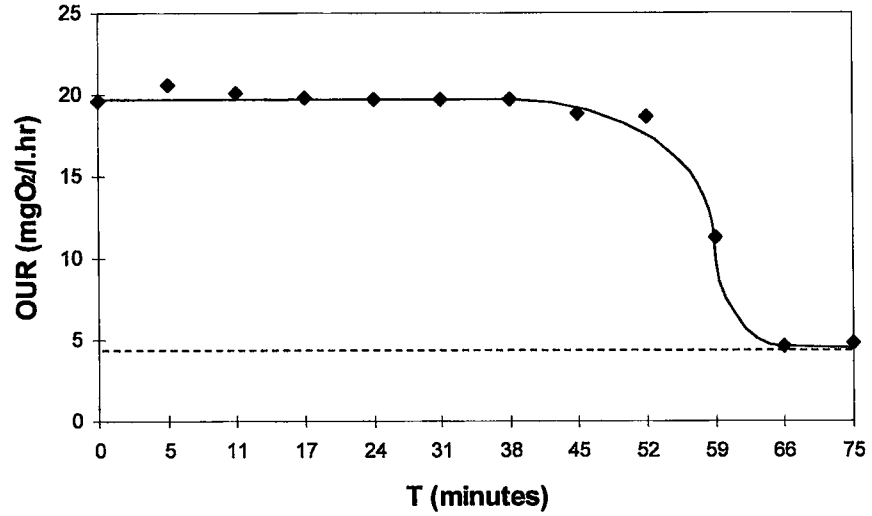

Figure A.14a OUR values versus time - b_H experiment - set 9 - day 6

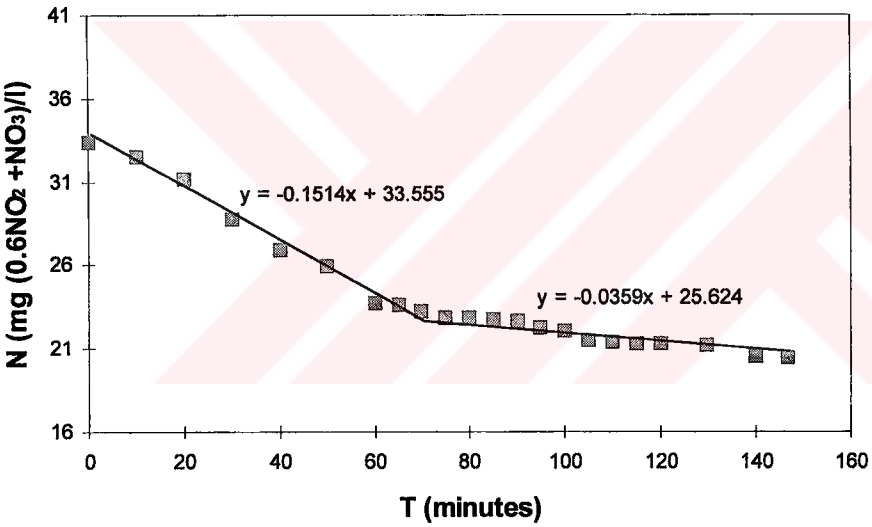

Figure A.14b $0.6NO_2^-$-N+NO_3^--N concentration versus time - b_{HD} experiment - set 9 - day 6

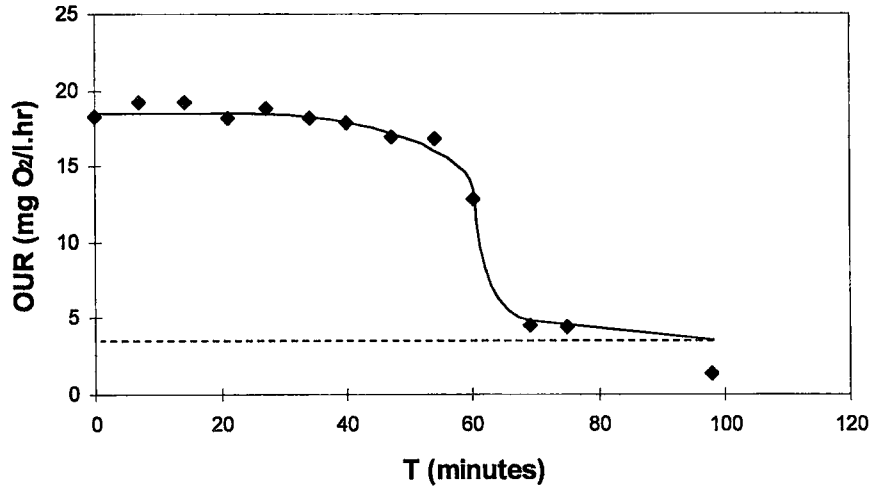

Figure A.15a OUR values versus time - b_H experiment - set 9 - day 7

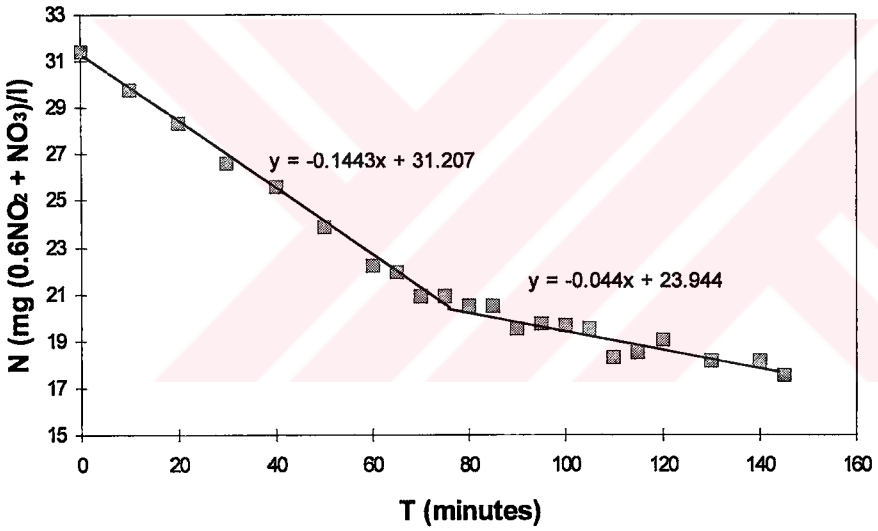

Figure A.15b $0.6NO_2^-$-N+NO_3^--N concentration versus time - b_{HD} experiment - set 9 - day 7

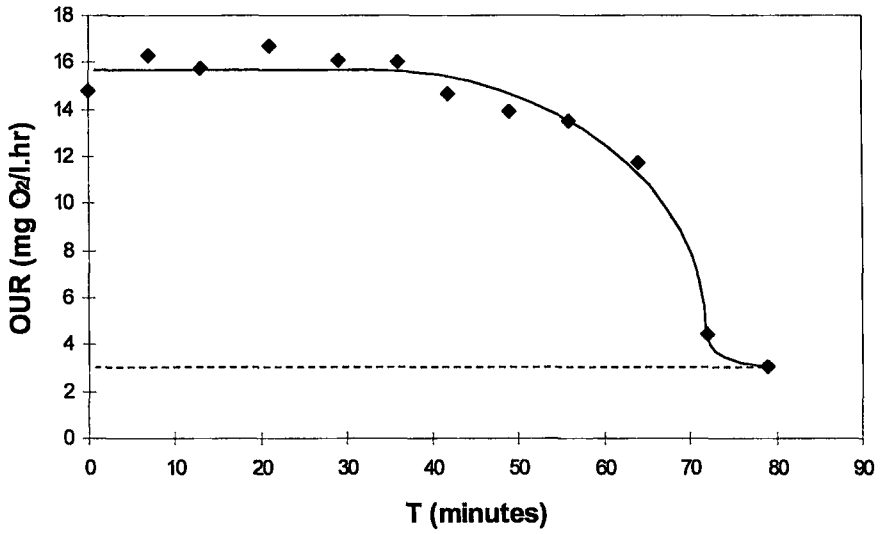

Figure A.16a OUR values versus time - b_H experiment - set 9 - day 8

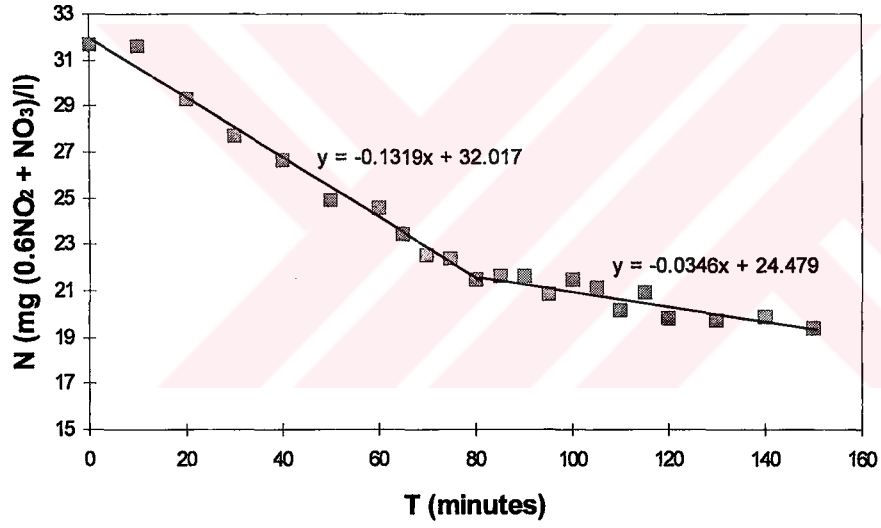

Figure A.16b $0.6NO_2^-$-N+NO_3^--N concentration versus time - b_{HD} experiment - set 9 - day 8

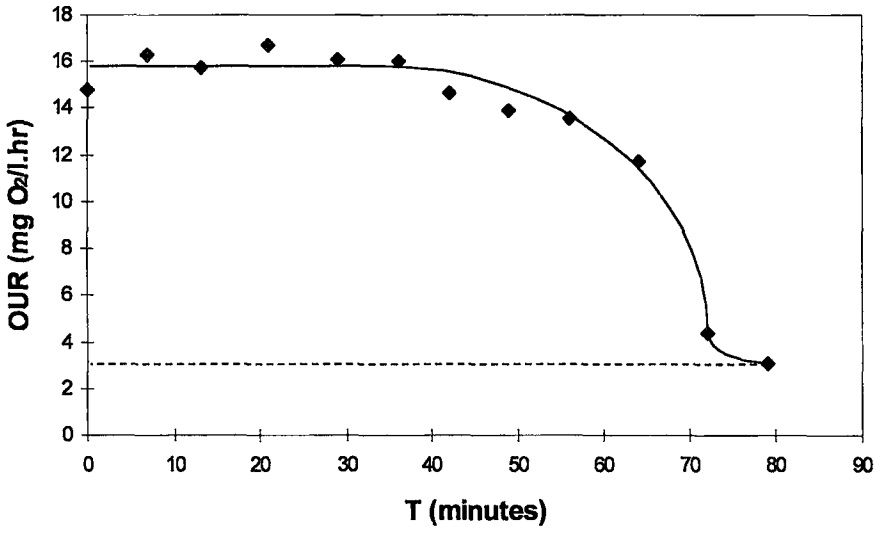

Figure A.17 OUR values versus time - b_H experiment - set 9 - day 9

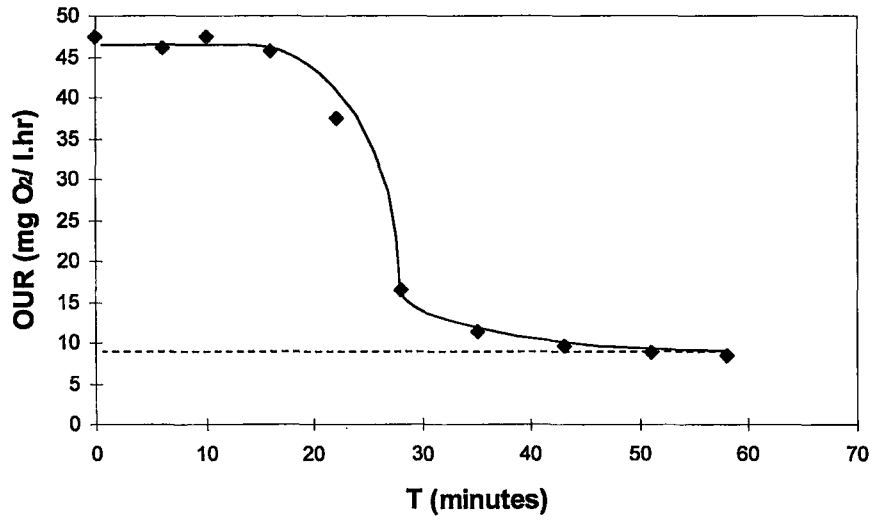

Figure A.18a OUR values versus time - b_H experiment - set 10 - initial day

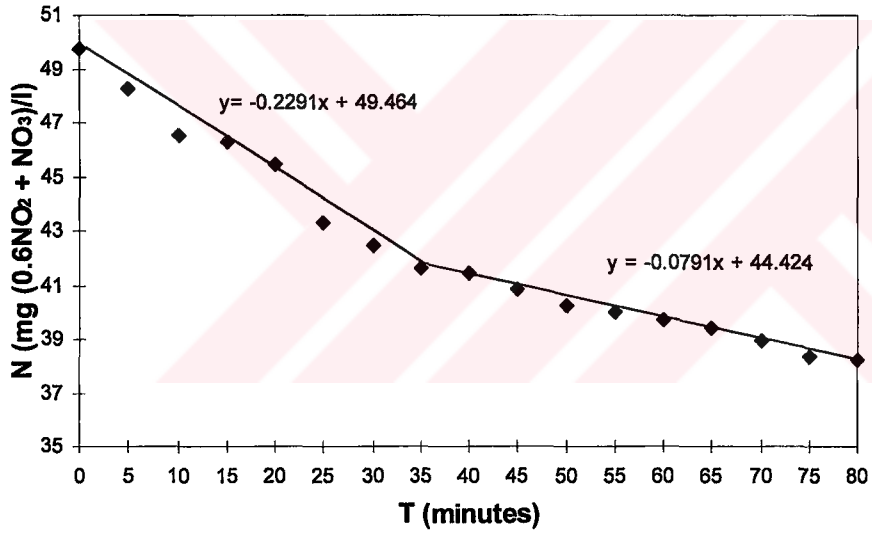

Figure A.18b $0.6NO_2^-$-N+NO_3^--N concentration versus time - b_{HD} experiment - set 10 - initial day

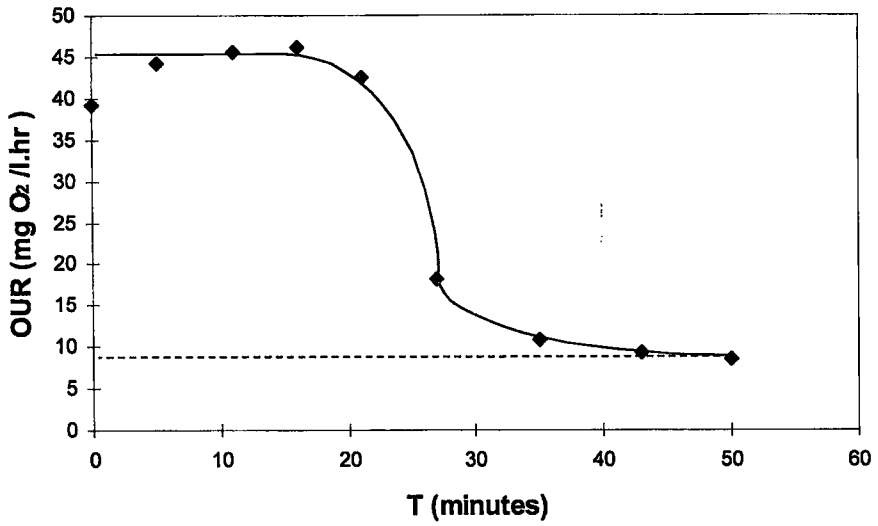

Figure A.19a OUR values versus time - b_H experiment - set 10 - day 1

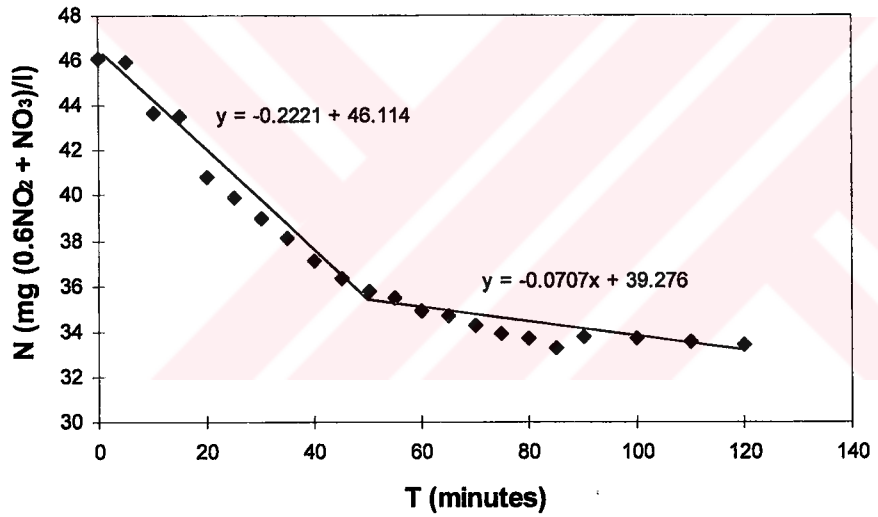

Figure A.19b $0.6NO_2^-$-N+NO_3^--N concentration versus time - b_{HD} experiment - set 10 - day 1

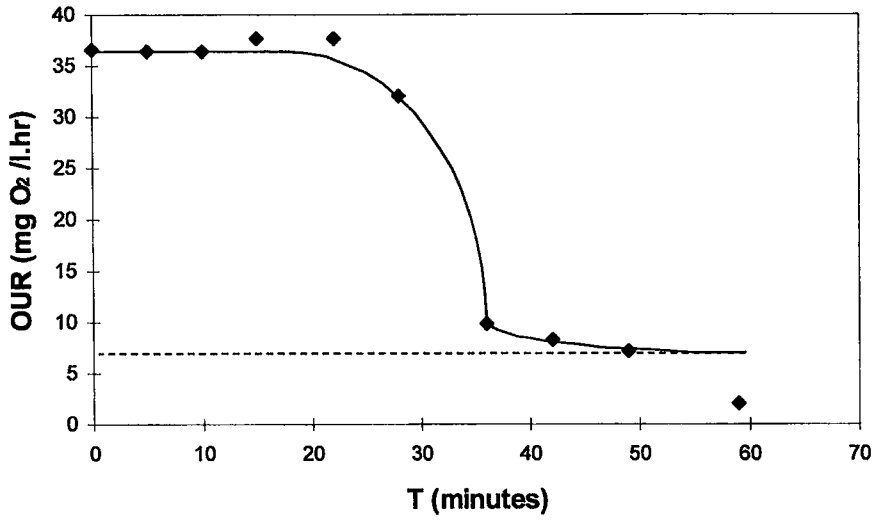

Figure A.20a OUR values versus time - b_H experiment - set 10 - day 2

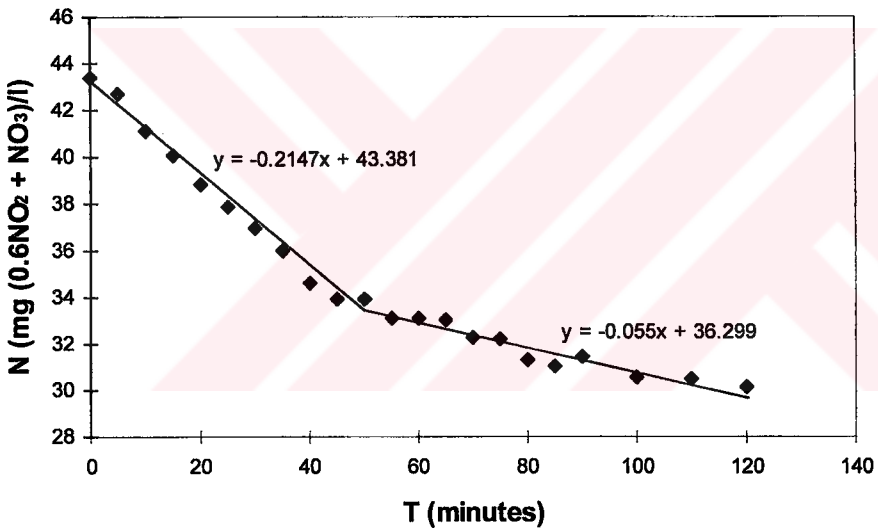

Figure A.20b $0.6NO_2^-$-N+NO_3^--N concentration versus time - b_{HD} experiment –set 10 - day 2

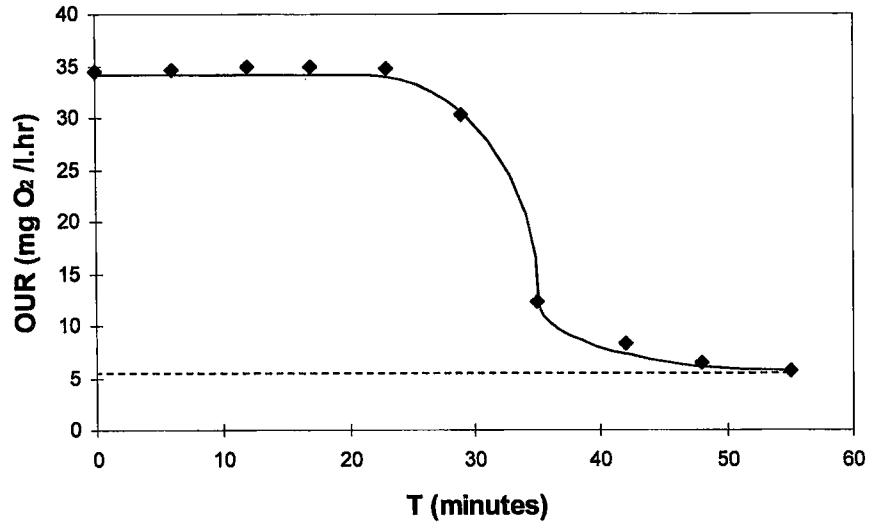

Figure A.21a OUR values versus time - b_H experiment-set 10- day 3

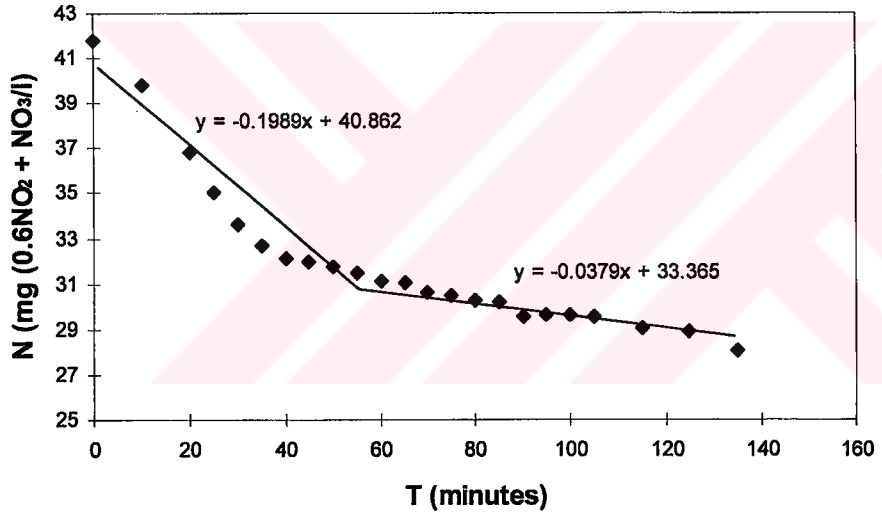

Figure A.21b $0.6NO_2^-$-N+NO_3^--N concentration versus time - b_{HD} experiment - set 10 - day 3

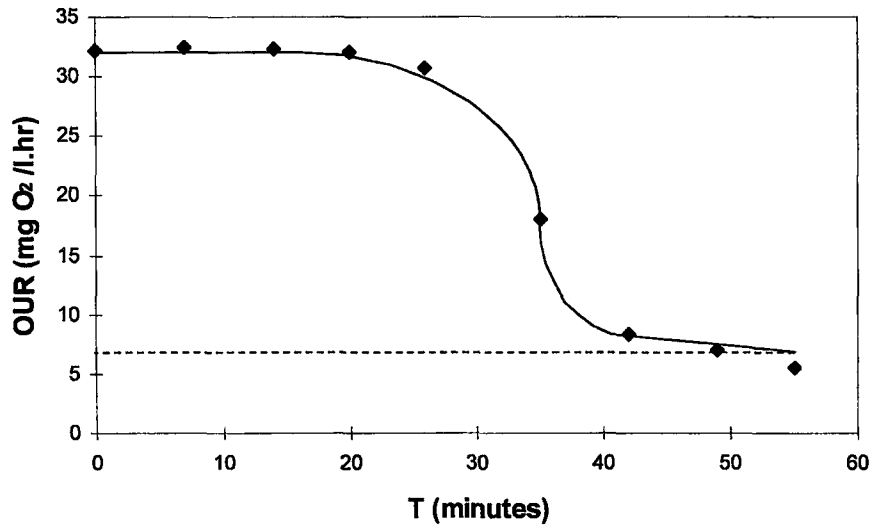

Figure A.22a OUR values versus time - b_H experiment - set 10 - day 5

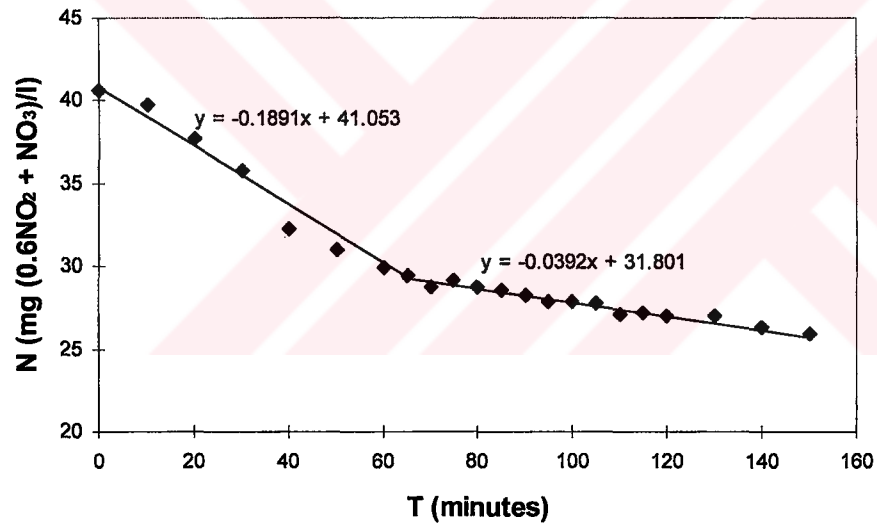

Figure A.22b $0.6NO_2^-$-N+NO_3^--N concentration versus time - b_{HD} experiment - set 10 - day 5

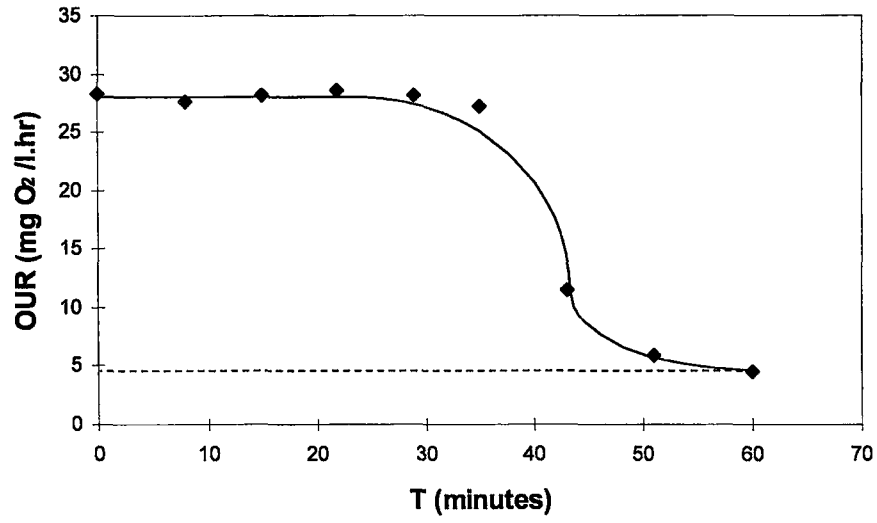

Figure A.23a OUR values versus time - b_H experiment - set 10 - day 6

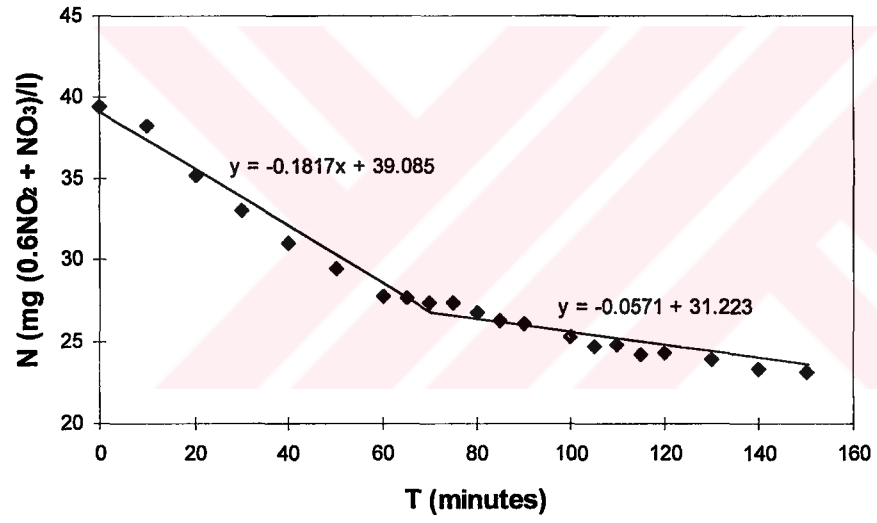

Figure A.23b $0.6NO_2^-$-N+NO_3^--N concentration versus time - b_{HD} experiment - set 10 - day 6

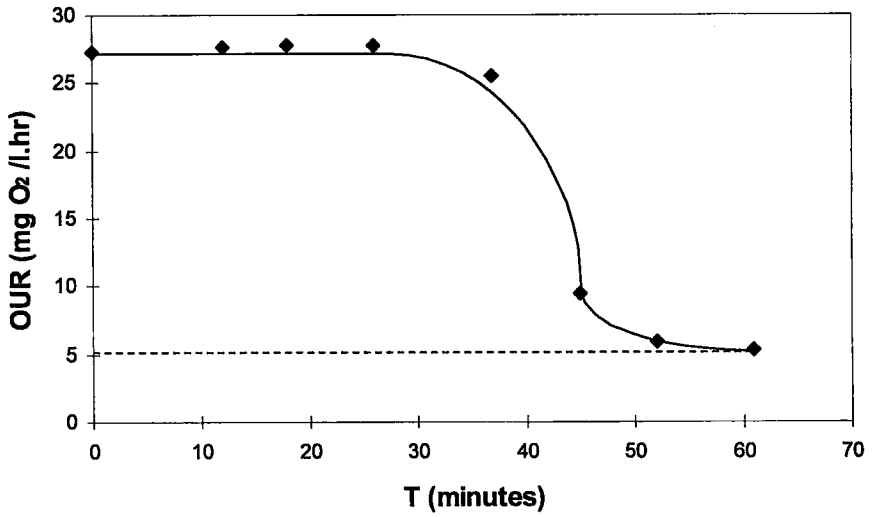

Figure A.24a OUR values versus time - b_H experiment - set 10 - day 7

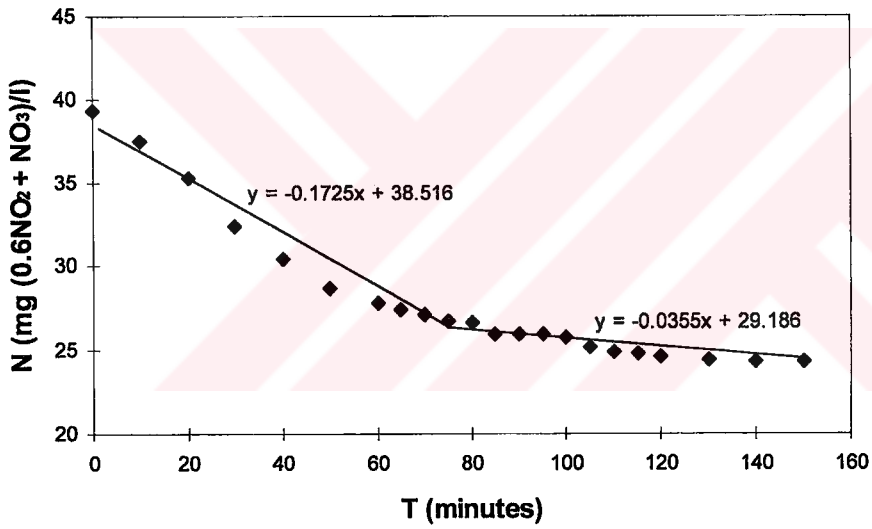

Figure A.24b $0.6NO_2^-$-N+NO_3^--N concentration versus time - b_{HD} experiment - set 10 - day 7

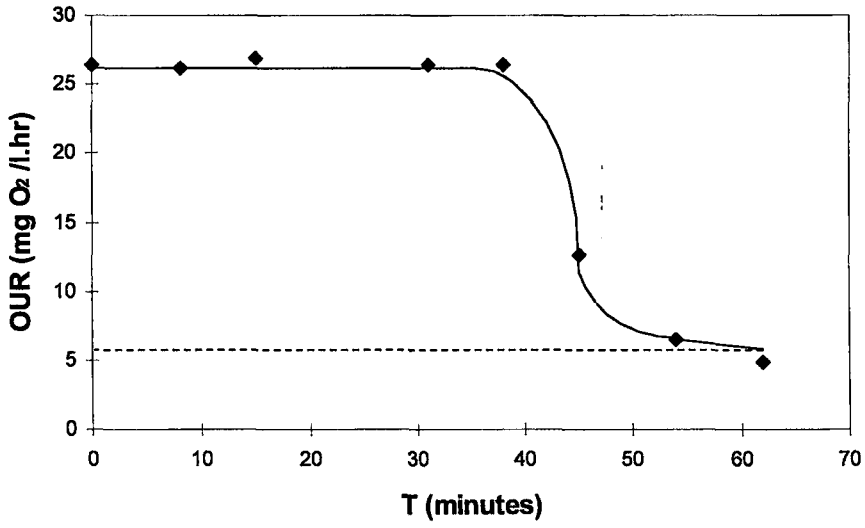

Figure A.25a OUR values versus time - b_H experiment - set 10 - day 8

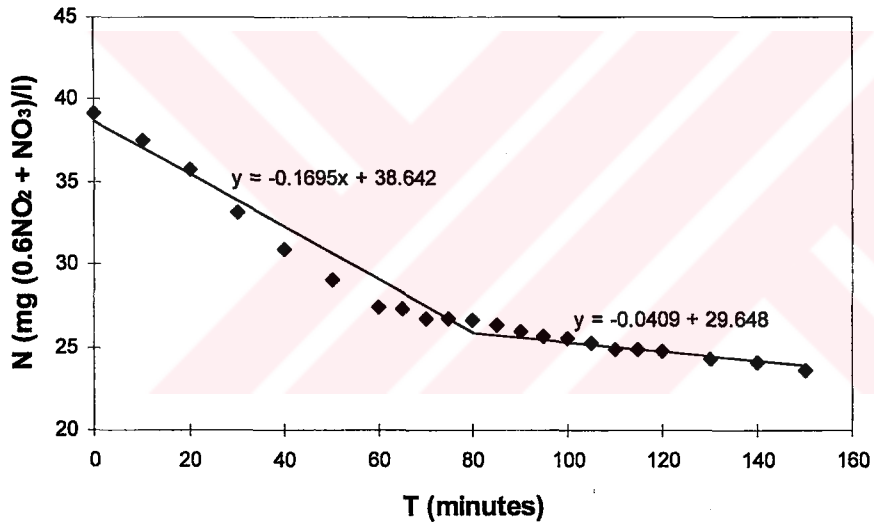

Figure A.25b $0.6NO_2^-$-N+NO_3^--N concentration versus time - b_{HD} experiment - set 10 - day 8

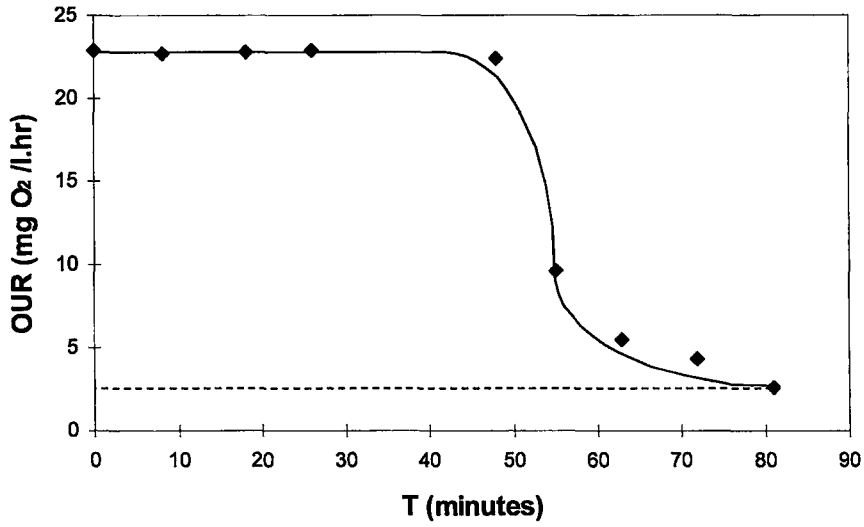

Figure A.26a OUR values versus time - b_H experiment - set 10 - day 9

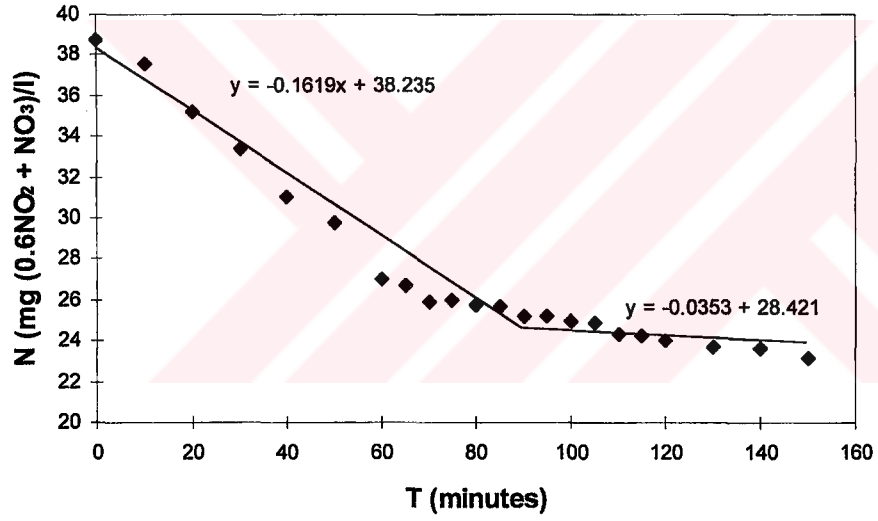

Figure A.26b $0.6NO_2^-$-N+NO_3^--N concentration versus time - b_{HD} experiment - set 10 - day 9

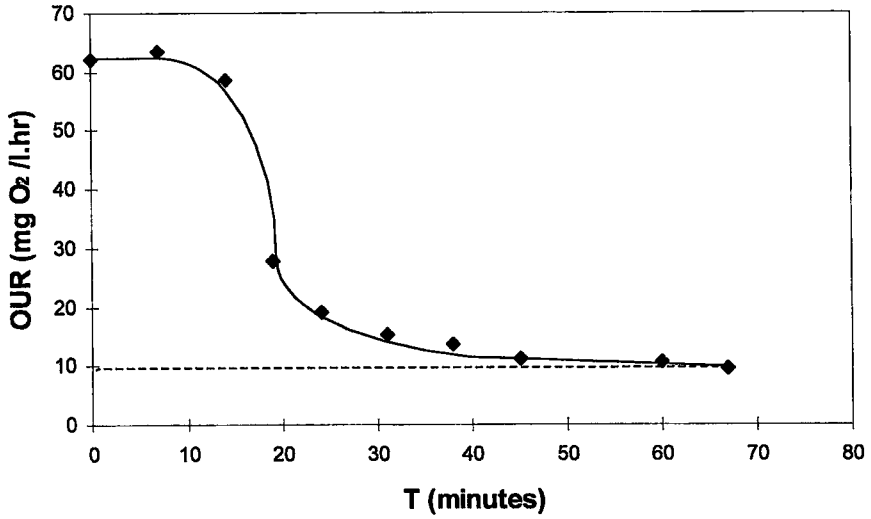

Figure A.27a OUR values versus time - b_H experiment - set 11 - initial day

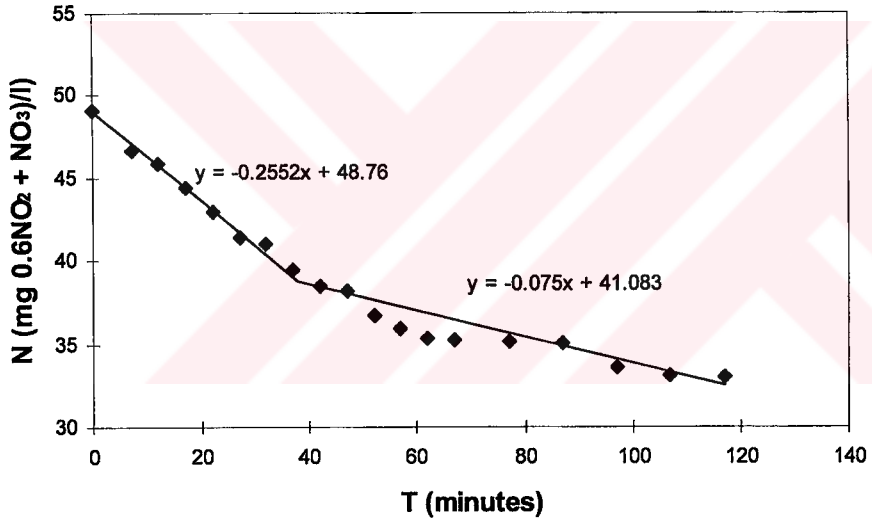

Figure A.27b $0.6NO_2^-$-N+NO_3^--N concentration versus time - b_{HD} experiment -set 11 -initial day

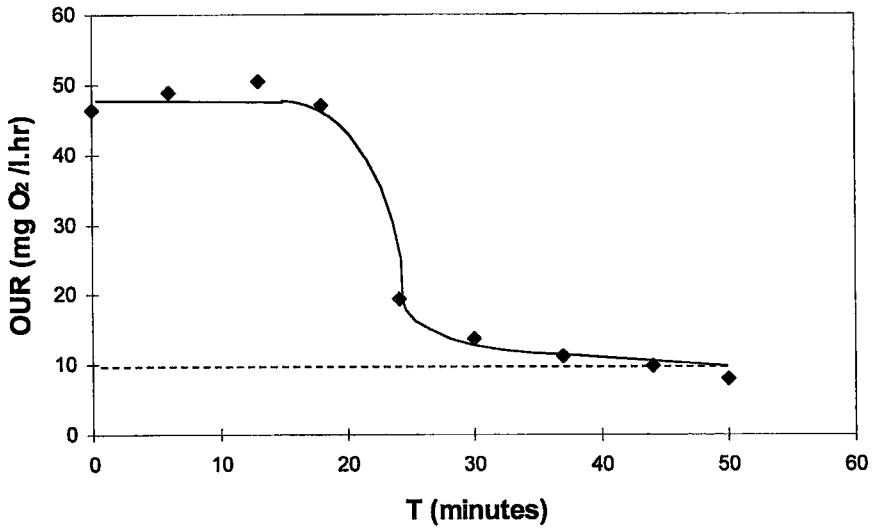

Figure A.28a OUR values versus time - b_H experiment - set 11 - day 1

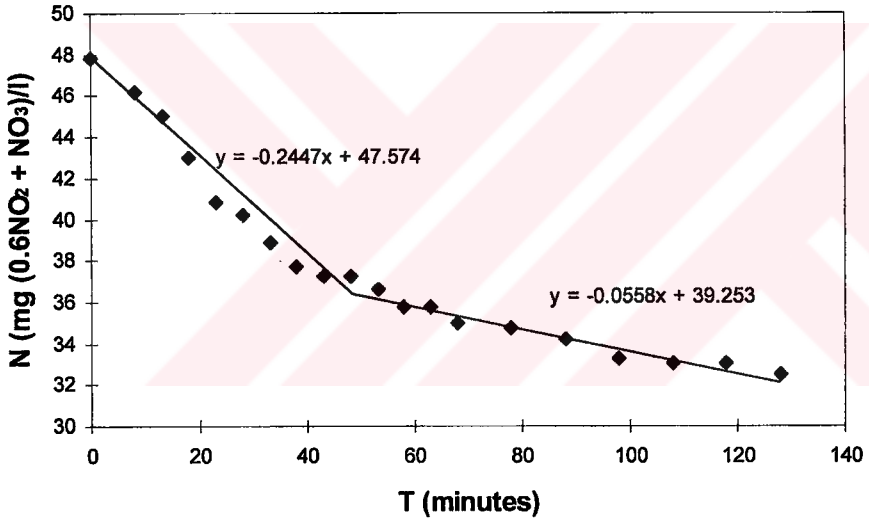

Figure A.28b $0.6NO_2^-$-N+NO_3^--N concentration versus time - b_{HD} experiment - set 11 - day 1

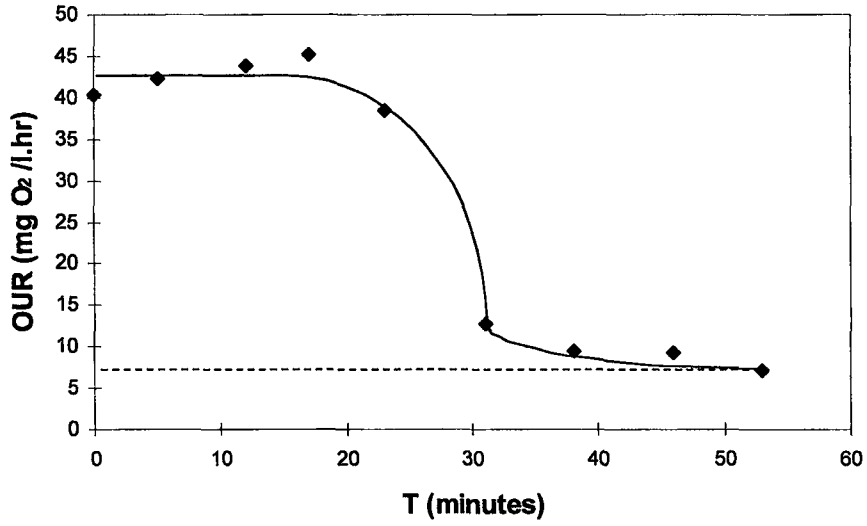

Figure A.29a OUR values versus time - b_H experiment - set 11 - day 2

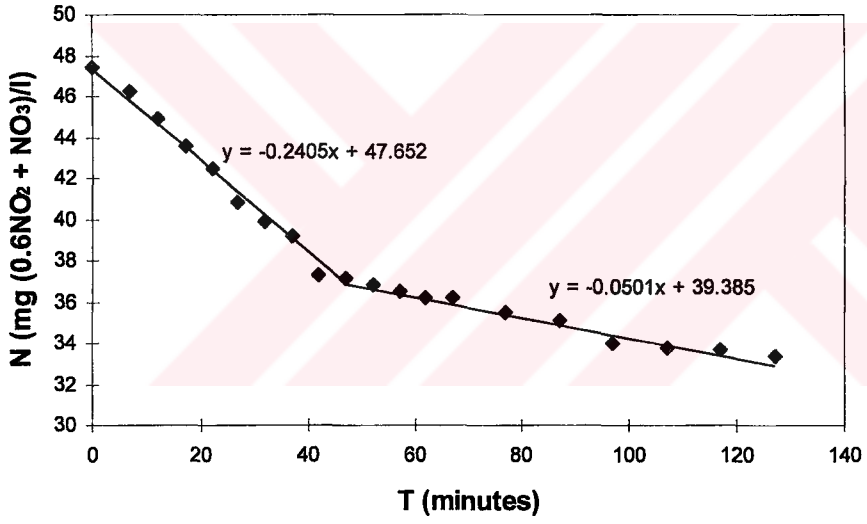

Figure A.29b $0.6NO_2^-$-N+NO_3^--N concentration versus time - b_{HD} experiment - set 11 - day 2

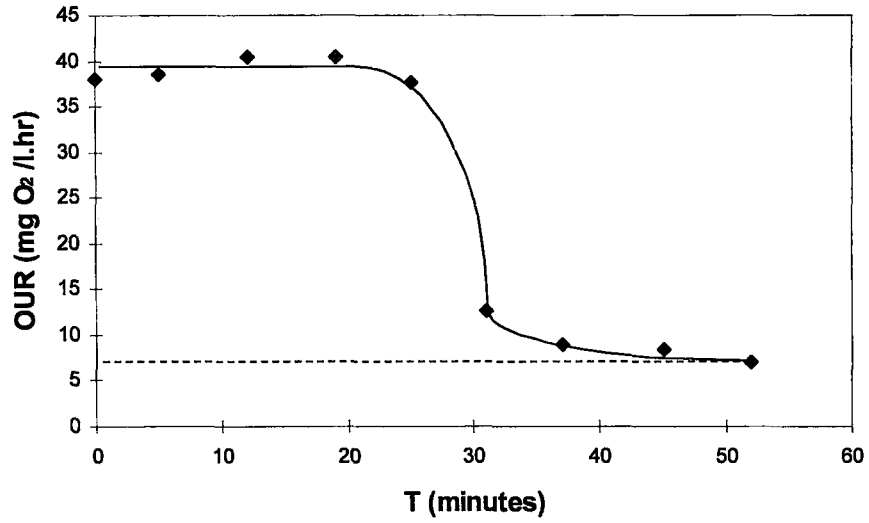

Figure A.30a OUR values versus time - b_H experiment - set 11 - day 3

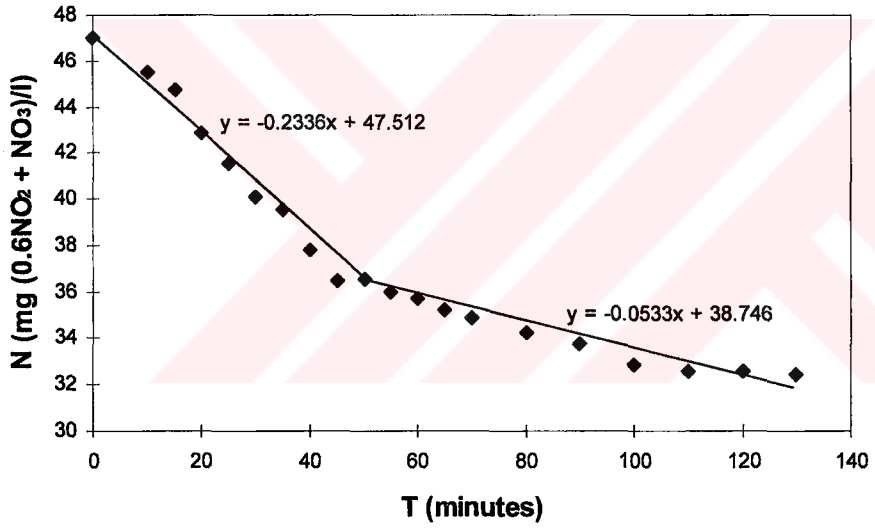

Figure A.30b $0.6NO_2^-$-N+NO_3^--N concentration versus time - b_{HD} experiment - set 11 - day 3

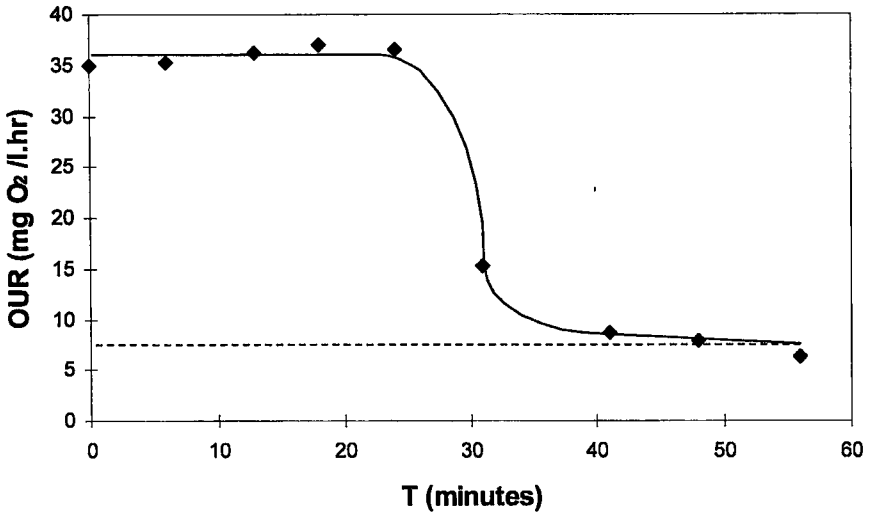

Figure A.31a OUR values versus time - b_H experiment - set 11- day 4

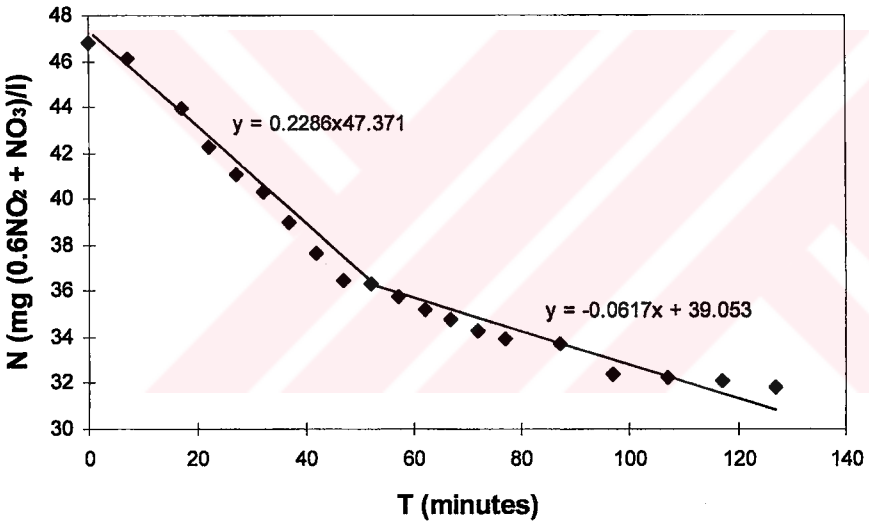

Figure A.31b $0.6NO_2^-$-N+NO_3^--N concentration versus time - b_{HD} experiment - set 11 - day 4

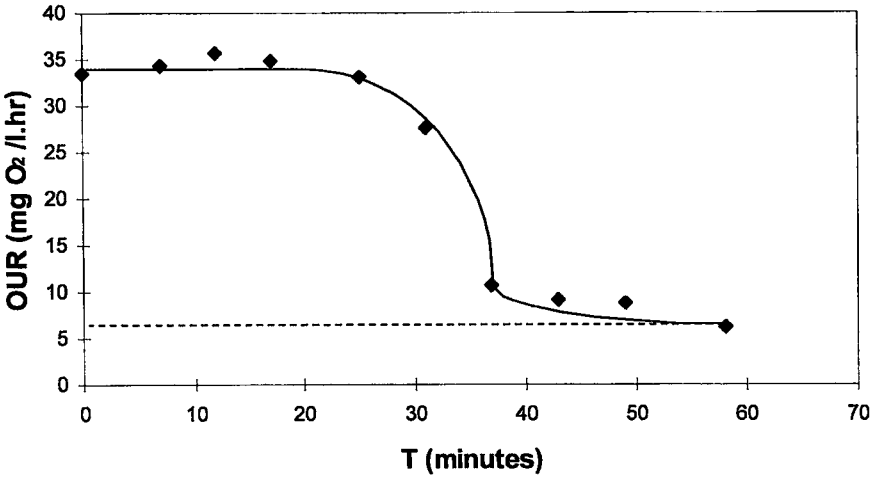

Figure A.32a OUR values versus time - b_H experiment - set 11- day 6

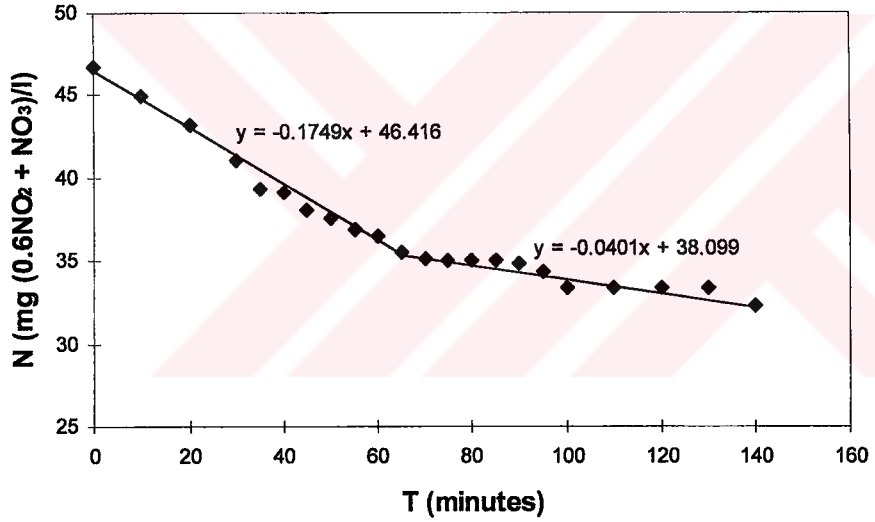

Figure A.32b $0.6NO_2^-$-N+NO_3^--N concentration versus time - b_{HD} experiment - set 11 - day 6

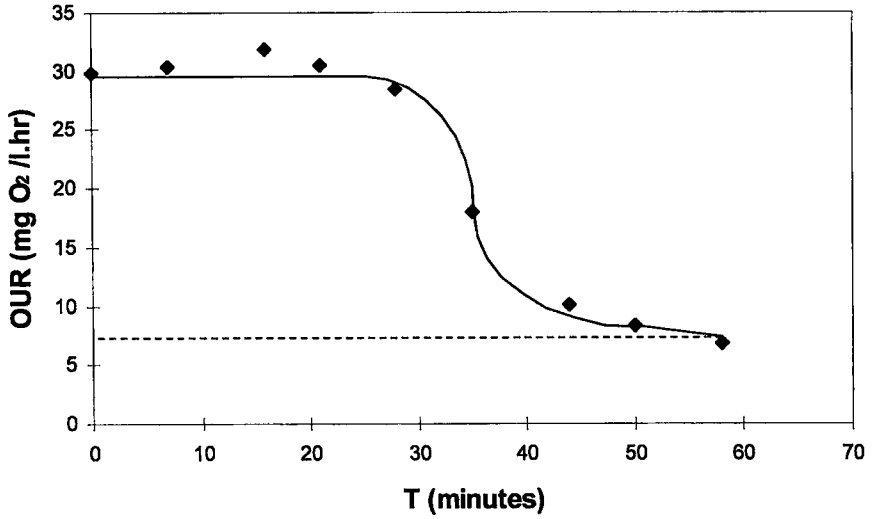

Figure A.33a OUR values versus time - b_H experiment - set 11 - day 7

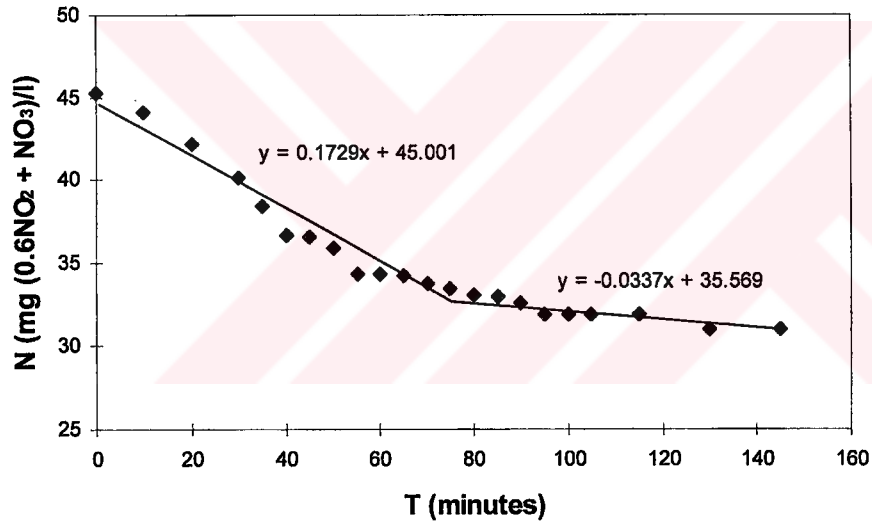

Figure A.33b $0.6NO_2^-$-N+NO_3^--N concentration versus time - b_{HD} experiment - set 11 - day 7

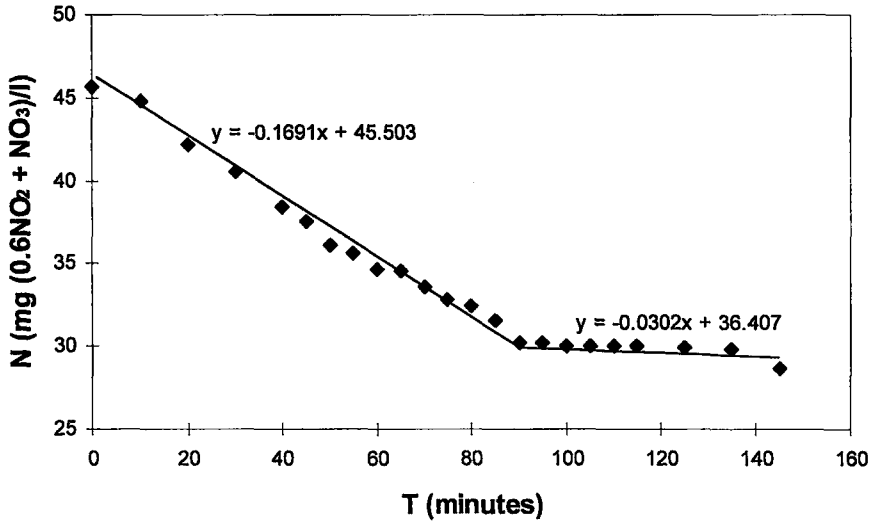

Figure A.34 Nitrate utilization rate versus time - b_{HD} experiment - set 11 - day 8

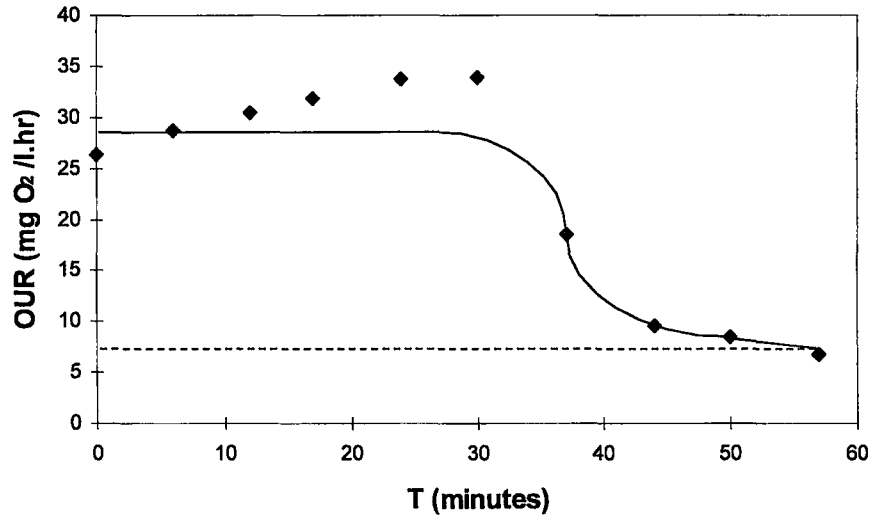

Figure A.35a OUR values versus time - b_H experiment - set 11 - day 9

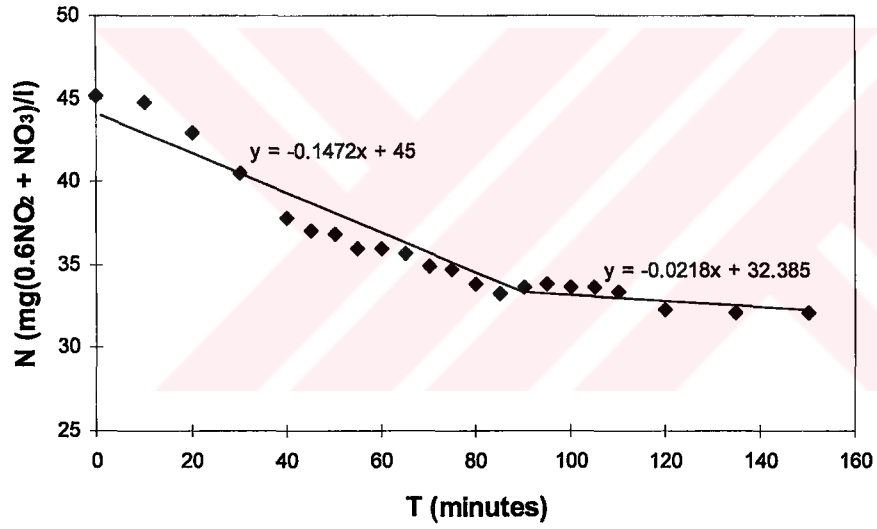

Figure A.35b $0.6NO_2^-$-N+NO_3^--N concentration versus time - b_{HD} experiment - set 11 - day 9

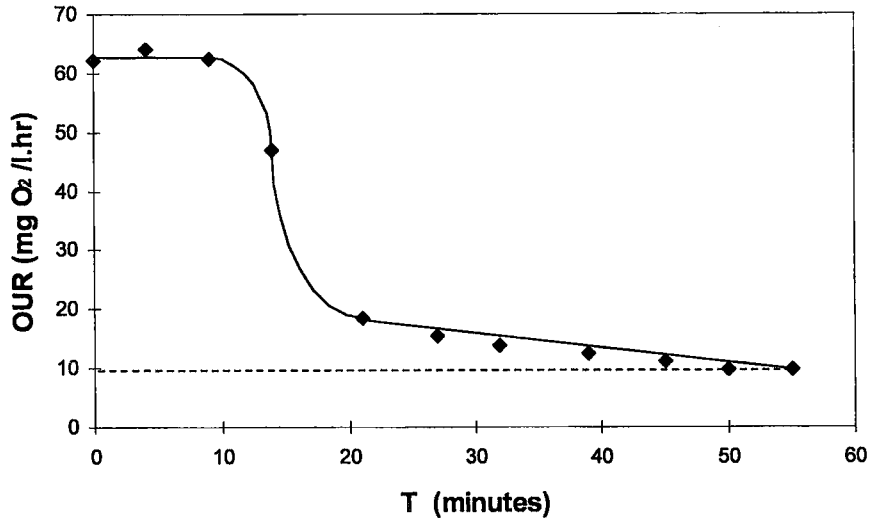

Figure A.36a OUR values versus time - b_H experiment - set 12 - initial day

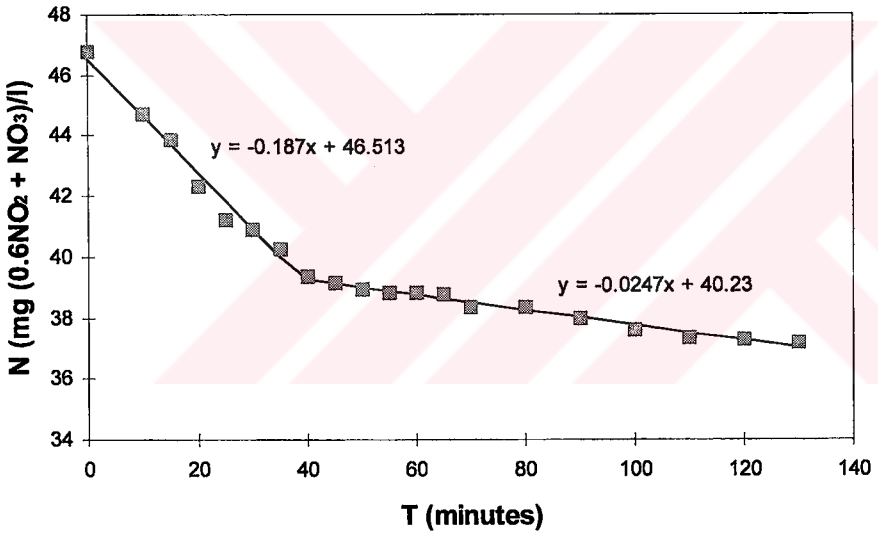

Figure A.36b $0.6NO_2^-$-N+NO_3^--N concentration versus time - b_{HD} experiment - set 12 - initial day

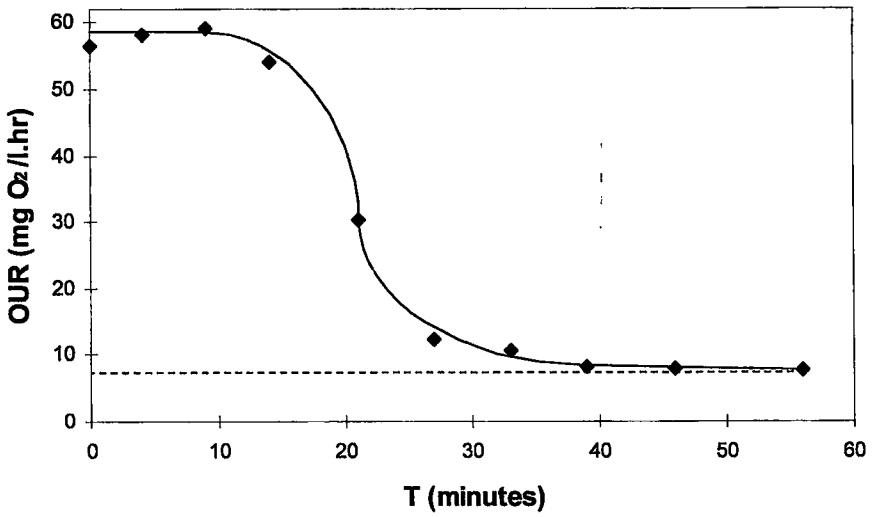

Figure A.37a OUR values versus time - b_H experiment - set 12 - day 1

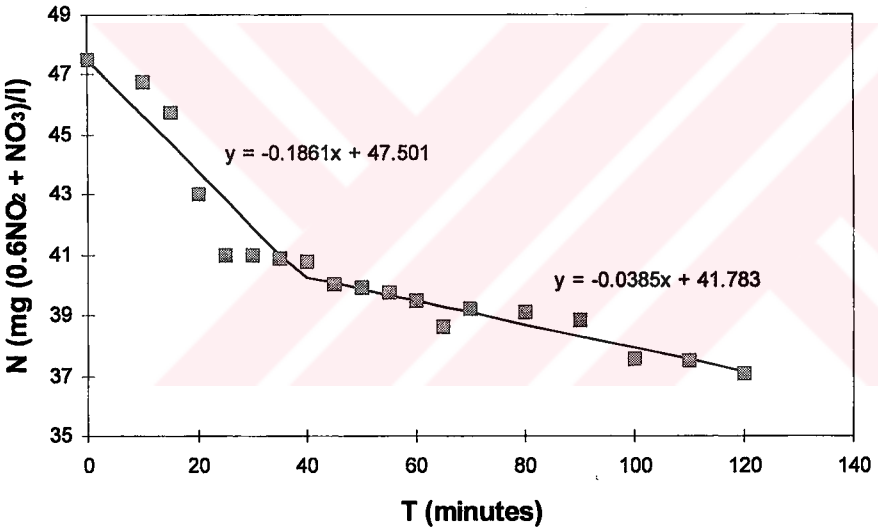

Figure A.37b $0.6NO_2^-$-N+NO_3^--N concentration versus time - b_{HD} experiment - set 12 - day 1

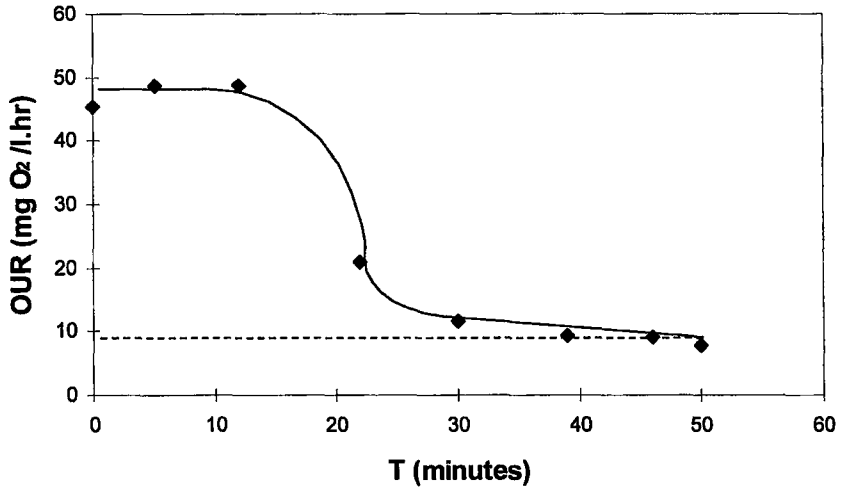

Figure A.38a OUR values versus time - b_H experiment - set 12 - day 2

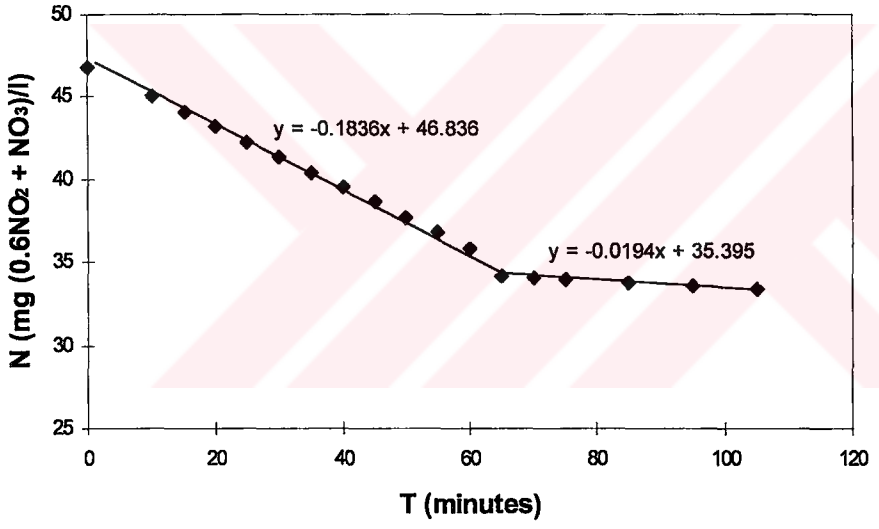

Figure A.38b $0.6NO_2^-$-N+NO_3^--N concentration versus time - b_{HD} experiment - set 12 - day 2

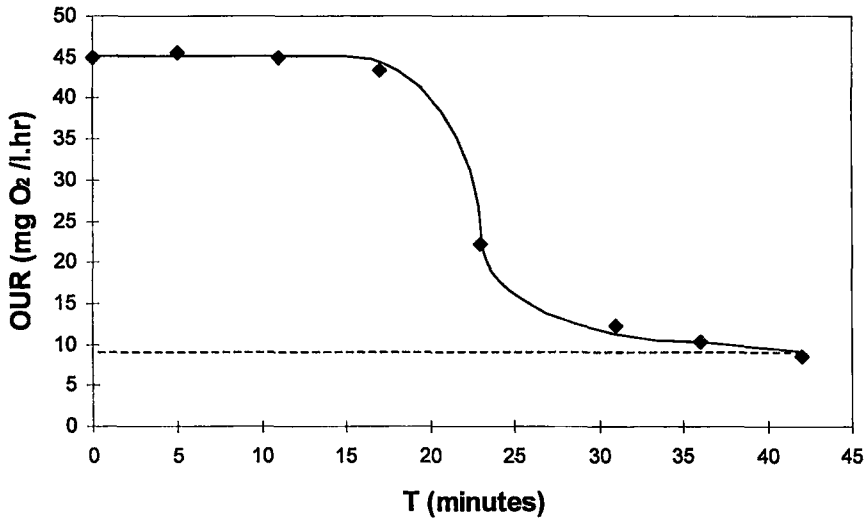

Figure A.39 OUR values versus time - b_H experiment - set 12- day 3

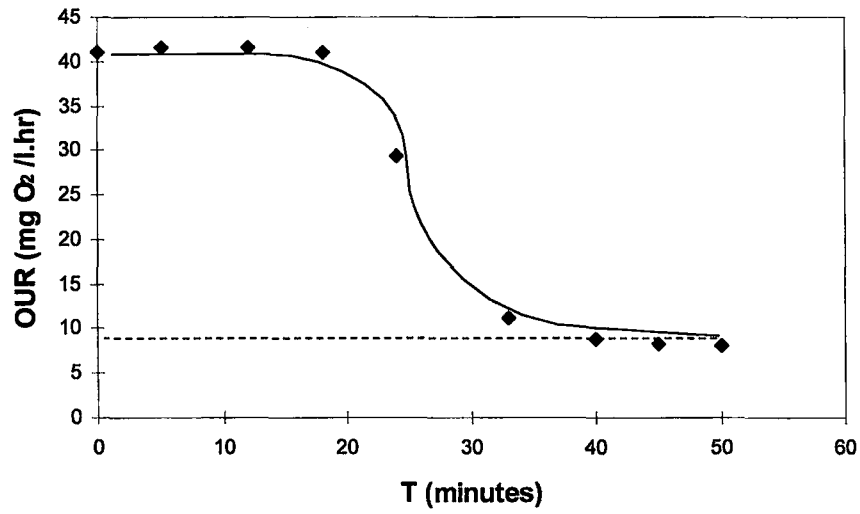

Figure A.40a OUR values versus time - b_H experiment - set 12- day 6

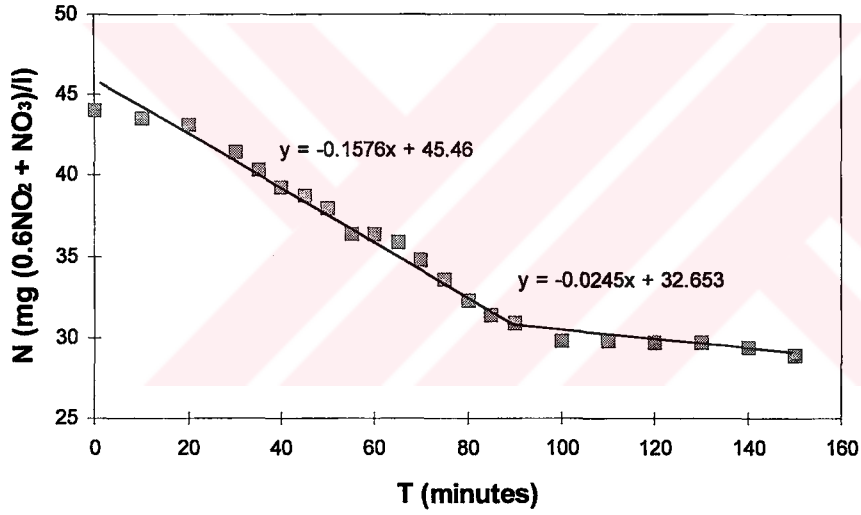

Figure A.40b $0.6NO_2^-$-N+NO_3^--N concentration versus time - b_{HD} experiment - set 12 - day 6

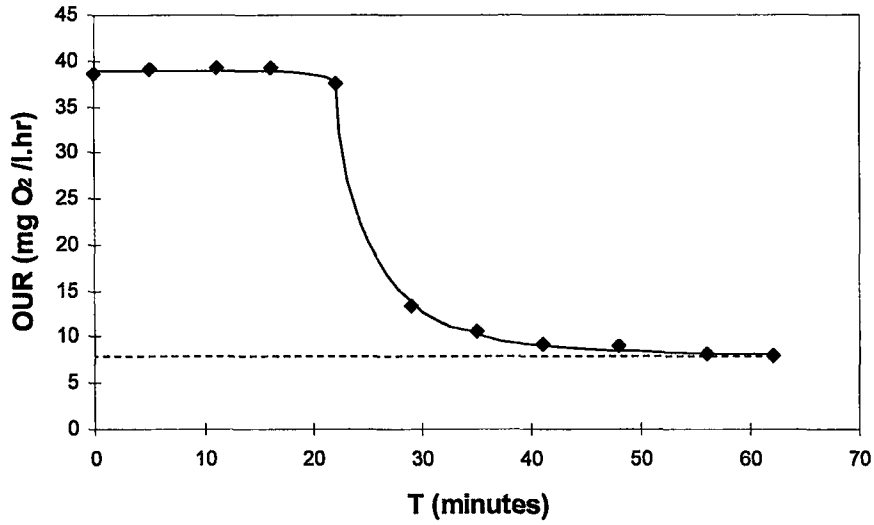

Figure A.41a OUR values versus time - b_H experiment - set 12 - day 7

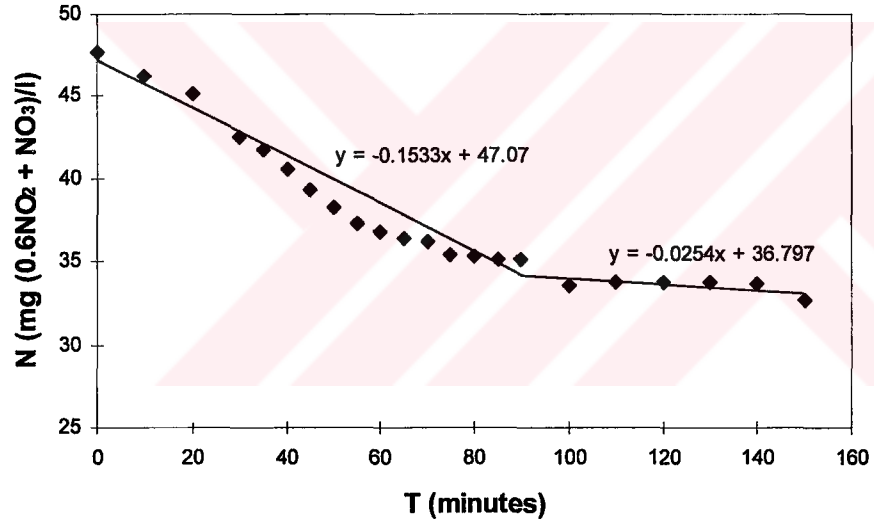

Figure A.41b $0.6NO_2^-$-N+NO_3^--N concentration versus time - b_{HD} experiment - set 12 - day 7

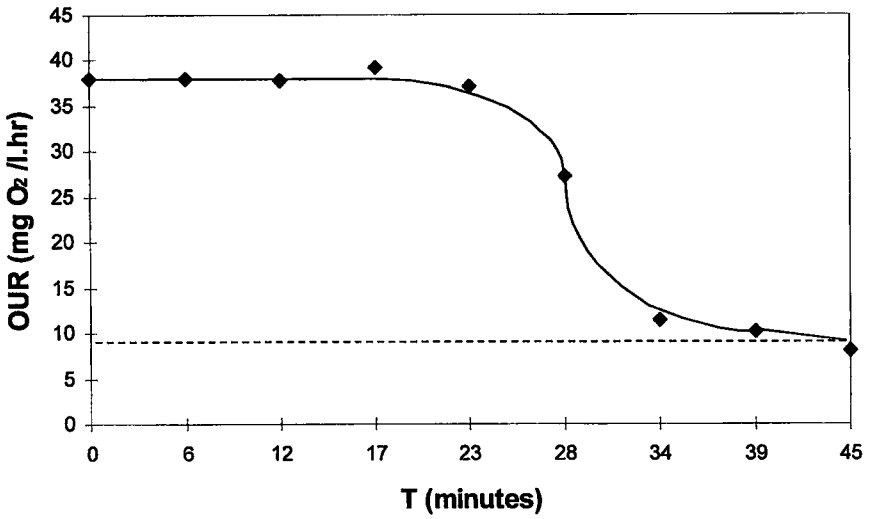

Figure A.42a OUR values versus time - b_H experiment - set 12 – day 8

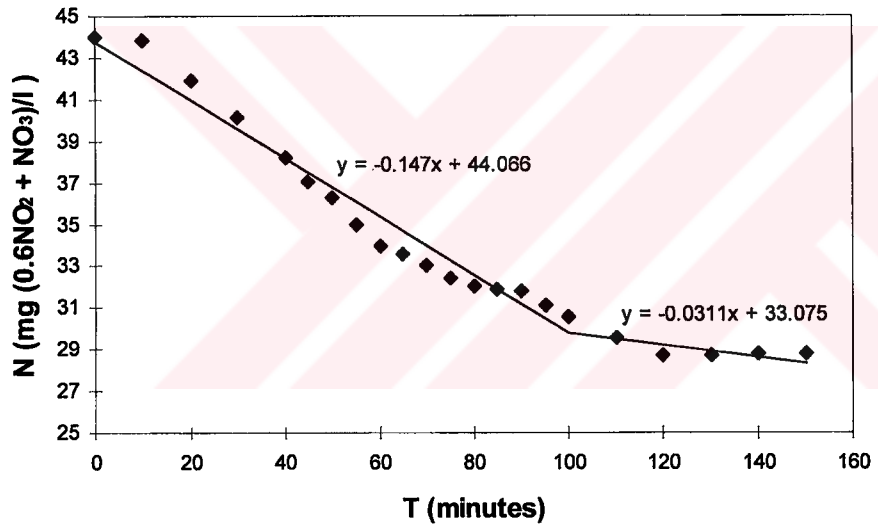

Figure A.42b $0.6NO_2^-$-N+NO_3^--N concentration versus time - b_{HD} experiment - set 12 - day 8

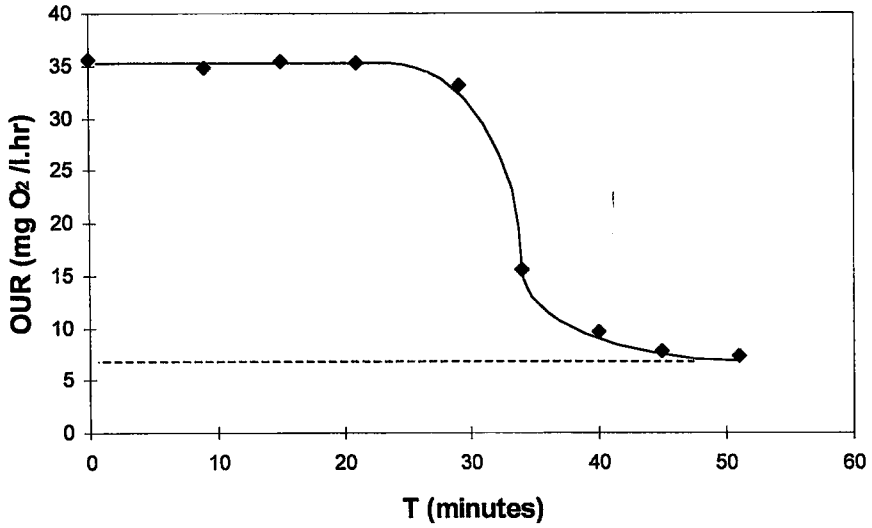

Figure A.43a OUR values versus time - b_H experiment - set 12 - day 9

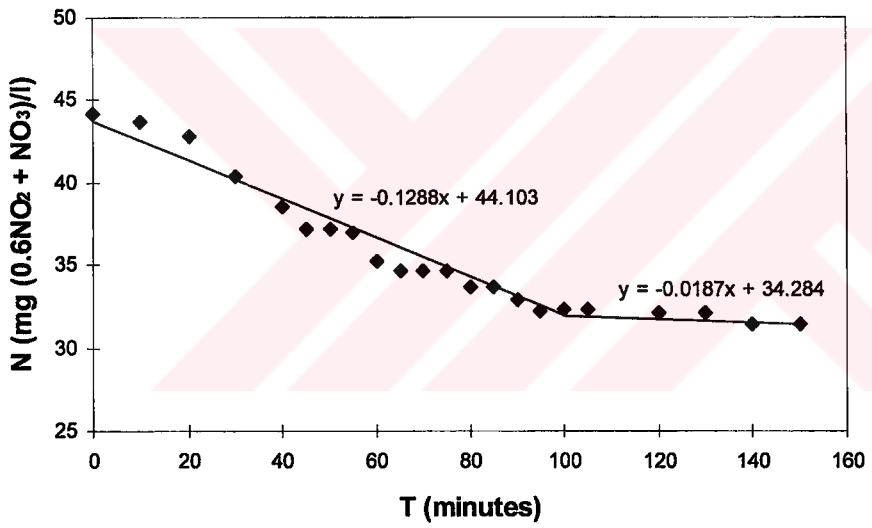

Figure A.43b $0.6NO_2^-$-N+NO_3^--N concentration versus time - b_{HD} experiment - set 12 - day 9

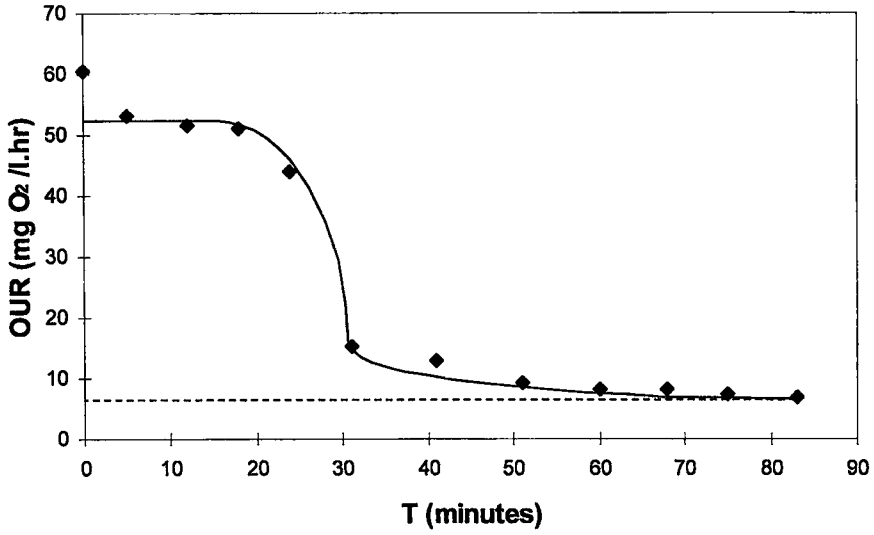

Figure A.44a OUR values versus time - b_H experiment - set 13 - initial day

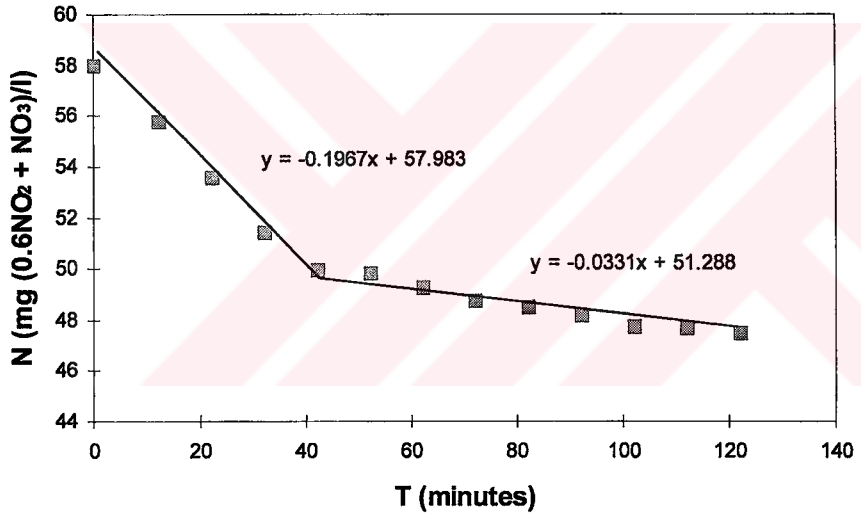

Figure A.44b $0.6NO_2^-$-N+NO_3^--N concentration versus time - b_{HD} experiment - set 13 - initial day

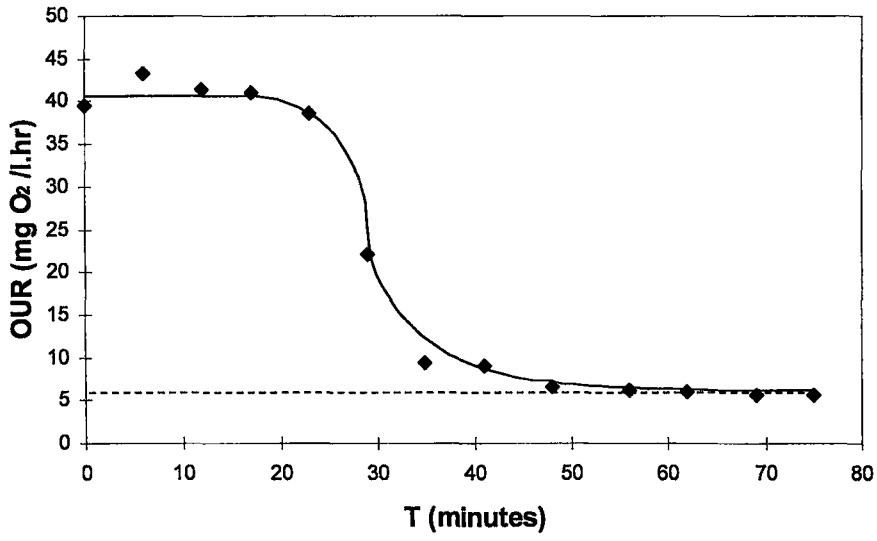

Figure A.45a OUR values versus time - b_H experiment - set 13 - day 1

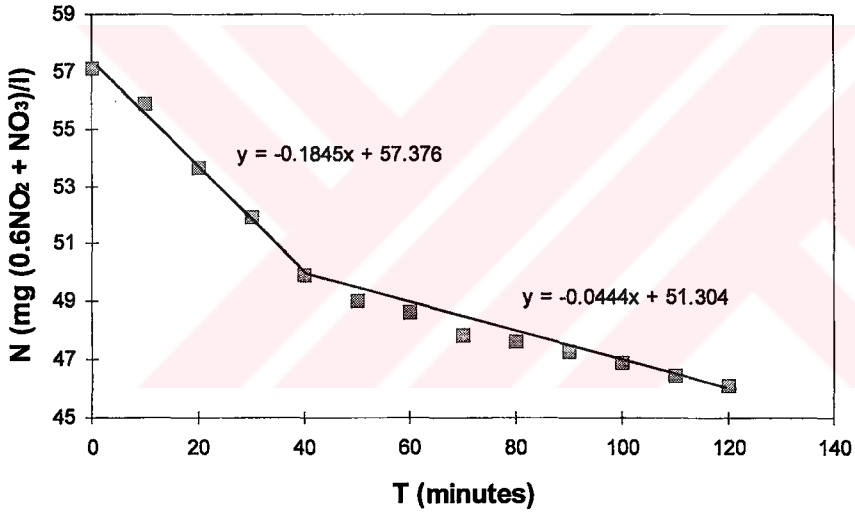

Figure A.45b $0.6NO_2^-$-N+NO_3^--N concentration versus time - b_{HD} experiment - set 13 - day 1

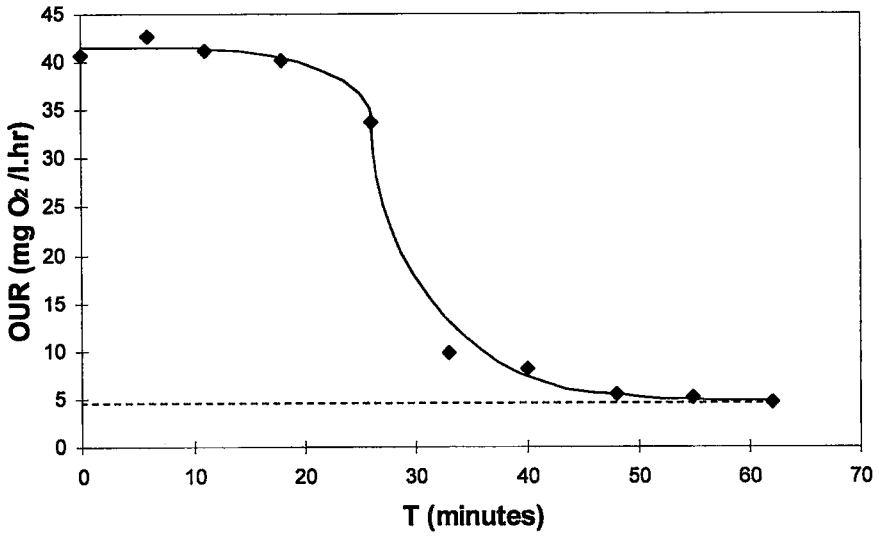

Figure A.46a OUR values versus time - b_H experiment - set 13 - day 2

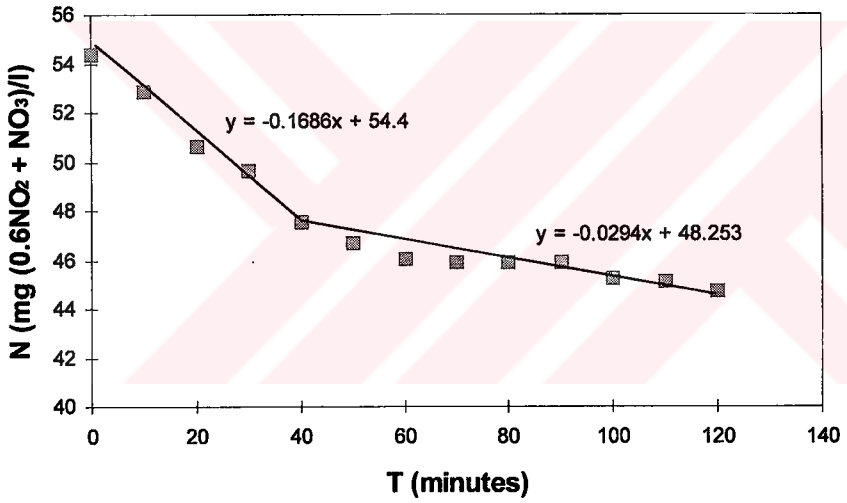

Figure A.46b $0.6NO_2^-$-N+NO_3^--N concentration versus time - b_{HD} experiment - set 13 - day 2

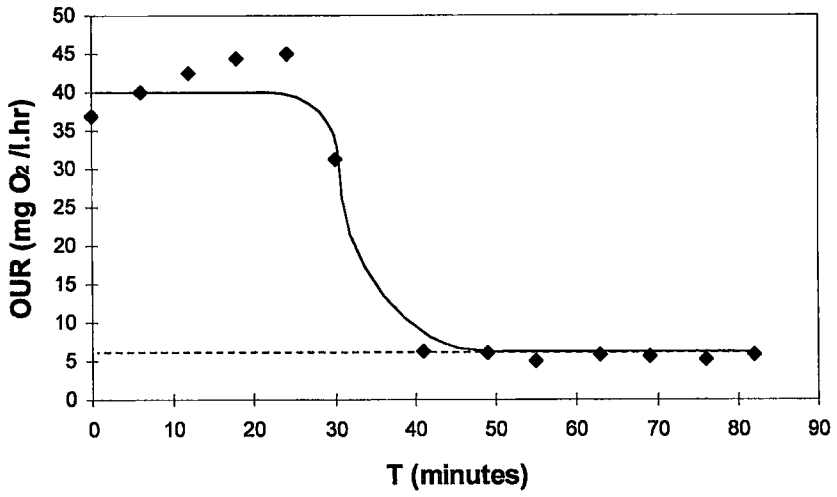

Figure A.47a OUR values versus time - b_H experiment - set 13- day 3

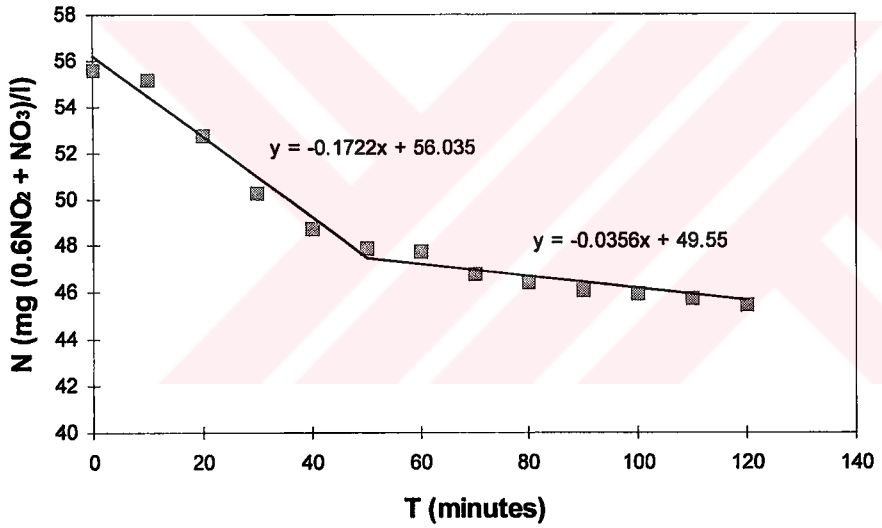

Figure A.47b $0.6NO_2^-$-N+NO_3^--N concentration versus time - b_{HD} experiment - set 13 - day 3

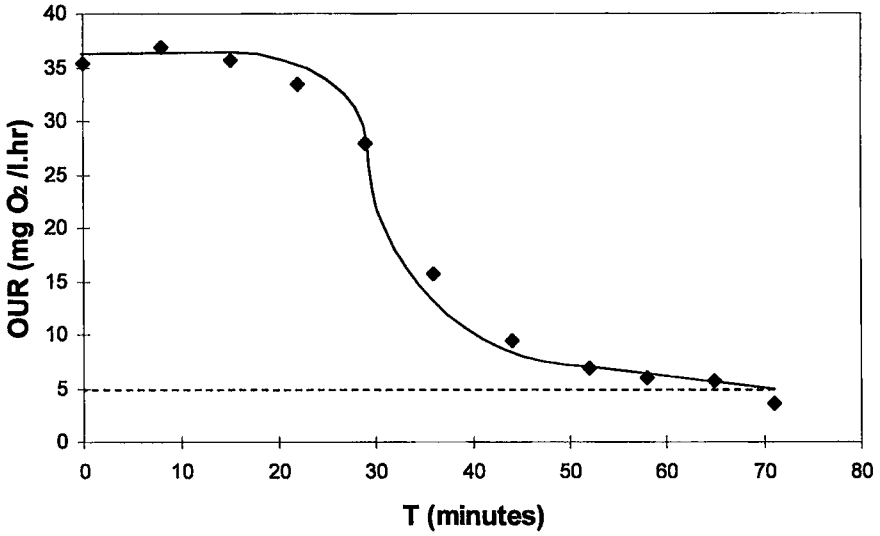

Figure A.48a OUR values versus time - b_H experiment - set 13- day 6

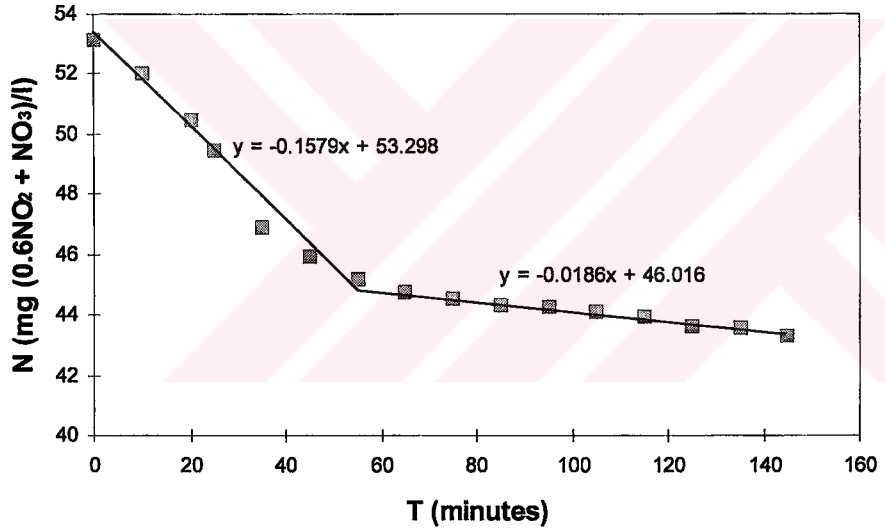

Figure A.48b $0.6NO_2^-$-N+NO_3^--N concentration versus time - b_{HD} experiment - set 13 - day 6

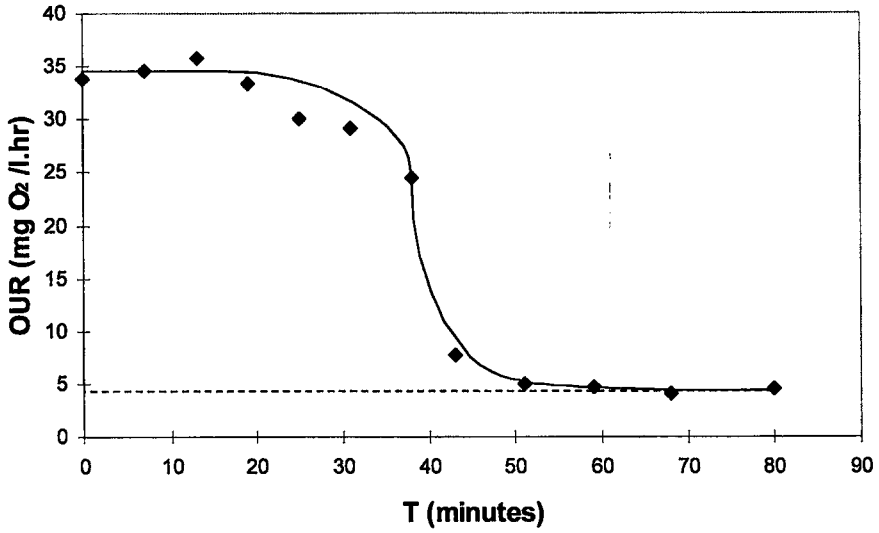

Figure A.49a OUR values versus time - b_H experiment - set 13 - day 7

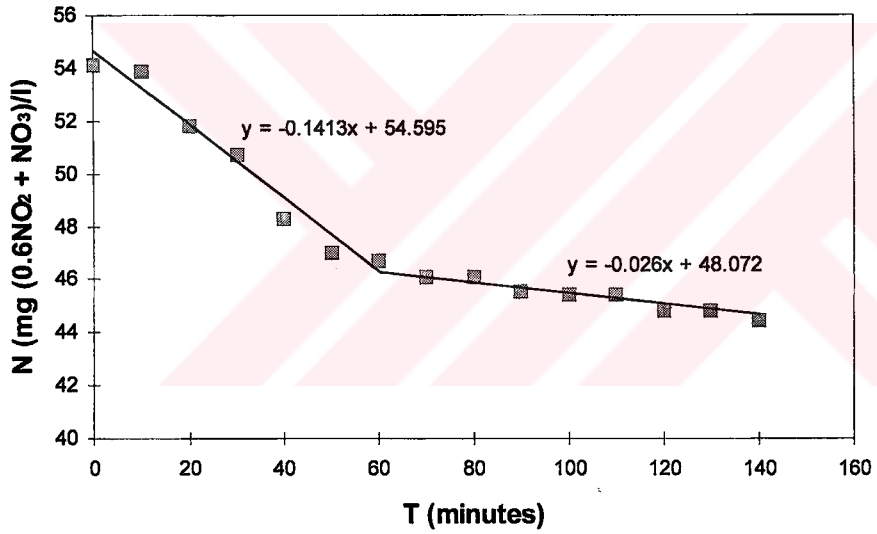

Figure A.49b $0.6NO_2^-$-N+NO_3^--N concentration versus time - b_{HD} experiment - set 13 - day 7

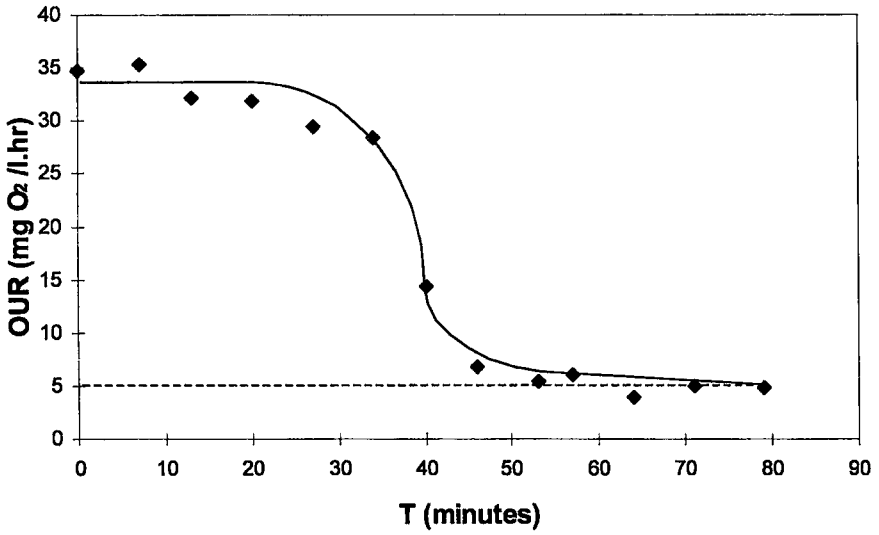

Figure A.50a OUR values versus time - b_H experiment - set 13 - day 8

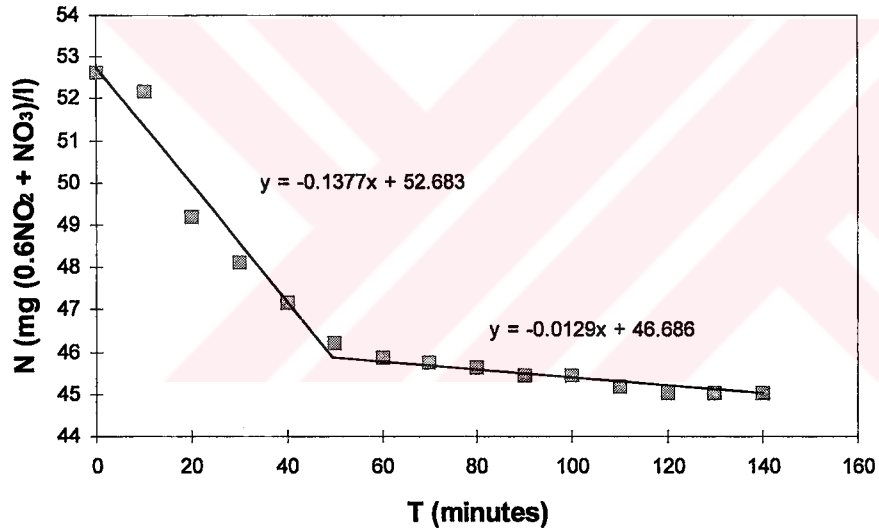

Figure A.50b $0.6NO_2^-$-N+NO_3^--N concentration versus time - b_{HD} experiment - set 13 - day 8

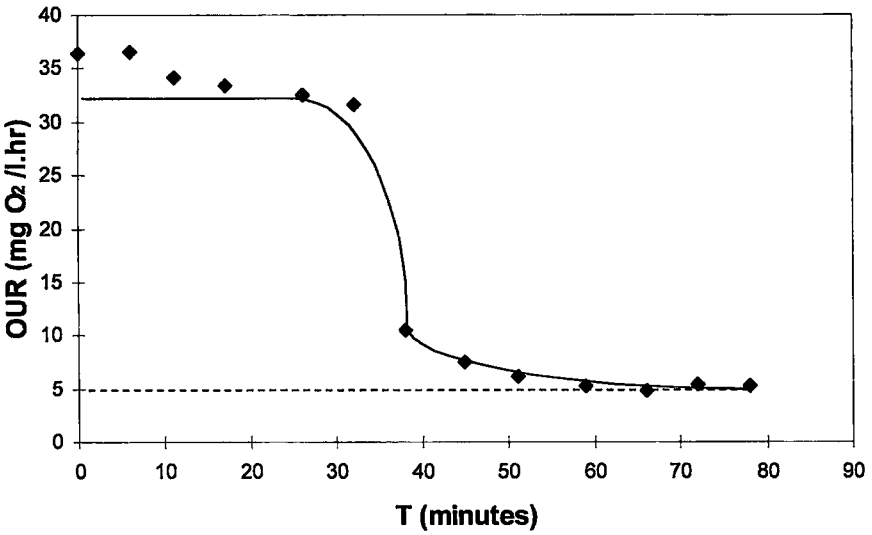

Figure A.51a OUR values versus time - b_H experiment - set 13 - day 9

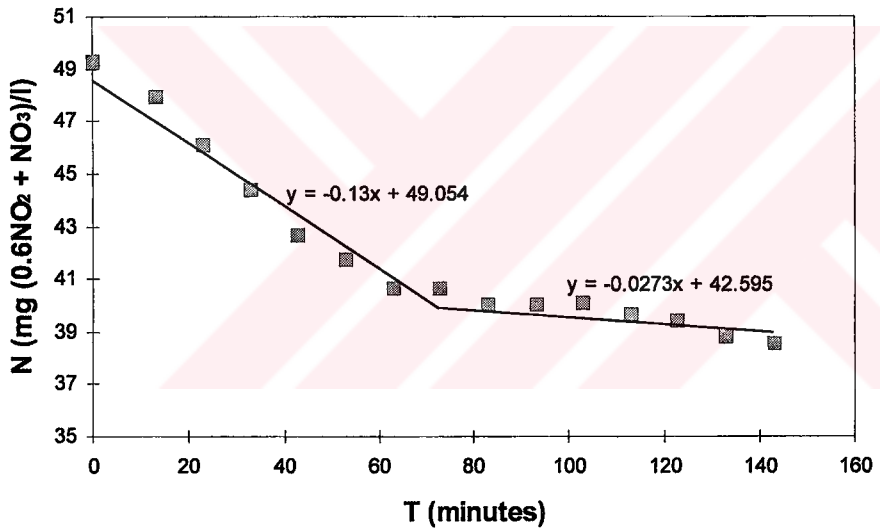

Figure A.51b $0.6NO_2^-$-N+NO_3^--N concentration versus time - b_{HD} experiment - set 13 – day 9

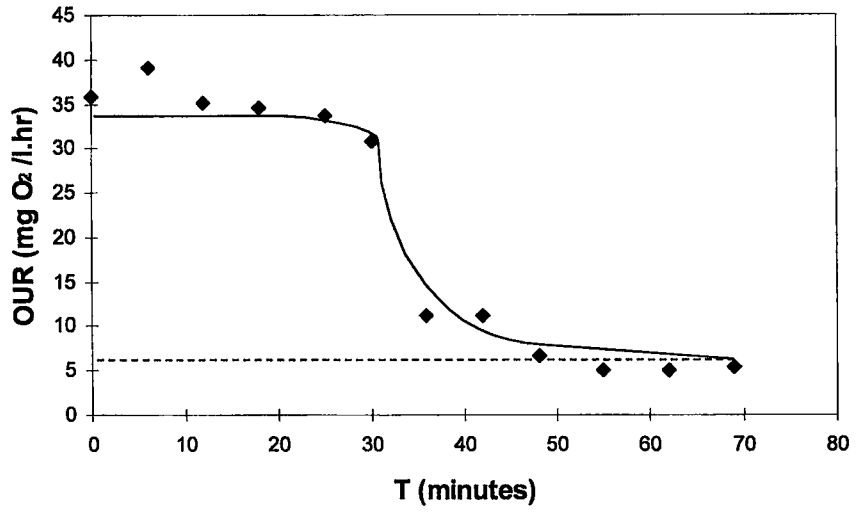

Figure A.52a OUR values versus time - b_H experiment - set 13 - day 10

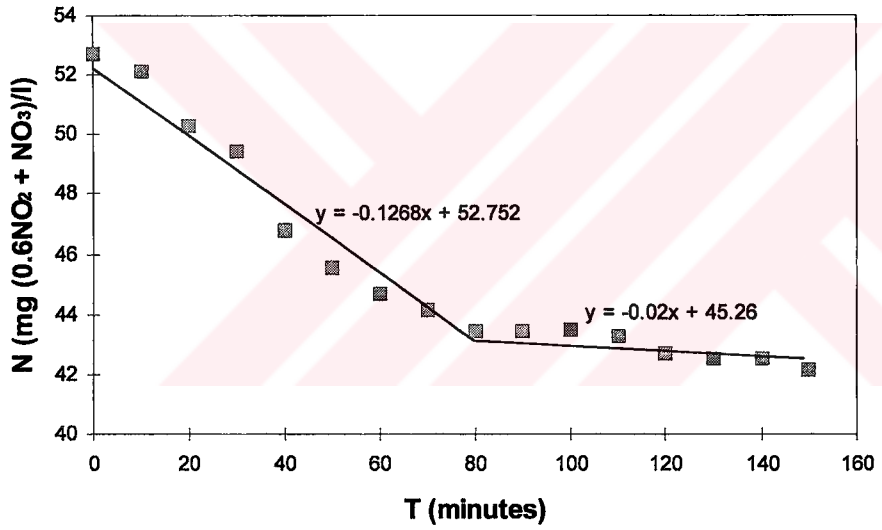

Figure A.52b $0.6NO_2^-$-N+NO_3^--N concentration versus time - b_{HD} experiment - set 13 - day 10

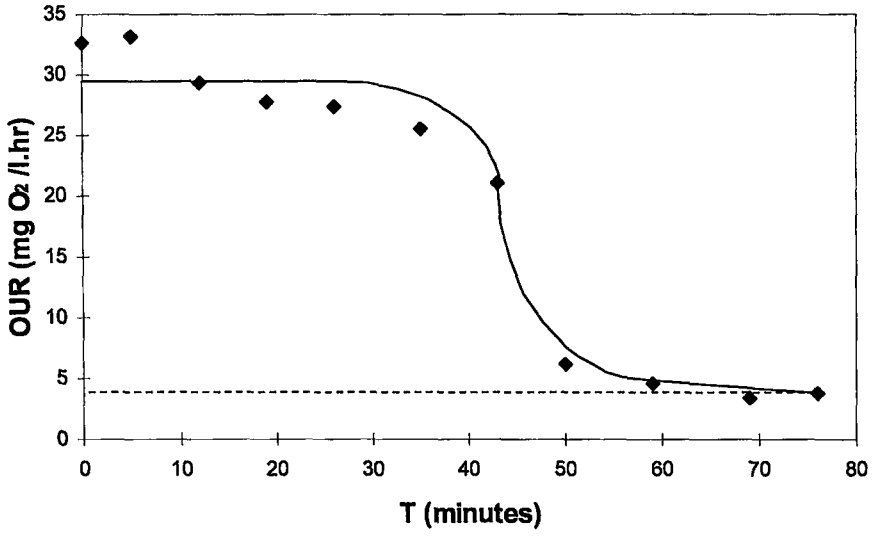

Figure A.53 OUR values versus time - b_H experiment - set 13 - day 13

CIRRUCULUM VITAE

Ebru Avcıoğlu was born in Ankara in 1968. She was graduated from TED Ankara College in 1986. She received her BS degree from the Environmental Engineering Department of the Middle East Technical University/Ankara. She completed her masters education at Drexel University/Philadelphia. She has been working as a research assistant at the Environmental Engineering Department of İstanbul Technical University since 1996.